UNIVERSIDADE DE SANTIAGO DE COMPOSTELA
Departamento de Enxeñería Química

Removal of Endocrine Disrupting Chemicals by the Ligninolytic Enzyme Versatile Peroxidase

Memoria presentada por
D. Roberto Taboada Puig
Para optar ó grado de Doutor pola
Universidade de Santiago de Compostela

Santiago de Compostela, decembro de 2012

UNIVERSIDADE DE SANTIAGO DE COMPOSTELA
Departamento de Enxeñería Química

Dª María Teresa Moreira Vilar, Catedrática do Departamento de Enxeñería Química e D. Juan Manuel Lema Rodicio, Catedrático do Departamento de Enxeñería Química da Universidade de Santiago de Compostela.

Informan:

Que a presente memoria, titulada "**Removal of Endocrine Disrupting Chemicals by the Ligninolytic Enzyme Versatile Peroxidase**" presentada por D. Roberto Taboada Puig, para optar ó grado de Doutor en Enxeñería Química no Programa de Doutoramento en Enxeñería Química e Ambiental, realizouse baixo a nosa inmediata dirección no Departamento de Enxeñería Química da Universidade de Santiago de Compostela.

E para que así conste, firman o presente informe en Santiago de Compostela, decembro de 2012

Os directores

Dª María Teresa Moreira Vilar   D. Juan Manuel Lema Rodicio

Chapter 6. Biocatalytic generation of Mn^{3+}-chelate as a chemical oxidant of organic compounds

Resumen general

Durante los últimos años de la década de 1990, se ha observado una preocupación creciente en torno a la producción, utilización y vertido de sustancias que son sospechosas de interferir con el sistema endocrino y, consecuentemente, que puedan ejercer algún efecto en la salud como cáncer, cambios de comportamiento y anomalías en la reproducción en los seres humanos así como en la vida salvaje. Estas sustancias se denominan Compuestos Disruptores Endocrinos (CDEs) y se definen como "un grupo de productos químicos (naturales, productos químicos sintéticos, industriales o subproductos) presentes en el medio ambiente y sospechosos de alterar las funciones del sistema endocrino y, en consecuencia, causar efectos de salud adversos en un organismo, su progenie o (sub)población". Dentro de los EDCs podemos distinguir en función de su origen, dos tipos de compuestos: (i) sustancias producidas por el hombre, por ejemplo, bisfenol A (BPA), triclosan (TCS) o el 17α–etinilestradiol (EE2), o (ii) hormonas naturales como estrona (E1), 17β-estradiol (E2) o estriol (E3). Existe un número considerable de efectos potenciales asociados a estos compuestos, tales como deformaciones morfológicas, inhibición del desarrollo, reducción de la calidad del esperma, inversión del sexo masculino al femenino y viceversa, etc. Los sistemas de tratamientos de aguas tradicionales, a pesar de conseguir una considerable eliminación de estos compuestos, no son capaces de eliminar los CDEs en su totalidad liberándolos al medioambiente. Aunque las concentraciones vertidas son muy bajas, estos compuestos pueden tener un efecto incluso a niveles de ng/L. En los últimos años se han desarrollado diferentes post-tratamientos para la eliminación de estos compuestos basados en procesos de oxidación avanzada como fotodegradación, fotocatálisis, ozonización, hipoclorito u óxidos de cloro, ultrasonidos, etc. No obstante, estos post-tratamientos por lo general son caros,

tienen poca especificidad y, en ocasiones, generan compuestos aún más tóxicos. Una alternativa que se plantea en este trabajo es la utilización de la enzima peroxidasa versátil (VP) de alto potencial redox, la cual se produce únicamente en ciertas cepas de hongos ligninolíticos. Se ha demostrado que, desde un punto de vista económico, puede considerarse una alternativa interesante ya que su coste de producción y utilización es equiparable a los procesos descritos anteriormente. El objetivo de esta tesis fue evaluar la capacidad de la enzima peroxidasa versátil para eliminar BPA, TCS, E1, E2 y EE2. Para abordar este objetivo se han abordado diferentes metas para llevar a cabo la eliminación de los CDEs mediante la enzima VP:

(i)   Identificación de un nuevo hongo de podredumbre blanca y purificación y caracterización del crudo enzimático producido.

(ii)   Estudio de la enzima libre en ensayos *batch* para la evaluación, a través de un análisis factorial, del efecto de los cofactores del ciclo catalítico en la eliminación de los CDEs.

(iii)   Inmovilización de la enzima para aumentar su estabilidad y aplicación a la eliminación de los CDEs.

(iv)   Estudio de la producción enzimática del complejo Mn^{3+}-malonato a partir de la enzima VP.

(v)   Desarrollo de un sistema enzimático de membrana para la eliminación en continuo de CDEs.

(vi)   Desarrollo de un sistema en dos etapas para la producción enzimática del complejo Mn^{3+}-malonato y su posterior utilización en la eliminación en continuo de CDEs.

(vii)   Identificación de los productos de degradación de BPA y TCS.

(viii) Desarrollo de un sistema de microfiltración-ultrafiltración para la polimerización en continuo de BPA.

Resumo xeral

Durante os últimos anos da década de 1990, houbo unha preocupación crecente sobre a produción, uso e eliminación de substancias sospeitosas de interferir co sistema endócrino e, consecuentemente,de ter un efecto sobre a saúde, como o cancro , alteracións de comportamento e anomalías reprodutivas en humanos, así como animais. Estas substancias son coñecidas como compostos desreguladores endócrinos (CDEs) e son definidas como "un grupo de produtos químicos (naturais, sintéticos ou produtos industriais) presentes no medio ambiente e sospeitosos de alterar as funcións do sistema endócrino e, consecuentemente, causar efectos adversos na saúde dun organismo, a súa descendencia, ou (sub)-poboación ". Entre os CDEs pódese diferenciar dacordo coa súa orixe, dous tipos de compostos: (i) sustancias producidas polo home, por exemplo, bisfenol A (BPA), triclosan (TCS) ou 17α-etinilestradiol (EE2), ou (ii) as hormonas naturais estrona (E1), 17β-estradiol (E2) e estriol (E3). Hai un considerable número de efectos potenciais asociados con estes compostos, como deformidades morfolóxicas, inhibición do crecemento, calidade reducida de espermatozoides ou a inversión do sexo masculino para feminino e viceversa, etc. Os sistemas tradicionais de tratamento de auga, a pesar de alcanzar a eliminación considerable destes compostos, non son quen de eliminar CDEs liberándoos no ambiente. Aínda que as concentracións liberadas son moi baixas, estes compostos poden ter un efecto a niveis de ng/L. Nos últimos anos desenvolvéronse diferentes pos-tratamentos para a eliminación destes compostos basados en procesos de oxidación avanzada como a fotodegradación, a catálise, ozonización, emprego de hipoclorito ou óxidos de cloro, ultrasóns, etc. Con todo, estes post-tratamentos xeralmente son caros, teñen especificidade limitada e ás veces incluso xéranse compostos máis. Unha alternativa que se propón neste traballo é a utilización da enzima de alto potencial redox versátil

peroxidase (VP), que é producida só por certas especiaes de fungos ligninolíticos. Ten sido demostrado que, dende un punto de vista económico, pode ser considerada una alternativa interesante xa que o custo de producción e uso é comparable cos procesos descritos anteriormente. O obxectivo deste traballo foi avaliar a capacidade do enzima peroxidasa versátil para eliminar o BPA, TCS, E1, E2 e EE2. Para acadar este obxectivo diferentes metas foron abordadas para levar a cabo a eliminación dos CDEs pola enzima VP:

(i) Identificación dun novo fungo de podredumbre branca e purificación e caracterización do crudo enzimático producido.

(ii) Estudo da enzima libre en ensaios *batch* para a avaluación, a través dun análisis factorial, do efecto dos cofactores do ciclo catalítico na eliminación dos CDEs.

(iii) Inmobilización da enzima para aumentar a súa estabilidade e aplicación á eliminación dos CDEs.

(iv) Estudo da producción enzimática do complexo Mn^{3+}-malonato a partir da enzima VP.

(v) Desenvolvemento dun sistema enzimático de membrana para a eliminación en continuo dos CDEs.

(vi) Desenvolvemento dun sistema en dos etapas para a producción enzimática do complexo Mn^{3+}-malonato e o seu posterior emprego na eliminación en continuo dos CDEs.

(vii) Identificación dos productos de degradación de BPA y TCS.

(viii) Desenvolvemento dun sistema de microfiltración-ultrafiltración para a polimerización en continuo de BPA.

Summary

During the last years of the 1990s, there has been a growing concern about the production, use and disposal of substances suspected of interfering with the endocrine system and consequently, that may have some effect on health as cancer, behavioral changes and reproductive abnormalities in humans as well as wildlife. These substances are known as endocrine disrupting compounds (EDCs) and are defined as "a group of chemicals (natural, synthetic chemicals, industrial products) present in the environment and suspected of altering the functions of the endocrine system and consequently, cause adverse health effects in an organism, its progeny, or (sub)-population." Among the EDCs two types of compounds can be distinguished according to their origin: (i) substances produced by man, for example, bisphenol A (BPA), triclosan (TCS) or 17α-ethinylestradiol (EE2), or (ii) natural hormones estrone (E1), 17β-estradiol (E2) and estriol (E3). There is a considerable number of potential effects associated with these compounds, such as morphological deformities, growth inhibition, reduced sperm quality investment male to female and vice versa, etc. The systems of traditional water treatment, despite achieving considerable elimination of these compounds, are not capable of removing completely releasing EDCs in the environment. Although concentrations expressed are very low, these compounds may have an effect even at levels ng/L. In recent years different post-treatments have been developed for removal of these compounds based on advanced oxidation processes as photodegradation, catalysis, ozonization, hypochlorite or chlorine oxides, ultrasound, etc. However, these post-treatments are usually expensive, have limited specificity and sometimes even toxic compounds are generated. An alternative that arises in this work is the use of the) high redox potential enzyme versatile peroxidase (VP) which is produced only by certain strains of ligninolytic fungi. It has been demonstrated

that, from an economic standpoint, it can be considered as an interesting alternative since its production and use costs are comparable to the previously described processes. The aim of this thesis was to evaluate the ability of the versatile peroxidase enzyme to remove BPA, TCS, E1, E2, EE2. To address this goal have addressed different goals to accomplish the removal of the enzyme EDCs by VP:

(i)   Identification of a new white-rot fungus and purification and characterization of enzymatic crude produced.

(ii)   Study of the free enzyme in batch experiments to evaluate, through factor analysis, the effect of the cofactors of the catalytic cycle in the removal of EDCs.

(iii)   Immobilization of the enzyme to increase its stability and application to the removal of EDCs.

(iv)   Study of the enzymatic production of Mn^{3+}-malonate complex from the enzyme VP.

(v)   Development of a membrane enzyme system for the continuous removal of EDCs.

(vi)   Development of a "two-stage" system for the enzymatic production of Mn^{3+}-malonate complex and subsequent use in the continuous removal of EDCs.

(vii)   Identification of the degradation products of BPA and TCS.

(viii) Development of a micro-ultrafiltration system for the continuous polymerization of BPA.

Chapter 1

General introduction

Chapter 1. General introduction

1.1. White-rot fungi

1.2. Lignin modifying enzymes

1.2.1. Laccase (Lac, E.C.1.10.3.2)

1.2.2. Lignin peroxidase (LiP, E.C.1.11.1.14)

1.2.3. Manganese peroxidase (MnP, E.C.1.11.1.13)

1.2.4. Versatile peroxidase (VP, E.C.1.11.1.16)

1.3. Endocrine disrupting chemicals

1.3.1. Bisphenol A

1.3.1.1. Health effects

1.3.1.2. Environmental risks

1.3.2. Triclosan

1.3.2.1. Health effects

1.3.2.2. Environmental risks

1.3.3. Natural and synthetic hormone substances: estrone, 17β-estradiol and 17α-ethinylestradiol

1.3.4. Physicochemical properties of EDCs

1.3.5. Post-treatments methods for the elimination of EDCs

1.3.5.1. Elimination of EDCs using AOPs

1.3.5.2. Degradation of EDCs by white rot fungi (WRF) and their lignin modifying enzymes (LMEs)

1.4. Conclusions

Chapter 1. General introduction

1.1. White-rot fungi

Lignin, one of the main constituents of wood together with cellulose and hemicelluloses, is the most recalcitrant compound of wood, due to its complex structure derived from the coupling monolignols and three alcohols (p-coumaryl, coniferyl and sinapyl) [1].

White-rot fungi (WRF) belong to the class of basidiomycetes and certain ascomycetes, and they constitute the most important rotting fungi since they are the only microorganims able to mineralize lignin producing carbon dioxide and water. The term "white-rot" has been traditionally used to describe forms of wood decay where lignin -as well as cellulose and hemicellulose- is broken down, leaving a light, white, rather fibrous residue completely different from the brown powder left by brown rot fungi [2]. Generally, WRF are unable to use lignin as a sole carbon source but they degrade it in order to gain access to cellulose and hemicellulose. Within this group, *Phanerochaete chrysosporium* is the most extensively studied species, although other fungi such as *Bjerkandera adusta*, *Trametes versicolor*, *Pleurotus ostreatus* are also well-known [2].

Delignification is based on the WRF capacity to produce one or more extracellular lignin-modifying enzymes (LMEs) which, thanks to their lack of substrate specificity, are also capable of degrading a wide range of xenobiotics also at relatively low concentrations since they are not induced by either lignin or other related compounds [3]. The use of fungal cultures has been considered as an environmental tool to remove organic pollutants such as polycyclic aromatic hydrocarbons, chlorinated and phenolic compounds, dyes, pharmaceutical compounds, among others. In **Table 1.1**, some examples of the use of white rot fungi in the removal of organic contaminants are shown.

Table 1.1. Removal studies of different kind of organic pollutants by WRF

Organic pollutants		White rot fungi	References
Polycyclic aromatic hydrocarbons	Anthacene, dibenzotiophene, fluoranthene, pyrene, chysene	*Phanerochaete chrysosporium, Bjerkandera adusta, Irpex lacteus, Lentinus tigrinus, Trametes versicolor*	[4-7]
Chlorinated and phenolic compounds	Hexacychlorohexane, dieldrin, aldrin, polychlorinated biphenyls	*Bjerkandera adusta, Pleurotus ostreatus, Phlebia brevispora, Phlebia aurea*	[8-10]
Dyes	Orange G, remazol brilliant blue R	*Bjerkandera adusta, Phanerochaete chrysosporium, Pleurotus ostreatus, Irpex lacteus*	[11, 12]
Pharmaceutical compounds	Naproxen, carbamazepine, norfloxacin, ciprofloxacin	*Pleurotus ostreatus, Trametes versicolor, Phanerochaete chrysosporium*	[13-16]

1.2. Lignin modifying enzymes

LMEs are oxidoreductases which catalyze the electron transfer from one substrate to another. LMEs act by generating free radicals that randomly attack the lignin molecule, breaking covalent bonds and releasing a range of phenolic compounds.

There are two main types of LMEs: peroxidases and laccases (phenol oxidases). The main LMEs are lignin peroxidase (LiP), manganese peroxidase (MnP), versatile peroxidase (VP) and laccases (Lac). In addition, these fungi secrete mediators of high molecular weight increasing the range of potentially biodegradable compounds. White-rot fungi start LMEs production during their secondary metabolism, since lignin oxidation provides no net energy to fungi [17]. These enzymes are responsible for generating highly reactive and non specific free radicals [18] that make them attractive for the development of advanced oxidation processes, where these enzymes may oxidize and degrade highly recalcitrant compounds (**Table 1.2**). The main lignin-modifying enzymes are described below.

Table 1.2. Removal studies of different kind of organic pollutants by LMEs

Enzymes	Organic pollutant	References
Laccase	Polycyclic aromatic hydrocarbons	[19]
	Chlorinated and phenolic compounds	[20-22]
	Dyes	[23-25]
	Pharmaceutical compounds	[26-28]
Peroxidases	Polycyclic aromatic hydrocarbons	[29, 30]
	Chlorinated and phenolic compounds	[31-33]
	Dyes	[34-36]
	Pharmaceutical compounds	[26, 27]

1.2.1. Laccase (Lac, E.C.1.10.3.2)

The enzyme laccase is a multi-copper oxidase that catalyzes one-electron oxidations by transferring one electron from four substrate molecules to one molecule of molecular oxygen which is reduced to water (**Figure 1.1**) [17].

Laccase shows low substrate specificity and can react with diphenols, aryl diamines, aminophenoles.

$$O_2 \diagdown \quad \diagup Laccase \diagdown \quad \diagup Substrate$$
$$H_2O \diagup \quad \diagdown Laccase_{OX} \diagup \quad \diagdown Substrate_{OX}$$
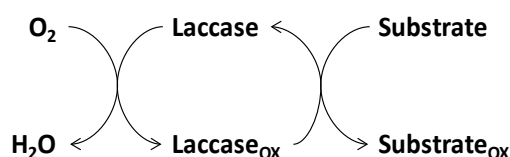
Figure 1.1. Catalytic cycle of Laccase

The redox potential of laccases is in the range between 780-800 mV. However, in presence of a mediator, laccase is able to oxidize also non-phenolic molecules [17, 37]. Laccase has various physiological functions depending on the producing species and their cellular location. It has been reported to be involved in virulence processes (yeasts, bacteria, pathogenic fungi), lignin degradation (white rot fungi) or deposition (plants), pigment synthesis (fungi, bacteria) and cuticle sclerotization in insects [38]. It has been isolated from cultures of *Aspergillus* and thermophilic fungi such as *Myceliophora thermophila*, *Chaemotium thermophilium*, among others [17].

1.2.2. Lignin peroxidase (LiP, E.C.1.11.1.14)

It was the first ligninolytic enzyme isolated in 1980's decade from the fungus *Phanerochaete chrysosporium* [39]. It is a glycoprotein with molecular mass between 38 and 47 kDa with a distinctive feature of an unusually low pH optimum near 3 [17]. It is able to catalyze the oxidation of phenolic and aromatic compounds with a similar structure to lignin. LiP shows a classical peroxidase mechanism: it can react with phenolic aromatic substrates forming phenoxy radicals, but it is unique in its ability to oxidize substrates of high redox potential (up to 1.4 V) [17]. It is an enzyme relatively specific to their substrates, being the

preferred substrate veratryl alcohol (VA) a natural metabolite that increases the enzyme activity and the rate of lignin degradation (**Figure 1.2**) [37].
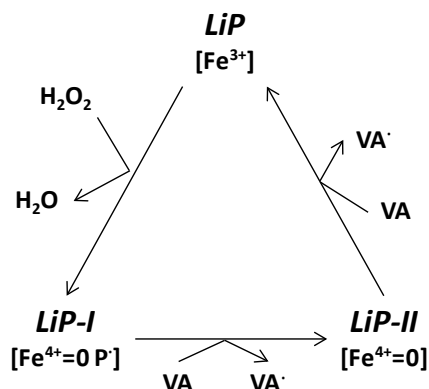
Figure 1.2. Catalytic cycle of LiP

1.2.3. Manganese peroxidase (MnP, E.C.1.11.1.13)

Manganese peroxidase is an extracellular enzyme discovered in *Phanerochaete chrysosporium* by Kuwahara et al. (1984) [40] and it is considered the most widespread ligninolytic peroxidase produced by almost all white-rot basidiomycetes and by various litter-decomposing fungi [17]. MnP is a glycoprotein with molecular weights between 32 and 62.5 kDa. This enzyme has a similar catalytic cycle to other peroxidases involving a two-electron oxidation; however, MnP is able to oxidize Mn^{2+}, resulting in the formation of diffusible oxidants (Mn^{3+}) capable of penetrating the cell wall matrix and oxidizing mainly phenolic substrates [37].

The catalytic cycle is initiated by binding of H_2O_2 to the native (ferric) enzyme and formation of an iron-H_2O_2 complex (**Figure 1.3**). Subsequent cleavage of the H_2O_2 oxygen-oxygen bond requires a two-electron transfer from the heme resulting in formation of MnP-I (Fe^{4+}). Afterwards, the O-O bond is heterolytically cleaved and a H_2O molecule released. Subsequent reduction proceeds through MnP-II (Fe^{4+}). Mn^{2+} ion acts as one electron-donor for this

porphyrin intermediate and is oxidized to Mn^{3+}. The reduction of MnP-II proceeds in a similar way and another Mn^{3+} is formed from Mn^{2+}, thereby leading to generation of native enzyme and release of the second water molecule. MnP is sensitive to high concentrations of H_2O_2 that cause reversible inactivation of the enzyme by forming MnP-III, a catalytically inactive oxidation state but can be rescued by Mn^{3+} [37, 41].

$$
\begin{array}{c}
\textbf{\textit{MnP}} \\
\textbf{[Fe}^{3+}\textbf{]}
\end{array}
$$
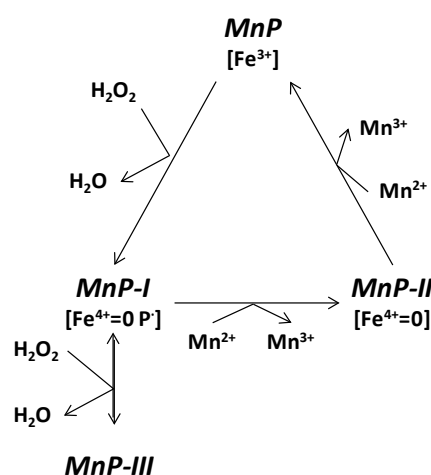
Figure 1.3. Catalytic cycle of MnP

Ions of Mn^{3+} are quite unstable in aqueous media. To overcome this drawback, they form complexes with organic acids, such as malonic or oxalic acid, secreted by the fungus in significant amounts that attack organic molecules non-specifically at location remote from the enzyme active site [37, 41]. These chelators could also accomplish other physiological functions; they enhance the dissociation of Mn^{2+} from the enzyme improving its activity; allow the fungus to control pH; sequester Ca^{2+} ions to increase the pore size of the plant cell wall and facilitate the penetration of the enzyme or react with O_2 to form H_2O_2 useful for the enzyme activity [37].

1.2.4. Versatile peroxidase (VP, E.C.1.11.1.16)

The enzyme VP is a peroxidase which combines the substrate specificity characteristics of the three other fungal peroxidases (MnP, LiP and *Coprinopsis cinerea* peroxidase). In this way, it is able to oxidize a variety of high and low redox potential substrates including Mn^{2+}, phenolic and non-phenolic lignin dimers, α-keto-γ-thiomethyl-butyric acid (KTBA), veratryl alcohol-dimethoxybenzenes, different types of dyes (Reactive Black 5), substituted phenols and hydroquinones [42, 43]. VP is only produced by fungi from the genera *Pleurotus*, *Bjerkandera* and *Lepista* [44]. It is interesting to underline that VP enzyme shows different optimal pHs for the oxidation of Mn^{2+} (pH 5) or aromatic compounds (pH 3), similar to those of optimal LiP and MnP activity [45].

The VP catalytic cycle (**Figure 1.4**) includes two-electron oxidation of the resting peroxidase (VP, containing, Fe^{3+}) by hydrogen peroxide to yield compound I (C-I_A, containing Fe^{4+}-oxo and porphyrin cation radical), whose reduction in two one-electron reactions, producing Mn^{3+}, results in the intermediate compound II (C-II_A, containing Fe^{4+}-oxo after porphyrin reduction) and then the resting form of the enzyme. Compounds C-I_B and C-II_B, which are in equilibrium with C-I_A and C-II_A respectively, are involved in the oxidation of veratryl alcohol and other high redox potential aromatic compounds [44]. The presence of Mn^{2+} at moderate concentrations was demonstrated to strongly inhibit the oxidation of LiP substrates, such as VA ([46]).

$$VP \quad [Fe^{3+}]$$

Figure content with:
- VP [Fe^{3+}]
- VA$^{\cdot}$, VA
- C-I$_B$ [Fe^{3+} Trp$^{\cdot}$]
- H$_2$O$_2$, H$_2$O
- Mn^{3+}, Mn^{2+}
- C-I$_A$ [Fe^{4+}=0 P$^{\cdot}$]
- Mn^{2+}, Mn^{3+}
- C-II$_A$ [Fe^{4+}=0]
- VA$^{\cdot}$, VA
- C-I$_B$ [Fe^{4+}=0 Trp$^{\cdot}$]
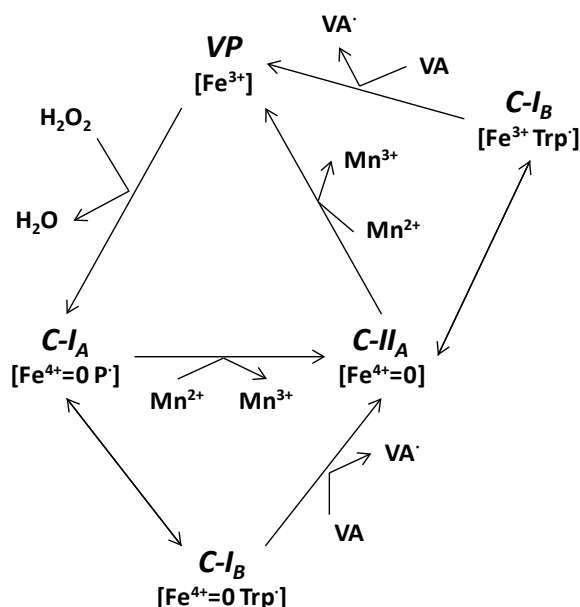
Figure 1.4. Scheme of VP catalytic cycle

1.3. Endocrine disrupting chemicals

Since the end of the 1990 there has been a growing concern about the exposure to substances which are suspected to interfere with the endocrine system, and thus, may cause health effects such as cancer, behavioural changes and reproductive abnormalities in human beings and wildlife (**Figure 1.5**).

Many of the thousands of anthropogenic chemicals currently released into the environment are endocrine disrupting compounds (EDCs; [47]). These are defined as "a group of chemicals (natural, synthetic, industrial chemicals or by-products) present in the environment and suspected to alter the functions of the endocrine system and, consequently, causing adverse health effects in an intact organism, or its offspring or (sub) population" [48].
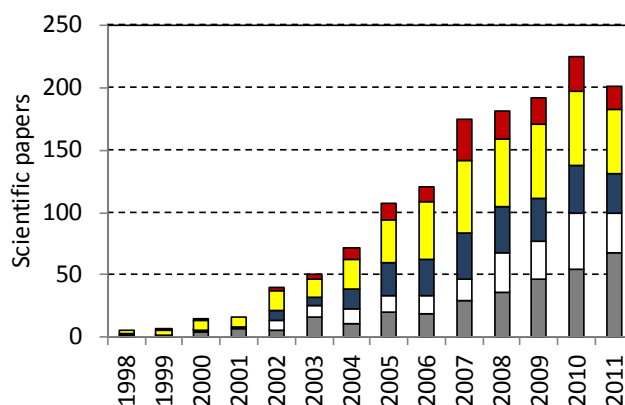
Figure 1.5. Impact of the EDCs in the environment. Scientific publications from 1998 to 2011 (ISI Web of knowledge). Bisphenol A (grey), triclosan (white), estrone (blue), 17β-estradiol (yellow) and 17α-ethinylestradiol (red).

Two classes of substances can cause endocrine disruption:

- <u>Man-made substances</u> which comprise: (i) synthetically-produced hormones, including oral contraceptives, such as ethynylestradiol (EE2), hormone replacement therapy and some animal feed additives, designed deliberately to interfere with and modulate the endocrine system; (ii) a variety of man-made chemicals, such nonylphenol present in cleaning agents or bisphenol A used in consumer goods and iii) various by-products from industrial processes such as dioxins.

- <u>Natural hormones</u> which include estrogens such as estrone (E1), 17β-estradiol (E2), and estriol (E3), progesterone and testosterone naturally found in the body of humans and animals, and phytoestrogens, such as isoflavonoides and coumestrol present in some plants.

This broad class of chemicals has been found in wastewater, surface waters, sediments, groundwater, and even drinking water [49]. Natural and synthetic EDCs are released into the environment, mainly through sewage

treatment systems before reaching the receiving bodies [49]. **Figure 1.6** shows the main distribution of EDCs in the environment.
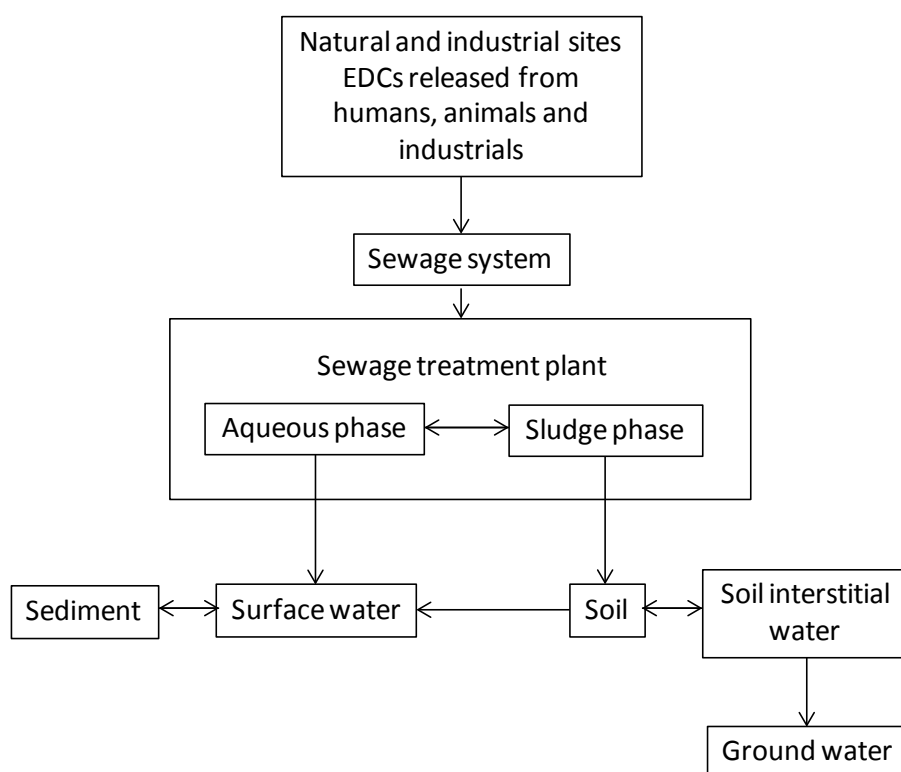
Figure 1.6. Distribution of EDCs in the environment.

Endocrine systems regulate a multitude of developmental, metabolic, and reproductive processes including embryonic development, gonadal formation, sex differentiation, growth, and digestion; therefore, endocrine disrupting compounds, may affect these processes by either binding to or blocking hormone receptors, thereby triggering or preventing hormonal response [50-52]. The typical effects of EDCs on animals are listed in **Table 1.3**.

Table 1.3. Effects of EDCs on animals

Invertebrates	References
Premature metamorphosis of larvae	[53]
Developmental inhibition	[54]
Delayed larval emergence	[55]
Reduced time to molt and altered sex ratios	[56]
Reduced overall growth	[57]
Identifiable protein expression changes	[58]
Miscarriage rate & reduced reproductive allocation	[59]
Increased female fecundity	[60]
Morphological deformities	[61]
Fish	
Reduced sperm quality and delayed ovulation	[62]
Complete inhibition of ovulation	[62]
Gonad structural changes in males and increased oocyte atresia	[63]
Decrease estrogen to androgen ratios in blood	
Increase estrogen to androgen ratios in blood	
Intersex condition	
Reduced numbers of mature spermatozoa	[64]
Feminized brains in embryos	[65]
Female skewed sex ratios in fry	
Amphibians	
Sex reversal male to female	[66]
Abnormal gut coiling, edema, microcephaly, and decreases in body length	[67]
Head malformations, scoliosis, and organogenesis suppression occur	[68]
Reptiles	
Abnormal seminiferous tubules in males	[69]
100% male to female sex reversal	
Oviduct abnormalities in females	[70]

1.3.1. Bisphenol A

Bisphenol A (BPA) is an industrial organic compound of formula $(CH_3)_2C(C_6H_4OH)_2$ with two phenol functional groups (**Figure 1.7**). Most BPA is used as an intermediate in the production of polycarbonate and epoxy resins, flame retardants, and other specialty products. Final products include adhesives, protective coatings, powder paints, automotive lenses, protective window glazing, etc. [71]. Polycarbonate is used in a number of household containers, including baby bottles, sippy cups, re-useable water bottles (sports bottles), pitchers, water carboys, tableware and food storage containers, whereas the epoxy resins act as a protective lining on the inside of metal-based food and beverage cans.
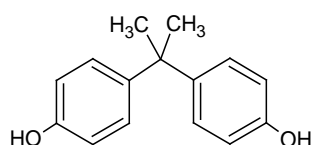
Figure 1.7. Molecular structure of Bisphenol A

The market for BPA has been growing with the increasing demand for polycarbonates and epoxy resins. Global demand for BPA is predicted to grow from 3.9 million tons in 2006 to about 5 million tons in 2010 [72]. The countries with the largest production of BPA are Germany, the Netherlands, USA and Japan [47].

1.3.1.1. Health effects

The production and use of BPA is a controversial issue all around the world. Results from standardized toxicity tests used globally for regulatory decision-making have supported the safety of current low levels of human exposure to BPA [73]. However, other reports on novel approaches and different endpoints describe various effects caused by BPA in laboratory animals at very low doses

according to estimated human exposures [74]. Many of these new studies evaluated developmental or behavioral effects that are not typically assessed in standardized tests.

The National Toxicology Program Center for the Evaluation of Risks to Human Reproduction (NTP) from the United States completed a review of BPA. The NTP uses five different terms to describe its level of concern about the different effects of chemicals: negligible concern, minimal concern, some concern, concern and serious concern. Regarding BPA, the NTP expressed "some concern for effects on the brain, behavior, and prostate gland in fetuses, infants and children at current human exposures to bisphenol A". The Program also expressed "minimal concern for effects on the mammary gland and an earlier age for puberty for females in fetuses, infant, and children at current human exposures to bisphenol A" and "negligible concern" for other outcomes. According to this, the NTP does not make any regulatory recommendations. With respect to neurological and developmental outcomes of BPA, the Program stated that "additional research is needed to fully assess the functional, long-term impacts of exposures to bisphenol A on the developing brain and behavior". The Program also stated that the current literature cannot yet be fully interpreted for biological or experimental consistency or for relevance to human health [75].

In the United States of America, current BPA food contact uses were approved under food additive regulations issued more than 40 years ago. This regulatory structure limits the oversight and flexibility of U.S. Food and Drug Administration (FDA). Once a food additive is approved, any manufacturer of food or food packaging may use the food additive. In March 2012, FDA concluded that "the scientific evidence at this time does not suggest that the very low levels of human exposure to BPA through the diet are unsafe".

However, the FDA recognizes potential uncertainties in the overall interpretation of these studies including the route of exposure used in the studies and the relevance of animal models to human health. Nevertheless, on 17th July 2012, the FDA banned the use of BPA in baby bottles and sippy cups.

Canada was the first country to take action on bisphenol A, thanks to the Chemicals Management Plan, developed by Canadian Environmental Protection Act (CEPA). This Plan was introduced in 2006 to review the safety of widely-used chemicals that have been in the marketplace for many years, as well as to update the knowledge and understanding of these chemicals. Although there is no general recommendation concerning BPA, the Canadian Government advised to reduce exposure of newborns and infants less than 18 months [76]. Consequently, the proposed ban applies only to baby bottles made of polycarbonate. All other containers made with other types of plastics can continue to be used safely.

Concerning the use of bisphenol A in Europe, in 2006 the European Food Safety Authority (EFSA) concluded that infants aged 3 and 6 months fed using polycarbonate infant feeding bottles have the highest exposure to BPA, though below the tolerable daily intake (TDI, 0.05 mg_{BPA}/kg). For this group of infants, the level of exposure to BPA decreases once feeding from polycarbonate bottles is phased out and other sources of nutrition become dominant. Even if the infant has sufficient capacity to remove BPA at worst-case exposure, the EFSA pointed out that an infant's system to remove BPA is not as developed as that of an adult and it gradually reaches the adult capacity after 6 months. Consequently, on April 1st, 2011, the European Commission adopted the EU No 321/2011 regulation that amends EU No 10/2011 related to the restriction of use of bisphenol A in plastic infant feeding bottles. The new EU regulation applied from

May 1st 2011 prohibits the use of Bisphenol A in the manufacture or import of polycarbonate infant feeding bottles.

As a general conclusion, it can be established that even when it is not clearly demonstrated that BPA can have a effect on human beings, most countries around the world are banning the use of BPA for the production of baby bottles or other household items that can be in close contact with infants. Thereby, to the list of countries that have banned the use of BPA, it is noteworthy that other world powers like the United Arab Emirates and China have joined the list of countries that do not allow the use of this endocrine disrupting compound.

1.3.1.2. Environmental risks

BPA emissions to the environment may be from several sources such as producing factories [77], installations that include BPA into plastic [71] and leachates from plastic wastes [78] and landfill sites [79]. Variable ranges of BPA concentrations have been detected: 5–320 ng/L in river waters [80, 81], 20–700 ng/L in sewage effluents [81, 82], 2–208 ng/m^3 in air, 0.2–199 ng/g in dust [83-86] and 0.1–384 ng/g in food-stuffs [85, 86].

Most studies of the effect of BPA on wildlife focus on endocrine systems. It was reported that BPA concentrations ranging from 1.1 to 12.8 mg/L are systemically detrimental to daphnids [87-89], mysids [87, 89] and freshwater (*Pimephales promelas*) and saltwater (*Menidia menidia*) fishes [87]. Based on reported EC$_{50}$ and LC$_{50}$ values that range from 1.0 to 10 mg/L, BPA is classified as "moderately toxic" and "toxic" to aquatic biota by the European Commission and the United States Environmental Protection Agency (US EPA), respectively [87]. However, studies of BPA effects on wildlife indicate that the compound may be harmful even at environmentally relevant concentrations (12 µg/L) or lower [90].

1.3.2. Triclosan

Triclosan is a type of bisphenol that exhibits antimicrobial activity (**Figure 1.8**). It is a synthetic, non-ionic, broad-spectrum antimicrobial agent, possessing mostly antibacterial, but also antifungal and antiviral properties [91]. Triclosan is fairly insoluble in aqueous solutions except for alkaline pH, and it is readily soluble in most organic solvents (**Table 1.6**).

It is used in many contemporary and professional health care products, such as hand soaps, hand washing solution, deodorants, etc. [91]. It is also incorporated into fabrics and plastics, including toys, toothbrush handles, cutting boards, pizza-cutter and mop handles, as well as surgical drapes and hospital over-the-bed table tops.
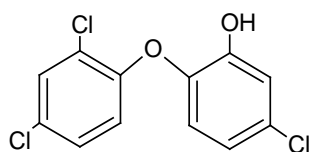
Figure 1.8. Molecular structure of triclosan

Depending on formulation and application, triclosan is recognized by the FDA as either an over-the-counter or a prescription drug. In addition, it is FDA-accepted for use as an antimicrobial pesticide for fungicide and bacteriostat applications [91].

1.3.2.1. Health effects

According to the FDA, there is no evidence that triclosan is hazardous to humans, there is no sufficient safety evidence to recommend changing consumer use of products that contain triclosan. In light of questions raised by recent animal studies of triclosan, FDA is reviewing all the available evidences on this ingredient in consumer products (www.fda.gov).

The Government of Canada completed its preliminary assessment of triclosan under the Canadian Environmental Protection Act [92] and the Pest Controls Products Act. The review concludes that triclosan is not harmful to human health, but in significant amounts it may cause harm to the environment [93].

The opinion of the European Commission, through the Scientific Committee on Consumer Products (SCPP), is that "taking into account the provided toxicological data, the continued use of triclosan as a preservative at the limit concentration of 0.3% in all cosmetic products is not safe for the consumer because of the magnitude of the aggregate exposure. However, its use at a maximum concentration of 0.3% in face products, toothpastes, hand soaps, body soaps/shower gels and deodorant sticks, is considered safe. However, the use of triclosan in other leave-on products (e.g. body lotions) and in mouthwash solutions is not considered safe for the consumer due to the higher level of exposure."

1.3.2.2. Environmental risks

The widespread use of triclosan results in the discharge of this compound to wastewater. Triclosan is transported through the domestic waste stream to wastewater treatment plants (WWTPs, **Figure 1.9**). Municipal wastewater treatment helps achieve removal efficiencies in the range of 51-95%, depending on the technical capabilities of sewage treatment systems [94-103]. Both the incomplete removal of triclosan from wastewater treatment plants (**Table 1.7**) and its presence in biosolids spread as fertilizers lead to triclosan being distributed in soils and surface waters.
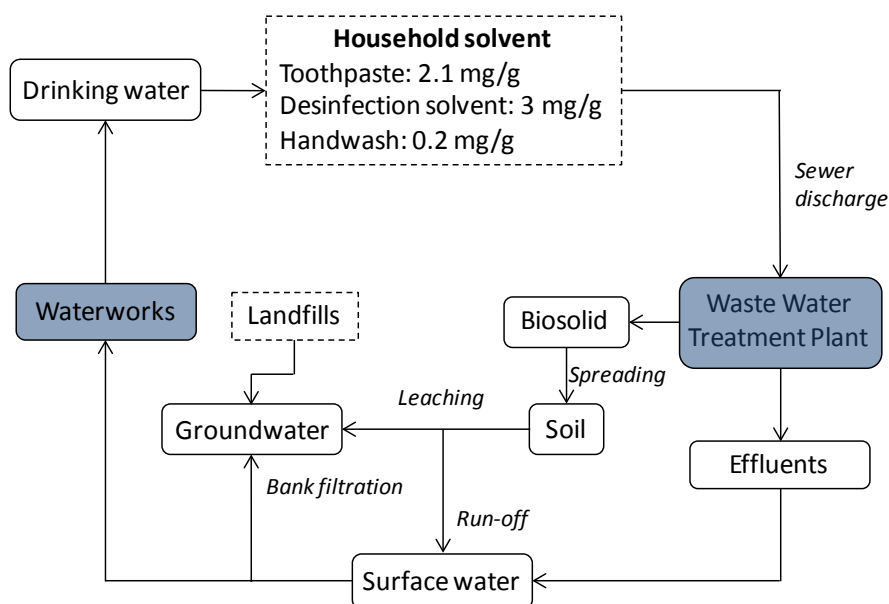
Figure 1.9. Life cycle of triclosan in the aquatic environment [104]

However, mass balance studies have demonstrated that triclosan also exhibits significant persistence, partitioning and sequestration in biosolids ($\log K_{OW}$~4.2; [99]). Approximately 50±19% of the incoming triclosan was observed to persist and become sequestered in biosolids in a typical WWTP comprising activated sludge treatment and anaerobic digestion [105]. Thus, the release of biocide into the environment includes the discharge of effluents into surface waters and the land application of digested sludge (**Table 1.4**).

1.3.3. Natural and synthetic hormone substances: estrone, 17β-estradiol and 17α-ethinylestradiol

Estrogens are a group of steroid compounds, named for their importance in the oestrus cycle, functioning as the primary female sex hormone. While estrogens are present in both men and women, they are usually presented at significant higher levels in women of reproductive age (**Table 1.5**). The natural estrogens, estrone (E1) and 17β-estradiol (E2), and the synthetic one, 17α-

ethinylestradiol (EE2), **Figure 1.10**, are the estrogens most commonly found in wastewater [106] while estriol (E3) is not usually detected in wastewaters [107].

Table 1.4. Environmental concentrations of triclosan

Environmental matrix		TCS Concentration	References
Surface water		1.4 ng/L-40000 ng/L	[97, 99, 101, 108-114]
Lake/river/streams with known input of raw wastewater			
Wastewater	Influent	20-86161 ng/L	[97, 98, 100, 101, 112, 115, 116]
	Effluent	23-5370 ng/L	[94, 96, 97, 103, 108, 112, 115, 117-119]
Sea water		<0.001-100 ng/L	[120, 121]
Sediment	Lake/River	<100-53000 µg/kg$_{d.w.}$	[122, 123]
	Marine	0.02-35 µg/kg$_{d.w.}$	[120]
Biosolid from WWTP		20-133000 µg/kg$_{d.w.}$	[94, 119, 123-126]
Activated/digested sludge		580-15600 µg/kg$_{d.w.}$	[100, 101, 115, 125]

d.w.: dry weight

Table 1.5. Daily excretion (µg) of estrogenic steroids in humans [127]

Category	Estrone	17β-Estradiol	Estriol	17α-Ethinylestradiol
Males	3.9	1.6	1.5	-
Menstruating females	8.0	3.5	4.8	-
Manopausal females	4.0	2.3	1	-
Pregnant women	600	259	6000	-
Women	-	-	-	35
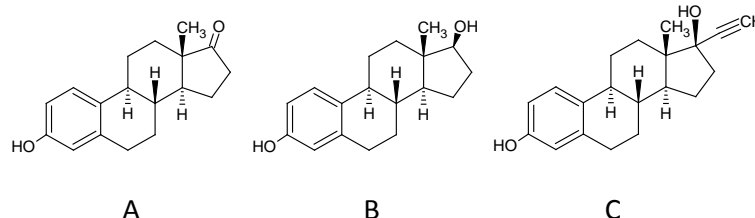
Figure 1.10. Molecular structure of (A) estrone, (B) 17β-estradiol and (C) 17α-ethinylestradiol

Estrone (E1)

Estrone, $C_{18}H_{22}O_2$, also known as oestrone (3-hydroxy-1,3,5(10)-estretrien-17-one) is a C-18 natural steroid hormone. Estrone is one of the naturally occurring estrogens, the others being estradiol and estriol. Estrone is produced primarily from androstenedione originating from the gonads or the adrenal cortex and from estradiol by 17-hydroxysteroid dehydrogenase. Androstenedione is also converted into estrone by aromatase (CYP19) to estrone and is expressed in stromal and carcinoma or parenchymal components of breast cancer tissue. Estrone concentrations in premenopausal mammals fluctuate according to the menstrual cycle. In premenopausal women, more than 50% of the estrone is secreted by the ovaries. In prepubertal children, men and nonsupplemented postmenopausal women the major portion of estrone is derived from peripheral tissue conversion of androstenedione. Interconversion of estrone and estradiol also occurs in peripheral tissue. In humans, during the follicular phase of the menstrual cycle estrone levels increase slightly. The production of estrone then increases markedly to peak at around day 13. The peak is of short duration and by day 16 the estrone levels will be low. A second peak occurs at around day 21 of the cycle and if fertilization does not occur, then the production of estrone decreases.

17β-estradiol (E2)

17β-estradiol, $C_{18}H_{24}O_2$, also known as estradiol and oestradiol, (17β)-estra-1,3,5(10)-triene-3,17-diol, is another natural steroid hormone. Like other steroids, E2 is derived from cholesterol, being androstenedione the key intermediary. Androstenedione is converted to testosterone and then to estradiol, by an alternative pathway, by the enzyme aromatase. In premenopausal women, estradiol is produced by granulose cells of the ovaries, smaller amounts of estradiol are also produced by the adrenal cortex, by the testes (in men) and fat cells are active precursors to estradiol, and will continue even after menopause.

17α-ethinylestradiol (EE2)

17α-ethinylestradiol, $C_{20}H_{24}O_2$, is the major endogenous estrogen in humans. It is a bioactive estrogen used in several formulations of combined oral contraconceptive pills. It was synthesized for the first time in 1938 by Hans Herloff Inhoffen and Walter Hohlweg [128]. It was approved by the FDA in the United States on 1943 and the FDA withdrew approval on 2004.

All humans as well as animals can excrete hormone steroids from their bodies, which end up in the environment through sewage discharge and animal waste disposal. Based on daily excretion of estrogens (**Table 1.5**), dilution factor and previous measurements, levels of estrogens in ng/l are expected to be present in aqueous environmental samples [127]. Those steroids have been detected in influents and effluents of sewage treatment plants and surface water [129-134]. As a consequence, the incomplete removal during wastewater treatment processes is considered the main source of estrogens in aquatic ecosystems (**Table 1.7**). It is clear that the three estrogens are not completely removed by WWTPs and they remain with fluctuating concentrations in effluent,

and discharge of such effluent may be the main reason for the wide occurrence of estrogens in surface waters, ground waters and even in drinking waters [49].

1.3.4. Physicochemical properties of EDCs

The physicochemical properties of BPA, TCS, E1, E2 and EE2 are shown in **Table 1.6.** Among these parameters, water solubility (S_w) and the octanol/water partition coefficient (K_{ow}) are key parameters on the fate of chemicals in the environment. In general, chemicals with logK_{ow} lower than 2.5 may be considered relatively hydrophilic, chemicals with 2.5<LogK_{OW}<4 yield medium sorption potential and chemicals with high K_{ow} values (greater than 4) have high sorption potential [135]. Therefore, TCS and EE2, which have high values of LogK_{ow} may be considered lipophilic substances. It can be observed that the natural estrogens, E1 and E2, are poorly soluble in water compared to the synthetic estrogen (EE2), BPA and TCS. All of them have low vapor pressures suggesting that volatilization is negligible. From the calculated carbon water coefficients (LogK_{oc}), adsorption to organic carbon is expected to be an important process resulting in the partitioning of the EDC onto soil and sediments.

Table 1.6. Physicochemical properties of EDCs [71, 119, 136]

EDC	M_w (g/mol)	S_w (mg/L)	Vapour pressure (Pa)	Sorption constant LogK_{oc}	LogK_{ow}
BPA	228.3	300±5	$5 \cdot 10^{-6}$	3.95	3.40
TCS	289.8	4.62	$6 \cdot 10^{-4}$	4.30	4.60
E1	270.4	1.30±0.08	$3 \cdot 10^{-8}$	3.67	3.43
E2	272.4	1.51±0.04	$3 \cdot 10^{-8}$	3.52	3.94
EE2	296.4	9.20±0.09	$6 \cdot 10^{-9}$	3.68	4.15

M_w: molecular weight; S_w: water solubility; K_{ow}: Octanol–water partition coefficient.

1.3.5. Post-treatments methods for the elimination of EDCs

Although conventional biological treatment processes have been reported effective at reducing levels of some EDCs in wastewater and sewage [137-140], the low levels of these contaminants in wastewater effluents are still a major concern for the receiving environment and downstream users because EDCs exert physiological effects at very low concentrations. A number of researchers have reported that conventional wastewater treatment efficiencies for degrading EDCs vary significantly throughout the year and that some EDCs are always present in effluent samples taken (**Table 1.7**).

Therefore, post-treatments methods for removal of these compounds are being investigated: (i) physical methods such as adsorption [141] or membrane separation [142]; (ii) chemical treatments, such as those based on oxidative catalysis [143], chlorination [144], ozonation [145] and other advanced oxidation processes (AOPs); (iii) microbial degradation with bacteria [145, 146] and fungi [147] and (iv) enzymatic treatment based on peroxidases [148].

Table 1.7. Occurrence and fate of EDCs in wastewater treatment plants

EDC	Influent (ng/L)	Effluent (ng/L)	Removal (%)	Reference
BPA	332–339	13–36	90 (mean)	[149]
	250–5620	< 43–4090	92 (mean)	[150]
	720–2376	16–1840	10–99	[151])
	281–3642	6–50	90–98	[152]
TCS	13,700–86,200	180–5,370	94 (mean)	[115]
	245	171	30 (mean)	[153]
	3,440	190	94 (mean)	[117]
	142–214	22.5–151	51 (mean)	[154]
	250–1,000	70–270	73 (mean)	[155]
	380	180	53 (mean)	[156]
	4,800–7,300	10–620	95 (mean)	[95]
	728	74–104	71 (mean)	[157]
	312	28	91 (mean)	[158]
	423–1,140	141–178	80 (mean)	[159]
	231–7,560	85–712	79 (mean)	[160]
	500–1,300	70–650	60 (mean)	[97]
	445	76	83 (mean)	[161]
	7,500–21,900	340–1,100	95 (mean)	[154]
E1	25–132	2.5–82	− 22 to 95	[129]
	44	17	61	[162]
	29–670	n.d.–72	− 111 to 100	[151]
	19–78	1–96	− 55 to 98	[163])
	20–130	< 0.3–11	n.a.	[150])
	57.8–83.3	6.3–49.1	41–89	[164]
	4–33	0–147	n.a.	[165]
E2	4.0–25	0.35–3.5	59–98	[129]
	11	1.6	85 (mean)	[162]
	35–125	n.d. –30	44–100	[151]
	2.4–26	0.2–14.7	− 18.5 to 98.8	[163]
	17–150	< 0.8	n.a.	[150]
	22.0	0.95	96	[166]
	0–11	0–158	n.a.	[165]
EE2	0.40–13	n.d. –1.7	52–100	[129]
	4.9–7.1	2.7–4.5	33–45	[167]
	< 0.3–5.9	< 0.3–2.6	n.a.	[150]
	3–70	n.d. –5	33.3–100	[151]
	< 0.7–14.4	< 0.7–4.1	71–93	[152]

n.d.: not detected; n.a.: n.a.

1.3.5.1. Elimination of EDCs using AOPs

The term advanced oxidation processes (AOPs) refers to processes in which the oxidation of organic contaminants occurs primarily through reactions with hydroxyl radicals ($\cdot$OH, standard redox potential (E^0) = 2.80 V) [168]. AOPs typically involve two stages: i) the formation of $\cdot$OH and ii) the reaction of these oxidants with organic contaminants in water. AOPs are considered a highly competitive technology for the removal of organic pollutants which, due to their high chemical stability and/or low biodegradability, are not successfully removed by conventional techniques [169]. The most common advanced oxidation processes are listed below:

- Photolysis: consists of the splitting or decomposition of a chemical compound by means of light energy or photons.

- Heterogeneous photocatalysis: it relies on the capacity of semiconducting materials to act as sensitizers for light-reduced redox processes due to their electronic structure. Photocatalysts include titanium dioxide (TiO_2), zinc oxide (ZnO), zinc sulfide (ZnS), ferric oxide (Fe_2O_3), silicon (Si), tin oxide (SnO_2), and cadmium sulfide (CdS), among others. TiO_2 has been the most widely cited photocatalyst in literature due to its properties: considerable activity, high stability, non-environmental impact and low cost [170].

- Strong oxidizers: it is based on the utilization of compounds with high redox potential such as ferrate (FeO_4^{2-}, E^0 = 2.20 V), ozone (O_3, E^0 = 2.08 V), hypochlorous acid (HOCl, E^0 = 1.48 V) and/or chlorine dioxide (ClO_2, E^0 = 1.46 V) and manganese oxide (MnO_2, E^0 = 1.23 V).

- Combination of UV and strong oxidizers: in order to enhance the removal of organic compounds from water, UV radiation with different oxidizers

has been studied, where the most common oxidizer is the hydrogen peroxide (H_2O_2, E^0 = 1.78 V).

- Sonolysis: it consists on the irradiation of ultrasound waves at low to medium frequency (20-1000 kHz) into a liquid medium. The high acoustic energy generates physical and chemical reactions, which result from the creation and collapse of cavitation bubbles. Theory describes pyrolysis in the cavitation bubbles and generation of ·OH radicals via the thermolysis of water molecules. These are reported to be the main reaction mechanisms responsible for the degradation of organic compounds in aqueous solutions [171].

As shown in **Figure 1.11**, the most documented degradation process for the treatment of EDCs is photodegradation, followed by the use of strong oxidizers (chlorination, ferrate and $MnSO_4$), ozonation and heterogeneous photocatalysis. Chlorination and ozonation of EDCs showed the fastest degradation kinetics followed by sonolysis, photocatalytic oxidation and finally photolysis.

In **Table 1.8**, a summary of the different AOPs applied for the removal of EDCs is displayed. In general, advanced oxidation processes have high degradation rate but they have low selectivity and high cost [172]). Moreover, it must be pointed out that under certain circumstances, AOPs can be a cause of concern themselves. These processes may render harmful by-products or transformation products due to their reactivity with water matrix components or micropollutants, which can have a similar or increased estrogenicity relative to the parent compound [173-179]. On this basis, the disappearance of the original compound does not necessarily imply that the treatment is efficient.
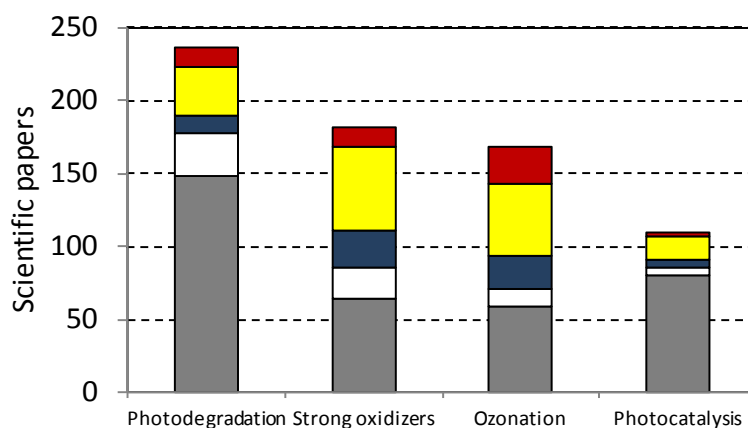
Figure 1.11. Scientific papers related to the application of AOPs for the removal of EDCs (ISI Web of knowledge; Years 1998 to 2011). BPA (grey), TCS (white), E1 (blue), E2 (yellow) and EE2 (red).

1.3.5.2. Elimination of EDCs by white rot fungi (WRF) and their lignin modifying enzymes (LMEs)

An environmentally friendly alternative for the elimination of EDCs may be the use of microorganisms. Among the different possible microorganisms, white rot fungi appear to be a good choice since they have been reported to degrade a wide range of organic pollutants [180]. Several authors have demonstrated the ability of different WRF not only to eliminate EDCs but also to reduce their estrogenic activity (**Table 1.9**).

The main drawback of using white rot fungi for the degradation of organic pollutants is the necessity of working in aseptic conditions and, consequently, the development of this alternative is costly and problematical. The capability of this fungal class to remove pollutants usually is related to the production and secretion of lignin modifying enzymes. Several works have demonstrated that the use of LMEs is a good environmental tool for the elimination of organic pollutants [181] and also EDCs (**Table 1.10).**

Table 1.8. Examples of results from different AOPs applied to degrade EDCs

Treatment method	EDC	Concentration	Removal (%)	Reference
Photodegradation	BPA	20 mg/L	100	[182]
	TCS	24.1 µM	H-L*: 23 h	[183]
	E1	3-20 mg/L	95 (60 min)	[184]
	E2	3-20 mg/L	60 (60 min)	
	EE2	0.5 µM	63 (60 min)	[185]
Photocatalysis (TiO$_2$)	BPA	10 mg/L	100	[186]
	TCS	31.0 µM	H-L: 70 min	[187]
	E1	10 µg/L	50-100 (7-60 min)	[188]
	E2	10 mg/L	H-L: 2.8 min	[143]
	EE2	10 mg/L	H-L: 2.4 min	
Ozonation	BPA	1–10 mg/L	100	[189]
	TCS	1.0 µM	H-L: 0.9 ms	[190]
	E1	5-15 mg/L	>80 (18 min)	[191]
	E2	400 µM	100 (55 min)	[192]
	EE2	8.4-67.6 µmol/L	76.3-100 (5-35 min)	[193]
Chlorination	BPA	1 mg/L	>90 (5 min)	[194]
	TCS	2.5-27.6 µM	H-L: 12 s	[195]
	E1	1 µM	H-L: 6.3 min	[144]
	E2	50 µg/L	100 (10 min)	[196]
	EE2	1 µM	H-L: 7.3 min	[144]
Chlorination and ozonation	E2	0.10 µM	75-99	[145]
	EE2	0.10 µM	75-99	

Table 1.8. Examples of results from different AOPs applied to degrade EDCs
(*cont.*)

Treatment method		EDC	Concentration	Removal (%)	Reference
Strong oxidizers	Ferrate (IV)	BPA	10 µmol/L	40 (4 min)	[197]
		TCS	3 µmol/L	83 (90 s)	[198]
		E1	10 µmol/L	>90 (4 min)	[197]
		E2	10 µmol/L	>90 (4 min)	
		EE2	10 µmol/L	>90 (4 min)	
	MnO$_2$	BPA	4.4 µM	99	[199]
		TCS	10 µmol/L	90 (96 min)	[200]
		E1	4 µM	100 (4 h)	[201]
		E2	3.7 µmol/L	70-90 (0.25-8 h)	[202]
		EE2	4 µM	90 (4 h)	[201]
	TiO$_2$	BPA	1 mg/L	99	[203]
	Fenton's reagent	BPA	22 nM	55	[204]
Combination of UV and strong oxidizer	UV and H$_2$O$_2$	E2	10 nmol/L	100	[205]
		EE2	10 nmol/L	100	
	UV/H$_2$O$_2$/Fe^{2+}	BPA	10 mg/L	>90	[206]
			700 µM	82	[207]
Sonolysis		BPA	500 µM	100	[208]
		TCS	10 µg/L	80-90 (40-60 min)	[209]
		E1	10 µg/L	90 (27 min)	[210]
		E2	10 µg/L	85 (27 min)	
		EE2	10 µg/L	80 (27 min)	

*H-L:half-life

The economic evaluation of the use of LMEs has been performed by Lopez et al. (2011) [211], who demonstrated that the enzymatic process based

on free peroxidase is economically competitive compared to photolysis, ozonolysis and Fenton processes.

Among the different enzymes, laccase is the most documented oxidative enzyme considered for the elimination of EDCs as shown in **Figure 1.12**. The main advantage related to the use of this enzyme over other oxidases and peroxidases is its availability (e.g. DeniLite®, the commercial laccase preparation from Novozymes, Denmark) due to the scale-up of its production. However, one of its major disadvantages is that the redox potential of laccase is low (0.5 - 0.8 V) when compared with other ligninolytic enzymes such as peroxidases, 1.45-1.51 [17] and it typically requires chemical mediators acting as the real oxidants, participating in the catalytic cycle of the enzyme [212, 213]. Most of these mediators are environmentally unsafe (HBT, for example) and may have an important economical impact on the treatment.
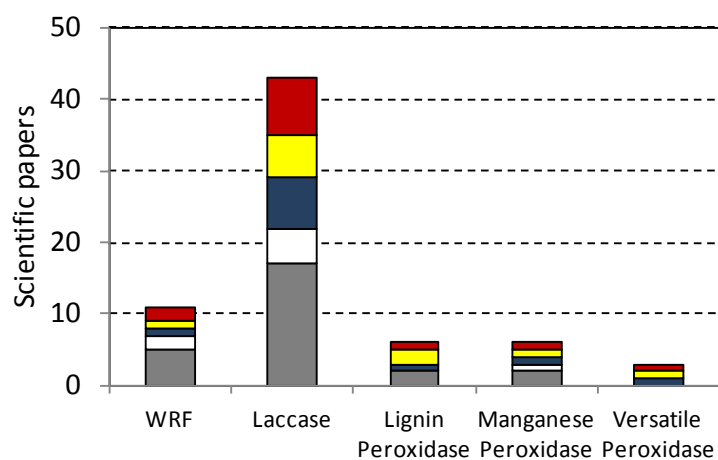
Figure 1.12. Impact of the *in vivo* and *in vitro* WRF processes in the elimination of EDCs from 1998 to 2011 (ISI Web of knowledge). BPA (grey), TCS (white), E1 (blue), E2 (yellow) and EE2 (red).

Table 1.9. Elimination of EDCs and reduction of estrogenicity by WRF

EDC	Fungus	Concentration	Removal (%)	Estrogenic activity reduction (%)	Reference
BPA	*Stropharia coronilla*	25 mg/L	---	100	[214]
	Stropharia rugosoannulata	25 mg/L	---	100	
	GM *Irpex lacteus*	100 mg/L	50 (3 d)	60	[215]
	Irpex lacteus	10 mg/L	>90 (14 d)	98 (14 d)	[147]
	Bjerkandera adusta	10 mg/L	75 (14 d)	90 (14 d)	
	Phanerochaete chrysosporium	10 mg/L	0 (14 d)	42 (14 d)	
	Phanerochaete magnoliae	10 mg/L	>90 (14 d)	85 (14 d)	
	Pleurotus ostreatus	10 mg/L	>90 (14 d)	100 (14 d)	
	Trametes versicolor	10 mg/L	>90 (14 d)	100 (14 d)	
	Pycnoporus cinnabarinus	10 mg/L	>90 (14 d)	85 (14 d)	
	Dichomitus squalens	10 mg/L	>90 (14 d)	86 (14 d)	
	Stereum hirsutum	200 mg/L	100 (14 d)	n.a.	[216]
	Heterobasidium Insulare	200 mg/L	100 (14 d)	n.a.	
	Pleurotus ostreatus	400 µM	80 (12 d)	n.a.	[217]
TCS	*Irpex lacteus*	10 mg/L	99 (14 d)	98 (14 d)	[147]
	Bjerkandera adusta	10 mg/L	0 (14 d)	22 (14 d)	
	Phanerochaete chrysosporium	10 mg/L	91 (14 d)	98 (14 d)	
	Phanerochaete magnoliae	10 mg/L	88 (14d)	98 (14 d)	
	Pleurotus ostreatus	10 mg/L	99 (14 d)	98 (14 d)	

EDC	Fungus	Concentration	Removal (%)	Estrogenic activity reduction (%)	Reference
	Trametes versicolor	10 mg/L	91 (14 d)	98 (14 d)	
	Pycnoporus cinnabarinus	10 mg/L	99 (14 d)	99 (14 d)	
	Dichomitus squalens	10 mg/L	99 (14 d)	98 (14 d)	
	Trametes versicolor	0.25 mM	60-90 (1-4 weeks)	n.a.	[218]
E1	*Phanerochaete sordida*	10 µmol/L	70-100 (3-6 d)	n.a.	[219]
E2	*Trametes versicolor*	10 mg/L	98	n.a.	[220]
	Ganoderma	10 mg/L	98	n.a.	
EE2	*Trametes versicolor*	10 mg/L	95	n.a.	[220]
	Ganoderma	10 mg/L	95	n.a.	
	Irpex lacteus	10 mg/L	100 (14 d)	72 (14 d)	[147]
	Bjerkandera adusta	10 mg/L	100 (14 d)	62 (14 d)	
	Phanerochaete chrysosporium	10 mg/L	63 (14 d)	15 (14 d)	
	Phanerochaete magnoliae	10 mg/L	13 (14 d)	0 (14 d)	
	Pleurotus ostreatus	10 mg/L	100 (14 d)	62 (14 d)	
	Trametes versicolor	10 mg/L	100 (14 d)	94 (14 d)	
	Pycnoporus cinnabarinus	10 mg/L	100 (14 d)	86 (14 d)	
	Dichomitus squalens	10 mg/L	100 (14 d)	78 (14 d)	

n.a.: not available

Table 1.10. Elimination of EDCs and reduction of estrogenicity by LMEs

LME	EDC	Fungus	Concentration	Removal (%)	Estrogenic activity reduction (%)	
Laccase	BPA	*Ganoderma lucidum*	2-20 mg/L	99-88.5	n.a.	[221]
		Trametes versicolor	1000 µM	100 (90 min)	n.a.	[222]
			50 µM	100 (20 min)	n.a.	[22]
			220 µM	50-70 (30-60 min)	40-60 (1-6 h)	[223]
		Trametes villosa	2.2 µM	100 (3 h)	n.a.	[224-226]
		Strain I-4 isolated from Japanese soil	5 mM	95-100 (1-3 h)	100 (24 h)	[227, 228]
		Coriolopsis polyzona	100 mg/L	45 (250 min)	n.a.	[229]
			5 mg/L	40-100 (1-4 h)	35-95 (1-4 h)	[230]
		Coriolus versicolor	100 µM	100 (1 h)	n.a.	[231]
			3 µmol/g$_{soil}$	80-100 (5 d)	n.a.	[232]
		Pycnoporus coccineus	3 µmol/g$_{soil}$	15 (5 h)		[233]
		Trametes sp.	200 µM	95-100 (1-3 h)	n.a.	[234]
			3 µmol/g$_{soil}$	90-100 (2-8 h)	n.a.	[233]
	TCS	*Cerrena unicolor*	50 µM	60 (120 min)	n.a.	[235]
		Trametes versicolor	5 mg/L	60 (6 h)	n.a.	[236]
		Trametes versicolor	100 µM	66 (90 min)	n.a.	[237]
		Ganoderma lucidum	2 mM	85	n.a.	[238]

LME	EDC	Fungus	Concentration	Removal (%)	Estrogenic activity reduction (%)	
		Coriolopsis polyzona	100 mg/L	55 (250 min)	n.a.	[229]
	E1	*Trametes* sp. Ha1	120-340 µM	62-100 (1 h)	n.a.	[239]
		Trametes versicolor	0.0004 µM	100 (1 h)	n.a.	[27]
		Myceliophthora thermophila	5 mg/L	100 (8 h)	n.a.	[213]
		Pycnoporus coccineus	3 µmol/g soil	20-60 (1-3 d)	n.a.	[232]
	E2	*Trametes* sp. Ha1	90-720 µM	93-100 (1 h)	n.a.	[239]
		Trametes versicolor	0.0004 µM	100 (1 h)	n.a.	[26]
		Myceliophthora thermophila	5 mg/L	100 (30 min)	n.a.	[213]
	EE2	*Trametes* sp. Ha1	110-990 µM	85-100 (1 h)	n.a.	[239]
		Trametes versicolor	0.0004 µM	100 (1 h)	n.a.	[26]
		Purchased from Sigma-Aldrich	5 mg/L	100 (30 min)	n.a.	[213]
		Pycnoporus coccineus	3 µmol/g_{soil}	40-80 (5-48 h)	n.a.	[232]
		Trametes sp.	3 µmol/g_{soil}	60-80 (4-8 h)	n.a.	[233]
LiP	BPA	*Phanerochaete sordida*	100 µM	>95 (24 h)	n.a.	[240]
		Phanerochaete chrysosporium	100 µM	52.5 (24 h)	n.a.	
			100 µM	40-50 (30-120 min)		[241]
	E1	*Phanerochaete sordida*	100 µM	60 (24 h)	100 (24 h)	[240]

Removal of EDCs by the ligninolytic enzyme Versatile Peroxidase

LME	EDC	Fungus	Concentration	Removal (%)	Estrogenic activity reduction (%)	
	E2	*Phanerochaete chrysosporium*	100 µM	25 (24 h)	>100 (24 h)	
		Phanerochaete sordida	100 µM	90 (24 h)	70 (24 h)	
	EE2	*Phanerochaete chrysosporium*	100 µM	38 (24 h)	>100 (24 h)	
		Purchased from Sigma-aldrich	19 µM	100 (20 min)	n.a.	[242]
		Phanerochaete sordida	100 µM	85 (24 h)	80 (24 h)	[240]
MnP	BPA	*Phanerochaete chrysosporium*	220 µM	90-100 (30-60 min)	40-90 (4-6 h)	[223]
		Pleurotus ostreatus	400 µM	100 (1 h)	n.a.	[217]
	TCS	*Trametes versicolor*	5 mg/L	100 (90 min)	n.a.	[237]
	E1	*Phanerochaete sordida*	10 µM	100 (1 h)	99-100 (1-2 h)	[243]
	E2	*Phanerochaete chrysosporium*	10 µM	100 (1 h)	80-100 (1-4 h)	[244]
VP	E1	*Bjerkandera adusta*	2.5 mg/L	100 (10 min)	n.a.	[148]
	E2			100 (5 min)		
	EE2			100 (10 min)		

n.a.: not available

1.4. Conclusions

The search of new technologies suitable for the treatment of wastewater containing EDCs is a challenge because, existing traditional WWTPs are not able to eliminate them completely. Even at concentrations of ng/L, EDCs have an impact in the endocrine system of the fauna producing morphological deformities, reduced overall growth, reduced sperm quality and delayed ovulation, reduced numbers of mature spermatozoa, sex reversal male to female among others.

Efforts have been put in the study of different post-treatments to remove the residual concentration of EDCs present in WWTP effluents. The most frequently used technologies for the removal of EDCs are advanced oxidation processes such as photocatalysis, photodegradation, sonolysis, ozonolysis, etc. In general, these processes have high degradation rate but they have low selectivity and high costs. In addition, AOPs can be a cause of concern itself since they may render harmful by-products or transformation products which can have similar or increased estrogenicity of that of the parent compound.

A biological alternative may be use of WRF or their LMEs to treat wastewater containing EDCs. From an operational point of view, the use of LMEs in *in vitro* systems, compared to the use of WRF in *in vivo* systems, is easier and cheaper since no aseptic conditions are needed. Among the LMEs, laccase is the most extensively studied enzyme for the degradation of BPA, TCS, E1, E2 and EE2 whereas peroxidases (LiP, MnP and VP) have not been studied in depth. Nevertheless, peroxidases have higher redox potential and consequently they are expected to provide better results of EDC removal (in terms of yield and degradation rate). In this PhD Thesis, the ability of the enzyme versatile peroxidase to eliminate the endocrine disrupting chemicals: BPA, TCS E1, E2 and EE2 will be studied.

Chapter 2

Materials and methods

Chapter 2. Materials and methods

2.1. Enzymatic and analytical methods

2.2. Determination of the concentrations of bisphenol A, triclosan, estrone, 17β-estradiol and 17α-ethinylestradiol by High Performance Liquid Chromatography

2.3. Determination of the concentrations of bisphenol A, triclosan, estrone, 17β-estradiol and 17α-ethinylestradiol by Gas Chromatography-Mass Spectrometry

2.4. Determination of the estrogenic activity by LYES

Chapter 2. Materials and methods

2.1. Enzymatic and analytical methods

Laccase activity was determined by measuring the oxidation of 5 mM 2,2'-azino-bis (3-ethylbenzothiazoline-6-sulfonic acid) (ABTS) in 100 mM sodium acetate buffer, pH 5 (ε_{436} = 29.3 mM^{-1} cm^{-1}) [245].

Mn-oxidizing peroxidase (MnP) activity was estimated by the formation of Mn^{3+}-tartrate complexes (ε_{238} = 6.5 mM^{-1} cm^{-1}) during the oxidation of 0.1 mM MnSO$_4$ in 100 mM tartrate buffer (pH 5) in the presence of 0.1 mM H$_2$O$_2$ [246], or by the oxidation of 1 mM 2,6-dimethoxyphenol (DMP) to coerulignone in 50 mM malonate buffer (pH 4.5), 1 mM MnSO$_4$ and 0.4 mM H$_2$O$_2$ [247]. The extinction coefficients at 468 nm (ε_{468}) were 27.5 mM^{-1} cm^{-1} referred to substrate concentration or 49.6 mM^{-1} cm^{-1} referred to product concentration.

Mn-independent oxidation of phenolic and non-phenolic compounds was estimated against 0.1 mM 2,6-dimethoxyphenol as described above and also against 2 mM veratryl alcohol, respectively. The veratryl alcohol oxidation was obtained by the formation of veratraldehyde in 100 mM sodium tartrate (pH 3) in the presence of 0.1 mM H$_2$O$_2$ [246]. The extinction coefficient considered (ε_{310}) was 9.3 mM^{-1} cm^{-1}. LiP activity was determined as the veratryl alcohol oxidation described above with the addition of 0.4 mM H$_2$O$_2$ [39].

All enzymatic activities were expressed as international units (U), defined as the amount of enzyme that transforms 1 μmol substrate/min or the amount of enzyme that releases 1 μmol product/min at 30ºC.

Protein concentration was determined by the method of Bradford [248] and reducing sugars by the method of Somogyi [249], using albumin and D-glucose as standards, respectively.

The total phenolic content was analyzed according to the Folin-Ciocalteau method [250]. Diluted samples (10 μL) were added to distilled water

(40 µL) followed by Folin-Ciocalteau reagent (25 µL). After 3 min, sodium carbonate (125 µL, 20% w/v) was added. Samples were left in the dark for 30 min before absorbance was measured at 725 nm (Powerwave XS, BioTek, Bad Friedrichshall, Germany). Results were expressed in terms of g of cathechol (CE)/L.

Total organic carbon (TOC) was measured in a Carbon Analyzer, Shimadzu TOC-5000. Total nitrogen (TN) was measured in an Organic Nitrogen Analyzer, Dohrmann Rosemount DN-1900.

The production of Mn^{3+}-chelate was determined spectrophotometrically in a 1 mL quartz cell in a Shimadzu UV-vis 160A spectrophotometer. The concentration of Mn^{3+}-chelate was determined using extinction coefficients of $\varepsilon_{238} = 6.5$ $mM^{-1}cm^{-1}$, $\varepsilon_{270} = 11.59$ $mM^{-1}cm^{-1}$, $\varepsilon_{290} = 5.89$ $mM^{-1}cm^{-1}$ and $\varepsilon_{270} = 5.6$ $mM^{-1}cm^{-1}$ for Mn^{3+} tartrate, malonate, lactate and oxalate, respectively [246, 251, 252].

2.2. Determination of the concentrations of bisphenol A, triclosan, estrone, 17β-estradiol and 17α-ethinylestradiol by High Performance Liquid Chromatography

Bisphenol A and Triclosan were quantified at a detection wavelength of 278 nm on a HP 1090 HPLC equipped with a diode array detector and a Lichrosphere100 C18 reversed-phase column (250 x 4.6 mm, particle size: 5 µm; LiChrocart, Merck) and an HP ChemStation data processor. Gradient elution started with 10% methanol in water, which was kept for 1 min, followed by an increase to 90% methanol within 4 min. This concentration was kept constant for 4 min, then linearly decreased back to 10% methanol in 1 min and kept constant for another 5 min. Flow rate was 1 mL/min, temperature 40ºC and the method was calibrated using external methanol standards.

The determination of E1, E2 and EE2 concentrations was also made by HPLC monitoring the absorbance at 220 nm. The injection volume was set at 200 µL, and the isocratic eluent (acetonitrile:50 mM phosphate, 60:40; pH 4.5) was pumped in at 0.8 mL/min.

2.4. Determination of the concentrations of bisphenol A, triclosan, estrone, 17β-estradiol and 17α-ethinylestradiol by Gas Chromatography-Mass Spectrometry

Concentration of BPA, TCS, E1, E2 and EE2 were measured by Gas Chromatography-Mass Spectrometry (GC-MS) (Saturn 2100T, Varian, USA). After agitation with acetonitrile (50% v/v), samples were extracted by solid phase extraction (SPE) with 60 mg OASIS HLB catridges (Water closet, Milford, MA, USA) previously supplemented with 3 mL of ethyl acetate, 3 mL of methanol and 3 mL of distilled water. The cartridges were dried with a nitrogen stream for 45 min and eluted with 3 mL of ethyl acetate. Finally, MTBSTFA (N-methyl-N-(tert-butyldimethylsilyl)-trifluoroacetamide) was added for derivatization of the compounds. **Table 2.1** summarizes the operational conditions and the detection/quantification limits for each compound.

Table 2.1. Operational conditions for the determination and quantification of EDCs by GC-MS.

Chromatographic parameters	
Split-splitless injector	
Column	CP Sil 8 CB-MS low bleed (30 m x 0.25 mm x 0.25 µm)
Splitless time	2 min
Injection temperature	280ºC
Gas flow (He)	1 mL/min
Injector (volume)	1 µL
Solvent	Ethyl acetate

Table 2.1. Operational conditions for the determination and quantification of EDCs by GC-MS (*cont.*)

Temperature program

Initial temperature	70ºC
Initial time	2 min
1st ramp	25ºC/min
Temperature 1	150ºC
2nd ramp	3ºC/min
Temperature 2	200ºC
3rd ramp	8ºC/min
Temperature 3	280ºC
Time 3	5 min

Mass Spectrometry

Ionization mode	Electronic impact
Filament current	10 µA
Ion ramp temperature	220ºC
Transference line temperature	280ºC
Voltage	1700 – 1750 V
Scan velocity	1s/scan
Mass spectrum	50-550 m/z
Quantification ion (m/z) / retention time (min)	
BPA	358, 207, 191, 73 / 26.09
TCS	349, 347, 345, 200 / 24.54
E1	218, 257, 343 / 31.54
E2	285, 326, 417 / 31.86
EE2	285, 368 / 32.43

Quantification limit

BPA	2.5 µg/L
TCS	5.0 µg/L
E1, E2	10 µg/L
EE2	40 µg/L

2.4. Determination of the estrogenic activity by LYES

The LYES (yeast estrogen screen-assay assisted by enzymatic digestion with lyticase) assay protocol was adapted from Schultis and Metzger (2004) [253]. The recombinant yeast *Saccharomyces cerevisiae* was kindly provided by the Laboratory of Microbial Ecology and Technology (Labmet, Ghent University, Belgium). Yeast cultures, pre-incubated for 48 h, were resuspended in fresh yeast-peptone-dextrose medium (yeast extract 10 g/L, casein peptone 20 g/L, dextrose 20 g/L in double-distilled water). Standards and samples from HPLC measurements (10 µL) were pipetted in a 96-well microtiter plate and evaporated for 30 min. Methanol (50% v/v) in double-distilled water was used as control. Each well was inoculated with 90 µL of yeast suspension. The plate was sealed with parafilm and incubated at 37ºC. After 24 h, 40 µL of a lyticase solution, 1 g/L (Sigma) diluted in Z-buffer, (10 x; 60 mM $Na_2HPO_4 \cdot 7\ H_2O$, 40 mM NaCl, 1 mM $MgSO_4 \cdot 7H_2O$, 50 mM 2-mercaptoethanol) were added. After 45 min of incubation at room temperature, 35 µL of Tween 80 (0.1% v/v; Merck) were added. After another 20 min of incubation (room temperature), 25 µL of a stock solution of chlorophenol red galactopyranoside (Sigma) at 1 g/L were added. Finally, absorbance at 550 nm and 630 nm were measured after 2 h. The estrogenic activity was calculated as shown in **equation [2.1],** where *x* is sample and *blk* is control:

$$Response = \left(Abs_{550nm}^{x} - Abs_{550nm}^{blk}\right) - \left(Abs_{630nm}^{x} - Abs_{630nm}^{blk}\right) \qquad \textbf{[2.1]}$$

Chapter 3

A new strain of Bjerkandera sp. Production, purification and characterization of versatile peroxidase

Chapter 3. A new strain of *Bjerkandera* sp. Production, purification and characterization of versatile peroxidase

3.1. Introduction

3.2. Materials and methods

    3.2.1. Identification of the fungus by sequencing the ITS region

    3.2.2. Fungal strain and culture conditions

    3.2.3. Preparation of the fungal inoculum

    3.2.4. Production profile of lignin modifying enzymes

    3.2.5. Purification of the enzymatic crude

    3.2.6. Gel electrophoresis and isoelectric focusing

    3.2.7. Amino acid composition and sequencing

    3.2.8. Kinetic studies and effects of pH and temperature

3.3. Results and discussion

    3.3.1. Identification of the fungus

    3.3.2. Production of lignin modifying enzymes in Erlenmeyer flasks

    3.3.3. Scale-up of the production of lignin modifying enzymes

    3.3.4. Effects of pH and temperature on the stability of the enzymatic crude

    3.3.5. Catalytic properties of the enzymatic crude

    3.3.6. Purification of the isoenzymes secreted by the new strain

    3.3.7. Physico-chemical properties of the isoenzymes

    3.3.8. Catalytic properties of the four purified isoenzymes

3.4. Conclusions

Chapter 3. A new strain of *Bjerkandera* sp. Production, purification and characterization of versatile peroxidase

3.1 Introduction

The degradation of recalcitrant compounds introduced by mankind in the environment implies an important ecological challenge as these compounds have complex structure and low bioavailability. Conventional physicochemical or biological treatment plants are only able to fulfil partial degradation while advanced oxidation processes such as UV exposure or ozonation render variable yields of degradation. A biological alternative may be based on the use of certain fungal strains, known as white rot fungi as this type of microorganisms have been reported to degrade a wide range of organic compounds such as dyes [17], polycyclic aromatic compounds [7], pharmaceutical and personal care products [15] etc. This ability is attributed to lignin modifying enzymes (LMEs) synthesized during secondary metabolism in response to nutrient limitation. Two ligninolytic peroxidases: lignin peroxidase (LiP) [39] and manganese peroxidase (MnP) [40], were described in *Phanerochaete chrysosporium* and reported in other white-rot fungi from the group of basidiomycetes [254, 255]. In addition, some fungi contain another lignin-degrading enzyme, versatile peroxidase (VP), also known as hybrid Mn-peroxidase, which combines properties of LiP that enables the Mn-independent oxidation of non-phenolic aromatic compounds, MnP for the oxidation of Mn^{2+} and plant peroxidases to carry out the oxidation of hydroquinones and substituted phenols [45, 256],

The manganese peroxidase component catalyzes the oxidation of Mn^{2+} to Mn^{3+} by H_2O_2 according to the **equation [3.1]**. The highly reactive Mn^{3+} is stabilized via chelation in the presence of dicarboxylic acid:

$$2\,Mn^{2+} +\, H_2O_2 \xrightarrow{MnP} 2\,Mn^{3+} + H_2O + \frac{1}{2}\,O_2 \qquad \textbf{[3.1]}$$
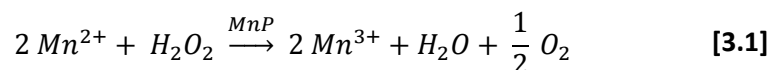
The lignin peroxidase enzyme catalyzes the oxidation of non-phenolic aromatic rings into aryl cation radicals by H_2O_2. Aryl cation radicals are unstable and undergo various subsequent reactions. A typical substrate is veratryl alcohol (3,4-dimethoxybenzyl alcohol), which is transformed into veratryl aldehyde (3,4-dimethoxybenzaldehyde) via the formation of veratryl cation and benzyl radicals, **equation [3.2]**:

$$Veratryl\ alcohol + H_2O_2 \xrightarrow{LiP} Veratraldehyde + H_2O\ + \frac{1}{2}\,O_2 \qquad \textbf{[3.2]}$$
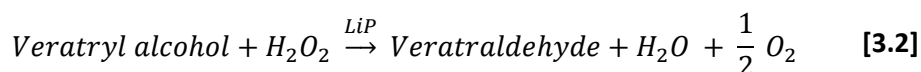
However, its catalytic cycle in the presence of Mn^{2+} is much higher than in the presence of other aromatic compounds [257].

LMEs are essential to lignin degradation and they are directly involved in the degradation of xenobiotic compounds [28, 233, 258-260]. In a previous work [261], the new fungal isolate, initially reported as *Antracophylum discolor*, showed high oxidative capability since it was able to degrade pentachlorophenol to an extent greater than well-known species such as *Phanerochaete chrysosporium*, *Lentinula edodes* and *Bjerkandera adusta* [262]. Even more, the new isolate presented higher capability for fungal growth on soils, which are particularly adverse conditions, completely different to those defined as the most favourable for fungal growth.

The possibility that this new isolate may be applied for a wide range of degradation conditions requires the comprehensive knowledge of the regulation mechanisms for LMEs production. This production depends on the nature and concentration of nitrogen and carbon sources, culture medium (including inducers and microelements) composition and environmental conditions.

The first aim of this work was to identify the new fungal strain. As a second objective, the significance of various nitrogen and carbon sources on the LMEs production was evaluated in order to produce the highest titres of LMEs. Finally, the purification and characterization of the different proteins secreted by the new fungal strain was performed.

3.2. Materials and methods

3.2.1 Identification of the fungus by sequencing the ITS region

For DNA extraction, five plugs of mycelium were inoculated into a 250 mL Erlenmeyer flask containing modified Kirk medium (**Table 3.2**) with glucose (10 g/L) and peptone (10 g/L). The cultures were incubated for 5 days at 25ºC in an orbital shaker. The mycelium was harvested by vacuum filtration, washed with sterile Milli-Q water and lyophilized. DNA was isolated as described elsewhere [263].

The genomic DNA was used as a template in PCR to amplify the ITS1 and ITS4 regions and the 5.8S rRNA gene. The primers used for the amplification were ITS1 (5'-TCCGTAGGTGAACCTGCGG-3') and ITS4 (5'-TCCTCCGCTTATTGATATGC-3') [264]. PCR was performed in 1 x PCR amplification buffer (Applied biosystems, CA, USA) with 1 mM MgCl$_2$ (Applied Biosystems), 1 µM of each primer, 50 µM of each deoxynucleoside triphosphate (Promega), 0.2 µg of DNA template, and 1.2 U of Taq DNA polymerase (Applied Biosystems), in a final volume of 50 µL, using a GeneAmp PCR System 2400 (PerkinElmer, NY, USA). Cycling parameters were 95ºC for 3 min followed by 35 cycles of 94ºC for 1 min, 52ºC for 40 s, and 72ºC for 1 min, and the final extension at 72ºC for 10 min. Control reactions lacking template DNA were performed in parallel. Amplified parameters were then sequenced using the two PCR primers, the BigDye Terminator v3.1 Cycle sequencing kit (Applied Biosystems), and the automated AI Prism 3730 DNA sequencer (Applied Biosystems). The sequence was compared by BLAST search [265] in GenBank.

3.2.2. Fungal strain and culture conditions

The new fungus, isolated from a Chilean forest in Temuco, was transferred from slant culture tubes (maintained at 4ºC and transferred every 12 months) to malt

extract agar plates and kept at 30ºC for 7 days before being used for inoculum preparation (**Table 3.1**).

Table 3.1. Composition of the main culture components (in g/L, unless otherwise indicated) in slant culture tubes, malt extract agar plates and Fernsbach flasks

	Slants	Plates	Fernsbach
Glucose	20	10	10
Agar	15	15	-
Peptone	5	-	5
Yeast extract	2	-	-
Malt extract	-	3.5	-
KH_2PO_4	1	-	2
$MgSO_4 \cdot 5H_2O$	0.5	-	0.5
$CaCl_2$	-	-	0.1
Mineral Salts*	-	-	10 mL/L
Thiamine	-	-	2 mg/L

*Tien and Kirk, 1988

3.2.3. Preparation of the fungal inoculum

The culture medium (**Table 3.1**) was inoculated with three malt agar plugs of mycelium in 100 mL Fernsbach flasks and it was incubated at 30ºC. After 7 days, Fernsbach fungal cultures were homogenized in a sterilized blender for 30 s and used as the inoculum.

3.2.4. Production profile of lignin modifying enzymes

Cultures were grown in the modified Kirk medium as shown in **Table 3.2**. Glucose, lactose and cheese whey were considered as three alternatives of carbon sources, whereas peptone and ammonium tartrate were evaluated as nitrogen sources. $MnSO_4$ (500 μM) and $CuSO_4$ (150 μM) were added to culture medium in order to stimulate peroxidase and laccase production, respectively.

All these experiments were performed in 250 mL Erlenmeyer flasks containing 90 mL of culture medium and inoculum (10% v/v) at 30^oC, 150 rpm and pH 4.5.

Table 3.2. Composition of the medium to produce lignin modifying enzymes

	Concentration
Carbon source	10 g/L*
Nitrogen source	0.5-10 g/L
Sodium acetate	2.72 g/L
KH_2PO_4	2 g/L
$CaCl_2$	100 mg/L
Mineral salts**	10 mL/L
Thiamine	2 mg/L
Tween 80	1 mL/L
$MnSO_4$	84.51 mg/L

*as reducing sugars
** Tien and Kirk (1988) [39]

Scale-up of the production

The production of LMEs was carried out at two different volumes: 1.5 L (Biostat®MD, Sartorius Stedim Biotech, Melsungen, Germany) and 20 L (Biostat® C-Plus, Sartorius Stedim Biotech, **Figure 3.1**). Experiments in the bioreactor with a final volume of 1.5 L were performed with a culture medium containing 10 g/L of glucose, 10 g/L of peptone, 1.25 mL/L Antifoam 204 (Sigma-Aldrich) and inoculum (10% v/v) at 30^oC, 150 rpm, pH 4.5 and 1.5 L/min of aeration (more details about medium composition in **Table 3.2**).

Experiments in the 20 L-bioreactor were performed with 25% (v/v) "straw water" medium containing 4 g/L of glucose, 1 g/L of peptone, 1.25 mL/L antifoam 204 and inoculum (10% v/v) at 30^oC, 150 rpm, pH 4.5 and air supply at 10 L/min. "Straw water" was produced by autoclaving straw with water (solid content of 74 g/L) at 121ºC during 20 min, and filtering the liquid after sterilization through Whatman No. 1 paper filters (Maidstone, United Kingdom).

Figure 3.1. Biostat C-Plus

3.2.5. Purification of the enzymatic crude

Purification was carried out from shaken cultures of the new fungus grown in modified Kirk medium containing 10 g /L glucose and 10 g/L peptone. After 6 d of incubation, the liquids were 45-fold concentrated by ultrafiltration (Filtron, 10 kDa-cut-off membrane) and dialyzed against 10 mM sodium tartrate (pH 5). The crude enzyme was loaded onto a Biorad Q-cartridge equilibrated with 10 mM sodium tartrate buffer at pH 5 (1 mL/min) and retained protein were eluted with a gradient of 0-0.25 M NaCl in the same buffer (60 min). Fractions with MnP activity were pooled separately, concentrated and 2 mL-samples applied onto a Sephacryl S-200 HR (Pharmacia K16/100) column equilibrated with the same buffer. Fractions with enzyme activity were pooled, concentrated in an AMICON ultrafiltration stirred cell (10 kDa) and dialyzed against 10 mM sodium tartrate

buffer at pH 5. The enzyme was applied to a Mono-Q anion-exchange-column (Pharmacia HR 5/5) using a linear gradient of 0-0.20 mM NaCl (20 min at 0.4 mL/min). The fractions that contained MnP activity were collected, concentrated, dialyzed and stored at -20ºC.

3.2.6. Gel electrophoresis and isoelectric focusing

SDS/PAGE was performed in 12% polyacrylamide gels. Isoelectric focusing (IEF) was performed in 5% polyacrylamide gels with a thickness of 1 mm and pH range of 2.5-10 (prepared with Biorad Ampholine, mixing 85% from pH 2.5-5 and 15% from 3.5-10) with 0.5 M H_3PO_4 and 0.5 M NaOH in anode and cathode sections, respectively. The pH gradient was measured on the gel by means of a contact electrode. Protein bands after SDS/PAGE and after IEF were stained with Coomasie Blue R-250 (Bio-Rad, NY, USA).

3.2.7. Amino acid composition and sequencing

The amino acid composition was determined with a Biochrom 20 autoanalyzer (Pharmacia, SW) after hydrolysis of 20 µg of protein with 6 M HCl at 110ºC for 24 h. N-terminal sequences were obtained by automated Edman degradation of 5 µg of protein in an Applied Biosystems (Perkin Elmer-model Procise™ 494).

3.2.8. Kinetic studies and effects of pH and temperature

The kinetic constants of the enzymatic crude was calculated for H_2O_2 (0-10 mM) and Mn^{2+} (0 – 10 mM), both estimated by the oxidation of DMP. The kinetic constants of MnP isoenzymes were calculated for H_2O_2 (estimated by the formation of Mn^{3+}-tartrate), Mn^{2+} (estimated as Mn^{3+}-tartrate) and 2,6-DMP by coerulignone formation). The kinetic constants of Mn-independent peroxidase activities were calculated for 2,6-DMP (estimated by coerulignone formation) and veratryl alcohol (estimated by veratraldehyde formation). All reactions were performed under the conditions described above.

The effect of temperature on the stability of the enzymatic crude was evaluated at a temperature range between 4 and 50ºC for 40 days. The effect of pH on the stability of the enzymatic crude and the isoenzymes, was examined in the pH range of 4-8 in 100 mM citrate-200 mM phosphate buffer by measuring the formation of Mn^{3+}-tartrate.

3.3 Results and discussion

3.3.1. Identification of the fungus

The sequences of the rDNA, including ITS1, 5.8S and ITS4, were identified as a suitable target for the analysis of fungal phylogeny (White et al. 1990). ITS is an ideal region to sequence for identification of species because they are easy to align. ITS region is variable among different fungal species and small DNA samples are used in the amplification process [266]. The amplified PCR products using the ITS1/ITS4 primers were size analyzed by agarose gel electrophoresis and were 604-bp in length. The nucleotide sequence (**Figure 3.2**) of the fungus showed 100% identity with ITS region of five unclassified basidiomycetes (accession numbers AF455417, AF455454, AM901877, AM930994, AM901992), one *Bjerkandera fumosa* (accession number AJ006673), and several strains of *Bjerkandera sp.* and *B. adusta* (accession numbers AY633927, EF441742).

CCTGCGGAAGGATCATTATCGAGTTTTGAACGGGGTTGTCTGCTGGCTCGCAAGGGCATG
TGCACGCCTGTCTCATCCACTCTCAACTTCTGTGCACTTTTCATAGGCCGGCTTGTGGG
TGCGTTCGCGCACTTGTAGGTGTCGGGCTTATGCTTTACTACAAACGATTCAGTTTTAG
AATGTCATACTTTGCTATAACGCAATTTATATACAACTTTCAGCAACGGATCTCTTGGC
TCTCGCATCGATGAAGAACGCAGCGAAATGCGATAAGTAATGTGAATTGCAGAATTCAG
TGAATCATCGAATCTTTGAACGCACCTTGCGCTCCTTGGTATTCCGAGGAGCATGCCTG
TTTGAGTCTCATGGAATTCTCAACCTTCGGCTTTATTGACGAAGGCTTGGACTTGGAGG
TCGTGCCGGCTCTCGTAGTCGGCTCCTCTGAAATGCATTAGTGCGAACGTTACCAGCCG
CTTCAGCGTGATAATTATCTGCGTTGCTGTGGAGGGTATTCTAGTGTTCGCGCTTCTAA
CCGTCTTCGGACAAATTTCTGAACTCATCAGGTGAGCTCAATAGGACTACCCGCTGAAC
TTAAGCATATCAATAA

Figure 3.2. Sequence of the rDNA of the new fungus. Subunit 18S rRNA (yellow), ITS1 (grey), 5.8S rRNA (white), ITS4 (red) and 28S rRNA (green)

Morphologically, the fungus presents the following macroscopic characteristics: fast growing reaching 9 cm in diameter after 5 days on malt extract agar plates at 30ºC and aerial mycelium abundant, woolly and white (**Figure 3.3**).
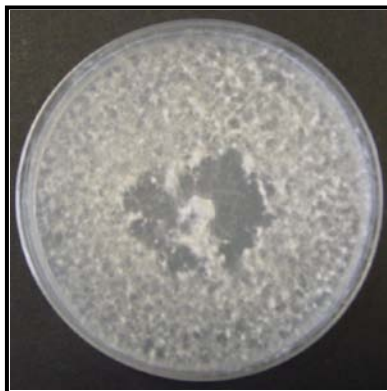
Figure 3.3. Macroscopic morphology of the fungus after 7 days of growth in solid medium

The microscopic characteristics of the morphology are: hyaline hyphae without clamp connection dividing into one-celled arthroconidia which remain barrel-shaped (~5 μm) and lack of sexual forms (**Figure 3.4**).

On the basis of morphological characteristics of the isolated fungus, the strain was similar to the anamorphic state of *Polyporus adustus* (Wild.) Fr. (=*B. adusta*) which shows a Geotrichum-like conidial state [267]. Other authors have identified similar isolates of *Bjerkandera sp*. as Geotrichum-like fungus [263, 268, 269]. Thus, it can be concluded that the new fungal strain is an anamorphous form of *Bjerkandera* sp. From now on, it is labelled as anamorph R1 of *Bjerkandera* sp.
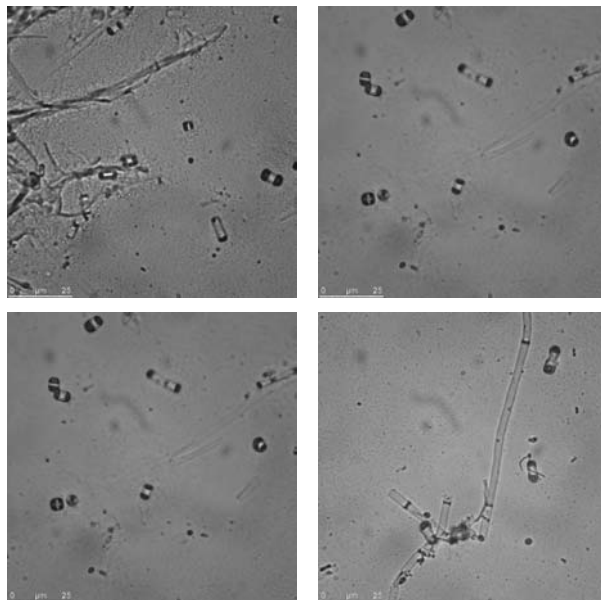
Figure 3.4. Microscopic morphology of the new fungus

3.3.2. Production of lignin modifying enzymes in Erlenmeyer flasks

The effect of three different carbon sources in the growth medium, glucose, lactose and cheese whey, were evaluated on the production of lignin modifying enzymes.

As shown in **Figure 3.5.a-b**, cheese whey was a poor growth substrate for the production of the enzyme both in the presence of peptone or ammonium tartrate as nitrogen source.

On the other hand, lactose was identified as a good carbon source when the nitrogen source was peptone ($\sim$ 1000 U/L on 12th day); however, when ammonium tartrate was used as nitrogen source, negligible growth of the fungus was observed (**Figure 3.5.c-d**). Laccase activity, even in a culture medium with $CuSO_4$ could not be detected. Among the three carbon substrates, glucose is the one that yielded the highest production of MnP (**Figure 3.6**).
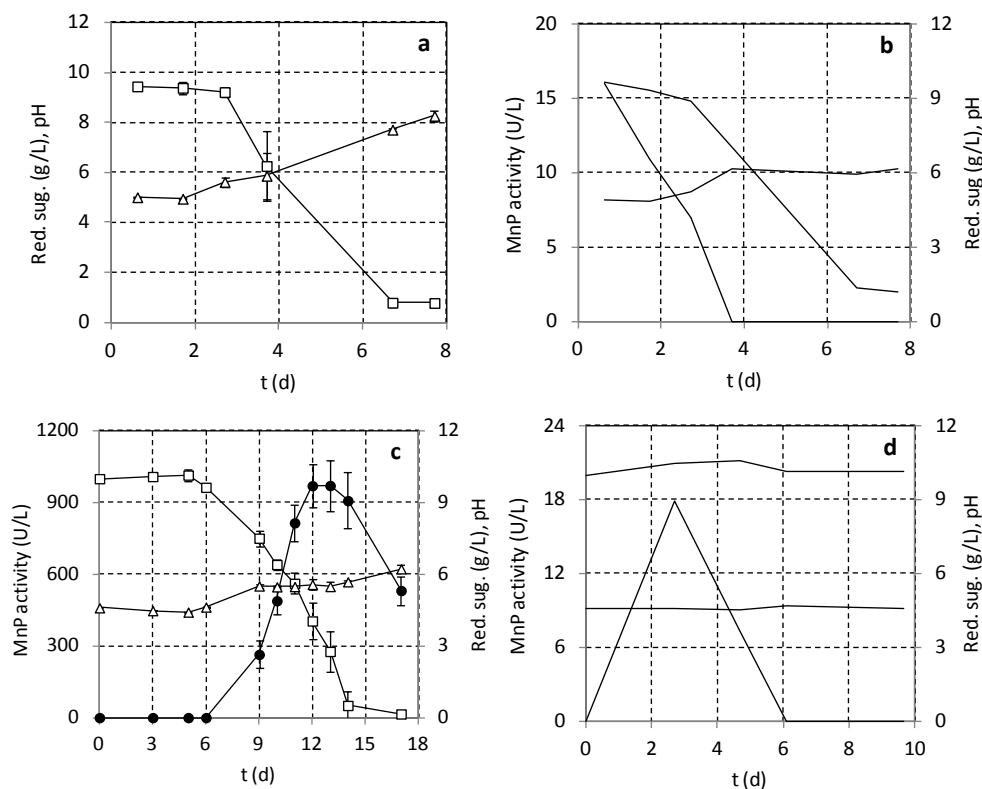
Figure 3.5. Time course experiment of the anamorph R1 of *Bjerkandera* sp. grown in Erlenmeyer Flasks in different media. Profiles of pH (△), reducing sugars (□) and MnP activity (●). 10 g/L cheese whey with 10 g/L peptone (a) and 50 mM ammonium tartrate (b); 10 g/L lactose with 10 g/L peptone (c) and 50 mM ammonium tartrate (d).

In order to obtain the highest production of peroxidase activity, three different concentrations, 0.5, 2 and 10 g/L, corresponding to N-limitation, sufficiency and excess, respectively, were investigated. Profiles of pH, consumption of glucose and MnP activity are shown in **Figure 3.6**.
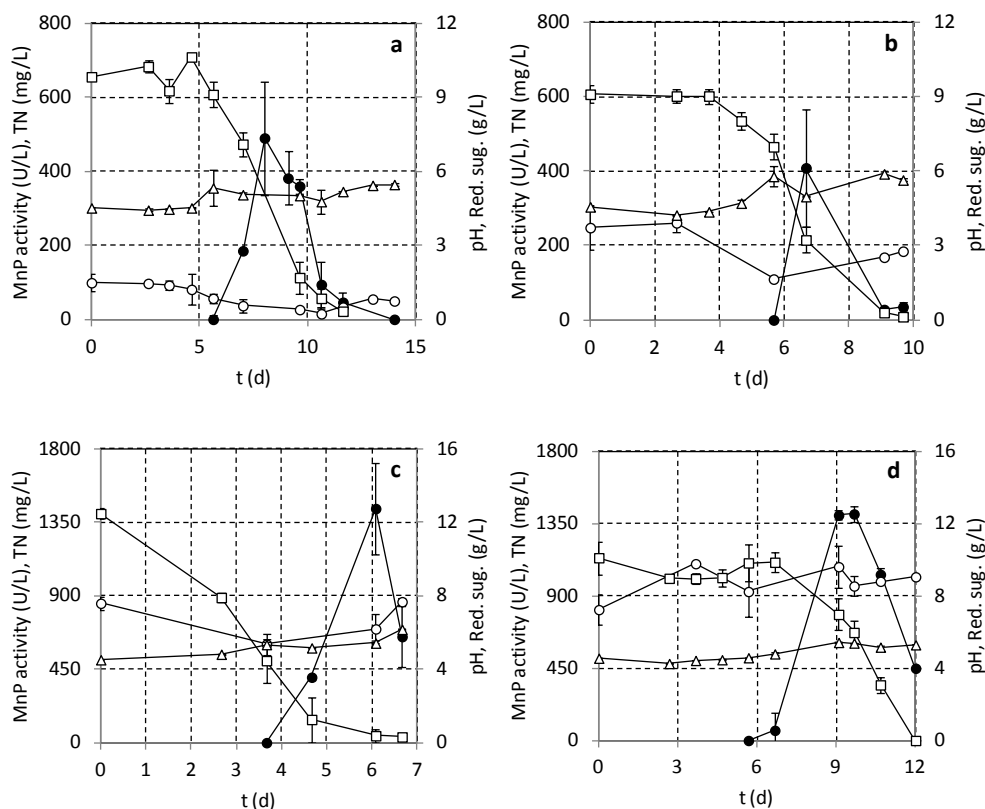
Figure 3.6. Time course experiment of the anamorph R1 of *Bjerkandera* sp. grown in Erlenmeyer flasks in different culture media. Profiles of pH (△), reducing sugars (□), MnP activity (●) and TN (○). Media: 10 g/L glucose and (a) 0.5 g/L peptone, N-limitation; (b) 2 g/L peptone, N-sufficiency; (c) 10 g/L peptone, N-excess (d) 50 mM ammonium tartrate, N-excess

In a N-limited medium (0.5 g/L) (**Figure 3.6.a**), the maximum peak of peroxidase activity: 500±180 U/L was obtained at day 8. Under sufficient nitrogen medium (2 g/L) (**Figure 3.6.b**), the activity reached a peak of 400±150 U/L at day 7 of incubation. Therefore, a significant difference between the medium with limitation or sufficiency of nitrogen was not observed. In a medium with high N concentration (10 g/L) (**Figure 3.6.c**), the maximum enzyme activity: 1435±278 U/L was obtained on the 6th day.

As shown in **Figure 3.6.c**, the highest level of MnP activity was achieved on day 6 (~1400 U/L) and it declined quickly. This fall could be attributed to the production of aryl alcohol oxidase (AAO) once one nutritional source is depleted. AAO is an enzyme involved in the production of H_2O_2 required as co-substrate by peroxidases [270]. AAO has been detected in another anamorph of *Bjerkandera adusta* [263]. A high level of H_2O_2 has been found in other basidiomycetes during secondary metabolism, causing the loss of peroxidase activity after few hours [271]. This effect could also affect the peroxidase activity in the new strain. When cultivating peptone as nitrogen source, high levels of H_2O_2 (5 mg/L) were detected at the moment of carbon source depletion.

Table 3.3. Summary of production of Mn-oxidizing peroxidase enzyme

Nitrogen source	Concentration (g/L)	MnP activity (U/L)	Time (d)	Production rate (U/L·d)
Peptone	0.5	490±153	8	61.2
	2.0	410±159	7	58.6
	5.0	1045±278	7	149
	10	1435±278	6	239
Ammonium tartrate	0.4	660±50	13	50.8
	1.8	752±71	10	75.2
	4.0	1013±40	7	145
	9.2	1400±27	9	156

Additionally, the influence of the type of nitrogen source was investigated. Either peptone or ammonium tartrate were added to the medium at equivalent concentrations of nitrogen (**Figure 3.6.d**). Both peptone and ammonium tartrate stimulated fungal growth and resulted in similar MnP

activity production. However, the production of enzyme was faster in the medium containing peptone, as shown in **Table 3.3**.

3.3.3. Scale-up of the production of lignin modifying enzymes

Taking into account the previous results, the production of ligninolytic enzymes was scaled-up in a 1.5-L fermenter using a modified Kirk medium supplied with 10 g/L of glucose and 10 g/L of peptone: 239 U/L·d. As shown in **Figure 3.7**, the peak of enzymatic activity reached was similar to the one observed in Erlenmeyer flasks with identical culture medium; however, the time required to reach the peak was shorter: 4.5 days. Hence, the MnP production rate hereby was slightly higher, 378 U/L·d. Presumably, the supply of air promoted growth due to the faster consumption of substrates, and consequently the production of enzyme took place previously to what occurred in Erlenmeyer flasks.

Figure 3.7. Fermentation profile of the anamorph R1 of *Bjerkandera* grown in 1.5 L bioreactor. Time course of pH (△), reducing sugars (□) and MnP activity (●).

The production of VP was also evaluated in a 20-L bioreactor. A new medium based on a residue (25% v/v), "straw-water", supplied with glucose and peptone was evaluated. The characteristics of the "straw-water" are displayed in **Table 3.4**.

Table 3.4. Composition of the "straw-water" medium

	Concentration
Reducing sugars	1.26±0.18 g/L
TOC	3.57 g/L
Proteins	233±38 mg/L
Phenolic content	299 mg$_{CE}$/L
pH	7.8

When using the "straw-water" medium to produce MnP, the activity peak reached, 450 U/L, was lower than in those fermentations carried out with modified Kirk medium (**Figure 3.8**). However, the time required to obtain this peak was considerably shorter, 2.25 days, which means that the MnP production rate is 200 U/L·d. Presumably, this may due to the fact that the substrates at the beginning of the fermentation in the 20-L fermenter were in lower concentrations than in Erlenmeyer flasks or 1.5-L bioreactors. Consequently, the total consumption of them was faster as well as the peak of enzyme activity. Moreover, due to the low amount of carbon and nitrogen sources, the fungus grew less and the secreted enzyme was also lower.

The on-line parameters (redox potential, pH and pO$_2$) allowed predicting when the moment of enzymatic peak. The increase of redox potential was indicative of the start of enzyme production, regardless the trend of dissolved oxygen (pO$_2$). When redox potential started to decrease and pH increased, the peak of enzyme was observed and shortly after, it started to fall.
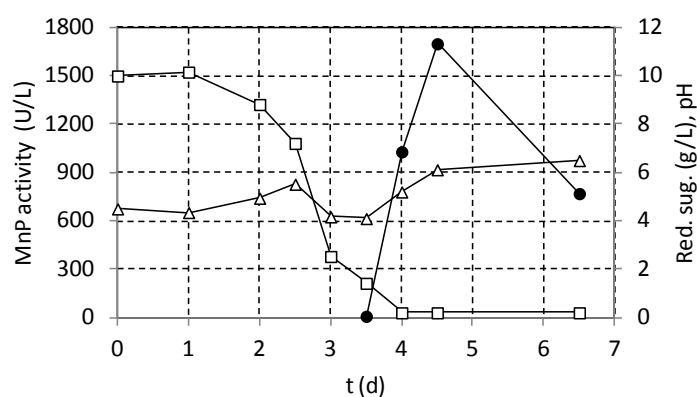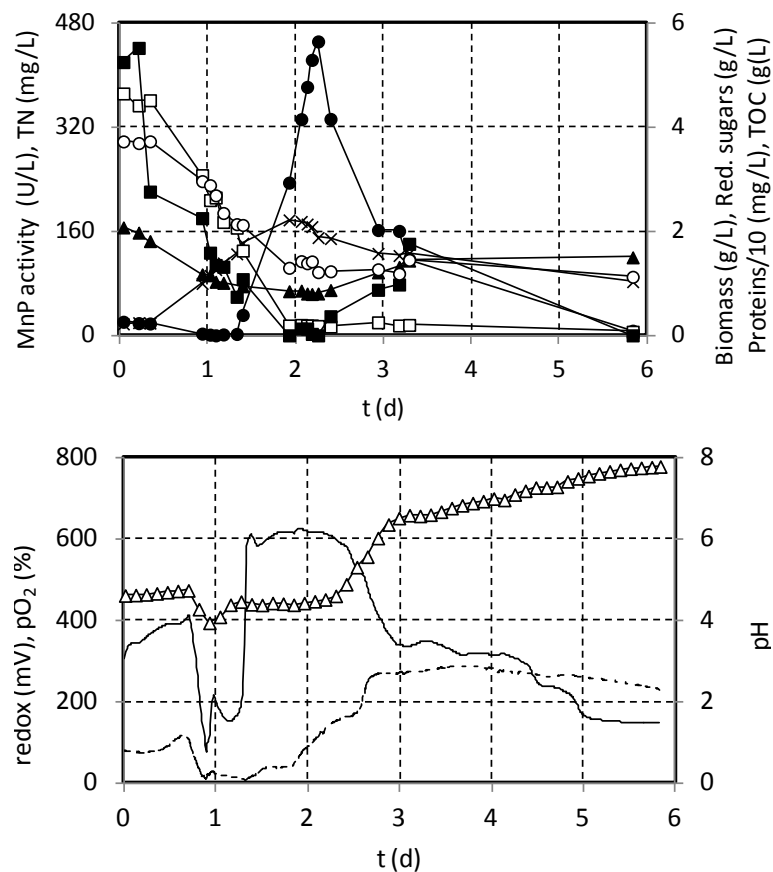
Figure 3.8. Fermentation profile of the anamorph R1 of *Bjerkandera* grown in a 20-L bioreactor. Time course of pH (△), reducing sugars (□), MnP activity (●), proteins (■), TOC (○), TN (▲), biomass (×), redox (▬) and pO₂ (- - -)

3.3.4. Effects of pH and temperature on the stability of the enzymatic crude

The effect of pH on the stability of the enzymatic crude is shown in **Figure 3.9**. The residual activity is shown as a percentage of the initial activity. When pH was maintained at 6, the enzyme retained 80% of the initial activity after 80 h of incubation. The stability of the enzyme decreased strongly at pH 3 and 8.
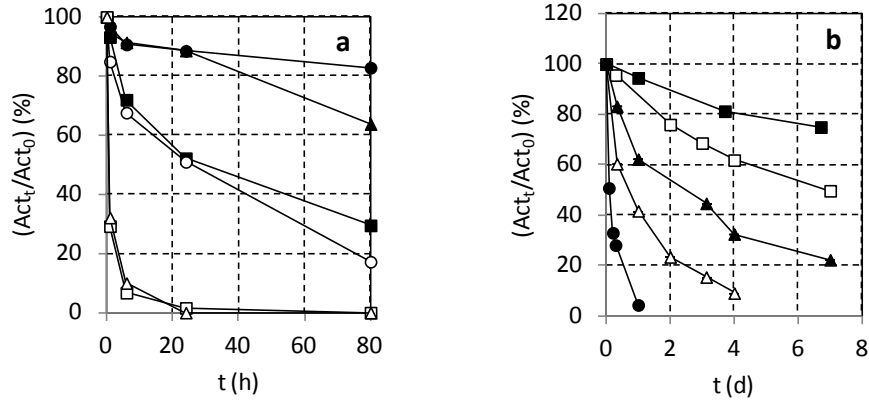
Figure 3.9. Effect of pH on MnP activity (a) at pH 3 (△), pH 4 (■), pH 5 (▲), pH 6 (●), pH 7 (○) and pH 8(□). Effect of temperature on MnP activity (b) at 4ºC (■), 25ºC (□), 30ºC (▲), 40ºC (△) and 50ºC (●).

Regarding the effect of temperature, the higher the temperature, the greater the enzymatic deactivation. For instance, the half-life of the enzyme was 7 days at 25ºC, whereas it was 2 h at 50ºC. The simplest model of enzymatic deactivation by temperature postulate that it is irreversible and it follows a first order kinetic. The active enzyme (E_a) suffers a structural change to form an inactive form (E_d):

$$E_a \xrightarrow{k_d} E_d \qquad \textbf{[3.3]}$$

Taking into account that the model considers that the deactivation of the enzyme follows a first order kinetic, the deactivation rate is:

$$r_d = k_d \cdot E_a \qquad \textbf{[3.4]}$$

In a discontinuous reactor, the **equation [3.5]** describes the mass balance:

$$\frac{dE_a}{dt} = -k_d \cdot E_a \rightarrow Ln\left[\frac{E_a(t)}{E_a(t=0)}\right] = -k_d \cdot t \qquad \textbf{[3.5]}$$

Considering that the enzymatic activity is proportional to the concentration of the enzyme, the **equation [3.6]** can be rewritten as:

$$Ln\left[\frac{Act_t}{Act_o}\right] = -k_d \cdot t \qquad \textbf{[3.6]}$$

The values of k_d can be calculated as the slope of representing $-Ln\left[\frac{Act_t}{Act_0}\right]$ against t; these values are shown in **Table 3.5**.

Table 3.5. Estimated values of k_d at different temperatures

T (K)	K_d (1/d)	R^2
277.15	0.0435	0.97
298.15	0.1010	0.96
303.15	0.2089	0.96
313.15	0.5554	0.98
323.15	2.9009	0.97

The effect of the temperature on the deactivation rate constant is described by the Arrhenius **equation**:

$$k_d = A \cdot e^{\left(\frac{-E_a}{R \cdot T}\right)} \qquad \textbf{[3.7]}$$

Where k_d is the deactivation constant rate, E_a is the activation energy, A is the pre-exponential factor, R is the universal gas constant and T is the temperature (in Kelvin). The value of E_a was calculated by means of a linear regression of Ln(k_d) against ($1/T$). Thereby, E_a was found to be 104 kJ/mol (R^2 = 0.98).

3.3.5. Catalytic properties of the enzymatic crude

The effect of Mn^{2+} concentration on the oxidation rate of 2,6-dimethoxyphenol by the enzymatic crude was evaluated in the range between 0 and 10 mM Mn^{2+} at different H_2O_2 concentrations: 0.10-0.80 mM (**Figure 3.10**).

Figure 3.10. Effect of Mn^{2+} concentration of the oxidation rate of 2,6-dimethoxyphenol at different H_2O_2 concentrations: 0.10 mM (■), 0.30 mM (□), 0.40 mM (●),0.50 mM (○) and 0.80 mM (△).

It can be observed that Mn^{2+} exerts a positive effect on the oxidation rate, which was dependent on the concentration of H_2O_2. There is a strong effect of Mn^{2+} concentration at very low H_2O_2 concentrations but beyond 0.75 mM, a pseudo-saturation region was reached, in which the reaction rate slightly increased with increasing Mn^{2+} concentration. The data corresponding to each series were fitted to the Michaelis-Menten model, **equation [3.8]**:

$$v = \frac{v_{max} \cdot [Mn^{2+}]}{[Mn^{2+}] + k_M}$$

[3.8]

Where v is the oxidation rate, v_{max} is the apparent maximum oxidation rate and k_M is the apparent Michaelis-Menten, the values are displayed at **Table 3.6**.

Table 3.6. Steady-state kinetic constants of the enzymatic crude, apparent K_M and v_{max}, and regression coefficient (R^2)

[H₂O₂] (mM)	v_{max} (U/L)	k_M (μM)	R^2
0.10	174	54.6	0.99
0.30	182	67.8	0.99
0.40	184	65.2	0.99
0.50	179	69.4	0.98
0.80	172	103	0.99

The values of k_M are affected by H_2O_2; at increasing H_2O_2 concentrations, k_M becomes higher, which implies a poorer affinity of the enzyme towards the substrate. Regarding v_{max}, an optimum point was observed at 0.40 mM H_2O_2. Real values of v_{max} and k_M cannot be determined since it would be imply experiments with no inhibitor, this being impossible because of the initiating character of H_2O_2 on the catalytic cycle.

Moreover, the effect of H_2O_2 concentration was also evaluated in the range 0.10-10 mM at different Mn^{2+} concentrations: 0.05-5.00 mM (**Figure 3.11**). The maximum oxidation rate was obtained at 0.4 mM H_2O_2, whereas the reaction rate drastically dropped at higher concentrations. The effect of Mn^{2+} was positive, since maximum oxidation rates corresponded to those of higher Mn^{2+} concentration. All data were fitted to a substrate inhibition kinetics, **equation [3.9]**:

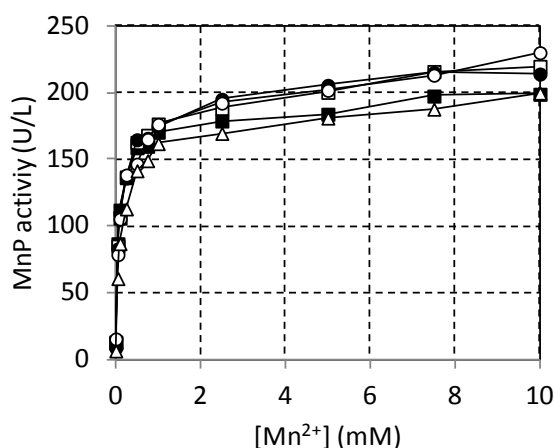$$v = \frac{v_{max} \cdot [H_2O_2]}{k_M + [H_2O_2] + \dfrac{[H_2O_2]^2}{k_S}}$$

[3.9]
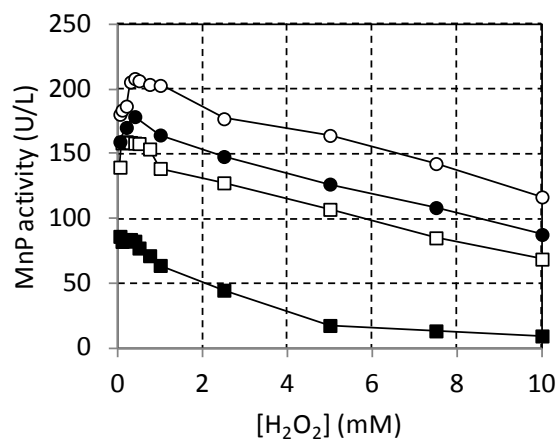
Figure 3.11. Effect of H_2O_2 concentration of the oxidation rate of 2,6-dimethoxyphenol at different Mn^{2+} concentrations: (■) 0.05 mM, (□) 0.50 mM, (●) 1.00 mM, (○) 5.00 mM.

Where v is the oxidation rate, v_{max} is the apparent maximum oxidation rate, k_M is the apparent Michaelis-Menten constant and k_S is the dissociation constant of the complex ES; the values are displayed at **Table 3.7**.

Table 3.7. Steady-state kinetic constants of the enzymatic crude, apparent K_M, k_S and v_{max}, and regression coefficient (R^2)

[Mn^{2+}] (mM)	v_{max} (U/L)	k_M (µM)	k_S (mM)	R^2
0.05	103	8.47	2.27	0.99
0.50	170	7.55	9.26	0.98
1.00	179	4.35	19.29	0.99
5.00	216	12.47	72.17	0.95

At increasing Mn^{2+} concentration, v_{max} increased which agrees with the results observed above; moreover, the higher the Mn^{2+} concentration, the higher the k_S values, which entail lower dissociation of the ES complex. Consequently, it can be established that manganese has a positive effect on the protection of the

enzyme against H_2O_2. Concerning the value of k_M, there is an optimum concentration at 1 mM.

3.3.6. Purification of the isoenzymes secreted by the new strain

To identify the enzymes with MnP activity, the enzymatic crude from 6 day cultures with modified Kirk medium with 10 g/L glucose and 10 g/L peptone, was analyzed. **Table 3.8** summarizes the results after each purification stage.

Table 3.8. Procedures for enzymatic crude purification

Step	Protein (mg)	Activity Total (U)	Specific (U/mg)	Purification Yield (%)	Factor (increase)
Ultrafiltration	2429	70344	29	100.0	1.0
Q-cartridge	445	63840	144	90.8	4.9
Sephacryl S-200	348	57041	164	81.1	5.7
Mono-Q					
R1B1	16	1933	121	2.7	4.2
R1B2	20	2598	130	3.7	4.5
R1B3	22	3290	150	4.7	5.2
R1B4	140	33320	238	47.4	8.2
TOTAL	198	41141	213.0	58.5	7.3

During low-performance anion exchange chromatography (**Figure 3.12.a**), only one fraction with MnP activity was detected. Absorption spectrum was monitored at 280 nm and 410 nm, which corresponds to the content of proteins and the heme absorption in the Soret region, respectively.
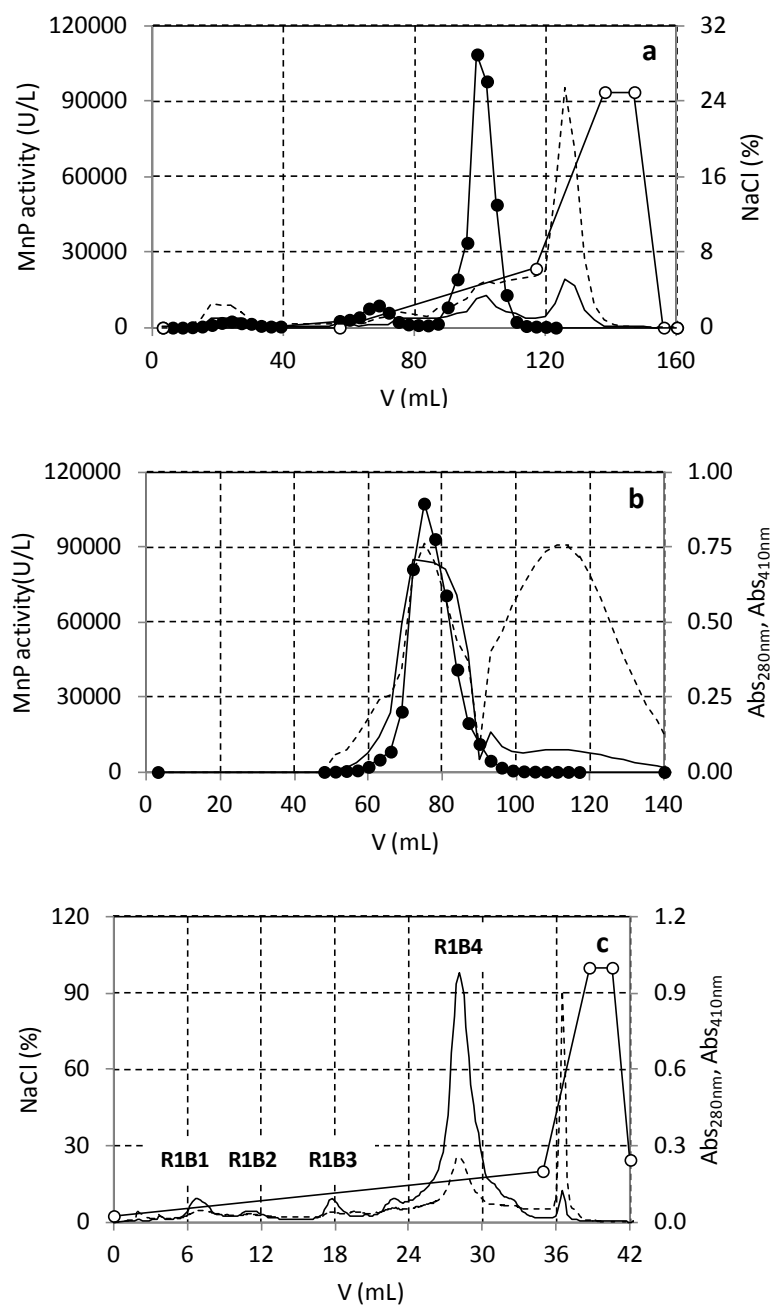
Figure 3.12. Purification of enzymatic crude. Profiles corresponding to (a) Q-cartridge column, (b) Sephacryl column and (c) Mono-Q column: MnP activity (●) NaCl (○), Abs_{280nm} (- - -) and Abs_{410nm} (−)

To complete the purification process two consecutive steps were required: an exclusion molar chromatography, using Sephacryl S-200 column (**Figure 3.12.b**) and a high-performance anion-exchange chromatography on Mono-Q (**Figure 3.12.c**). Four hemeproteins peaks were obtained exhibiting MnP activity and high A_{410}/A_{280} ratio. These proteins were labelled R1B1, R1B2, R1B3, and R1B4. The last one was the major fraction with a yield around 48%.

3.3.7. Physico-chemical properties of the isoenzymes

As shown in **Figure 3.13**, each fraction contains one protein band on SDS-PAGE. The molecular mass of the denatured peroxidases was estimated to be 49 kDa for R1B3, 47 kDa for R1B4, 45 kDa for R1B2 and 42 kDa for R1B1.
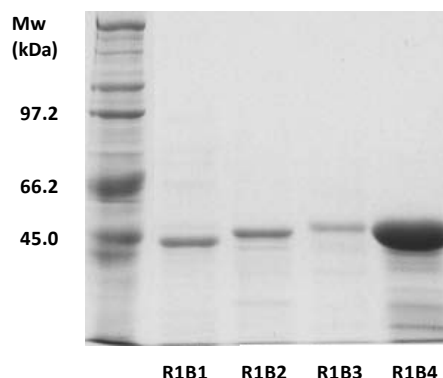
Figure 3.13. Estimation of relative molecular masses of the isoenzymes

The analytical IEF of the main peak, R1B4, showed p*I* around 3.5. The N-terminal sequence of the peroxidase R1B4 from the anamorph described in this work was the same as the N-terminal sequence of BOS2 enzyme reported for the wild strain of *B. adusta* [272]: VAXPDGVNTATNAAXXALFAVRDDI. These results, together with the molecular and morphological analysis, corroborate that the new fungus corresponds to a new anamorph of *Bjerkandera* sp.

The effect of pH on the stability of the isoenzymes is shown in **Figure 3.14**. The residual activity is shown as a percentage of the initial activity. When pH was maintained in 6, the enzyme retained about 70% of the initial activity, even after 1 month of incubation. The enzyme stability strongly decreased at pHs 4 and 8.
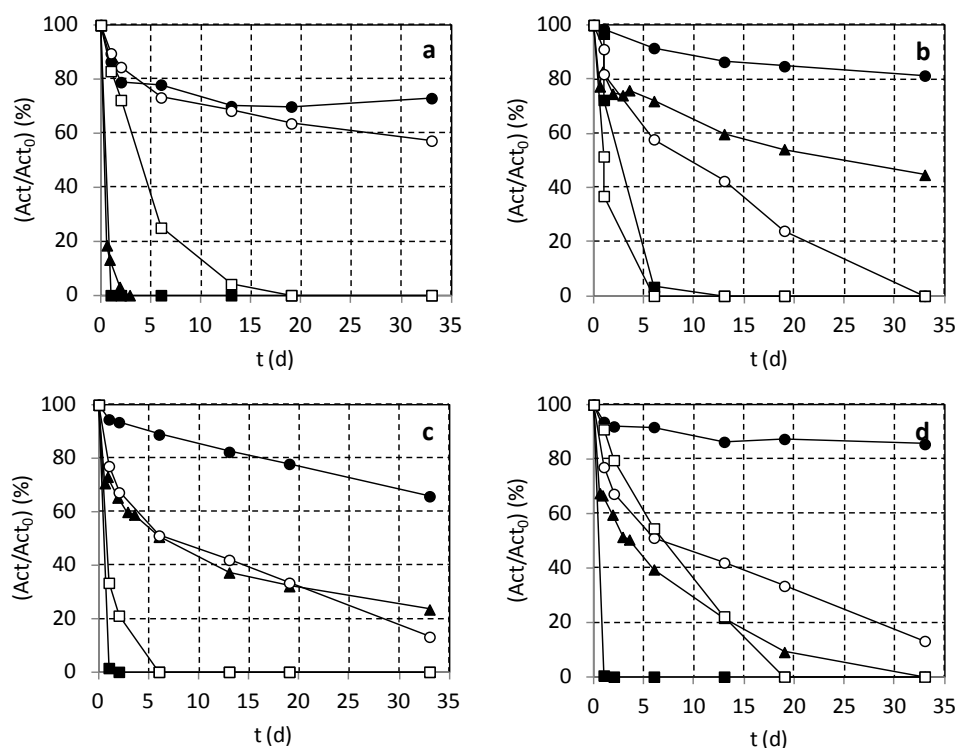
Figure 3.14. Effect of pH on stability of isoenzymes (a) R1B1, (b) R1B2, (c) R1B3 and (d) R1B4:pH 4 (■), pH 5 (▲), pH 6 (●), pH 7 (○) and pH 8 (□)

3.3.8. Catalytic properties of the four purified isoenzymes

The four fractions showed high peroxidase activity on Mn^{2+} and Mn-mediated peroxidase activity on DMP. The K_M and V_{max} for Mn^{2+} were obtained from the formation of Mn^{3+}-tartrate and from the Mn^{2+}-dependent oxidation of DMP (**Table 3.9**).

Table 3.9. Kinetic parameters of the four purified isoenzymes

	R1B1		R1B2	
	K_M	v_{max}	K_M	v_{max}
Substrate	**(µM)**	**(U/mg)**	**(µM)**	**(U/mg)**
H_2O_2 [*]	15.9±0.8	122.5±2.1	21.3±3.5	49.6±0.9
Mn^{2+}	45.1±2.0	84.2±1.0	14.3±1.8	24.4±0.1
$DMP + Mn^{2+}$	33.5±1.7	53.1±1.0	20.1±1.8	20.2±0.4
DMP	99.63	0.15	56.9±6.5	0.31±0.00
Veratryl alcohol	ns [†]	Ns	ns	Ns
	R1B3		**R1B4**	
	K_M	v_{max}	K_M	v_{max}
Substrate	**(µM)**	**(U/mg)**	**(µM)**	**(U/mg)**
H_2O_2 [*]	25.5±1.9	83.0±1.5	19.3±1.8	1009±152
Mn^{2+}	33.0±0.8	36.0±0.3	26.9±2.8	1037±46
$DMP + Mn^{2+}$	26.0±1.2	29.6±0.3	37.9±2.2	412±19.0
DMP	26.6±4.8	0.60±0.0	47.4±2.1	1.14±0.00
Veratryl alcohol	ns	ns	1287±3.29	24.7±0.0

[*]Mn^{2+} (0.1 mM) was used as substrate
[†]ns, no substrate

The kinetic constants show high affinity for H_2O_2 and Mn^{2+}. Mn^{2+}-independent peroxidase activity against DMP was detected with all four proteins. R1B3 presented the highest affinity for DMP, R1B2 and R1B4 showed a K_M value around 50 µM, and very slow oxidation of DMP by R1B1 was observed. However, Mn-independent activity on non-phenolic compounds, such as veratryl alcohol (pH 3), by R1B1, R1B2 and R1B3 was not detected while R1B4 oxidized this aromatic alcohol with K_M value of 1.2 mM.

The four peroxidases R1B1, R1B2, R1B3 and R1B4 showed high affinity for Mn^{2+} but also had Mn-independent activity on DMP. Only the fraction R1B4 could be considered as a versatile peroxidase, since it was the only one able to

oxidize efficiently Mn^{2+} and phenolic and non-phenolic compounds in absence of this ion. In view of the results obtained in this study, the enzyme produced by this new anamorph of *Bjerkandera* sp. can be classified as versatile peroxidase.

3.4. Conclusions

A new fungus from Temuco (Chile) was isolated and studied to produce ligninolytic enzymes. The fungus was identified by sequencing the ITS region to belong to the species *Bjerkandera*. After the study of both macroscopic and microscopic morphological characteristics, it was identified as an anamorphous form of *Bjerkandera* sp and classified as anamorph R1 of *Bjerkandera* sp.

Among the lignin modifying enzymes evaluated during the fermentation of the fungus, only peroxidases were detected in the enzymatic crude. Even in a medium supplied with $CuSO_4$ the fungus was not able to produce laccase. Three different carbon sources were evaluated to produce MnP and glucose was identified as the most suitable substrate for growth and MnP production. Moreover, two different nitrogen sources, peptone and ammonium tartrate, at four different levels were studied. The highest enzyme production rate, 239 U/L·d, was obtained with a modified Kirk medium supplied with 10 g/L glucose and 10 g/L peptone. The stability of the enzymatic crude was evaluated at different temperatures and pH values. It was found that the enzymatic crude was more stable at pH 6 and, as expected, the higher the temperature, the shorter the half-life.

Three purification steps, anion exchange, exclusion molar chromatography-high performance and anion exchange, were necessary to purify the enzymatic crude. Four hemeproteins were obtained, R1B1, R1B2, R1B3 and R1B4. Among the four isoenzymes, only R1B4 was identified as a versatile peroxidase. The stability against pH was evaluated and, as observed with the enzymatic crude, the highest stability was observed at pH 6.

Chapter 4

Immobilization of the enzyme versatile peroxidase through the formation of combined cross-linked enzyme aggregates, CLEA®s

Chapter 4. Immobilization of the enzyme versatile peroxidase through the formation of combined cross-linked enzyme aggregates, CLEA®s

Chapter 4. Immobilization of the enzyme versatile peroxidase through the formation of combined cross-linked enzyme aggregates, CLEA®s

4.1. Introduction

From an operational point of view, the use of free enzymes presents several disadvantages, mainly focused on technological and economic issues: complex recovery and reuse of the biocatalyst, necessity for product purification from the protein, potential source of complexity when operating in continuous mode, enzyme liability under extreme reaction conditions (temperature, pH, and presence of organic solvents), etc. These drawbacks can be overcome through the immobilization of the enzyme, which facilitates the separation of the biocatalyst from the reaction medium, increases its molecular weight and, in general, improves the stability of the protein against denaturation [273].

Immobilization of macromolecules can be defined as a method to restrict mobility. The first immobilization technique was developed in 1916 by Nelson and Griffin when they realized that the enzyme invertase "exhibited the same activity when absorbed on a solid (charcoal or aluminium hydroxide) at the bottom of the reaction vessel as when uniformly distributed throughout the solution". Up to now, more than 5000 publications and patents have been published on enzyme immobilization. A classification of immobilization methods according to different chemical and physical principles could be as follows:

1. Immobilization on supports. Support binding can be physical, ionic or covalent; however, physical bonding is generally too weak to keep the enzyme attached to the support under industrial conditions or high concentrations of reactants or products and high ionic strength. Ionic

binding is generally stronger and covalent binding of the enzyme to the support even much more [274]

2. <u>Entrapment</u>. In this type of immobilization, a polymeric network is synthesized in the presence of the enzyme where the biocatalyst is physically retained.

3. <u>Cross linking</u>. The use of support leads to "dilution of activity" of immobilized enzymes, due to the introduction of a large portion of non-catalytic mass ranging from 99.9% to 90.0%, which implies lower space-time yield and lower productivity [275].

4.1.1. Cross-linked enzyme aggregates, CLEA®s

The technique of protein cross-linking via the reaction of a cross-linker with reactive amino groups on the protein surface was initially developed in the 1960s [276]. Carrier-free immobilization strategies based on the synthesis of cross-linked enzyme crystals (CLECs), cross-linked dissolved enzymes (CLEs) and cross-linking enzyme aggregates (CLEA®s), have been proposed to conventional immobilization methods on solid supports [277-279].

The production of CLEs has several drawbacks, such as low activity retention, poor reproducibility, low mechanical stability and difficult handling of the gelatinous aggregate. The production of CLECs improved the stability against denaturation by heat, organic solvents or proteolysis. CLECs have been formulated as robust and highly active immobilized enzymes for use in industrial biotransformations; however, an inherent disadvantage of CLECs is the constraint of crystallizing the enzyme, which is a laborious procedure that requires high purity enzyme [280]. Comparable results were achieved when immobilizing the enzyme in CLEA®s [278]. In this immobilization procedure, protein molecules can be precipitated to form physical aggregates which are

chemically bonded to each other by means of the addition of a cross-linker (**Figure 4.1**).
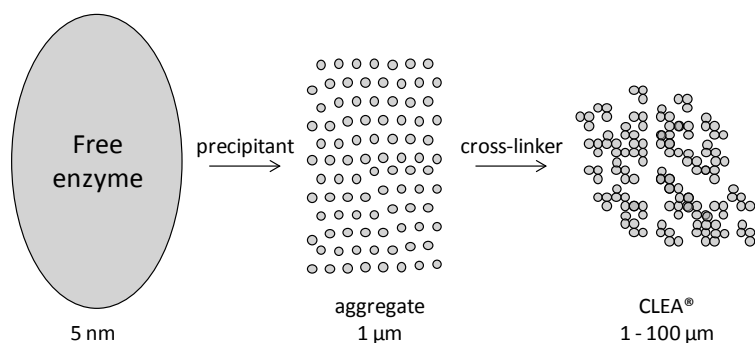
Figure 4.1. Preparation of CLEA®s

Precipitation step

The physical aggregation of proteins into supermolecular structures can be induced by the addition of salts (e.g. ammonium sulphate), organic solvents (e.g. acetone, methanol, ethanol etc.), or non-ionic polymers (e.g. polyethylene glycol) to protein solutions without perturbation of the original three-dimensional structure of the protein [281]. The choice of the precipitating agent depends on the type of enzyme to be immobilized, as shown in **Table 4.1**.

Cross-linking step

The solid aggregates are held together by non-covalent bonding and readily collapse and redissolve when dispersed in the medium. Chemical cross-linking of the aggregates will produce cross-linked enzyme aggregates in which the preorganized superstructure of the aggregates and, hence, their activity will be maintained. Glutaraldehyde (GLU) is generally the cross-linking agent of choice as it is inexpensive and readily available in commercial quantities. The amount of glutaraldehyde necessary to immobilize through the formation of CLEA®s is dependent on the type of enzyme.

Table 4.1. Conditions for the production of CLEA®s for a number of enzymes.

Organism	Enzyme	Precipitant	[GLU]	Reference
Candida antarctica	Lipase A	DME	100 mM	[280]
	Lipase B	DME	150 mM	
Thermomyces lanuginosus	Lipase	*tert*-butyl alcohol	100 mM	
Rhizomucor miehei	Lipase	*tert*-butyl alcohol	100 mM	
Aspergillus niger	Phytase	Ethyl lactate	100 mM	
Dactylium dendroides	Galactose oxidase	*tert*-butyl alcohol	100 mM	
Porcine	Trypsin	Ammonium sulphate	100 mM	
Aspergillus niger	Glucose oxidase	Ethyl acetate	100 mM	
Aspergillus oryzae	β-galactosidase	2-propanol	100 mM	
Rhodococcus erythropolis	Alcohol dehydrogenase	Ammonium sulphate	8 mM	
Candida boidinii	Formate dehydrogenase	Ammonium sulphate	8 mM	
Coriolus versicolor	Laccase	Polyethylene glycol	100 mM	
Coriolopsis polizona	Laccase	Polyethylene glycol	8 µM	[277]

4.2. Materials and methods

4.2.1. Production and concentration of versatile peroxidase

Versatile peroxidase (VP) was obtained from submerged cultures of the anamorph R1 of *Bjerkandera* sp. The fungus was grown in a 42 L fermenter, BIOSTAT®C+ from Sartorius Stedim Biotech (Melsungen, Germany) as described in **section 3.2.4**, using skimmed cheese whey and peptone as carbon and nitrogen sources, respectively.

4.2.2. Determination of manganese-dependent activity of VP

Manganese-dependent activity (MnP) of VP was measured photometrically (Powerwave XS, Bio-Tek, Bad Friedrichshall, Germany) by monitoring the oxidation of 2,6-dimethoxyphenol (DMP) at 468 nm and 30ºC (ε_{468} = 49.6 mM^{-1}cm^{-1}) as described in **section 2.1**. In case of combined CLEA®s, glucose (4.53 mM) was used as the reaction substrate.

4.2.3. Preparation of CLEA®s

CLEA®s were prepared under various conditions using 100 µL of a 10 U/mL VP solution (corresponding to 500 µg of protein) and 900 µL of precipitant, i.e. polyethylene glycol (70% w/w, PEG; Fluka), acetone (100%; Merck), 2-propanol (100%; Merck), n-propanol (100%; Merck) or 2-butanol (100%; Merck). Glutaraldehyde (GLU, Grade II, Sigma-Aldrich; 25% in H_2O) was added as cross-linker at a concentration of 18 mM. Assays were incubated at 30ºC, 100 rpm for 21.5 h when using PEG and at 4ºC, 100 rpm and 4 h for the other precipitants. Using PEG as precipitant, the effect of GLU was also evaluated, varying its concentration from 18 to 200 mM.

For investigations on combined CLEA®s, cross-linking was conducted using 70% PEG, 72 mM GLU and concentrations of 0.1 – 100 µg/L of bovine serum albumin (BSA) or 0.35 - 350 mg/L of glucose oxidase from *Aspergillus*

niger (Sigma-Aldrich; GOD) in a total volume of 1 mL. After incubation for 21.5 h at 30°C and 100 rpm, 9 mL of sodium malonate buffer (10 mM, pH 5.0) were added. After thorough mixing, the activity of the suspension was determined before and after the solution was centrifuged for 30 min at 8000 *g*. The pellets were repeatedly washed with the above mentioned buffer until no MnP activity was detected in the supernatant. Pellets were resuspended in 10 mL sodium malonate buffer and stored at 4°C until further use. All assays were performed in triplicate. The activities of CLEA®s were calculated by subtracting the activities in the supernatants after centrifugation from the suspension activity to correct for non cross-linked enzyme [279]. The conversion yield was calculated by dividing CLEA®-activity by the initial activity added.

4.2.4. Biochemical enzyme characterization

The apparent Michaelis-Menten constant: K_M and the inhibition constant: K_I of different enzyme preparations: VP-CLEA®s, combined CLEA®s and a mixture of non cross-linked VP and GOD (free VP-GOD), were determined based on the MnP activity using DMP as substrate. The concentration ranges used for K_M and K_I determinations were 1 µM-100 mM for H_2O_2, 20 µM-184 mM for glucose and 1 µM-50 mM for Mn^{2+}.

Kinetic parameters were calculated by curve fitting the plot of reaction rate versus substrate concentrations using Kaleidagraph 3.5 (SYNERGY© software, Reading, PA, USA). The results of the kinetic experiments of purified VP are published elsewhere [272].

The stability of free VP and of the CLEA®s was tested using 100 U/L of MnP activity. Enzyme was incubated for 20 h at 25ºC in organic solvents (Merck) and residual activity was determined as described above. The organic solvents were acetone (36%, v/v), methanol (44%, v/v), ethanol (55%, v/v), acetonitrile (10%, v/v), dimethyl sulfoxide (20%, v/v) and n-propanol (20%, v/v). The thermal

inactivation of CLEA®s and of soluble VP at 50ºC was investigated at pHs 4.5 and 5.5 using 10 mM sodium malonate buffer. One hundred microunits of CLEA®s or free VP were incubated in 900 µL of buffer solution. Residual activity was measured every 30 min.

To evaluate the enzyme tolerance towards hydrogen peroxide, a series of reactions were carried out involving DMP oxidation either by VP-GOD-CLEA®s or by free VP at different peroxide concentrations (1 µM - 100 mM). The influence of the glucose concentration: 18 µM - 180 mM, on MnP activity of VP-GOD-CLEA®s and with free VP-GOD was assessed in presence of 1 mM DMP, 50 mM sodium malonate and 1 mM $MnSO_4 \cdot H_2O$. The effect of pH for the oxidation of Mn^{2+} was evaluated by means of the DMP protocol at 30°C in a range between 3.0 and 7.5 using sodium malonate buffer. All assays were performed in triplicate.

4.3. Results and discussion

4.3.1. Preparation of VP CLEA®s

Cross-linking of versatile peroxidase has not been reported in literature so far, thus as a first stage in the research, an experimentation protocol is compulsory to choose the optimal precipitation agent and subsequently, the optimal concentration of the cross-linking chemical. The physical aggregation of protein molecules into supramolecular structures can be induced by the addition of salts, organic solvents, or non-ionic polymers to protein solutions without perturbation of the original three-dimensional structures of the protein [281]. Four different organic solvents were evaluated for their ability to aggregate VP prior to cross-linking experiments. The aggregation efficiency was calculated by subtracting the supernatant activity after centrifugation (8000 g, 10 min) from the suspension activity and thus, expressed related to the initial activity. The recovery of the initial activity after aggregation was 112.6±15.8%, 95.1±7.8%, 97.9±9.5% and 78.4±3.3% for acetone, 2-propanol, n-propanol and 2-butanol, respectively. The best result was achieved for acetone with a recovery percentage higher than 100% (**Figure 4.2.a**), which is in agreement with experiments carried out for three lipases and one trypsin [279]. In a combined aggregation and cross-linking step, a high inactivation of the enzyme was observed when using glutaraldehyde (18 mM) as cross-linker (**Figure 4.2.a**).
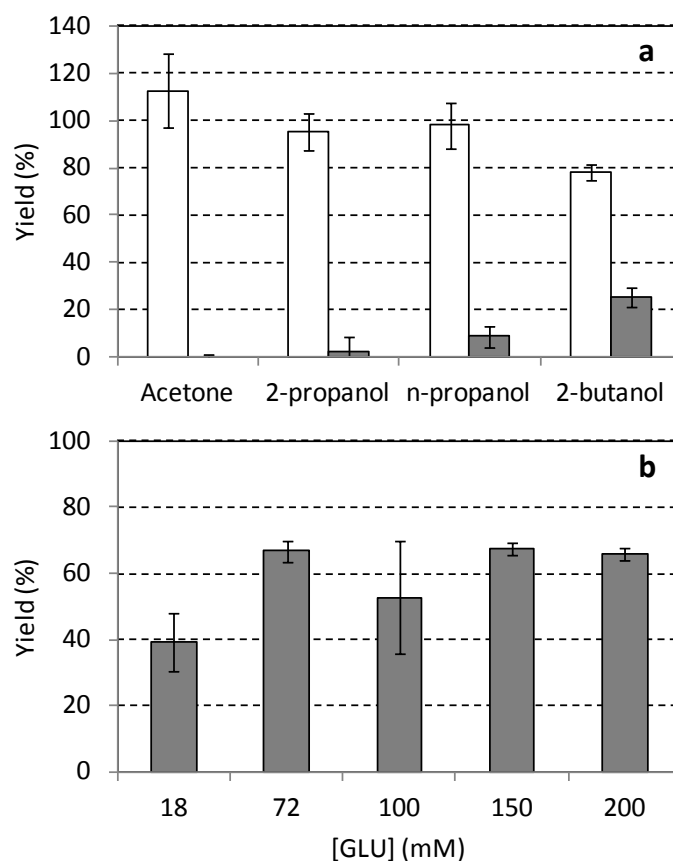
Figure 4.2. Aggregation and cross-linking efficiency. (a) Effect of different organic solvents on aggregation yield (white column) and CLEA® yield (grey column); (b) Effect of GLU concentration on VP-CLEA®s production using PEG as precipitant.

The combined aggregation and cross-linking using a non-ionic polymer, PEG, as precipitant led to a CLEA® yield (ratio between CLEA® activity and initial activity) of 39.1±8.7%. GLU is cheap and versatile; however, a number of enzymes are inactivated by this cross-linking chemical. Therefore, once PEG was identified as the best precipitant, a range of GLU concentrations: 18 – 200 mM was tested with the purpose of determining the optimum amount of GLU, i.e. high CLEA® yield with low enzymatic deactivation (**Figure 4.2.b**). The CLEA® yield increased at increasing GLU concentration up to 72 mM. Beyond this

concentration, higher CLEA® yields were not obtained. This value is in agreement with the concentration determined for other enzymes. The optimum GLU concentration for CLEA®s formation of three lipases, one laccase, one phytase, one galactose oxidase, one trypsin, one glucose oxidase and one β-galactosidase was found to be 100 mM whereas the glutaraldehyde concentration for CLEA®s production of one alcohol dehydrogenase and one formate dehydrogenase was 8 mM [282].

4.3.2. Production of combined VP-GOD-CLEA®s

The addition of "proteic feeders" facilitates obtaining CLEA®s in cases where the protein concentration in the enzyme preparation is low and/or the enzyme activity is vulnerable to high concentrations of GLU required for cross-linking [283]. The co-aggregation of the target enzyme with a "proteic feeder" was described to improve enzymatic stability, recovery yield and activity [277]. BSA was used to improve the stability of laccase CLEA®s [277], as well as the recovery of lipase CLEA®s [283] and aminoacylase CLEA®s [284]. In this work, the use of BSA in a range of 0.1-100 µg/L led to the inactivation of the enzyme and, consequently, led to the reduction of the CLEA® yield (**Figure 4.3.a**).

Combined CLEA®s were produced by performing the co-aggregation of VP at different GOD concentrations (3.5 – 350 mg/L, (**Figure 4.3.b**), using the optimal conditions as mentioned above. The co-aggregation and cross-linking of VP with GOD resulted in a higher yield of immobilized MnP activity compared to VP-CLEA®s. Using a ratio VP:GOD (w/w) of 5:3.5, a CLEA® yield of 89.2±1.9% was obtained. Combined VP-GOD-CLEA®s used in further experiments were produced under these conditions.
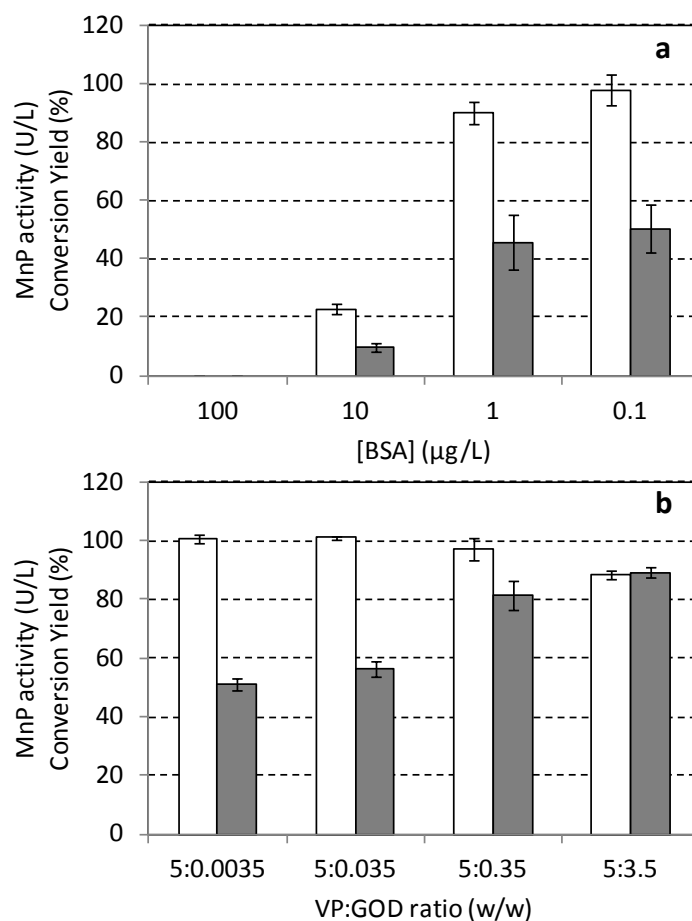
Figure 4.3. Effect of the addition of proteic feeder on the MnP activity of the VP enzyme (white column) and on the production of CLEA® (grey column). (a) Bovine serum albumin (BSA) and (b) Glucose oxidase.

The immobilization procedure involves the covalent binding between free amino residues of the enzyme, using glutaraldehyde as a functional coupling agent. Even though both enzymes (VP, GOD) have comparable levels of amino acids with tertiary amino groups, the different accessibility of those residues could explain the observed differences in yield. Manganese peroxidase from *Phlebia radiata* and GOD from *Aspergillus niger* were co-immobilized on porous

silica beads, obtaining a higher loss of enzymatic activity (69.1%) than the value obtained in this study [285].

Catalytic cascade reactions drastically reduce the operational time and costs as well as the consumption of auxiliary chemicals and energy [286], as fewer unit operations and lower reactor volumes are needed. For instance, the co-immobilization of a chloroperoxidase and a soybean peroxidase with GOD into polyurethane foams was successfully performed [287]. Other authors immobilized two or more enzymes in combi-CLEA®s such as co-immobilized catalase with GOD or galactose oxidase [282] and combi-CLEA®s composed of the (S)-selective oxynitrilase from *Manihot esculenta* and the non-selective recombinant nitrilase from *Pseudomonas fluorescens* EBC 191 [288]. In this work, the use of GOD not only led to an improvement in the CLEA®-yield but VP-GOD-CLEA®s exerted MnP activity upon glucose addition; thereby, demonstrating a functional catalytic cascade in which H_2O_2 produced by GOD serves as a substrate for VP.

Among the different parameters affecting MnP activity, the concentration of H_2O_2 is the most crucial parameter for the action of the enzyme [35]. An excessively concentrated chemical would cause the inactivation of the enzyme, whereas a too low concentration may limit the reaction rate. In addition, the continuous or sensor-controlled addition of H_2O_2 has the disadvantage that high local concentrations may occur around the entry point, resulting in an inactivation of the enzyme. These hot spots can be avoided by the *in situ* formation of hydrogen peroxide from oxygen and glucose. Specific activities of 172 μmol_{O2}/(min·mg) for GOD of *Aspergillus niger*, i.e., a H_2O_2 production rate of 172 μmol/(min·mg) GOD as well 250 μmol Mn^{3+}/(min·mg) corresponding to a H_2O_2 consumption of 125 μmol/(min·mg) were considered in this study [289]. The ratio VP:GOD used was 5:3.5; consequently, the theoretical

ratio of H_2O_2 produced:H_2O_2 consumed is 1. At lower GOD concentrations MnP activity is probably limited due to the available H_2O_2.

4.3.3. Characterization of VP-GOD-CLEA®s

4.3.3.1. Catalytic properties

Calculations of the apparent kinetic parameters of the VP-GOD-CLEA®s in comparison with free VP and a mixture of free VP and free GOD are depicted in **Table 4.2**. The kinetic parameters were calculated by curve fitting the plot of reaction rate versus substrate concentrations (**Figure 4.4**)

Table 4.2. Apparent kinetic parameters of VP-GOD-CLEA®s for the oxidation of DMP

		H_2O_2	Mn^{2+}	Glucose
Free VP	K_M (µM)	37.9±8.5	52.1±6.5	-
	K_I (mM)	3.2±0.5	-	-
	v_{max} (U/L)	141.1	101.6	-
	R^2	0.99	0.99	-
Free VP-GOD	K_M (µM)	36.3±6.3	80.6±1.4	8001 ±144
	K_I (mM)	3.0±0.3	-	-
	v_{max} (U/L)	144.5	107.7	111.8
	R^2	0.99	0.99	0.99
VP-GOD CLEA®s	K_M (µM)	27.5±4.5	73.7±10.0	640±86.3
	K_I (mM)	13.9±1.7	-	-
	v_{max} (U/L)	157.5	153.0	143.3
	R^2	0.99	0.99	0.99

Compared to free VP, a lower affinity of VP-GOD-CLEA®s was observed for Mn^{2+}, evidenced by an increase of K_M (52.1±6.5 µM and 73.7±10.0 µM, respectively). The immobilization process is known to potentially change the

enzyme conformation, which could result in an increase of K_M due to alterations of the binding site of the enzyme or steric hindrance [290]. But, similarly to that observed for a solution containing free VP plus GOD (80.6±1.4 µM), the increase of K_M probably reflected an interference with compounds from the GOD formulation or GOD itself.

No significant differences were found in the K_M value for H_2O_2 (37.8±8.5 µM, 36.3±6.3 µM and 27.5±4.5 µM, for free VP, free VP-GOD and VP-GOD-CLEA®s, respectively). The changes of the K_M values, indicative of mass transfer limitations for the immobilized enzymes, were obviously minor, thus underlining an advantage of the applied methodology. However, an increase in the H_2O_2 inhibition constant: K_I was observed (3.24±0.49, 3.01±0.30 and 13.87±1.71 mM, respectively). This was confirmed by the results obtained at non limiting H_2O_2-concentrations (**Figure 4.4.b**). In a range of 1 – 100 mM H_2O_2, VP-GOD-CLEA®s had higher activity compared to the non cross-linked VP, for instance at 20 mM H_2O_2, the residual activities were 50 and 10%, respectively, compared to the maximum activity at 0.4 mM H_2O_2.

4.3.3.2. Stability against aqueous organic solvents, pH and high temperature

Van Aken et al. (2000) observed that immobilized MnP on porous silica gels was more stable than free MnP in the presence of high H_2O_2 concentrations [285]. This effect was also observed for reactions catalyzed by chloroperoxidase CLEA®s (CPO-CLEA®s) where the peroxide tolerance of CPO-CLEA®s was much higher than the free chloroperoxidase [291]. However, a significant increase in the stability of MnP from *B. adusta* against H_2O_2 after immobilization in glutaraldehyde-agarose gel was also obtained [292].
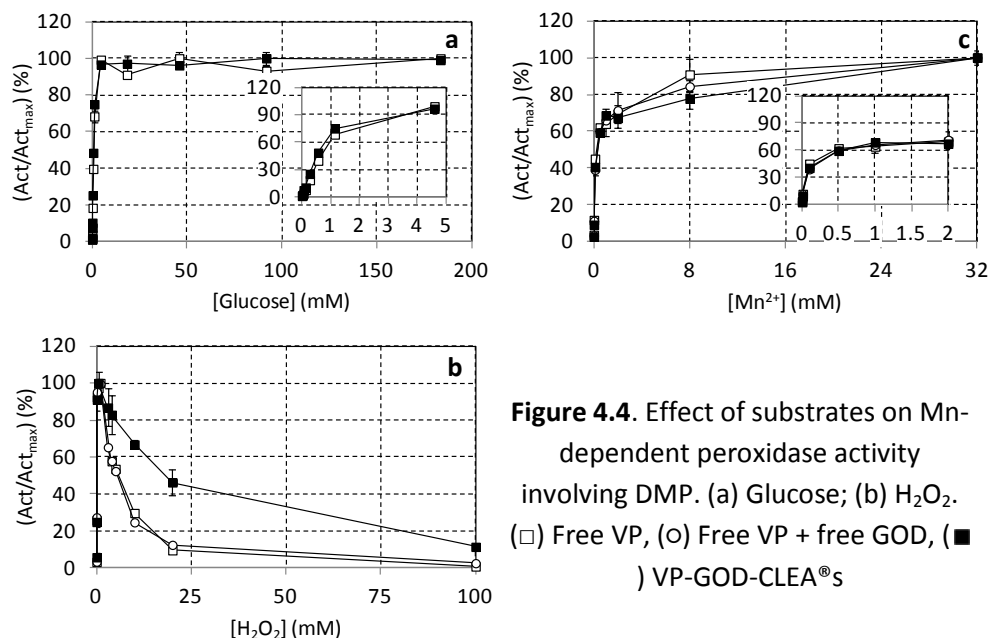
Figure 4.4. Effect of substrates on Mn-dependent peroxidase activity involving DMP. (a) Glucose; (b) H_2O_2. (□) Free VP, (○) Free VP + free GOD, (■) VP-GOD-CLEA®s

The stability of enzymes is highly dependent on the reaction conditions used, such as temperature, pH, presence of denaturants, etc. Cross-linking is reported to increase the stability of enzymes. CLEA®s of *Alcaligenes* sp. lipases had higher stability in organic solvents than the free enzyme and retained high activity in dioxan [293]. CLEA®s of *Coriolopsis polyzona* laccase showed higher stability against different denaturants and higher thermoresistance compared to the free enzyme [277]. The stability of the free VP and VP-GOD-CLEA®s against organic solvents was evaluated. With the exception of ethanol (55% v/v) where VP-GOD-CLEA®s had a residual activity of 12.8±0.9% compared to free VP (2.6±0.4%), cross-linking did not improve stability under the tested conditions (**Figure 4.5**). Moreover, the stability of the free VP, free VP + free GOD and VP-GOD-CLEA®s at different pH was evaluated. As shown in **Figure 4.6,** the immobilization of the VP enzyme through the formation of combined CLEA®s did

not improve the enzymatic stability at acid and basic pH values compared to free VP or free VP + free GOD.
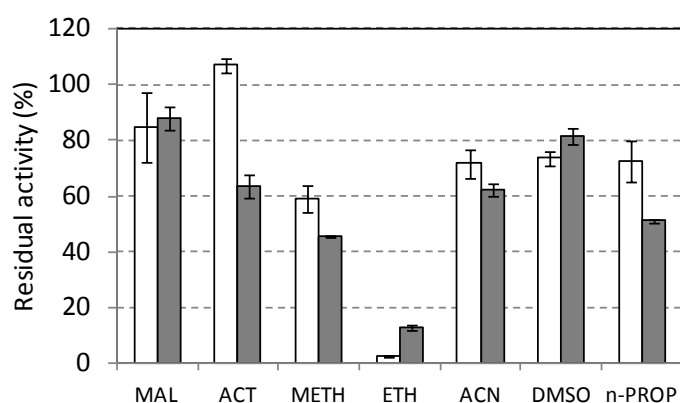
Figure 4.5. Stability, residual activity (%) after 20 h, of free VP (white column) and VP-GOD-CLEA®s (grey column) against organic solvents. Control (Na-malonate, 10 mM, pH 4.5; MAL), acetone (ACT), methanol (MET), ethanol (ETH), acetonitrile (ACN), dimethylsulfoxide (DMSO) and n-propanol (n-PROP).
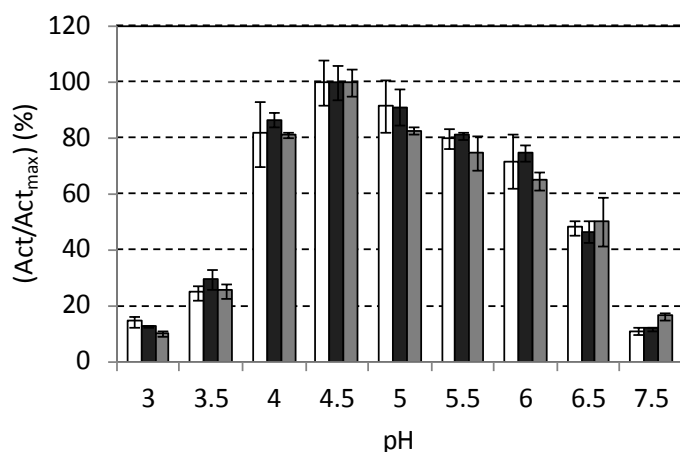
Figure 4.6. Stability, residual activity (%), of free VP (white column), free VP + free GOD (black column) and VP-GOD-CLEA®s (grey column) at different pH

Upon incubation at pH 4.5 or 5.5 for 150 min at 50 °C, no significant differences in the residual activity were measured between free VP and VP-GOD-

CLEA®s (**Figure 4.7**). For instance, activities at the end of the experiment differed less than 10% between VP-GOD-CLEA®s (14.6±0.6 U/L) and free VP (14.9±1.4 U/L) at pH 4.5.
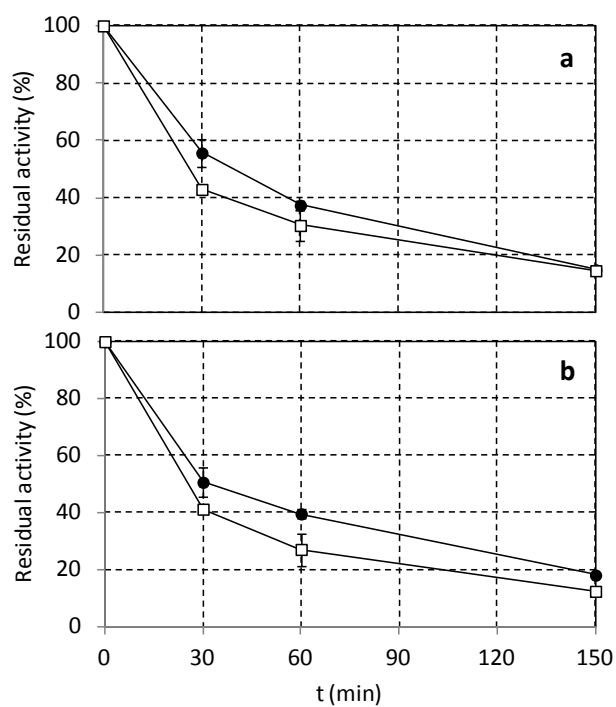
Figure 4.7. Stability, residual activity (%), at 50ºC at pH (a) 4.5 and (b) 5.5.
(●) Free VP and (□) VP-GOD-CLEA®s

4.4. Conclusions

No cross-linking of versatile peroxidase has been reported so far in the literature. A number of factors affecting the production of CLEA®s have been evaluated: type of precipitants, glutaraldehyde concentration, proteic feeder and glucose oxidase concentration.

Five different precipitants were evaluated in the preparation of VP-CLEA®s: four aqueous organic solvents (acetone, 2-propanol, n-propanol and 2-butanol) and one non-ionic polymer (polyethyleneglycol). The best results in terms of aggregation yield were obtained when using PEG.

The glutaraldehyde is the most common "cross-linker" used in immobilization techniques because its ability to form covalent bonds; however, it can have a negative effect on the enzyme since it can inactivate the enzymatic activity. For this reason, the effect of the "cross-linker" glutaraldehyde concentration was evaluated in the range 18 – 200 mM. The best results in terms of CLEA® yield were observed at 72 mM GLU concentration.

Two different proteic feeders, bovine serum albumin and the enzyme glucose oxidase, were evaluated to increase the CLEA® yield, since they can provide amino groups to form covalent bonds. BSA was discarded because its use led to high deactivation of the VP enzyme. Different VP:GOD (mg/mg) ratio values were evaluated with the purpose of finding the best results in terms of VP-GOD-CLEA®s yield. An optimum ration was found to be 5:3.5.

The co-aggregation of VP with GOD through the formation of combined CLEA®s (VP-GOD-CLEA®s) did not improve the enzymatic stability in presence of aqueous organic solvents or at different pH values or at high temperature, compared to free VP or free VP + free GOD. Nevertheless, the co-aggregation of VP and GOD increased the stability of VP against H_2O_2.

Finally, the use of GOD not only improved the CLEA®-yield but VP-GOD-CLEA®s affected MnP activity upon glucose addition; thereby demonstrating a functional catalytic cascade in which H_2O_2 produced *in situ* by GOD serves as a substrate for VP.

Chapter 5

Versatile peroxidase: a suitable tool for the treatment of endocrine disrupting chemicals

Chapter 5. Versatile peroxidase: a suitable tool for the treatment of endocrine disrupting chemicals

5.1. Introduction

5.2. Materials and methods

5.2.1. *In vivo* elimination of endocrine disrupting chemicals

5.2.2. *In vitro* elimination of endocrine disrupting chemicals

5.2.2.1. Evaluation through response surface methodology of the batch elimination of EDCs by free VP

5.2.2.2. Batch elimination of EDCs by VP-GOD-CLEA®s

5.2.3. Identification of degradation products of BPA, TCS, E1, E2 and EE2

5.3. Results and discussion

5.3.1. *In vivo* removal of endocrine disrupting chemicals

5.3.2. Evaluation through response surface methodology of the batch elimination of EDCs by free VP

5.3.2.1. Bisphenol A and triclosan

5.3.2.2. Estrogeni compounds

5.3.3. Batch removal of EDCs by VP-GOD-CLEA®s

5.3.4. Identification of degradation products of BPA, TCS, E1, E2 and EE2

5.3.4.1. Bisphenol A

5.3.4.2. Triclosan

5.3.4.3. Estrone, 17β-estradiol and 17α-ethinylestradiol

5.4. Conclusions

Chapter 5. Versatile peroxidase: a suitable tool for the treatment of endocrine disrupting chemicals

5.1. Introduction

The catalytic cycle of VP depends on the combined action of several compounds, referred to as substrates, cofactors and mediators, which initiate and participate in the catalytic cycle. These compounds are hydrogen peroxide which initiates the catalytic cycle, $MnSO_4$ which reduces the compounds C-I_A and C-II_A, **Figure 1.4**, and Na-malonate, necessary to chelate and stabilize the ion Mn^{3+} produced. From a theoretical point of view, the molar ratio between H_2O_2 and Mn^{2+} has to be 1:2 (**Equation [3.1]**), whereas the ratio between Mn^{3+} and Na-malonate should be, at least, 1:3.

Response surface methodology is a multivariate technique that mathematically fits the experimental domain studied in the theoretical design through a response function. RSM has been extensively studied on biotechnology namely optimization of medium composition [294], however, up to our knowledge, this is the first report for EDCs elimination optimization by enzymatic catalysis with RSM. The application of experimental design and response surface methodology (RSM) in oxidation of EDCs process can result in improved elimination, reduced process variability, time and overall costs. Additionally the factors that influence the experiments are identified, optimized and possible synergic or antagonistic interactions that may exist between factors can be evaluated. Only a few recent studies aiming the oxidation of EDCs by MnP or VP are available (**Table 5.3**. As shown, the ratios mentioned above (Mn^{2+}:H_2O_2 and Mn^{2+}:Na-malonate) differ from theory, depending on the study. Therefore, in order to perform the degradation of the EDCs in the best possible conditions, an optimization process was carried out where the effect of Na-malonate and

$MnSO_4$ concentration and the initial MnP activity were evaluated. Moreover, an attempt to identify the degradation products after the degradation reactions of the five EDCs with VP, was conducted.

5.2. Materials and methods

5.2.1. *In vivo* removal of endocrine disrupting chemicals

Static fungal cultures were prepared to evaluate the ability of the anamorph R1 of *Bjerkandera* sp. to remove BPA, TCS, E1 E2 and EE2. Experiments were carried out in Erlenmeyer flasks. EDCs were added, immediately after inoculation of three plugs containing active mycelium, from stock solutions to provide a concentration of 100 µg/L. The composition of the growth medium was: 4 g/L glucose, 1 g/L peptone and 25% (v/v) "straw water" (**Table 3.4**). Abiotic controls were prepared to verify any possible adsorption or evaporation. All the cultures were evaluated in triplicate and incubated for 7 days. Samples were taken at the end of the experiment to analyze residual enzymatic activity and to carry out the extraction and determine the concentration of EDCs by GC-MS.

5.2.2. *In vitro* removal of endocrine disrupting chemicals

5.2.2.1. Evaluation through response surface methodology of the batch elimination of EDCs by free VP

The enzymatic removal of BPA, TCS, E1, E2 and EE2 was carried out in batch experiments with free VP. Three operational variables (independent variables) affecting the Mn-oxidizing catalytic cycle of VP: Na-malonate (*[Na-malonate]*, x_1, mM) and MnSO$_4$ (*[MnSO$_4$]*, x_2, mM) concentration and initial MnP activity (*Act.$_0$*, x_3, mM) and their interactions were evaluated. To study the effect of the above indicated variables, a factorial design with three levels for each variable was used; these levels were represented by -1, 0 and 1 (**Table 5.1**).

Other parameters were: 0.4 mM H$_2$O$_2$ concentration (**Figure 6.6**), 30ºC, and 10, 5, 2.5, 2.5, 2.5 mg/L initial concentrations for BPA, TCS, E1, E2 and EE2, respectively.

Table 5.1. Levels and actual values of the variables tested

Factor	Variable	Unit	-1	0	1
x_1	[Na-malonate]	mM	1	10	50
x_2	[MnSO$_4$]	mM	0.05	0.5	1
x_3	Act.$_0$	U/L	25	50	100

Samples were taken after 0, 2, 4, 6, 8 and 10 min in BPA experiments, after 0, 2, 5, 8, 10, 20, 40 and 60 min in TCS assays, and after 0.5, 1, 5 and 10 min in estrogens experiments to analyze residual enzymatic activity and EDC concentration. Independent experiments were carried out for BPA and TCS, whereas the elimination of the three estrogens was performed in the same experiments. A Full Factorial Design (FFD) was used (**Figure 5.1**), in which the central point (0,0,0) was repeated three times.
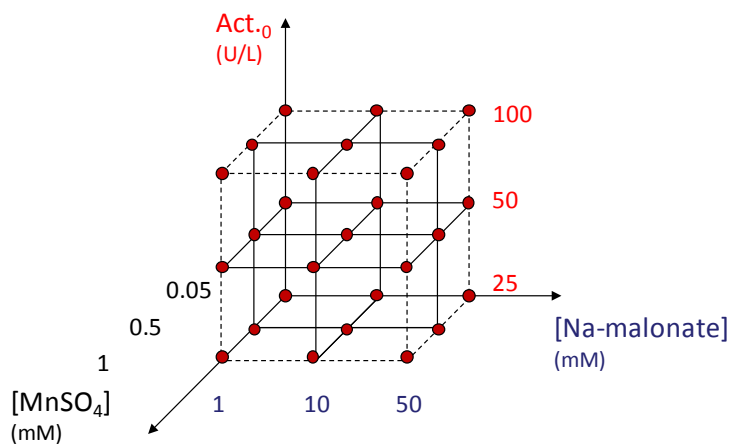

Figure 5.1. Full Factorial Design to evaluate the batch elimination of EDCs

Two variables were defined as response variables (dependent variables): maximum degradation rate (v_{max}, Y_1, mg/L·min, **equation [5.1]**), degradation

extent (Y, Y_2, %, **equation [5.2]**). These response variables were calculated as follows:

$$v_{max} = \frac{([EDC]_t - [EDC]_0)}{t} \qquad \textbf{[5.1]}$$

Where *[EDC]* is the EDC concentration in mg/L and *t* is the time required to take the first sample in min.

$$Y = \left(\frac{([EDC]_{tf} - [EDC]_0)}{[EDC]_0} \right) \cdot 100 \qquad \textbf{[5.2]}$$

Where *L* is the length of the spectrophotometer quartz cell and t_f is the time at the end of the experiment.

In order to optimize the conditions to maximize both Y_1 and Y_2 and minimize Y_3, three dimensional response surface methodology (RSM), was applied. Thereby, relationships between manipulated variables and one or more response variables can be determined [295]. When three generic variables are considered, the standard response surface methodology equation is **equation [5.3]**:

$$\begin{aligned} Y = {} & b_0 + b_1 \cdot x_1 + b_2 \cdot x_2 + b_3 \cdot x_3 + b_{12} \cdot x_1 \cdot x_2 + b_{13} \cdot x_1 \cdot x_3 \\ & + b_{23} \cdot x_2 \cdot x_3 + b_{11} \cdot x_1^2 + b_{22} \cdot x_2^2 + b_{33} \cdot x_3^2 \end{aligned} \qquad \textbf{[5.3]}$$

Where, *Y* is the response variable (controlled); x_1, x_2 an x_3 are the independent variable (manipulated); b_0 is the regression coefficient at center point; b_1, b_2 and b_3 are the linear coefficients; b_{12}, b_{13} and b_{23} are the second-order coefficients; and b_{11}, b_{22} and b_{33} are the quadratic coefficients [296]. When the values of the independent variables are coded (dimensionless), the

coefficients have the same dimensions and, subsequently, the same units of the dependent variable.

5.2.2.2. Batch elimination of EDCs by VP-GOD-CLEA®s

The enzymatic removal of BPA, TCS, E2 and EE2 was carried out in batch experiments using combined CLEA®s representing 250 mU of MnP activity. The final volume was 5 mL, containing 50 mM sodium malonate buffer (pH 5.0), 1 mM $MnSO_4$ and initial concentration of each compound of 10 mg/L. This concentration was higher than the water solubility of NP and EE2, thus all the assays contained 5% (v/v) methanol arising from the stock solutions to increase solubility. Assays containing heat inactivated enzyme (15 min, 95 °C) served as control. The experiment was conducted for 10 minutes at 30 °C, started by addition of glucose in case of combined CLEA®s. The residual concentration of each compound in the supernatant was measured by HPLC. Glucose (4.59 mM) was used to oxidize the native form of VP. All assays were performed in triplicate.

5.2.3. Identification of degradation products of BPA, TCS, E1, E2 and EE2

In order to identify the possible degradation products of the VP-mediated elimination of BPA, TCS, E1, E2 and EE2, five independent batch assays with the best oxidation conditions (**Table 5.2**) were carried out. Samples were taken after 10 minutes to be analyzed by GC-MS.

The five EDCs are nonvolatile and/or thermally unstable, consequently a process of derivatization is necessary. In this process, the original compound is chemically changed, producing a new compound that has properties more amenable to GC-MS.

Table 5.2. Conditions of batch experiments for the identification of degradation products

	[Na-malonate] (mM)	[MnSO$_4$] (mM)	MnP activity (U/L)	[H$_2$O$_2$] (mM)
BPA	30	0.60	70	0.40
TCS	30	0.60	70	0.40
E1	41	0.82	86	0.40
E2	41	0.82	86	0.40
EE2	41	0.82	86	0.40

Therefore, all the analyzed samples were derivatized with N-methyl-M-(tert.-butyldimethylsilyl)trifluoroacetamide (MTBSTFA, **Figure 5.2**) which provides greater thermal and hydrolytic stability to the compound by formation of methyl-terbutyl-silyl derivates [297, 298].
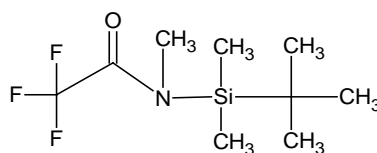
Figure 5.2. Chemical structure of MTBSFA

The procedure consisted in comparing the GC-MS chromatograms of the samples after 10 minutes with the chromatogram of a sample at time zero, in order to find new peaks which correspond with degradation products. Afterwards, the mass spectrum of each new peak was analyzed with the purpose of identify the compound. It was assumed the way how these molecules might suffer a fragmentation process.

5.3. Results and discussion

5.3.1. *In vivo* elimination of endocrine disrupting chemicals

The ability of the fungus anamorph R1 of *Bjerkandera* sp. to eliminate five endocrine disrupting compounds, BPA, TCS, E1, E2 and EE2 was evaluated in static cultures. As shown in **Figure 5.3**, the concentration of each EDC in the abiotic control was markedly lower than 100 μg/L, after seven days of incubation, which suggest that, presumably, there is elimination due to adsorption, volatilization or photodegradation. However, refer to this final concentration, a degradation related to the action of the fungus was observed. The fungus was able to eliminate completely the bisphenol A and the three estrogens, whereas the elimination of TCS was almost complete, 95.90±0.26%.
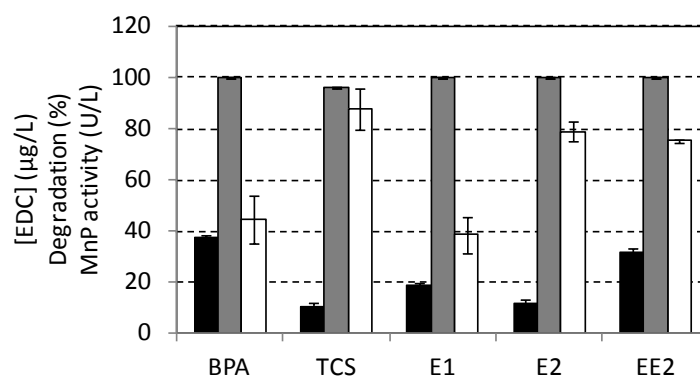

Figure 5.3. Degradation of EDCs by anamorph R1 of *Bjerkandera* sp. Concentration of EDC in abiotic control at the end of the experiment (black column), degradation after seven days (grey column) and MnP activity (white column)

In order to relate the elimination of the disruptor compounds with the action of the VP enzyme, the MnP activity was also measured at the end of the

experiment to find out that in all experiments at least it was 40 U/L, suggesting that the disappearance of the EDCs is due to oxidative action of VP.

5.3.2. Evaluation through response surface methodology of the batch elimination of EDCs by free VP

There are few studies of *in vitro* incubations of BPA, TCS, E1, E2 and EE2 with these MnP ov VP (**Table 5.3**), nevertheless, all the experiments reported a good degradation extent.

Table 5.3. Degradation conditions of EDCs with MnP or VP

[Na-malonate] (mM)	[MnSO$_4$] (mM)	[H$_2$O$_2$] (mM)	Initial MnP Activity (U/L)	Reference
50	0.1	GOD[*]	600	[244]
50	0.1	GOD	600	[243]
50	0.1	GOD	600	[237]
50[**]	2.0	2.0	10000[***]	[217]
50	0.050	GOD	100	[223]
1 - 10	0.033	1 – 10 µM/min	10 - 50	[148]

*GOD: Glucose (25 mM) and glucose oxidase (3.33 nkat/mL)
**sodium lactate
***measured as oxidation of guaiacol

The effect of factors affecting the Mn-oxidizing catalytic cycle of the enzyme versatile peroxidase, [Na-malonate] (x_1), [MnSO$_4$] (x_2) and MnP activity (x_3), were evaluated by response surface methodology. The results of this study are divided in two different sections, BPA and TCS, and the three estrogens.

5.3.2.1. Bisphenol A and triclosan

The oxidation of bisphenol A and triclosan by the action of free VP was carried out separately. The data resulting from the 27 individual experiments to evaluate the effect of [Na-malonate], [MnSO$_4$] and initial MnP activity on the elimination of BPA and TCS are displayed in **Table 5.4**.

Tabla 5.4. Full Factorial Design matrix with response for the experiments with BPA and TCS

Run	x_1	x_2	x_3	Y_1^{BPA}	Y_2^{BPA}	Y_1^{TCS}	Y_2^{TCS}
1	1	-1	-1	1.37	59.4	1.44	100
2	1	-1	-0.33	3.02	83.3	1.88	100
3	1	-1	1	3.88	92.0	1.98	100
4	1	-0.05	-1	4.00	97.9	2.01	100
5	1	-0.05	-0.33	4.89	97.9	2.37	100
6	1	-0.05	1	4.89	97.9	2.40	100
7	1	1	-1	2.51	97.9	1.07	100
8	1	1	-0.33	4.89	97.9	2.45	100
9	1	1	1	4.89	97.9	2.45	98.0
10	-0.63	-1	-1	0.69	60.5	1.01	72.6
11	-0.63	-1	-0.33	1.57	67.3	0.96	84.4
12	-0.63	-1	1	1.53	70.9	0.96	100
13	-0.63	-0.05	-1	1.55	89.2	1.16	90.2
14	-0.63	-0.05	-0.33	3.87	100	2.45	100
15	-0.63	-0.05	1	4.24	100	2.39	100
16	-0.63	1	-1	1.81	67.2	0.74	71.8
17	-0.63	1	-0.33	4.28	100	2.45	100
18	-0.63	1	1	4.43	100	2.45	100
19	-1	-1	-1	0.49	38.1	0.37	58.8
20	-1	-1	-0.33	0.95	61.2	0.95	75.4
21	-1	-1	1	0.82	75.4	0.79	96.5
22	-1	-0.05	-1	1.47	92.8	0.88	98.7
23	-1	-0.05	-0.33	5.00	100	1.01	100
24	-1	-0.05	1	3.77	100	1.17	100
25	-1	1	-1	2.75	78.1	0.59	60.7
26	-1	1	-0.33	5.00	100	1.50	98.7
27	-1	1	1	5.00	100	2.06	100

Experimental data were fitted to a second order polynomial model with the purpose of explaining the mathematical relationship between the independent variables and the response variables, **equations [5.4-5.7]**.

$$Y_1^{BPA} = 5.98 + 1.13 \cdot x_1 + 0.99 \cdot x_2 + 0.41 \cdot x_3 + 0.24 \cdot x_1 \cdot x_2 - 0.48 \cdot x_1 \\ \cdot x_3 + 0.06 \cdot x_2 \cdot x_3 - 2.87 \cdot x_1^2 - 0.99 \cdot x_2^2 + 0.54 \cdot x_3^2$$

[5.4]

$$Y_2^{BPA} = 125 + 12.6 \cdot x_1 + 8.12 \cdot x_2 + 3.82 \cdot x_3 - 0.40 \cdot x_1 \cdot x_2 - 1.79 \cdot x_1 \\ \cdot x_3 - 2.75 \cdot x_2 \cdot x_3 - 41.7 \cdot x_1^2 - 6.02 \cdot x_2^2 + 2.01 \cdot x_3^2$$

[5.5]

$$Y_1^{TCS} = 2.79 + 0.29 \cdot x_1 + 0.47 \cdot x_2 + 0.45 \cdot x_3 + 0.29 \cdot x_1 \cdot x_2 - 0.15 \cdot x_1 \\ \cdot x_3 + 0.00 \cdot x_2 \cdot x_3 - 0.83 \cdot x_1^2 - 0.36 \cdot x_2^2 - 0.29 \cdot x_3^2$$

[5.6]

$$Y_2^{TCS} = 110 + 4.53 \cdot x_1 + 14.9 \cdot x_2 + 11.6 \cdot x_3 + 3.20 \cdot x_1 \cdot x_2 - 1.27 \cdot x_1 \\ \cdot x_3 - 13.8 \cdot x_2 \cdot x_3 - 34.7 \cdot x_1^2 - 8.60 \cdot x_2^2 + 1.57 \cdot x_3^2$$

[5.7]

The fit of the data was successful in the case of the response variables Y_1 R^2 = 0.9244 and 0.8914 for BPA and TCS, respectively, whereas in the case of the response variable Y_2 was poor, R^2 = 0.8479 and 0.7159 for BPA and TCS, respectively.

Regarding the enzymatic activity level, in the case of BPA, the best elimination yield for all conditions tested were obtained at 100 U/L since it was higher than 70% in all experiments. No deactivation of the enzyme was observed in. In the case of TCS, for all conditions tested the maximum elimination yield (≥ 90%) was observed at 100 U/L. Concerning to the Mn^{2+} concentration, there is a clear positive relation with response variables, v_{max} and degradation extent. Although the elimination yield of TCS was in all cases higher than 90%, higher the Mn^{2+} concentration shorter the time required to obtain this value and, consequently, higher is Y_1. Concerning the Na-malonate concentration, it has an optimum at 10 mM (**Figure 5.4**).

Eibes et al. (2010) [148] observed that increasing the concentration up to 10 mM of sodium malonate has a negative effect on the degradation of

pharmaceuticals by VP produced by *Bjerkandera adusta*, nevertheless Eibes et al. (2005) [299] observed that the best malonic acid concentration in the degradation of anthracene was 20 mM. Mielgo et al. (2003) [35] obtained the best decolorization rates of Orange II (OII) when no malonic acid was added but they observed a noticeable loss of decolorizing capacity at a concentration of sodium malonate of 50 mM compared to 10 mM. Taboada-Puig et al. (2011) [300] obtained the highest Mn^{3+}-malonate enzymatic production at a sodium malonate concentration of 30 mM and a drop was observed at 50 mM.
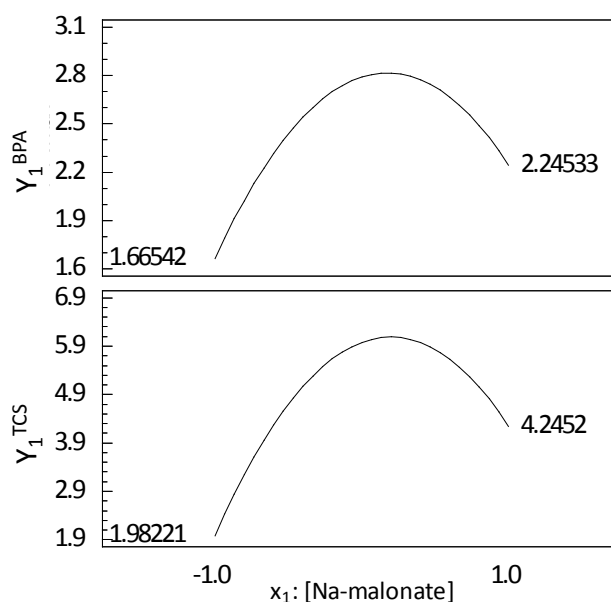

Figure 5.4. Effect of Na-malonate concentration on Y_1^{BPA} and Y_1^{TCS}.

The effect of sodium malonate concentration depends on the target compound to be oxidized, however all authors found that high concentrations of sodium malonate reduced oxidative capacity of the enzyme. This could be explained due to the Mn^{3+} ion is stronger chelated at higher sodium malonate

concentration and, consequently, it is more stable but it is a weaker oxidant [301].

In order to evaluate the effect of the concentration of sodium malonate in the chelation of Mn^{3+}, some experiments were performed by directly measuring spectrophotometrically (λ = 268 nm; ε = 11.59 mM^{-1} cm^{-1}) the formation of Mn^{3+}-malonate. As shown in **Figure 5.5a**, there is a positive relation between Mn^{3+} concentration and Mn^{3+}-malonate. Nevertheless, the sodium malonate has a negative effect on the production of Mn^{3+}-malonate and an optimum Na-malonate concentration is observed to be 10 mM.
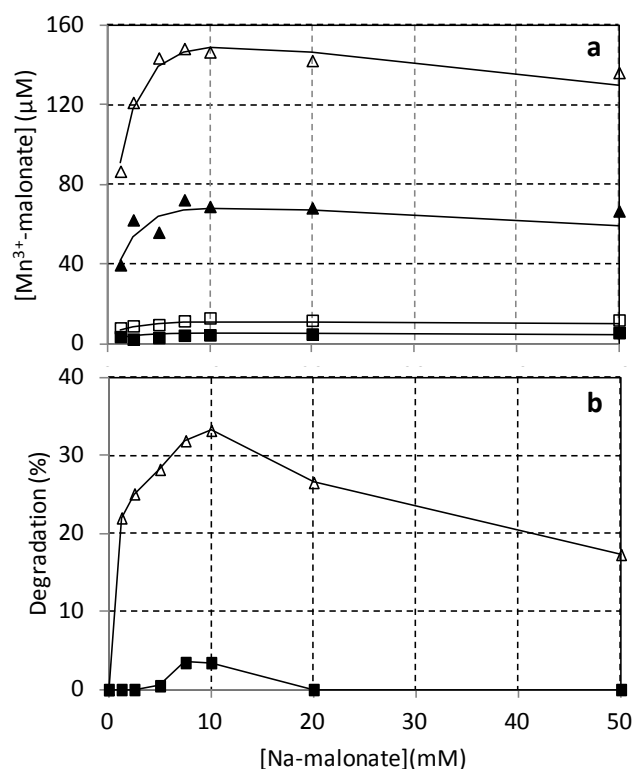

Figure 5.5. Effect of Na-malonate on (a) the Mn(III) chelation and (b) Orange II degradation. Mn^{3+} concentration: 10 μM (■), 20 μM (□), 100 μM (▲), 200 μM mM (△)

Furthermore, the ability of chemically generated Mn^{3+}-malonate to oxidize Orange II, was carried out. The effect of Na-malonate concentration was analyzed (0-50 mM) at two different Mn^{3+} concentrations (10 and 200 µM).

The initial concentration of OII was 34.25 µmol/L and the reaction was followed by spectrophotometry (λ = 480 nm) for 10 min [34]. As shown in **Figure 5.5b**, the capability of the chemically generated Mn^{3+}-malonate to oxidize the dye OII was lower at high sodium malonate concentration. As shown in **Figure 5.5a**, the concentration of Mn^{3+}-malonate, with Mn^{3+} = 0.2 mM, was very similar, 149 µM, 146 µM and 130 µM for 10 mM, 20 mM and 50 mM Na-malonate concentration, respectively, therefore, a similar OII decolorization yield was expected, however there are clear differences since the degradation yield was 33%, 27% and 17%. These results support those ones observed during the oxidation of BPA and TCS, where Mn^{3+} in presence of high Na-malonate concentration is a weaker oxidizing.

The analysis of variance (ANOVA) is a way of presenting the calculations for the significance of the effect related to a particular factor, especially for data in which the influence of several factors is being considered simultaneously. Analysis of variance decomposes the sum of squared residuals from the mean into non-negative components attributable to each factor, or combination of factor interactions. The F-test was applied for the 1% of significance level (α = 0.01), **Figure 5.6**.

In both responses Y_1^{BPA} and Y_1^{TCS}, the three independent variables, concentration of Na-malonate and $MnSO_4$, and MnP activity had a positive effect. The quadratic terms of Na-malonate concentration and $MnSO_4$ concentration had a negative effect on both response variables. In the case of Y_1^{BPA} also the interaction between Na-malonate concentration and VP activity ($x_1 \cdot x_3$), had a negative effect, whereas the interaction between Na-malonate and

MnSO$_4$ concentration had a negative effect in Y_1^{TCS}. Regarding the degradation extent, Na-malonate and MnSO$_4$ concentration had a positive effect on Y_2^{BPA}.
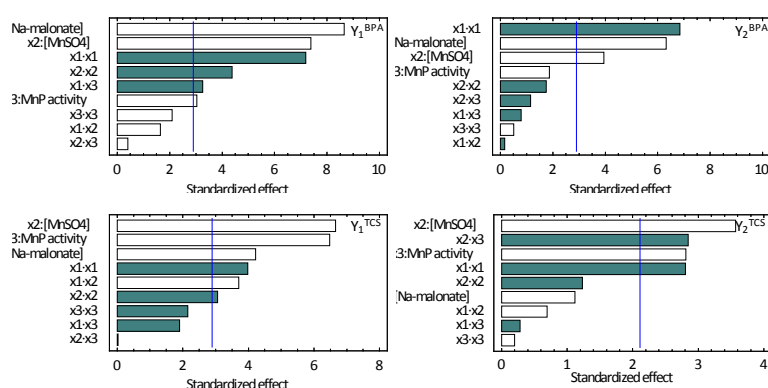

Figure 5.6. Standardized pareto chart for Y_1^{BPA}, Y_2^{BPA}, Y_1^{TCS} and Y_2^{TCS}. White bars: positive effect, grey bars: negative effect

Three-dimensional response surface model (RSM) as a function of two factors, maintaining all other factors at fixed levels, hereby in at central point, is helpful in understanding both the main and the interactions effects of these two factors. RSM has been successfully applied in this study to maximize Y_1 and Y_2 by using a non-linear optimization algorithm (**Table 5.5**).

Table 5.5. Combination of factor levels which maximizes v$_{max}$ (Y_1) and the degradation extent (Y_2)

Factor	Units	Y_1^{BPA}	Y_2^{BPA}	Y_1^{TCS}	Y_2^{TCS}
[Na-malonate]	mM	28.9	28.6	31.4	26.7
[MnSO$_4$]	mM	0.79	0.73	0.88	0.65
MnP activity	U/L	100	100	100	100

As a result of this analysis, it was found that the optimum level of the independent variables that maximizes both response variables are, approximately, 30.0 mM, 0.74 mM and 100 U/L for Na-malonate and MnSO$_4$ concentration, and MnP activity, respectively.

5.3.2.2. Estrogenic compounds

The oxidation of E1, E2 and EE2by VP was carried in the same experiments. The data resulting from the 27 individual experiments to evaluate the effect of x_1, x_2 and x_3 on the elimination of the three estrogenic compounds are displayed in **Table 5.6**.

Table 5.6. Full Factorial Design matrix with response for the experiments with E1, E2 and EE2. E_r: estrogenicity reduction

Run	x_1	x_2	x_3	Y_1^{E1}	Y_2^{E1}	Y_1^{E2}	Y_2^{E2}	Y_1^{EE2}	Y_2^{EE2}	E_r (%)
1	1	-1	-1	9.10	84.8	6.48	100	6.61	100	87.2
2	1	-1	-0.33	10.12	100	7.35	100	7.86	100	96.0
3	1	-1	1	10.32	100	7.97	100	8.12	100	91.7
4	1	-0.05	-1	9.89	100	9.13	100	8.32	100	99.3
5	1	-0.05	-0.33	14.07	97.5	16.51	99.0	14.31	98.5	98.0
6	1	-0.05	1	13.78	97.9	17.20	98.3	14.90	98.5	94.7
7	1	1	-1	9.22	86.1	7.22	100	7.66	100	90.5
8	1	1	-0.33	14.59	100	15.30	100	15.22	100	86.2
9	1	1	1	15.40	100	16.73	100	16.22	100	95.2
10	-0.63	-1	-1	7.34	86.8	4.23	96.8	5.31	96.8	97.6
11	-0.63	-1	-0.33	8.54	100	6.21	100	6.29	100	100
12	-0.63	-1	1	9.05	95.7	6.36	100	6.83	99.0	100
13	-0.63	-0.05	-1	7.96	100	6.91	100	6.08	100	100
14	-0.63	-0.05	-0.33	12.08	100	12.36	100	10.51	100	100
15	-0.63	-0.05	1	12.31	100	13.13	100	11.25	100	95.5
16	-0.63	1	-1	9.68	83.7	5.34	91.2	6.14	88.0	85.7
17	-0.63	1	-0.33	10.84	100	11.95	100	10.76	100	98.5
18	-0.63	1	1	14.65	94.9	18.36	100	13.91	100	100
19	-1	-1	-1	8.21	79.2	4.90	95.3	5.37	95.6	98.5
20	-1	-1	-0.33	10.10	100	7.69	100	7.29	100	100
21	-1	-1	1	8.83	83.5	4.75	100	5.18	100	99.3
22	-1	-0.05	-1	5.95	77.7	2.49	78.6	3.24	77.7	86.9
23	-1	-0.05	-0.33	9.17	100	7.88	100.0	7.53	100	93.3
24	-1	-0.05	1	8.38	81.4	3.50	83.4	4.62	83.4	76.3
25	-1	1	-1	7.18	69.9	3.44	70.3	4.76	71.7	87.5
26	-1	1	-0.33	9.41	100	8.37	100	8.11	100	100
27	-1	1	1	11.02	95.5	10.18	1000	9.16	100	99.1

Experimental data were fitted to a second order polynomial model with the purpose of explaining the mathematical relationship between the independent variables and the response variables. The value of the coefficients of the polynomials are displayed in **Table 5.7**.

Table 5.7. Coefficients of the second order polynomials of Y_1^{E1}, Y_2^{E1}, Y_1^{E2}, Y_2^{E2}, Y_1^{EE2} and Y_2^{EE2}, and the regression coefficient

	Y_1^{E1}	Y_2^{E1}	Y_1^{E2}	Y_2^{E2}	Y_1^{EE2}	Y_2^{EE2}
x_0	13.1	108	16.5	99.4	13.5	98.8
x_1: [Na-malonate]	1.19	0.02	2.34	-1.51	1.92	-1.58
x_2: [MnSO$_4$]	1.83	5.05	3.16	3.01	2.40	3.14
x_3: MnP activity	1.65	4.32	2.89	4.08	2.57	4.00
$x_1 \cdot x_2$	0.80	2.80	1.93	2.84	1.27	3.04
$x_1 \cdot x_3$	0.37	-0.33	0.26	1.24	0.52	1.18
$x_2 \cdot x_3$	0.31	-0.25	0.78	-3.06	0.83	-3.03
x_1^2	-1.53	-4.55	-4.75	5.02	-2.93	5.09
x_2^2	-1.18	-10.1	-2.31	-4.83	-1.89	-4.96
x_3^2	-0.59	-5.91	-1.84	-4.62	-0.89	-4.04
R^2	0.8344	0.7243	0.8338	0.6275	0.8780	0.6327

As observed in the results from the BPA and TCS experiments, the accuracy of the fit was better for the response variable Y_1 than for the degradation extent, Y_2. Presumably, this may be due to that the reaction time was longer that the necessary and at the end of the experiments, regardless of the conditions tested, the degradation extent was almost complete (**Table 5.7**). Consequently, there is no dependency between Y_2 and x_1, x_2 and x_3, therefore from now on the analysis is focused in the results of the response variable Y_1.

The results of the analysis of variance for Y_1^{E1}, Y_1^{E2} and Y_1^{EE2} are shown in **Table 5.8**. The ANOVA table partitions the variability in Y_1 into separate pieces for each of the independent variables x_1, x_2 and x_3. It then tests the statistical significance of each independent variable by comparing the mean square against an estimate of the experimental error. In this case, the three individual effects have *P-values* less than 0.01, indicating that they have a significantly effect on response variables at the 99.0% confidence level.

Table 5.8. Analysis of variance for Y_1^{E1}, Y_1^{E2} and Y_1^{EE2}

	P-value		
	Y_1^{E1}	Y_1^{E2}	Y_1^{EE2}
x_1: [Na-malonate]	**0.0009**	**0.0006**	**0.0001**
x_2: [MnSO$_4$]	**0.0000**	**0.0000**	**0.0000**
x_3: MnP activity	**0.0000**	**0.0001**	**0.0000**
$x_1 \cdot x_1$	0.1107	0.0122	0.0190
$x_1 \cdot x_2$	0.0298	**0.0073**	**0.0080**
$x_1 \cdot x_3$	0.2803	0.6782	0.2280
$x_2 \cdot x_2$	0.0348	0.0275	**0.0087**
$x_2 \cdot x_3$	0.3885	0.2539	0.0789
$x_3 \cdot x_3$	0.3232	0.1109	0.2389

The interaction between Na-malonate and MnSO$_4$ concentration had a positive effect in both Y_1^{E2} and Y_1^{EE2}, whereas the quadratic term of MnSO$_4$ concentration had a significant negative effect on Y_1^{EE2} (**Figure 5.7**). RSM was applied in this study to maximize Y_1^{E1}, Y_1^{E2} and Y_1^{EE2} by using a non-linear optimization algorithm.
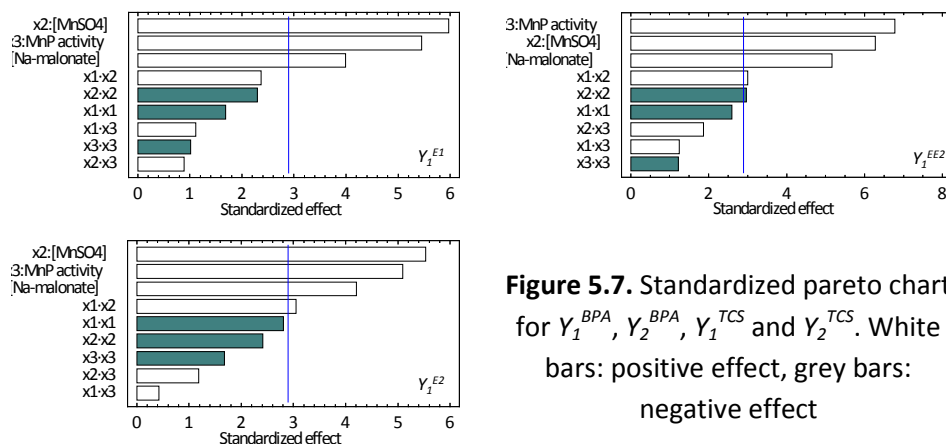
Figure 5.7. Standardized pareto chart for Y_1^{BPA}, Y_2^{BPA}, Y_1^{TCS} and Y_2^{TCS}. White bars: positive effect, grey bars: negative effect

RSM was applied in this study to maximize Y_1^{E1}, Y_1^{E2} and Y_1^{EE2} by using a non-linear optimization algorithm. The results are displayed on **Table 5.9**. Summarizing, the best results in terms of maximum rate of degradation of estrogens are, approximately, 41 mM and 1.00 mM Na-malonate and MnSO$_4$ concentration, respectively, and 100 U/L MnP activity.

Table 5.9. Combination of factor levels which maximizes Y_1^{E1}, Y_1^{E2} and Y_1^{EE2}

Factor	Units	Y_1^{E1}	Y_1^{E2}	Y_1^{EE2}
[Na-malonate]	mM	44.5	37.2	41.0
[MnSO$_4$]	mM	1.00	1.00	0.99
MnP activity	U/L	100	100	100

Concerning the estrogenic activity, threre was not a correlation between the conditions and the reduction of the estrogenicity. However, as shown in **Table 5.6**, for all experiments the reduction was higher than 80% suggesting that the products originated during the enzymatic treatment have no estrogenic activity.

5.3.3. Batch elimination of EDCs by VP-GOD-CLEA®s

The removal of BPA, TCS, E2 and EE2 was tested by using VP-GOD-CLEA®s, free VP-GOD, with glucose as enzymatic substrate in batch experiments. The mixture of free VP and GOD as well as VP-GOD-CLEA®s were able to eliminate more than 90% of all pollutants except TCS, of which 40.7±2.3 and 25.6±2.5% were removed, respectively (**Figure 5.8**).
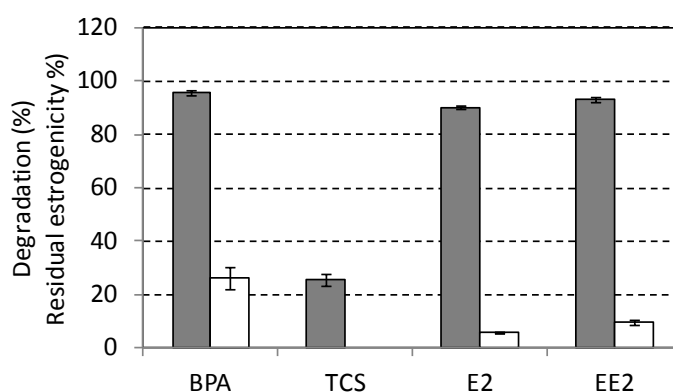

Figure 5.8. Results from the elimination of BPA, TCS, E2 and EE2 by VP-GOD-CLEA®s. Grey bars: degradation extent, white bars: residual estrogenicity.

All processes proved to be very effective in eliminating four of the studied EDCs, however, another important aspect concerning the removal of this kind of compounds is the residual estrogenicity. A 10-min treatment with free VP reduced the estrogenic activity of BPA, E2, and EE2 by 73.6±4.2%, 94.2±0.4% and 90.3±1.0%, respectively, whereas VP-GOD-CLEA®s treatment reduced estrogenicity of BPA, E2 and EE2 by 72.9±10.7%, 72.5±4.1%, and 60.4±5.9%, respectively (**Figure 5.8**). This difference could be due to a modification of the catalytic properties of the enzyme upon insolubilization [283]. The estrogenic activity of TCS could not be determined using the LYES as already described for the YES-assay by Cabana et al. (2007) [230].

5.3.4. Identification of degradation products of BPA, TCS, E1, E2 and EE2

The identification of the main degradation products by GC-MS is not straightforward since in most cases the mass spectrum of the originated compounds is similar to its parent compound's one or the suggested metabolite is not commercially available. However, in this chapter, the tentative identification of the degradation products of bisphenol A, triclosan, estrone, 17β-estradiol and 17α-ethinylestradiol, was performed by the analysis of the results obtained by GC-MS.

During the derivatization of the EDCs, the hydroxyl group from each molecule reacts with the MTBSTFA resulting in the loss of a hydrogen atom and the formation of methyl-terbutyl-sylil derivatives ([297], **Figure 5.9**).
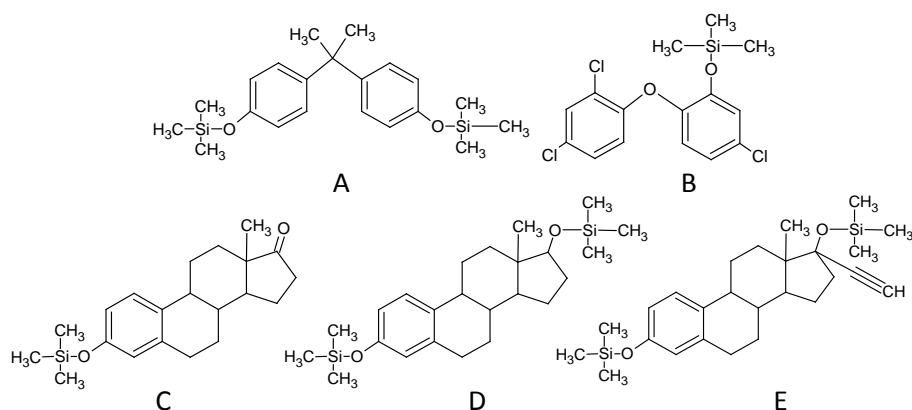

Figure 5.9. Derivatized structures of (A) BPA, (B) TCS, (C) E1, (D) E2 and (E) EE2

5.3.4.1. Bisphenol A

Three different degradation products, BPA_1, BPA_2 and BPA_3, were detected at three different retention times, 10.5, 11.9 and 27.7 min, respectively, during the treatment of bisphenol A with VP (**Figure 5.10**).

Figure 5.10. Degradation of BPA by VP. Chromatogram of the sample at t = 10 min

BPA$_1$

On the basis of the mass spectrum (MS, **Figure 5.11**) of the degradation product *BPA$_1$*, it may be 4-(2-hydroxypropan-2-yl)phenol.
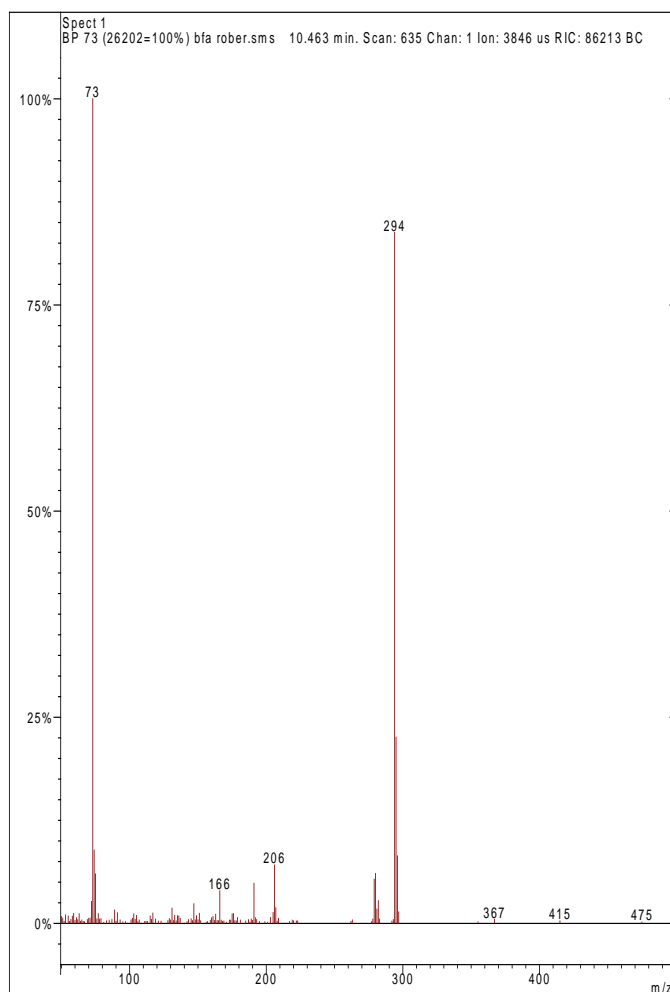

Figure 5.11. Mass spectrum of *BPA$_1$*

This compound has a molecular ion of m/z: 294 and, after the loss of the tert-butyil-sylil derivative, as well as the oxygen, the main quantification ion is m/z =

206 (**Figure 5.12**). Moreover, a new breakdown of the molecule form the quantification ion m/z = 166 (**Figure 5.12**).
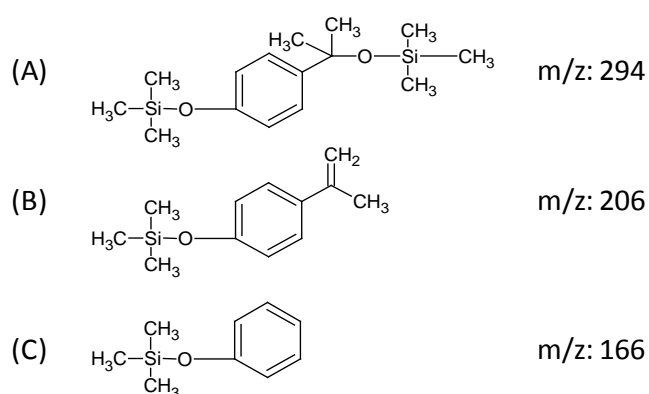

Figure 5.12. Molecular structure of 4-(2-hydrpxypropan-2-yl)phenol (A) and the two quantification ions: m/z = 206 (B) and m/z = 166 (C).

The compound 4-(2-hydrpxypropan-2-yl)phenol was also identified as a degradation product in the elimination of BPA with the bacteria *Sphingobium xenophagum* [302] and *Sphingomonas* sp. strain TTNP3 [303]. During the elimination of BPA by the oxidative action of Ferrate (IV), Li et al. (2008) [197] also found that BPA_1 is an oxidation product.

BPA$_2$

On the basis of the mass spectrum (**Figure 5.13**) of the degradation product *BPA$_2$*, it was not possible to identify this degradation product since it is the same than *BPA$_1$* except for the quantification ion m/z = 239.
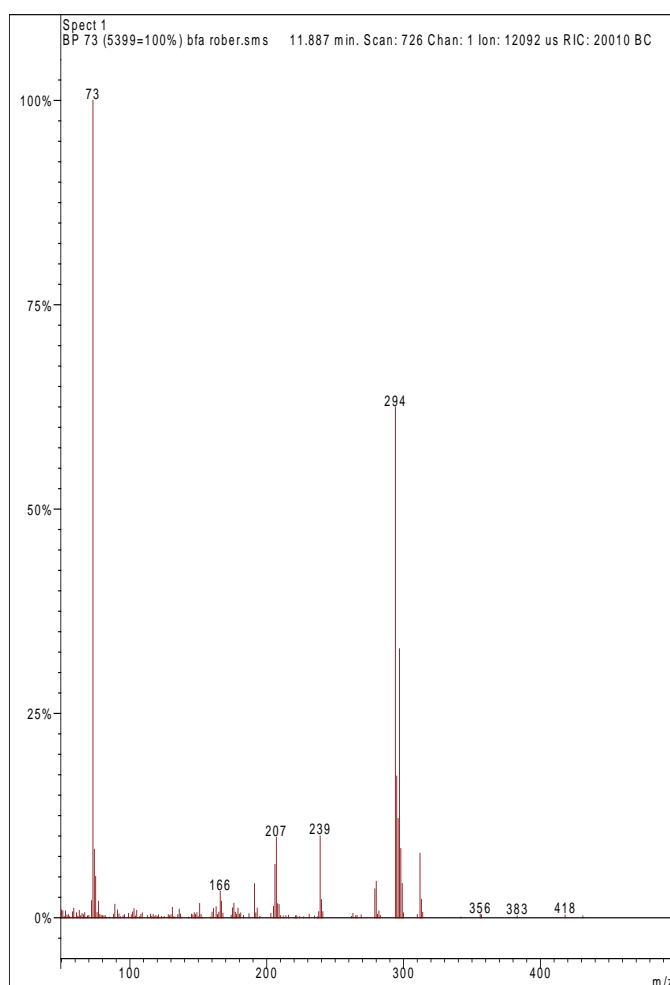

Figure 5.13. Mass spectrum of *BPA$_2$*

BPA$_3$

On the basis of the MS (**Figure 5.14**) of the degradation product *BPA$_3$*, it may be 2,2-bis(4-hydroxyphenyl)-1-propanol.

Spect 1
BP 446 (3921=100%) bfa rober.sms   27.648 min. Scan: 1731 Chan: 1 Ion: 24031 us RIC: 10052 BC
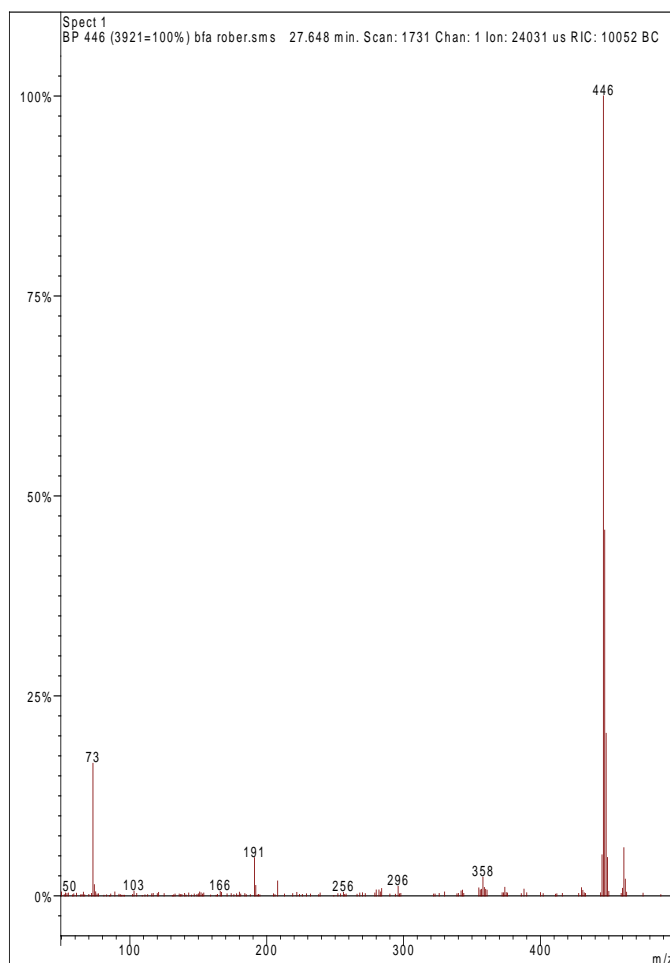
Figure 5.14. Mass spectrum of *BPA$_3$*

This compound has a molecular ion of m/z: 460 and, after the ionization, the four main quantification ions are m/z = 446, m/z = 358, m/z = 256 and m/z = 191 (**Figure 5.15**). The compound 2,2-bis(4-hydroxyphenyl)-1-propanol was also identified by Lobos et al. (1992) [304] and Spivack et al. (1994) [305] as a

degradation product in the elimination of BPA with a gram negative bacteria. Sasaki et al. (2009) [306] also detected *BPA₃* as a degradation product in the reaction between BPA and the cytochrome P450 monooxygenase.
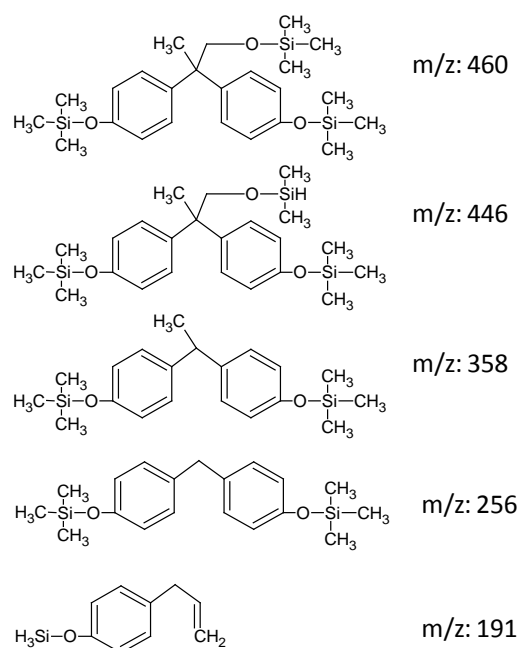

Figure 5.15. Molecular structure of 2,2-bis(4-hydroxyphenyl)-1-propanol, m/z = 460, and the quantification ions: m/z = 446, m/z = 358, m/z = 256 and m/z = 191.

It was demonstrated by Kitamura et el. (2005) [307] that when the propane bridge of BPA was substituted with a hydrophilic group, the estrogenic activities of these compounds were markedly inhibited, showing the specific nature of this response (compare BPA_3 and with BPA). In fact, the EC_{50} (half maximal effective concentration) values of BPA_3 increased 17.5-fold against BPA, 11 and 0.63 µM, respectively.

Gültekin and Ince (2007) [308] summarized the results of many studies in which AOPs were used to degrade EDCs and concluded that in general, the

analysis of estrogenic activity showed that the effluent either exhibited no hormonal activity or much less that of the original sample. They prepared a list of oxidation by-products and found that phenol and p-hydroquinone were the two most commonly observed products regardless of the AOP technique used for degrading bisphenol A. Hydroxyacetophenone was identified in photo-Fenton and photocatalytic processes, while methylbenzofuran was observed in photo-Fenton, some TiO_2 and ozonation processes. Similarly, Gözmen et al. (2003) [207], after applying Fenton reactions, detected the following by products: o-monohydroxylated BPA, dihydroxylated BPA, m-monohydroxylated BPA, phenol, catechol, hydroquinone, benzoquinone, resorcinol, 4-isopropenylphenol, 4-hydroxymandelic acid, 4-hydroxy benzoic acid, butendionic acid, 4-oxobutenoic acid, acetic acid and formic acid.

The polymerization at level of C-C bond formation was previously proposed for BPA and the dimer produced by laccase of *T. villosa* was identified as 5,5'-bis[1-(4-hydroxy-phenyl)-1-methyl-ethyl]-biphenyl-2,2'-diol [226]. More recently, Huang and Weber (2005) [309] proposed possible reaction pathways in which the polymerization mechanism of BPA also occurs through C–O bonds.

5.3.4.2. Triclosan

Two different degradation products, TCS_1 and TCS_2, were detected at two different retention time, 9.8 and 27.7 min, respectively, during the treatment of triclosan with VP (**Figure 5.16**).
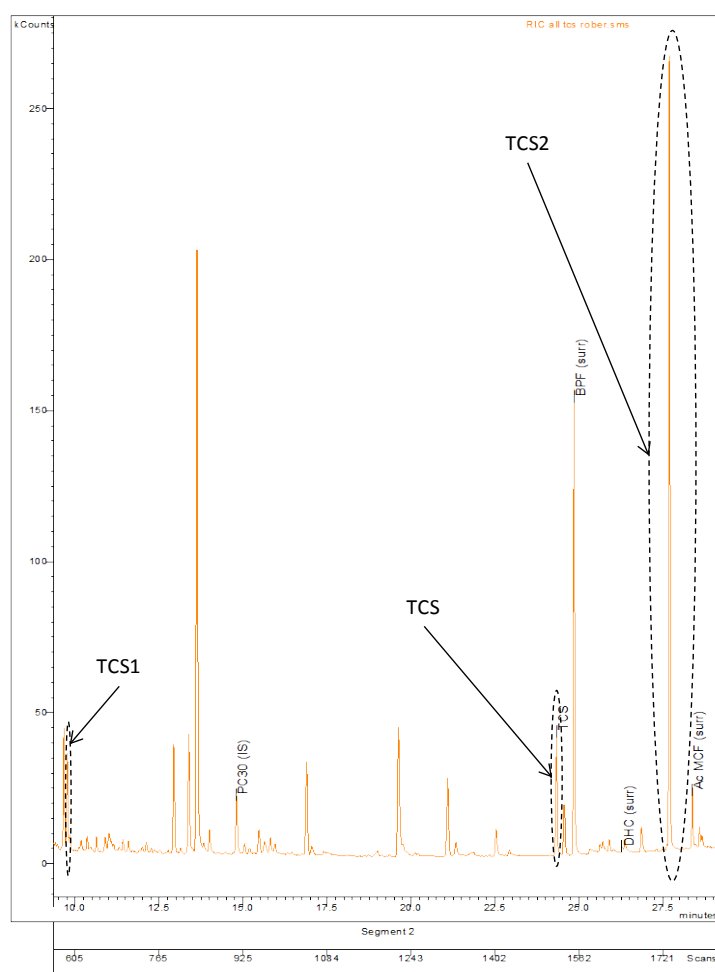

Figure 5.16. Degradation of TCS by VP. Chromatogram of the sample at t = 10 min

TCS$_1$

On the basis of the MS (**Figure 5.17**) of the degradation product *TCS$_1$*, it may be 4-chlorocatechol. This compound has a molecular ion of m/z: 288, and after the ionization, the two main quantification ions are m/z = 166 and m/z = 138 (**Figure 5.18**).
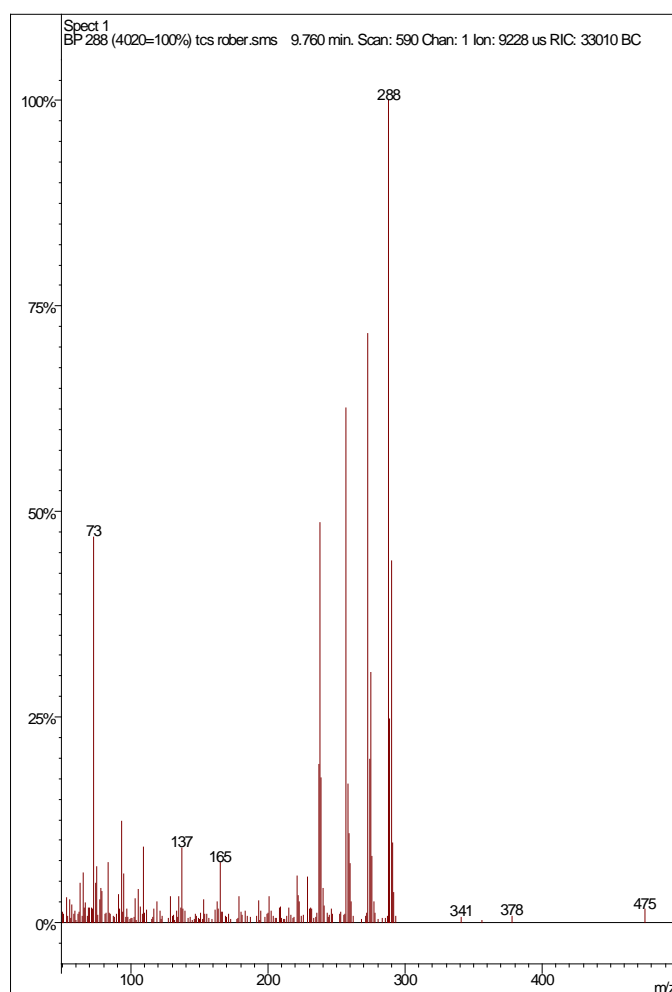

Figure 5.17. Mass spectrum of *TCS$_1$*

The compound 4-chlorocatechol was also identified by Sirés et al. (2007) [310] as a degradation product in the treatment of BPA by electro-fenton. The same degradation product was also found by Yang et al. (2001) [198] as a intermediate in the elimination of BPA by$[FeO_4]^{2-}$. On the basis of the mass spectrum, the degradation product TCS_1 may also be the compound chlorohydroquinone. This compound has a molecular ion of m/z: 288 (**Figure 5.19**). After the ionization, the two main quantification ions are m/z = 166 and m/z = 138 (**Figure 5.19**).
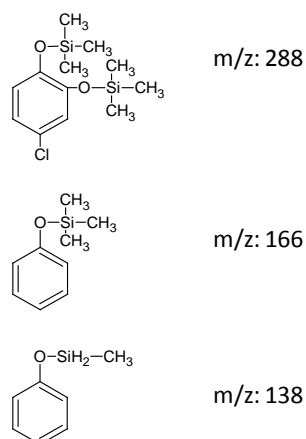

Figure 5.18. Molecular structure of 4-chlorocatechol, m/z = 288, and the quantification ions: m/z = 166 and m/z = 138

The compound chlorohydroquinone was also identified as a degradation product after the elimination of triclosan by the ligninolytic enzyme laccase [238]. The same metabolite was detected by Sirés et al. (2007) [310] as a degradation product during the treatment of triclosan by the advanced oxidation process electro Fenton. Yang et al. (2001) [198] also identified the chlotohydroquinone as a degradation product after the oxidation of triclosan by ferrate.
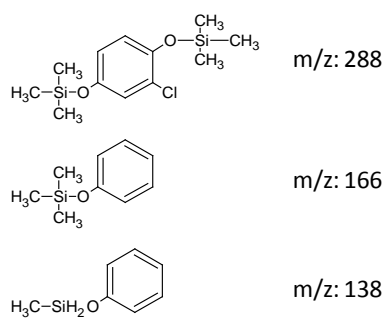
Figure 5.19. Molecular structure of chlorohydroquinone, m/z = 288, and the quantification ions: m/z = 166 and m/z = 138

TCS$_2$

According to the MS of TCS_1, it may be a hydroxylated form of triclosan.
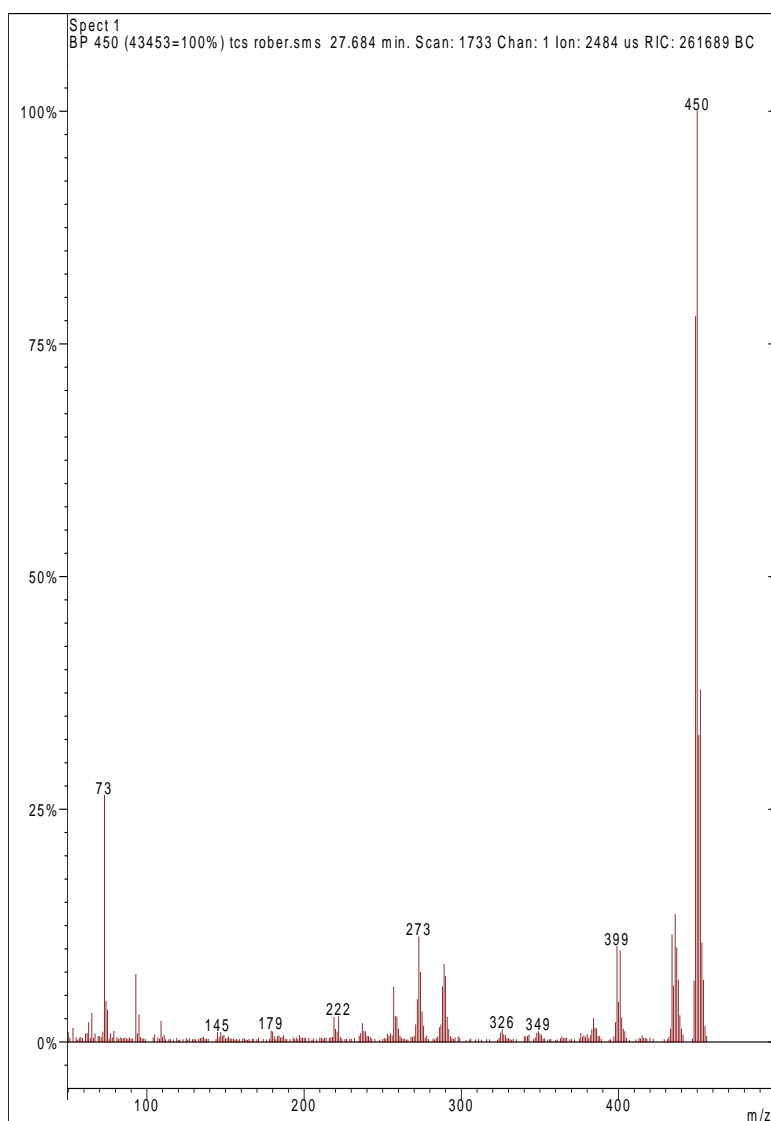

Figure 5.20. Mass spectrum of TCS_2

The hydroxyl group can be introduced in six different positions of the triclosan molecule (**Figure 5.21**).
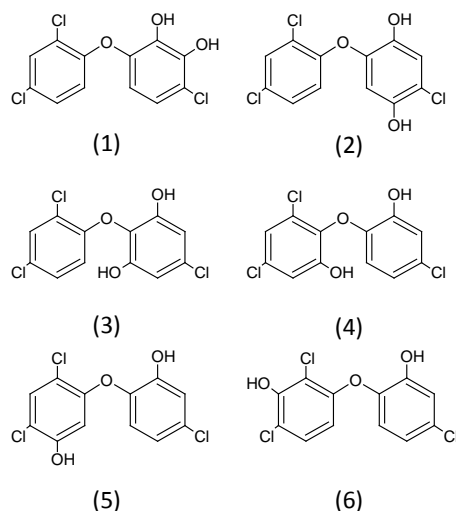
Figure 5.21. Different hydroxylated forms of triclosan

TCS$_2$ was also identified as a degradation product in the phototransformation of triclosan in presence of TiO$_2$ [311]. The same degradation product was also detected by Sankoda et al. (2011) [312] by using a system also based in TiO$_2$.Wu et al. (2010) [313] identified a hydroxylated form of triclosan in an *in vivo* system with rats and in an *in vitro* system with rat liver S9 and microsome. Taking as a model the hydroxylated form (6), the derivatized form and the main quantification ions are shown in **Figure 5.22**.

Murugesan et al. (2010) [238] enhanced the transformation of TCS by laccase in the presence of redox mediators. They identified by-products using LC, ESI-MS and GC-MS. In the absence of redox mediator, 56.5% TCS removal was observed within 24 h, concomitant with formation of new products with molecular weights greater than that of TCS. These products were dimers and trimers of TCS, as confirmed by ESI-MS analysis. The use of 1-hydroxybenzotriazole (HBT) and syringaldehyde as mediators significantly enhanced TCS transformation and resulted in products with lower molecular weights than TCS, including 2,4-dichlorophenol, dechlorinated forms of 2,4-DCP

and 2-chlorohydroquinone. These results confirmed the involvement of two mechanisms of laccase-catalyzed TCS removal: (i) oligomerization in the absence of redox mediators, and (ii) ether bond cleavage followed by dechlorination in the presence of redox mediators.
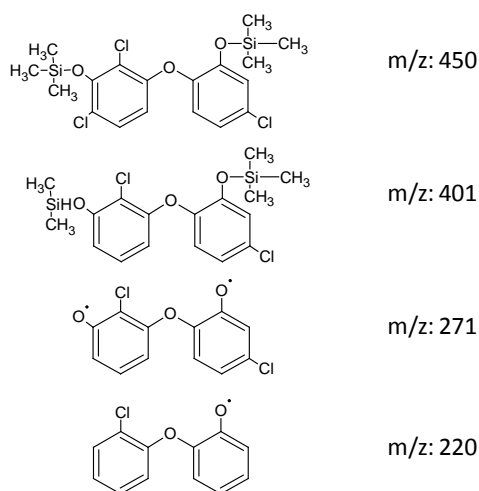
Figure 5.22. Molecular structure of the hydroxylated triclosan, m/z = 450, and the main quantification ions: m/z = 401, m/z = 271 and m/z = 220

Cabana et al. (2007) [230] found that the elimination of TCS by laccase from *Coriolopsis polyzona* produces essentially dimers. They show that the polymerization could occur at the level of C-C bond formation, which could be located between phenol moieties of EDCs. By using MS equipped with an electrospray atmospheric pressure ionization (ESI) source in the negative ion monitoring mode (ESI-MS), the authors detected chloroform-soluble metabolites, the molecular weights of the degradation by-products were 288, 574, 860 and 1146 amu.

5.3.4.3. Estrone, 17β-estradiol and 17α-ethinylestradiol

Six, four and three metabolites from the degradation of E1, E2 and EE2, respectively, were detected, but none of them could be identified. However, two of the metabolites of E2 (E21 and E22, **Figure 5.23**) appeared in the chromatograms obtained by GC-MS at the same time of those found by Lloret et al. (2012) [314] (32.0 and 32.15 min) using laccase, corresponding to the by-products coded as metE2-1 and metE2-2, respectively. In both studies, these metabolites presented similar m/z values (374 and 414 for E21 and E22, respectively).

A more exhaustive study will be required to identify the degradation products detected after the degradation of EDCs using VP. This could be carried out by using some additional preparative steps (ultrafiltration and settling), other analytical techniques (like TLC, NMR, etc) and by comparing the results with standards to ensure their identification. Additionally, it will be considered the possibility that the degradation products could either be produced by the cleavage of the aromatic rings of the EDC (rendering smaller species) or by oxidative coupling reactions, producing dimers, oligomers and polymers.

Mao et al. (2009) [242] degraded natural and synthetic estrogens using LiP from *P. chrysosporium* and by applying MS indentified two peaks (m/z = 268.8 and 541.0) related to the molecular ions of two reaction products, estrone (MW 270) and a dimer of 17β-estradiol (MW 542). The molecular ion of 17β-estradiol (E2, m/z = 270.7) appeared in the spectrum of the reaction sample, reflecting incompleteness of the reaction.
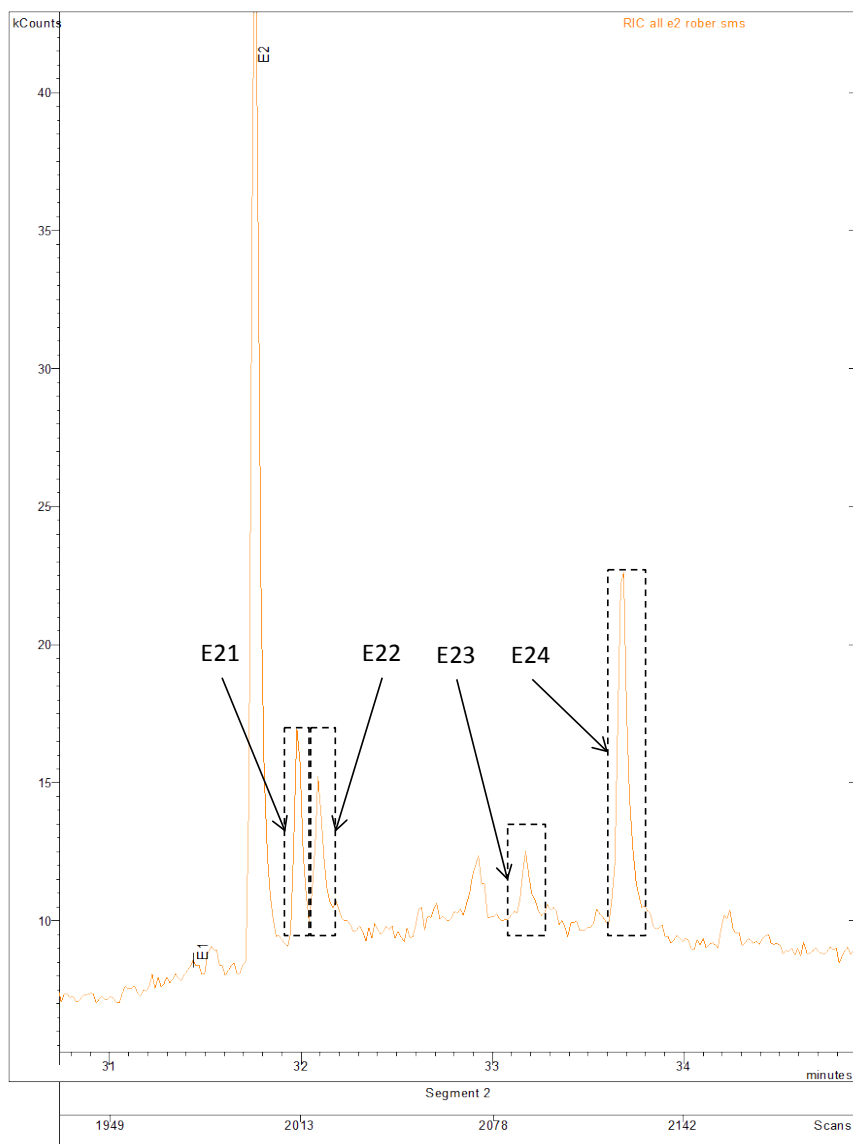
Figure 5.23. Degradation of E2 by VP. Chromatogram of the sample at t = 10 min

When samples were prepared at stronger reaction conditions, E2 did not appear in the mass spectrum, nor did estrone, indicating the intermediate nature of estrone. The molecular ion of an E2 trimmer (m/z = 811.0) was also

identified in samples that were prepared under stronger reaction conditions, suggesting that E2 tends to polymerize under LiP catalysis, likely via oxidative coupling that has been previously observed for the reactions mediated by horseradish peroxidase (HRP) and laccases [230]. It has been shown that such enzyme-mediated polymerization can effectively reduce the estrogenicity of parent estrogens [26].

In a subsequent study the same researchers found that during the degradation of E2 by LiP the presence of natural organic matter and/or veratryl alcohol impacts the formation and distribution of the products [315]. They found six products (three dimers and two trimers of E2, and an unidentified by-product with MW of 270) the major products appeared to be oligomers resulting from E2 coupling. These products likely formed colloidal solids in water that can be removed via ultrafiltration or settled during ultracentrifugation.

Tanaka et al. (2009) [239] conducted the degradation of estrone, 17β-estradiol and 17α-ethynyletstradiol using laccase from *Trametes* sp. Ha1. They proposed that the initial reaction products are dimmers. In fact, one of the purified initial oxidation products of EE2, detected by high resolution MS, was a dimer with m/z = 590.2007. They observed that the initial oxidation rates increased proportionally to the estrogen concentrations, while in the later stage of the reaction the dimers concentration decreased. Finally, based on the initial reaction product (dimers of estrogens) and the time course of oxygen consumption in the reaction they suggest that the estrogens were oligomerized in the oxidation.

Nicotra et al. (2004) [316] used laccase from *Mycelyopthora* and *Trametes* strains for degrading E2 in organic solvents or in a biphasic system. They observed that laccase oxidation generates an oxygen radical that can delocalize to carbon-located radicals. Subsequent coupling of these reactive

intermediates produces C-C or C-O dimers, which could be further oxidized to generate oligomers and polymers. Accordingly, in addition to a brown precipitate (due likely to the formation of insoluble oligomeric and polymeric derivatives), thin-layer chromatography (TLC) showed the formation of two products more polar than E2. These compounds were isolated by flash chromatography and analyzed by MS. The mass values of the molecular peaks (542 m/z in both cases) were consistent with a dimeric structure for all the derivatives.

Taking together the results of the presented studies, it can be concluded that the more common mechanism of degradation observed when using ligninolytic enzymes is polymerization/ oligomerization, being dimmers and trimmers of the EDCs, the most frequently detected by-products. However, depending on the operational conditions and the ligninolytic enzyme used (for example, using lacasses without redox mediators), smaller by-products could be also formed. This information suggest, that when ligninolytic enzymes are used for degrading EDCs special care should be taken in the selection of the pretreatment of the samples before using the analytical techniques. These should include steps for separating both, the soluble (low molecular weight compounds) and less soluble (oligomers and polymers) fractions, and then applying the most adequate technique in each case for analyzing the by-products.

5.4. Conclusions

The capability of the fungus anamorph R1 of *Bjerkandera* to oxidize five endocrine disrupting chemicals, BPA, TCS, E1, E2 and EE2, and to reduce their estrogenic activity, was demonstrated through *in vivo* static experiments. In addition, the effect of three important variables of the Mn-oxidizing catalytic cycle of the enzyme versatile peroxidase, concentrations of Na-malonate and $MnSO_4$ and the initial enzymatic activity, in the *in vitro* oxidation of the above mentioned EDCs, was evaluated by response surface methodology.

Among the evaluated variables, the effect individual effect of Na-malonate and $MnSO_4$ presented the most significant effect on both maximum degradation rate as well as degradation extent. Moreover, the quadratic term of the Na-malonate concentration had a very significant effect. This fact reflects that at very low concentrations of the organic acid there is not enough chelating agent to stabilize the ion Mn^{3+}, and at very high concentrations the Mn^{3+} is so trapped that is not able to oxidize the organic pollutants. The optimum conditions for the degradation were estimated to be 30-40 mM Na-malonate concentration, 0.8-1 mM $MnSO_4$ concentration and an initial enzymatic activity of 100 U/L.

An attempt to identify the degradation products was performed in *in vitro* experiments. Three metabolites of BPA were found after 10 minutes of reaction, *BPA₁* (4-(2-hydrpxypropan-2-yl)phenol), *BPA₂* (not identified) and BPA₃ (2,2-bis(4-hydroxyphenyl)-1-propanol) and two degradation products of, *TCS₁* (4-chlorocatechol or chlotohydroquinone) and *TCS₂* (hydroxylated triclosan). Concerning the estrogenic compounds, six, four and three degradation products were found for E1, E2 and EE2, respectively, after 10 minutes of reaction, however, the identification was not successful.

Chapter 6

Biocatalytic generation of Mn^{3+}-chelate as a chemical oxidant of organic compounds

Chapter 6. Biocatalytic generation of Mn^{3+}-chelate as a chemical oxidant of organic compounds

6.1. Introduction

6.2. Materials and methods

6.2.1. Influence of organic acids, Mn^{2+}, H$_2$O$_2$, enzymatic activity and pH on Mn^{3+}-chelate formation

6.2.2. Batch production of Mn^{3+}-chelate and its application to the process of oxidizing several organic compounds

6.2.3. "Two-stage" system for the continuous production of the Mn^{3+}-complex and decolorization of an azo dye, Orange II

6.2.4. Determination of the concentrations of the dye Orange II and anthracene

6.3. Results and discussion

6.3.1. Influence of key parameters on the batch production of Mn^{3+}-chelate

6.3.1.1. Effects of the type and concentration of organic acid

6.3.1.2. Effect of MnSO$_4$ concentration

6.3.1.3. Effect of H$_2$O$_2$ concentration

6.3.1.4. Effect of pH

6.3.1.5. Effect of VP concentration

6.3.2. Effect of temperature on the stability of the Mn^{3+}-malonate complex

6.3.3. Application of the Mn^{3+}-chelate for oxidizing recalcitrant compounds

6.3.3.1. Azo dye, Orange II

6.3.3.2. Endoxrine disrupting chemicals, bisphenol A and triclosan

Chapter 6. Biocatalytic generation of Mn^{3+}-chelate as a chemical oxidant of organic compounds

6.1. Introduction

Lignin is one of the most widespread substances in nature. One widely held principle concerning lignin degradation by fungi is the necessity of primary attack by extracellular oxidoreductases including lignin peroxidase (LiP), manganese peroxidase (MnP) and laccase [317]. In addition, a short list of fungi contains another lignin-degrading enzyme: versatile peroxidase (VP). VP is also known as hybrid Mn-peroxidase and combines properties of LiP and MnP, i.e., it is able to oxidize Mn^{2+} and non-phenolic aromatic compounds [45]. Nevertheless, the catalytic efficiency of VP in the presence of Mn^{2+} is considerably higher than its efficiency in the presence of other aromatic substrates [257].

The catalytic cycle of VP includes successive conversions in which the enzyme is oxidized by H$_2$O$_2$ to a two-electron-oxidized intermediate, compound I. Compound I removes one electron from the substrate and passes the electron to a one-electron-oxidized species, compound II. At this stage of the catalytic cycle, organic substances and Mn^{2+} can serve as electron donors. Compound II removes another electron from the substrate, and subsequently, the enzyme returns to its native form. The oxidation of Mn^{2+} generates Mn^{3+}, which is a strong oxidative species (1.54 V) and acts as a mediator in the degradation of organic compounds[4]. That is, target substrates are oxidized by Mn^{3+} and not directly by the enzyme. This ion is rather unstable and requires the presence of organic acids that form Mn^{3+} chelates, which can then non-specifically oxidize organic molecules [45, 318, 319]. The formation of complexes with dicarboxylic acids alters the potential of Mn^{3+}. The more strongly chelated Mn^{3+} is, the more stable. Increased stability inhibits dismutation to Mn^{2+} and Mn^{4+} but also makes

Mn^{3+} a weaker oxidant [301]. Mn^{3+}-chelates have several advantages over proteins when used as oxidants. They are more tolerant to protein-denaturing conditions such as low and high temperatures, wide range of pH, oxidants, detergents and proteases. Such chelates may also penetrate microporous barriers that prevent the passage of proteins.

The main drawback related to the application of enzymatic systems is that consumption and destabilization of the enzyme in the process are evidenced, which renders low degradation productivity and limits the applicability of the enzymatic process [35, 320].

A more efficient enzymatic system would accomplish two main objectives: maximization of Mn^{3+}-chelate production and minimal consumption and deactivation of the enzyme. In this sense, separation of the catalytic cycle of the enzyme and degradation of the target recalcitrant compound by Mn^{3+} reactive species may be useful to accomplish both goals.

In this study, three different groups of compounds were considered as target substances: an industrial azo dye (Orange II), natural and synthetic estrogens (estrone, 17β-estradiol and 17α-ethinylestradiol) with endocrine disrupting potential and a polycyclic aromatic hydrocarbon (anthracene). These compounds are considered to be persistent and recalcitrant pollutants and present diverse chemical structures and physico-chemical properties. A number of different key parameters were evaluated to fuffil the development of a "two-stage" process. In this sense, the influence of specific factors that may directly affect the VP catalytic cycle and the stability of the complex were studied: type and concentration of organic acids, Mn^{2+}, H_2O_2 as well as temperature and pH. Finally, both the enzymatic and degradation reactors were coupled in a continuous operation to oxidize the dye.

6.2. Materials and methods

6.2.1. Influence of organic acids, Mn^{2+}, H$_2$O$_2$, enzymatic activity and pH on Mn^{3+}-chelate production

The effects of several parameters, such as enzymatic activity, organic acid (type and concentration), concentrations of Mn^{2+} and H$_2$O$_2$ and pH on the formation of Mn^{3+}-chelate were evaluated. The reactions were started by the addition of H$_2$O$_2$ and followed for 60 min in a Shimadzu UV-vis 160A spectrophotometer.

Several organic acids, malonic (Sigma-Aldrich, St. Louis, MO, USA), oxalic (Panreac, Montcada, Reixac, Spain), tartaric (Sigma-Aldrich) and lactic (Panreac, Montcada) acid, were evaluated at variable concentrations from 5 to 50 mM to evaluate the production of Mn^{3+}-chelate in the presence of 2 mM MnSO$_4$ and 0.40 mM H$_2$O$_2$ at pH 4.5. All acid solutions were prepared from their sodium salts. The effect of initial MnSO$_4$ concentration between 1 and 4 mM was determined at pH 4.5 in the presence of 5, 10, 30 and 50 mM malonate with 0.40 mM H$_2$O$_2$. The effect of H$_2$O$_2$ concentration, from 0.02 to 4 mM, on the formation of the Mn^{3+}-chelate was evaluated in the presence of 30 mM malonate and 2 mM MnSO$_4$ at pH 4.5. The effect of pH (ranging from 3 to 9) was evaluated in the presence of 30 mM malonate, 2 mM MnSO$_4$ and 0.40 mM H$_2$O$_2$. Titers of MnP activity were systematically changed from 5 to 100 U/L to evaluate the production of the complex in the presence of 30 mM malonate, 2 mM MnSO$_4$ and 0.40 mM H$_2$O$_2$ at pH 4.5. The stability of the Mn^{3+}-chelate was studied at three temperatures, -18ºC, 4ºC and room temperature.

6.2.2. Batch production of Mn^{3+}-chelate and its application to the process of oxidizing several organic compounds

The potential oxidation capacity of the Mn^{3+}-chelate was evaluated for different organic compounds after batch production of the Mn^{3+}-chelate to supply a

sufficient amount of the complex. Batch production was conducted in a stirred Amicon ultrafiltration cell (8200) with 150 mL of working volume and a 10 kDa cut-off polyethersulfone membrane (Millipore PBGC06210, **Figure 6.1**). Prior to batch production, the enzyme was dialyzed in 10 mM malonate buffer (pH 4.5). The standard composition of the reaction medium in the enzymatic reactor was: 100 U/L VP, 0.40 mM H_2O_2, 30 mM malonate and 2 mM Mn^{2+}. After 15 min in the Amicon cell, N_2 was used to flush the system to assure a head space pressure of 2 bar and allow the production of the complex at a rate of 2.9±0.5 mL/min for 30-45 min. The complex was then measured and an average concentration of 350 µM Mn^{3+}-chelate was obtained, which was later applied in the batch oxidation experiments.
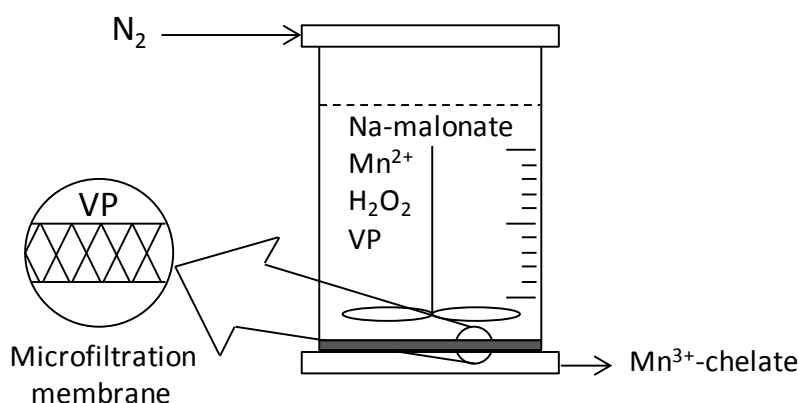
Figure 6.1. Schematic diagram for the batch production for the batch production of Mn^{3+}-malonate in a stirred AMICON ultrafiltration cell 8200

Four different groups of compounds: one azo dye (Orange II); two endocrine disrupting chemicals (EDCs) bisphenol A (BPA, Sigma-Aldrich) and triclosan (TCS, Sigma-Aldrich); natural and synthetic estrogens, estrone (E1, Sigma-Aldrich), 17β-estradiol (E2, Sigma-Aldrich) and 17α-ethinylestradiol (EE2, Sigma-Aldrich); and one polycyclic aromatic hydrocarbon, anthracene (Janssen

Chimica, NJ, USA), were selected as target compounds for the oxidation reaction. The experiments were performed in batch on a small scale, from 1 mL cuvettes to 100-mL Erlenmeyer flasks**.** Control experiments in the absence of the complex were also conducted in parallel.

Oxidation of the Orange II dye was performed in a 2 mL quartz spectrophotometer cell with 1 mL reaction mixture for 10 min. Decolorization was spectrophotometrically measured at 480 nm [34] by adding the stock solution of the dye (100 mg/L) and Mn^{3+}-chelate. Different initial concentrations of Orange II, from 10 to 27 mg/L, and Mn^{3+}-chelate, from 70 to 200 µM, were evaluated.

Transformation of the estrogen compounds was performed in 100 mL Erlenmeyer flasks with a reaction volume of 20 mL. The three estrogens, E1, E2 and EE2, were incubated separately. The reaction mixture consisted of 200 µL of the estrogen solution (250 mg/L) and 19.8 mL of the Mn^{3+} complex.

Elimination of the BPA and TCS was performed in 50 mL Erlenmeyer flasks with a reaction volume of 10 mL. The two disruptors were incubated separately. The reaction mixture consisted of the endocrine disrupting chemical, 5 mg /L and 10 mg/L for TCS and BPA, respectively, and the oxidizing complex Mn^{3+}-malonate (495 µM).

Oxidation of anthracene was carried out in 25 mL Erlenmeyer flasks with a reaction volume of 10 mL with magnetic stirring at room temperature (25ºC) in darkness. The reaction mixture consisted of 4 mL of anthracene stock solution in acetone (12.5 mg/L) and 6 mL of the Mn^{3+}-complex. Flasks containing Mn^{2+}, malonate and H$_2$O$_2$ (Control 1) and Mn^{2+} and malonate (Control 2) at identical concentrations to those used in the Amicon Cell, instead of the retentate mixture, were also set up as control experiments. Samples were taken after 4 h and 2, 3 and 6 days.

6.2.3. "Two-stage" system for the continuous production of the Mn^{3+}-complex and the decolorization of the azo dye, Orange II

The enzymatic system used for the continuous production of Mn^{3+}-malonate is presented in **Figure 6.2**. This system consists of a stirred tank reactor (200-mL working volume) operated in continuous mode coupled to a 10 kDa cut-off ultrafiltration membrane (Prep/Scale-TFF Millipore), which permits the recycling of the enzyme to the reaction vessel. The additional volume of the ultrafiltration unit and the interconnecting tubing was 65 mL and the total volume of the reaction system accounted for 265 mL. Cofactors were added to the reactor from two stock solutions: H$_2$O$_2$ and a mixture of Mn^{2+} and sodium malonate at pH 4.5. These two stock solutions were fed into the reactor by independent variable-speed peristaltic pumps. The operational parameters were: initial MnP activity, 100 U/L; H$_2$O$_2$ feed rate, 8 µM/min; Na-malonate feed rate, 330 µM/min; MnSO$_4$ feed rate, 16 µM/min and hydraulic retention time (HRT), 60 min. The enzyme was recycled at a recycling:feed flow ratio of 12:1. The enzyme solution was provided as a single addition of VP at the beginning of the experiment. Samples from the filtrate were taken and measured for Mn^{3+}-malonate concentration.
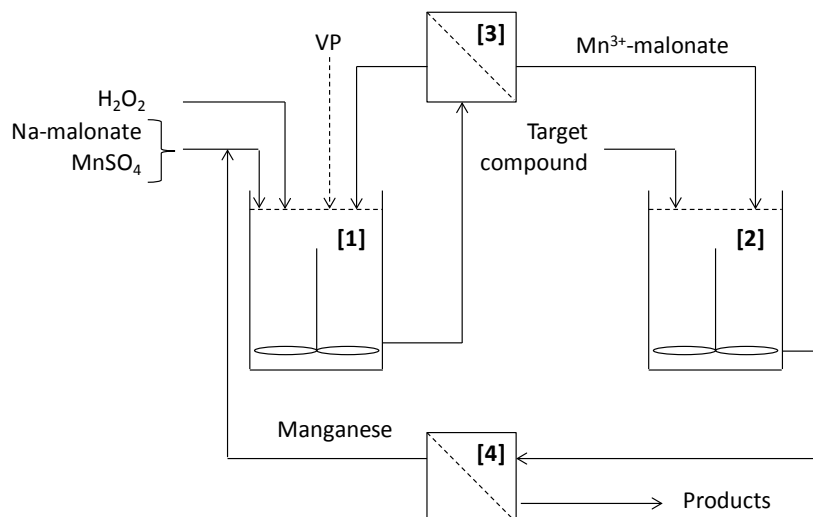
Figure 6.2. Schematic diagram of the "two-stage" system for the Mn^{3+}-malonate production. [1] Enzymatic reactor, [2] Oxidation reactor, [3] Ultrafiltration membrane and [4] Osmosis reverse system.

The Mn^{3+}-malonate generated in the enzymatic reactor was used in a second stage to carry out the decolorization of the azo dye Orange II. The second reactor (200-mL working volume) was fed with 2.5 mL/min of Mn^{3+}-malonate and 2.5 mL/min of a stock solution of the dye (50 mg/L). The reaction was performed at room temperature and 150 rpm. Finally, Mn^{2+} was recovered and reintroduced into the enzymatic reactor using a reverse osmosis system.

6.2.4. Determination of the concentrations of Orange II and anthracene

Decolorization of the Orange II was spectrophotometrically measured at 480 nm and monitored for 15 min [34].

The determination of anthracene concentration was performed as follows, with an HP 1090 HPLC, equipped with a diode array detector for monitoring the absorbance at 253 nm, a 4.6 mm × 200 mm Spherisorb ODS2 reverse-phase column (5 µm; Waters) and an HP ChemStation data processor. The injection volume was set at 10 µL, and the isocratic eluent (80% acetonitrile

and 20% water) was pumped in at 0.4 mL/min. A calibration curve was plotted to correlate the area and the concentration of the stock solutions, which ranged between 0.1 and 10 mg/L.

6.3. Results and discussion

6.3.1. Influence of key parameters on the batch production of Mn^{3+}-chelate

Formation of the Mn^{3+}-chelate in batch mode was spectrophotometrically monitored for 11 h. The reaction medium was similar to that used for the determination of MnP activity, except for the lack of a phenolic substrate (2,6-dimethoxyphenol), allowing the direct monitoring of Mn^{3+}-chelate formation. **Figure 6.3** shows a typical time course of Mn^{3+}-chelate generation by VP [251].
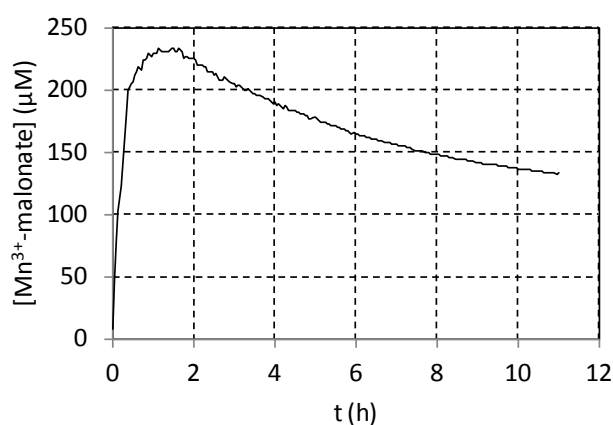
Figure 6.3. Time course of Mn^{3+}-malonate production by VP. Conditions were: 30 mM Na-malonate, 2 mM MnSO$_4$, 0.40 mM H$_2$O$_2$, pH 4.5.

A steady slope in the generation of the Mn^{3+}-chelate from the beginning of the experiment was observed, reaching a maximum of approximately 240 µM. After the maximum, a slight decay was detected at very slow rate in an incubation period between 1.5 and 11 h, which was indicative of substantial stability over the evaluation period. The kinetics of Mn^{3+}-chelate formation requires the evaluation of the effect of certain major parameters such as the type and concentration of organic acids, levels of Mn^{2+} and H$_2$O$_2$, pH, T, enzymatic activity and storage time.

6.3.1.1. Effect of the type and concentration of organic acid

Organic acids such as oxalic and malonic acid are secreted by fungi [252]. Organic acids play an important role in Mn-dependent enzymatic reactions by facilitating the release of Mn^{3+} from the active site of the enzyme and stabilizing the metal ion by chelation [252].

In this study, the type and concentration of organic acid affected both the rate of generation of the Mn^{3+}-chelate and the peak levels achieved (**Figure 6.4**).
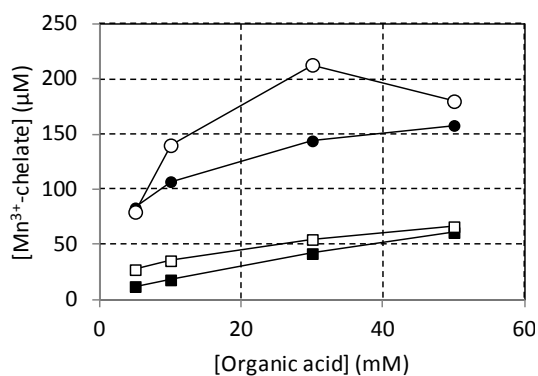
Figure 6.4. Effect of type and concentration of organic acids: (■) Lactic acid, (□) tartaric acid, (●) oxalic acid and (○) malonic acid.

Low levels of Mn^{3+}-chelate were found for tartaric and lactic acid and intermediate levels were detected when oxalic acid was used, while the highest titers were achieved in the presence of malonic acid. According to these results, malonate enhanced the stability of the Mn^{3+}-chelate. Accordingly, this compound was considered the organic acid to be used in the production of the Mn^{3+}-chelate. This result agrees with those obtained by [321] and [252], who reported that malonate presented the strongest chelating strength. Nevertheless, [322] and [323] found that the acids with the strongest chelating potential were malic and oxalic acid, respectively.

Considering the range of concentrations evaluated, the value of 30 mM allowed the highest production of Mn^{3+}-malonate with a maximum peak higher than 200 µM. At lower concentrations, the titer and generation rate of the Mn^{3+}-chelate were both lower. At concentrations higher than 30 mM, there was a slight decrease in the titers achieved. Mielgo et al. (2003) [35] observed that the highest levels of decolorization of Orange II by MnP were obtained when no malonic acid was added, whereas [318] reported that MnP activity increased with higher malonate concentration, reaching a maximum near 50 mM. Thus, the type and concentration of the organic acid used is dependent on the application.

6.3.1.2. Effect of MnSO$_4$ concentration

The effect of initial MnSO$_4$ concentrations in the range of 1 to 4 mM was evaluated in the presence of 5, 10, 30 and 50 mM malonate. The highest peak titer corresponded to a concentration of 2 mM Mn^{2+}, and no further increase was observed at a higher concentration of Mn^{2+}. Decay of the Mn^{3+}-chelate after the maximum level was significantly faster at higher concentrations of MnSO$_4$ (**Figure 6.5**).
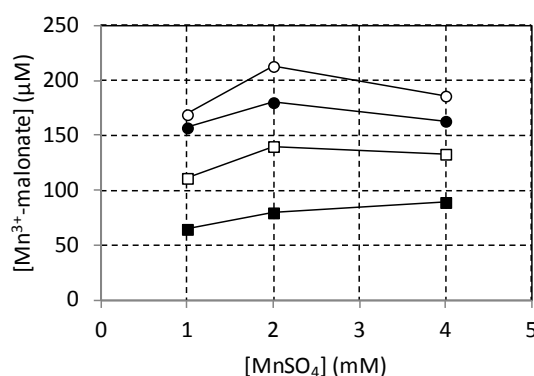

Figure 6.5. Effect of the concentration of Mn^{2+} at different Na-malonate levels: (■) 5 mM, (□) 10 mM, (●) 30 mM and (○) 50 mM.

6.3.1.3. Effect of H_2O_2 concentration

The effect of initial H_2O_2 concentration on the generation of the Mn^{3+}-chelate was evaluated in the presence of 30 mM malonate and 2 mM $MnSO_4$, at pH 4.5. The inactivation of VP in the absence of substrate (DMP) occurred during the incubation of the enzyme with H_2O_2, with inactivation especially evident at high concentrations of H_2O_2. As shown in **Figure 6.6.**, the enzymatic production of Mn^{3+}-malonate reached its peak at a H_2O_2 concentration of 0.40 mM. Higher concentrations of H_2O_2 did not correlate with a significant increase in the titers of the complex, suggesting an imbalance in the cyclic process of oxidation and reduction of the mediator and destabilization of the enzyme during the reaction. Inactivation of the peroxidase by H_2O_2 probably occurred due to formation of the catalytically inactive compound III [252, 319]. Among the different parameters evaluated, the concentration of H_2O_2 was found to be crucial for the enzyme activity. The concentration of H_2O_2 had to be strictly controlled, as an excessively concentrated reagent would cause the inactivation of the enzyme. On the contrary, an excessively low concentration would limit the reaction rate and extent.
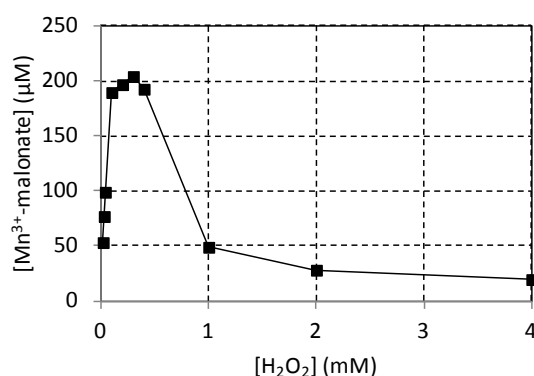

Figure 6.6. Effect of the H_2O_2 concentration on the production of Mn^{3+}-malonate

6.3.1.4. Effect of pH

With the objective of evaluating the influence of pH on the production of the Mn^{3+}-chelate, pH was adjusted from 3 to 9. As shown in **Figure 6.7**, the highest concentration of the complex was obtained at pH 4-4.5, whereas at more basic or acid pH, the production sharply dropped due to enzyme deactivation. The same optimal pH value has been found when the inactivation of a similar VP enzyme was evaluated [324].

Another aspect to be considered when evaluating the effect of pH on the generation of the Mn^{3+} complex is the chemical equilibrium of Mn^{3+}. It is known that Mn^{3+} is a strong oxidant, as observed from **equation [6.1]**.

$$Mn^{3+} + e^- \leftrightarrow Mn^{2+} \quad E^0 = 1.54\,V \qquad \textbf{[6.1]}$$
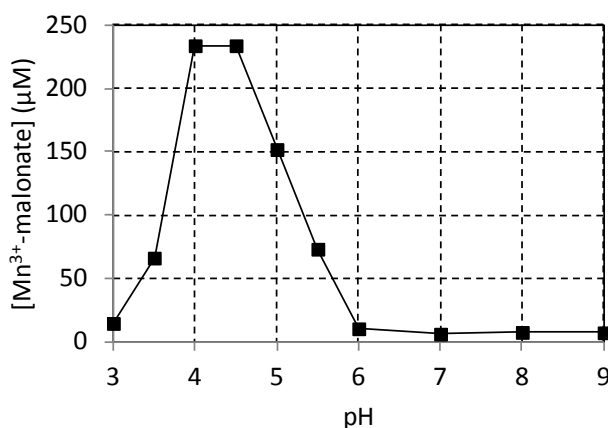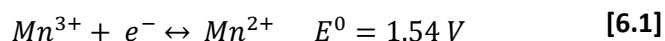

Figure 6.7. Effect of pH on the production of Mn^{3+}-malonate.

In an alkaline medium, the two cations precipitate, but the extent of Mn^{3+} precipitation is higher than that of Mn^{2+} due to differences of the solubility of the products Mn(OH)$_3$ and Mn(OH)$_2$ (K_{sp}, 10^{-36} and 10^{-13}, respectively). Thus, if

the pH of the medium is alkaline, the chemical equilibrium is described by **equation [6.2]**.

$$Mn(OH)_3 + e^- \leftrightarrow Mn(OH)_2 \quad E^0 = 0.10\,V \qquad \textbf{[6.2]}$$
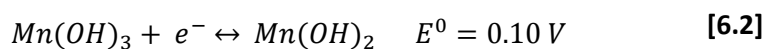
The oxidation potential of Mn^{3+}/Mn^{2+} in basic medium is very low compared to that achieved at acid pH [325]. For this reason, it is much more convenient to use the complex at acid pH values, at which both Mn^{3+} and Mn^{2+} are soluble in the reaction medium. On the contrary, if a basic pH is used, insoluble hydroxides will form.

6.3.1.5. Effect of VP concentration

The influence of MnP activity was analyzed in experiments performed with variable titers of the enzyme, ranging from 5 to 100 U/L. These experiments were carried out in a stirred Amicon ultrafiltration cell (8200) with 150 mL of working volume and a 10 kDa cut-off polyethersulfone membrane. As shown in **Figure 6.8**, the initial MnP activity had a significant effect on the production of the Mn^{3+}-chelate. Enzymatic activity of 100 U/L led to the highest levels of the Mn^{3+}-chelate out of the range tested. Further increases had no significant effect on the production of the Mn^{3+}-chelate. Taking this into account, it was considered that the best initial activity for the production of Mn^{3+}-malonate was 100 U/L.

6.3.2. Effect of temperature on the stability of the Mn^{3+}-malonate complex

The stability of Mn^{3+}-malonate at different temperatures was studied by incubating the complex at -18ºC, 4ºC and room temperature (**Figure 6.9**). The half-life of the complex at room temperature was found to be approximately 3.75 h. This value was increased at low temperatures, especially when the Mn^{3+}-chelate was kept frozen at -18ºC. According to these results, the application of

the complex should be conducted immediately after its production, and its storage is only recommended at a temperature that will keep it frozen.
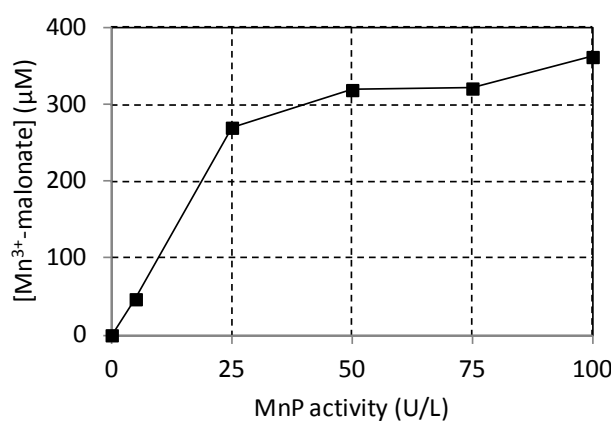
Figure 6.8. Effect of the initial enzymatic activity on the production of Mn^{3+}-malonate.
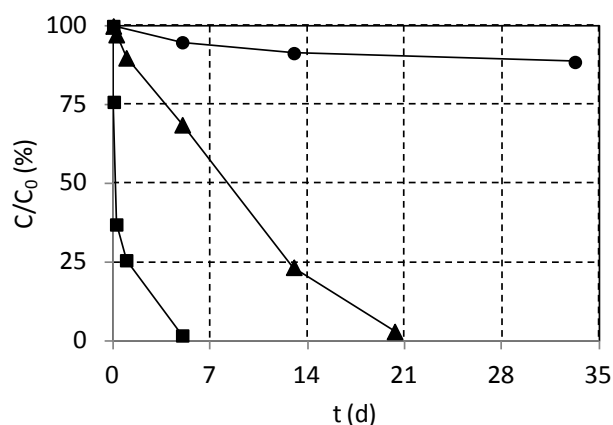
Figure 6.9. Stability of the complex Mn^{3+}-malonate at different temperatures: (■) room temperature, (▲) 4ºC and (●) -18ºC

6.3.3. Application of the Mn^{3+}-chelate for oxidizing recalcitrant compounds

The Mn^{3+}-chelate produced in an Amicon cell was later used for the oxidation of three different groups of compounds: an azo dye (Orange II), natural and synthetic estrogens (E1, E2 and EE2) and one polycyclic aromatic hydrocarbon

(anthracene). The oxidation of these compounds was performed in batch at room temperature (25ºC). Control experiments in the absence of the complex were also conducted in parallel.

6.3.3.1. Azo dye, Orange II

The capability of the complex to decolorize Orange II was evaluated with different initial concentrations of the dye, ranging from 11 to 27 mg/L and with an initial concentration of the complex of 165 µM. In all cases, the complex was able to oxidize the dye, reaching a similar percentage of decolorization (80-85%). Moreover, as shown in **Figure 6.10,** the higher the initial concentration of the Orange II was, the higher the maximum rate of decolorization.
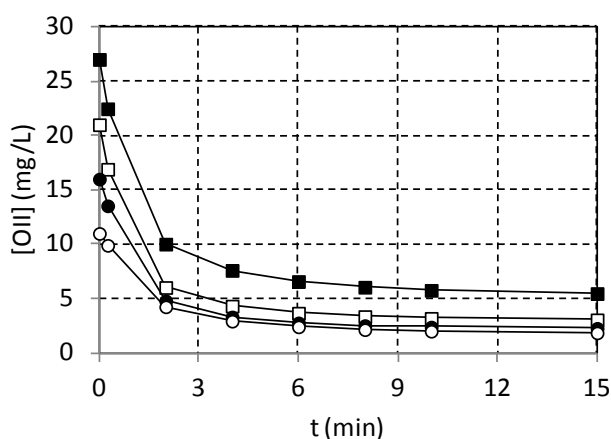
Figure 6.10. Removal profile of Orange II by Mn^{3+}-malonate (165 µM) at different initial concentrations of the dye: (○) 11 mg/L, (●) 16 mg/L, (□) 21 mg/L and (■) 26 mg/L.

Different concentrations of the Mn^{3+}-chelate, ranging from 70 to 200 µM, were evaluated to maximize the extent and rate of decolorization. Results are shown in **Figure 6.11**. It was observed that the higher the initial concentration of the complex was, the higher the maximum rate of oxidation and the decolorization extent.
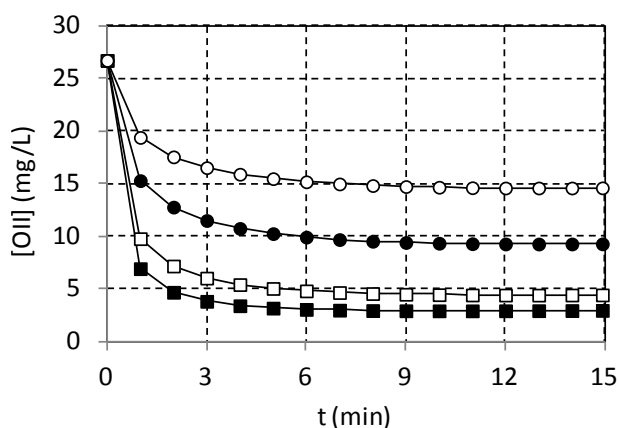
Figure 6.11. Removal profile of Orange II (27 mg/L) by Mn³⁺-malonate at different initial concentrations of the dye: (○) 70 µM, (●) 110 µM, (□) 165 µM and (■) 200 µM.

6.3.3.2. Endocrine disrupting chemicals, bisphenol A and triclosan

The capability of the complex to eliminate two different EDCs: bisphenol A and triclosna, was evaluated in batch experiments. The initial concentration of the oxidizing complex was 495 µM and the concentration of TCS and BPA was 5 and 10 mg/L, respectively. Samples were taken after 10, 40 and 60 min and they were analyzed for residual concentration by HPLC. As shown in **Figure 6.12,** almost the complete transformation of both compounds was after 10 minutes of reaction. These results agree with those observed in **Chapter 5**, in which the enzyme VP was able to eliminate these EDCs in 10 minutes.
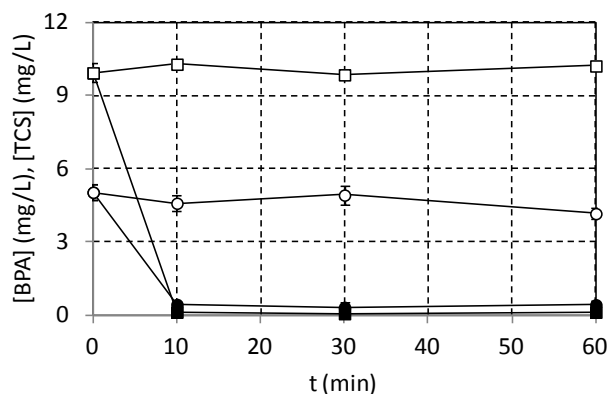
Figure 6.12. Removal profile of (■) BPA and (●) TCS by the oxidative action of the complex Mn^{3+}-malonate. Sample (black symbols) and control (white symbols)

6.3.3.3. Natural and synthetic hormones, estrone, 17β-estradiol and 17α-ethinylestradiol

The capacity of the complex to oxidize three different estrogens: estrone, 17β-estradiol and 17α-ethinylestradiol, was evaluated in batch. The initial concentration of the complex was 350 μM and the concentration of each estrogen was 2.5 mg/L. Samples were taken after 1 min and 0.25, 1, 6 and 12 h and analyzed for estrogen concentration by HPLC. As shown in **Figure 6.13,** the transformation of the three estrogens was immediately evidenced.

Previous results have demonstrated the ability of lignin-modifying enzymes to oxidize estrone [243], 17β-estradiol and 17α-ethinylestradiol [244]. The enzymatic transformation of these compounds was performed in 1 h of treatment, whereas in the present study, the complete disappearance of E1, E2 and EE2 was achieved immediately after being added to the oxidative system.
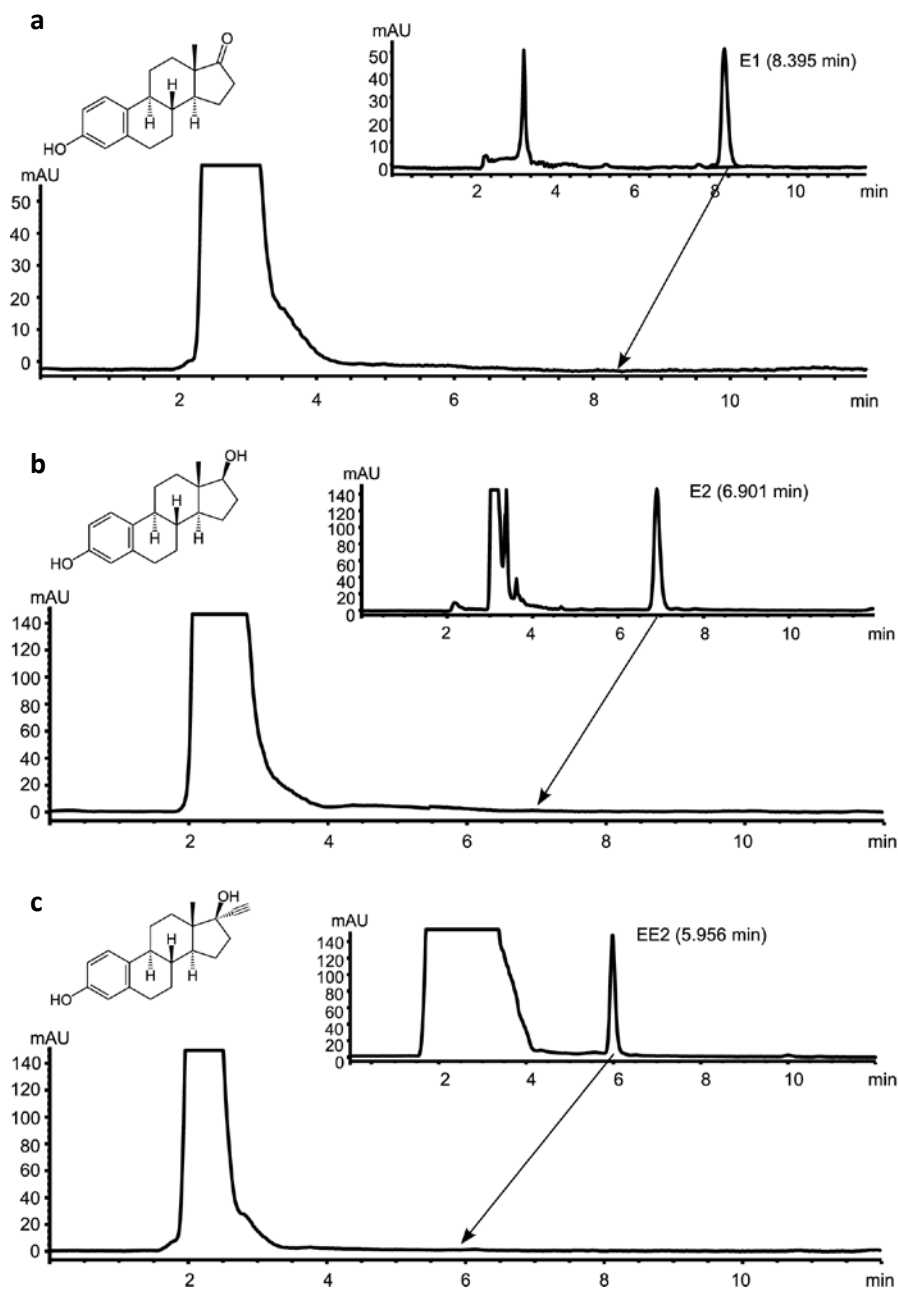
Figure 6.13. Chromatograms of the estrogens (a) E1, (b) E2 and (c) EE2 after 1 min. A chromatogram of a standard solution containing the initial concentration of each estrogen is shown in the upper right corner.

6.3.3.4. Polycyclic aromatic hydrocarbon, anthracene

The ability of the complex to oxidize a solution containing anthracene was also evaluated. The low solubility of anthracene in water was countered by the addition of acetone to a final concentration of 36% (v/v), which permitted to increase its concentration in the aqueous phase from 0.07 to 10 mg/L [299]. The final transformation percentage after 6 days was approximately 90% (**Figure 6.14**).
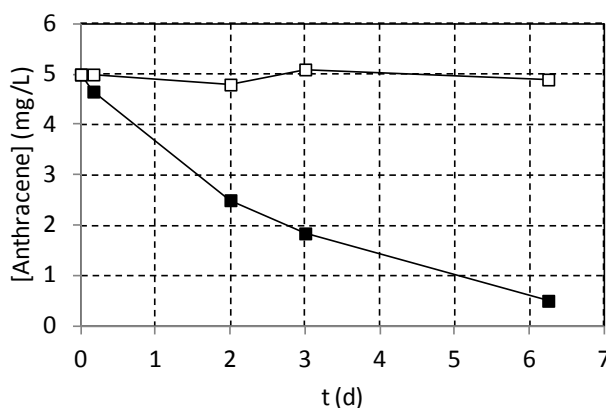
Figure 6.14. Removal profile of anthracene by the oxidative action of the complex Mn^{3+}-malonate. (■) Sample and (□) control.

During the oxidation of anthracene, a rapid disappearance of the hydrocarbon was initially observed, followed by a slower rate of transformation. Considering that the half-life of the Mn^{3+} complex at room temperature is approximately 4 h, the oxidation of anthracene may partially be attributed to the formation of reactive oxygen species, such as hydroxyl or phenoxy radicals that subsequently oxidize the polycyclic aromatic hydrocarbon (PAH). In this case, the Mn^{3+} complex would act as a direct oxidant during the first hours, oxidizing the PAH, as well as triggering an oxidative cascade through the formation of active oxidant intermediate compounds such as quinones. Considering that

anthraquinone is the main metabolite produced during the oxidation of anthracene by ligninolytic enzymes [19, 326], one possible explanation for the behavior of the reaction is based on the autocatalytic effect of anthraquinone. In previous studies of enzymatic oxidation of anthracene by MnP [299], the oxidation rate was observed to be significantly faster than that obtained in the "two-stage" system in this study. One possible application for the Mn^{3+}-malonate complex (for degrading compounds with low solubility such as anthracene) would be in a biphasic system like that proposed by Eibes et al. (2007) [320]. In such a system, the aqueous phase was replaced by fresh Mn^{3+}-chelate in each of several cycles would produce an increase in the anthracene oxidation rate. Mn^{3+}-chelates, not being proteins, can solve problems related to the use of organic solvents for increasing the solubility of certain compounds, as the solvent would not interfere with the enzyme and may have little effect on the stability of the complex.

The oxidation rates of the three types of compounds using Mn^{3+}-malonate as an oxidizing agent were in agreement with those observed using the VP enzyme in a one-stage process. The azo dye and the estrogens were easily transformed by Mn^{3+}-malonate, whereas the transformation of anthracene was slower. This broad degradation capacity supports the use of the Mn^{3+} complex for the treatment of other xenobiotics.

6.3.4. A continuous process for the production of the Mn^{3+}-chelate and decolorization of the Orange II dye in a "two stage" process

Continuous production of the Mn^{3+}-malonate complex was carried out in a stirred reactor coupled with an external ultrafiltration membrane. Conditions were set based on the previous results obtained in batch reactions. The differences from the previous experiments presented in this study include the ultrafiltration system used, the optimized conditions for Mn^{3+}-malonate

generation and the scale of the ultrafiltration system (1 mL cuvette cell, 150 mL Amicon cell and 265 mL Prep/Scale Millipore System). In the second system used, the enzyme is retained within the cell, and the application of N_2 pressure allows low molecular compounds to flow through the membranes. In the third system, the enzyme is recirculated using peristaltic pumps, retaining the enzyme within the "two-stage" system. In both systems, mixing in the reactors is provided by magnetic stirring.

In the batch operation, a ratio of Na-malonate/Mn^{2+}/H_2O_2 of 75/5/1 (30, 2 and 0.4 mM) was optimal for the production of the complex. In the continuous system, a ratio of 41.6/3.1/1 (330, 16.65 and 8 µmol/L·min) was used. It is important to note that scaling up the amounts used in the batch operation to provide adequate feeding rates in the continuous mode is not straightforward. Optimal values reported for the one-stage operation of a similar system were taken into consideration to determine the H_2O_2 feeding rate [34]. Thus, an H_2O_2 volumetric feeding rate of 8 µmol/L·min (considering a reaction volume of 265 mL) was used as the initial value. López et al. (2004) [34] have found that volumetric feeding rates of H_2O_2 in the range of 5-15 µmol/L·min caused no enzyme inactivation but, at the same time, limited the decolorization rate of the system significantly. In our case, a low peroxide feeding rate was sufficient to maintain high levels of production of the Mn^{3+}-malonate complex. The scale-up of the "two-stage" system from an optimized batch process to a continuous system increased the generation of the Mn^{3+} complex from 350 to 400 µM.

The amount of Mn^{3+}-malonate produced increased during the first 5 h and then remained stable for the next 5 h and production reached a maximal level of approximately 10 µmol/L·min (**Figure 6.15**).
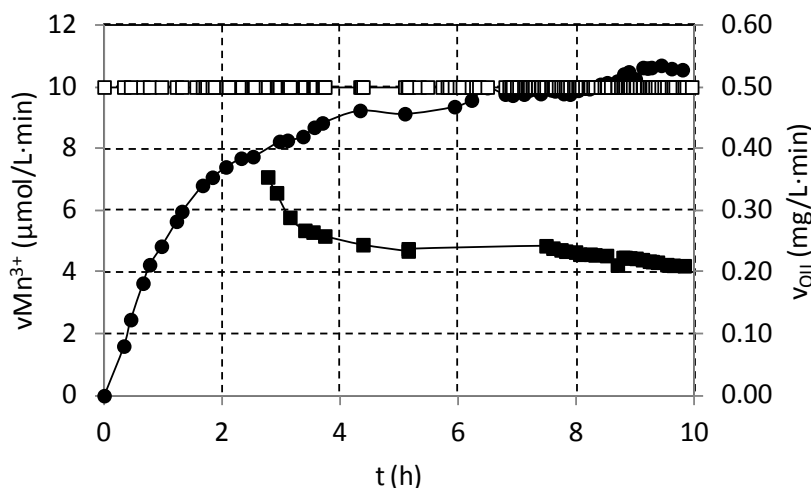
Figure 6.15. Profile of continuous production of Mn^{3+}-malonate and continuous removal of Orange II: (●) production rate of Mn^{3+}-malonate, (□) feeding rate of Orange II and (■) outlet rate of Orange II.

The continuous reactor used for Mn^{3+}-malonate production was coupled with an oxidation system operating with the azo dye Orange II. Similar to previous results, this compound presented an intermediate oxidation rate, and spectrophotometric monitoring was simple and straightforward. Decolourization of Orange II was directly proportional to the concentration of the complex; at the beginning of the operation of the system, the level of decolorization was low but later increased to approximately 54% (v_{OII} = 0.23 mg/L·min) as the concentration of the complex reached 400 µM (v_{Mn3+} = 10 µmol/L·min). During the operation of the system, the reverse osmosis recovery, defined as the relation between the Mn^{2+} in the recirculation line and the feeding line, was 96%. Continuous decolorization of the dye by MnP in an enzymatic membrane bioreactor was performed previously by López et al. (2004) [34]. Fairly constant decolorization (to levels greater than 90%) was reached over 150 min, but the average VP consumption was 37 U/L·h. Whereas, in this study, decolorization

levels between 50% and 60% were maintained for 7 h without loss of enzyme activity.

Previously, other systems for the generation and use of Mn^{3+}-chelates in a "two-stage" reactor system have been reported [327, 328]. Both studies proposed enzyme immobilization on different supports, the NH_2-Emphaze polymer (Pierce Chemical Co., Rockford, IL) and FSM-16 (a mesoporous material), respectively. The Emphaze-MnP column system requires NaCl to prevent the adsorption of Mn^{3+}-chelate to the support matrix, and salt conditions must be controlled carefully. However, this study reports the continuous production of Mn^{3+}-chelate in reactions catalyzed by free VP from *B. adusta* in a stirred reactor coupled to an external ultrafiltration membrane. Hence, this system does not require enzyme immobilization or additives such as NaCl.

6.4. Conclusions

The ability of the enzyme versatile peroxidase to produce the oxidizing species Mn^{3+}-malonate was evaluated. Four parameters affecting the catalytic cycle of the enzyme and, consequently, the production of the chelate Mn^{3+}-malonate, such as type and concentration of the organic acid, Mn^{2+} and H$_2$O$_2$ concentrations, initial enzymatic activity and pH of the medium, were evaluated. The conditions which allowed the highest production were: 30 mM Na-malonate, 2 mM MnSO$_4$, 0.4 mM H$_2$O$_2$, 100 U/L initial activity and pH 4.5.

The capability of the complex to oxidize different xenobiotic compounds, such as the azo dye Orange II, the polycyclic aromatic hydrocarbon anthracene and three estrogens, was assessed. For all contaminants, the oxidation extent was higher than 80%, thereby demonstrating that the complex is a strong and versatile oxidant.

Moreover, a new set-up, the "two-stage" system in which the Mn^{3+}-malonate complex can be produce in a continuous mode and can be applied in a second reactor to oxidize different organic compound, was designed and patented (ES 2373729 B2). In a first approach, the enzyme was able to produce Mn^{3+}-malonate in a continuous mode with a rate 10 µmol/L·min and it was able to continuously decolorize Orange II with a rate of 0.27 mg$_{OII}$/L·min.

In **chapter 7** the optimization of the continuous production is studied by the response surface methodology.

Chapter 7

Continuous reactors for the elimination of endocrine disrupting chemicals

Chapter 7. Continuous reactors for the elimination of endocrine disrupting chemicals

7.1. Introduction

7.2. Materials and methods

7.2.1. Evaluation of the continuous production of Mn^{3+}-malonate in the "two-stage" system by response surface methodology

7.2.2. Design of a process control system

7.2.3. Description and operation of three configurations of continuous-based reactors: "two-stage" system, enzymatic ultrafiltration system, microfiltration reactor with immobilized CLEA®s for the continuous removal of EDCs

7.2.3.1. Enzymatic ultrafiltration system

7.2.3.2. "Two-stage" system

7.2.3.3. Microfiltration system

7.3. Results and discussion

7.3.1. Evaluation of the continuous production of Mn^{3+}-malonate in the "two-stage" system by response surface methodology

7.3.2. Design of the control system of the enzymatic reactor in the "two-stage" system

7.3.3. Continuous elimination of bisphenol A, triclosan, estrone, 17β-estradiol and 17α-ethinylestradiol in the "two-stage" system

7.3.4. Continuous elimination of bisphenol A, triclosan, estrone, 17β-estradiol and 17α-ethinylestradiol in an enzymatic ultrafiltration system

7.3.5. Continuous elimination of bisphenol A by CLEA®s in a microfiltration system

7.4. Conclusions

Chapter 7. Continuous reactors for the elimination of endocrine disrupting chemicals

7.1. Introduction

In **chapters 5 and 6** was demonstrated the ability of the lignin modifying enzyme versatile peroxidase (VP) and the oxidizing complex Mn^{3+}-malonate, respectively, to eliminate the compounds BPA, TCS, E1, E2 and EE2 in batch experiments. In the present chapter, the continuous elimination of these disruptors by VP and Mn^{3+}-malonate was studied.

The major drawback when operating conventional continuous reactors with free enzymes is the large consumption of the biocatalyst, which may be lost with the treated effluent. Nevertheless, the recovery and reutilization of the enzyme is imperative when a continuous prolonged operation is attempted since the cost of the biocatalyst may limit its application.

The retention of the enzyme by an ultrafiltration membrane is a very interesting alternative to overcome the washing out of the catalyst with the treated effluent [34, 314]. In this system, the enzyme the reactor is connected with an ultrafiltration membrane which enables the recovery of the free enzyme back to the reaction vessel; thereby, by using an enzymatic membrane reactor, it is possible to separate the biocatalysts from products and /or other substrates by a semi permeable membrane that creates a selective physical/chemical barrier [34]. This set-up is very interesting because allows the use of enzymes in free form avoiding their immobilization, which usually is related with high costs.

This system was successfully applied for the continuous elimination of dyes by the oxidative action of the enzyme manganese peroxidase [34] and it was also used for the continuous treatment of estrogens by the action of the lignin modifying enzyme laccase [314]. However, the main drawback related to the application of enzymatic systems is the consumption and destabilization of

the enzyme in the process, mainly due to the conditions in which the reaction has to be performed, i.e. presence in the medium of protein-denaturant compounds, extreme temperatures, very acidic or very basic pH, oxidants, detergents, proteases, organic solvents, etc.

In **chapter 6** of the present thesis dissertation, a new system ("two-stage" system) was presented in order to overcome the high deactivation of the enzyme due to the reaction conditions. In this system, the continuous production and use of the complex Mn^{3+}-malonate to treat the azo dye Orange was performed. However, the conditions (Na-malonate, $MnSO_4$ and H_2O_2 feeding rate, hydraulic retention time and enzymatic activity) selected to perform this oxidation were not the optimal ones. Therefore, the key goal of this chapter was to study the effect of Na-malonate and H_2O_2 feeding rate and hydraulic retention time of the enzymatic reactor on the continuous production of the oxidizing chelate Mn^{3+}-malonate. As second aim, after having optimized the catalytic conditions, the ability of the complex to continuously eliminate BPA, TCS, E1, E2 and EE2 was evaluated. In addition, with the objective of comparing the Mn^{3+}-malonate mediated elimination with the enzymatic oxidation, the elimination of the same five EDCs by the direct action of the enzyme VP in a continuous enzymatic ultrafiltration membrane reactor was carried out. Finally, the elimination of BPA was evaluated by using VP-GOD-CLEA®s in a microfiltration membrane reactor.

7.2. Materials and methods

7.2.1. Evaluation of the continuous production of Mn³⁺-malonate in the "two-stage" system by response surface methodology

Three operational variables (manipulated variables) affecting the continuous production of the oxidizing complex Mn^{3+}-malonate in the "two-stage" system (**Figure 6.2**): Na-malonate ($v_{malonate}$, x_1, µM/min) and H_2O_2 (v_{H2O2}, x_2, µM/min) feeding rates and hydraulic retention time (HRT, x_3, min) and their interactions, were evaluated. To study the effect of the above-indicated variables, a factorial design with three levels (low, center and high) for each variable was used; these levels were represented by -1, 0 and 1 (**Table 7.1**).

Table 7.1. Levels and actual values of the variables tested

Factor	Variable	Unit	-1	0	1
x_1	$v_{malonate}$	µM/min	200	250	300
x_2	v_{H2O2}	µM/min	10	25	40
x_3	HRT	min	30	50	70

A Central Composite Face Centered (CCFC) design was used (**Figure 7.1**), in which the central point (0,0,0) was repeated four times.

Three variables were defined as response variables (controlled variables): Mn^{3+}-malonate production rate (v_{Mn3+}, Y_1, µM/min, **equation [7.1]**), Mn^{3+}-malonate concentration ([Mn^{3+}], Y_2, µM, **equation [7.2]**) and enzymatic deactivation rate (E.D., Y_3, U/L·h, **equation [7.3]**). These response variables were calculated as follows:

$$v_{Mn3+} = \frac{Q_O \cdot [Mn^{3+}]}{V}$$

[7.1]
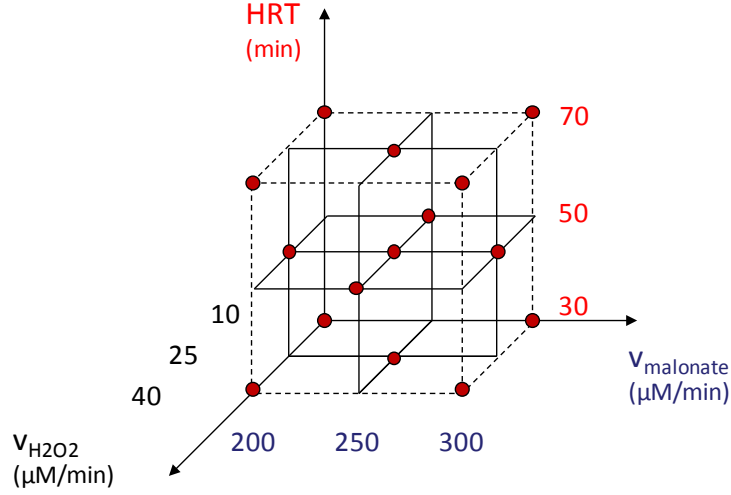
Figure 7.1. Central Composite Face Centered design to evaluate the continuous production of Mn^{3+}-malonate

Where Q_O is the output system flow rate in mL/min.

$$[Mn^{3+}] = \frac{Abs_{270nm}}{\varepsilon_{270nm} \cdot L} = \frac{Abs_{270nm}}{11.59 \; mM^{-1}cm^{-1} \cdot 1 \; cm} \qquad \textbf{[7.2]}$$

Where L is the length of the spectrophotometer quartz cell.

$$E.D. = \frac{(Act_0 - Act_1)}{(t_1 - t_0)} \qquad \textbf{[7.3]}$$

In order to optimize the conditions to maximize both Y_1 and Y_2 and minimize Y_3, three dimensional response surface methodology (RSM), was applied. Thereby, relationships between manipulated variables and one or more response variables can be determined [295]. When three generic variables are considered, the standard response surface methodology equation is the following:

$$Y = b_0 + b_1 \cdot x_1 + b_2 \cdot x_2 + b_3 \cdot x_3 + b_{12} \cdot x_1 \cdot x_2 + b_{13} \cdot x_1 \cdot x_3 \\ + b_{23} \cdot x_2 \cdot x_3 + b_{11} \cdot x_1^2 + b_{22} \cdot x_2^2 + b_{33} \cdot x_3^2 \qquad \textbf{[7.4]}$$

Where, Y is the response variable (controlled); x_1, x_2 an x_3 are the independent variable (manipulated); b_0 is the regression coefficient at center point; b_1, b_2 and b_3 are linear coefficients; b_{12}, b_{13} and b_{23} are second-order coefficients; and b_{11}, b_{22} and b_{33} are quadratic coefficients [296]. When the values of the independent variables are coded (dimensionless), the coefficients have the same dimensions and, subsequently, the same units of the dependent variable.

The rest of the parameters were: 200 U/L MnP activity, 30ºC, v_{Mn2+} = 25 µM/min manganese feeding rate and 200 mL working volume. The additional volume held by ultrafiltration unit and the interconnecting tubing was 65 mL.

7.2.2. Design of a process control system

A method for the design and analysis of a Multi-Input-Multi-Output (MIMO) process, for a steady-state process, is the Relative Gain Array (RGA). RGA provides a quantitative analysis of interactions between controlled and manipulated variables. Moreover, it also provides a method for matching variables controlled and manipulated to make a control system. This methodology consists of making a matrix of relative gains. The relative gain is calculated as the increment having a controlled variable with respect to an increase of a manipulated variable, divided by the restrictions that we impose on each variable, **equation [7.5]**:

$$K_{ij} = \frac{\dfrac{\left[Y_i^2 - Y_i^1\right]_{x2=0,x3=0}}{\Delta Y}}{\dfrac{\left[x_j^2 - x_j^1\right]_{x2=0,x3=0}}{\Delta x}} \qquad \textbf{[7.5]}$$

Where K_{ij} is the gain, Y_i are the controlled variables, x_j are the manipulated variables and ΔY and Δx are the restrictions. The transfer function (G) can be written, on the steady state, as the matrix of gains, **equation [7.6]**:

$$G = \begin{bmatrix} K_{1,1} & K_{1,2} & K_{1,3} \\ K_{2,1} & K_{2,2} & K_{2,3} \\ K_{3,1} & K_{3,2} & K_{3,3} \end{bmatrix} \qquad \text{[7.6]}$$

Where the rows are gains of the controlled variables and the columns are the relative gains of the manipulated variables. The relative gain, λ_{ij}, is defined as the ratio between the "open-loop gain" and the "closed-loop gain", **equation [7.7]**:

$$\lambda ij = \frac{\left(\dfrac{\partial y_i}{\partial u_j}\right)_u}{\left(\dfrac{\partial y_i}{\partial u_j}\right)_y} \qquad \text{[7.7]}$$

Where the term $\left(\dfrac{\partial y_i}{\partial u_j}\right)_u$ refers to partial derivative evaluated with all manipulated variables constant except u_j (open-loop gain) and, similarly, the term $\left(\dfrac{\partial y_i}{\partial u_j}\right)_y$ denotes the partial derivative with all controlled variables constant except y_i (closed-loop gain). It can be demonstrated that the RGA matrix can be calculated as the *Hadamard* product (element by element) between the transfer function and the transpose of its inverse, **equation [7.8]**:

$$RGA = G \otimes (G^{-1})^T \qquad \text{[7.8]}$$

The characteristics of this matrix are:

1- All elements of a row or column must sum to one $\sum_{i=1}^{n} K_{i,j} = \sum_{j=1}^{n} K_{i,j} = 1$

2- The RGA is insensitive to scaling of the variables

3- Each of the rows of the matrix represents a controlled variable, while each column represents a manipulated variable

The matrix is interpreted as follows:

- If $\lambda_{i,j} = 0$, the manipulated variable x_j has no effect on the controlled variable Y_i

- If $\lambda_{i,j} = 1$, the manipulated variable x_j is affecting the controlled variable Y_i without any interaction of other control loops

- If $\lambda_{i,j} < 0$, the control system will be unstable

- If $0 < \lambda_{i,j} < 1$, implies that other control loops are interacting with the control loop of these two variables:

    o If $\lambda_{i,j} = 0.5$, the effect of pairing these two variables may be affected by another control loop

    o If $\lambda_{i,j} < 0.5$, the other control loops are influencing the pairing of these two variables

    o If $\lambda_{i,j} > 0.5$, the pairing of these two variables is good but can still be influenced by the other control loops

- If $\lambda_{i,j} > 1$, implies that this coupling is dominant in the system but still can be affected by other variables of the system in the opposite direction.

- If $\lambda_{i,j} > 10$, avoid this pairing

In conclusion, the desired value for each of the relative gains is the unit.

To evaluate the sensitivity of a matrix to possible errors, the condition number of singular value decomposition (γ) is defined. If γ = 1, the matrix is "well-conditioned", whereas if the condition number is high (> 10), the matrix of gains G is "bad-conditioned" and can be singular (det (G) = 0). In such case, at least two process variables are coupled together and their regulation with a decentralized controller (not multivariate) may be difficult or impossible.

Furthermore, in such case the RGA matrix is very sensitive to errors in the gain matrix (G) and the pairing indicated may not be valid.

7.2.3. Description and operation of three configurations of continuous-based reactors: "two-stage" system, enzymatic ultrafiltration system, microfiltration reactor with immobilized CLEA®s for the continuous removal of EDCs

Three different membrane system configurations were employed to continuously oxidize BPA, TCS, E1, E2 and EE2. In the *enzymatic ultrafiltration system*, **Figure 7.2**, the enzyme is in direct contact with the organic pollutants and the matrix where they are contained; therefore, it is expected that the deactivation of the biocatalyst will be high due to the conditions of the reaction (high pH and presence of denaturants). To overcome the high deactivation rate, a "two-stage" system, **Figure 6.2**, was design. In this configuration, the enzyme avoids the contact with the pollutant and, consequently, a lower deactivation rate is expected. Finally, a third configuration, microfiltration system, **Figure 7.3**, was developed. In this configuration, the enzyme is used in its immobilized form, VP-GOD-CLEA®s, thereby it can be retain in the system by a microfiltration membrane. This system is expected to provide lower deactivation since the pressure of the system is lower than in an ultrafiltration membrane and glucose is used as substrate in the cascade catalytic cycle.

7.2.3.1. Enzymatic ultrafiltration system

The enzymatic reactor corresponds to a stirred tank reactor [1] operated in a continuous mode coupled to an ultrafiltration membrane [2], which permits the recycling of the soluble enzyme to the reaction vessel (**Figure 7.2**). A stirred tank of 200 mL working volume was coupled with a polyethersulfone synthetic membrane (Prep/Scale-TFF Millipore) with a nominal molecular weight cutoff of 10 kDa. The additional volume held by ultrafiltration unit and the

interconnecting tubing was 75 mL. The reactor was equipped with temperature and pH sensor. Two stock solutions (A) 36.6 mM Na-malonate, 0.75 mM $MnSO_4$ and EDCs and (B) 0.99 mM H_2O_2, were fed into the reactor by independent variable speed peristaltic pumps.
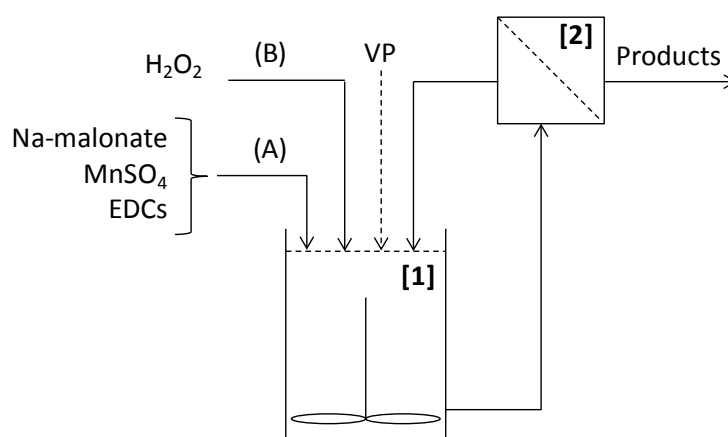
Figure 7.2. Schematic diagram of the enzymatic ultrafiltration membrane system for the continuous elimination of BPA, TCS, E1, E2 and EE2. [1] Enzymatic reactor, [2] ultrafiltration membrane

Experiments in the enzymatic reactor were performed by pumping the two stock solutions, thus initiating the catalytic cycle of VP. The feeding rate of the solution (A) was 3.92 mL/min from the stock solution containing 36.6 mM Na-malonate and 0.75 mM $MnSO_4$ which correspond to addition rates of 520 and 10.68 µmol/L·min, respectively. The feeding rate of the solution (B) was 1.58 mL/min of H_2O_2 from the stock solution with concentration of 0.99 mM which corresponds to an addition rate of 5.70 µmol/L·min. The enzyme was recycled in a recycling:feed flow ration of 12:1. The addition of the enzymatic stock was carried out according to a fed-batch addition strategy to maintain a MnP activity around 100 and 200 U/L. Experiments were performed at 30ºC. Samples were taken from permeate to measure the residual concentration of EDCs and from

the reactor to estimate the enzymatic activity. In order to avoid the oxidation of the DMP by the complex Mn^{3+}-malonate which may interfere in the determination of MnP activity, samples taken from the reactor were dialyzed through a PD-10 column (Amersham Biosciences, Björkgatan, Uppsala, Sweden).

Two experiments were carried out in order to evaluate the effect of the matrix in which the EDCs are contained. The values of the concentration and the addition rates of the EDCs are displayed in **Table 7.2**.

Table 7.2. EDCs concentration and addition rates in solution (A)

EDC	Experiment 5		Experiment 6	
	Concentration (mg/L)	Addition rate (µg/L·min)	Concentration (mg/L)	Addition rate (µg/L·min)
BPA	2.12	30.22	8.25	117.6
TCS	1.32	18.82	1.43	20.38
E1	1.18	16.82	1.34	19.10
E2	1.74	24.80	1.86	26.51
EE2	1.75	24.94	1.89	26.94
Matrix	Real wastewater		Distilled water	

7.2.3.2. "Two-stage" system

Elimination experiments in the "two-stage" system were carried out by pumping the Mn^{3+}-malonate, produced in the enzymatic reactor **[1]**, and a stock solution containing the EDCs, to the oxidation reactor **[2]** (**Figure 6.2**). The conditions to produce the complex Mn^{3+}-malonate were those found as optimum conditions to maximize the production rate of the complex, **Table 7.3**.

The oxidizing reactor consisted of a 200 mL stirred tank working at room temperature. The solution containing the complex Mn^{3+}-malonate, coming from the ultrafiltration membrane, was fed at 5.3 mL/min, as well as the stock

solution containing the EDCs was fed at 5.3 mL/min; therefore, the hydraulic retention time in the oxidizing reactor was 19 min, approximately.

Table 7.3. Conditions for the continuous production of Mn^{3+}-malonate to oxidize EDCs in the "two-stage" system

$v_{malonate}$ = 250 µM/min	pH 4.5
v_{Mn2+} = 25 µM/min	HRT = 50 min
v_{H2O2} = 25 µM/min	MnP activity = 200 U/L

Samples were taken from oxidation reactor outlet to measure the residual concentration of EDCs, by HPLC or GC-MS, and from the reactor to estimate the enzymatic activity and Mn^{3+}-malonate concentration. In order to avoid the oxidation of the DMP by the complex Mn^{3+}-malonate which may interfere in the determination of MnP activity, samples taken from the reactor were dialyzed through a PD-10 column (Amersham Biosciences, Björkgatan, Uppsala, Sweden). Four experiments were carried out to evaluate the effect of the concentration of the EDCs and the effect of the matrix in which the EDCs are contained, on the degradation rate. The values of the concentration and the addition rates of the EDCs are shown in **Table 7.4**.

Table 7.4. EDCs concentration and addition rates in the oxidizing reactor of the "two-stage" system

	Experiment 1		Experiment 2	
EDC	**Concentration (mg/L)**	**Addition rate (µg/L·min)**	**Concentration (mg/L)**	**Addition rate (µg/L·min)**
BPA	2.22	58.83	8.76	232.14
TCS	1.70	45.05	1.47	38.95
E1	1.11	29.41	1.33	35.24
E2	1.90	50.35	1.92	50.88
EE2	1.60	42.40	1.88	49.82
Matrix	Distilled water		Real wastewater	

Table 7.4. EDCs concentration and addition rates in the oxidizing reactor of the "two-stage" system (*cont.*)

EDC	Experiment 3		Experiment 4	
	Concentration (µg/L)	Addition rate (µg/L·min)	Concentration (µg/L)	Addition rate (ng/L·min)
BPA	101.84	2.70	2.20	58.22
TCS	49.24	1.30	1.19	31.54
E1	n.s.	----	3.77	99.83
E2	73.45	1.95	1.28	33.90
EE2	162.27	4.30	6.05	160.29
	Real wastewater		Real wastewater	

n.s. not spiked

The real wastewater used in this work was taken from the outlet of the secondary clarifier of the wastewater treatment plant from Calo-Milladoiro (Ames, Spain). The characteristics of the water are shown in **Table 7.5**.

Table 7.5. Characteristics of the real wastewater from Calo-Milladorio treatment plant

ANION	Concentration (mg/L)	CATION	Concentration (mg/L)		Concentration (mg/L)
Cl^-	78.24	Li^+	0.00	TC	18.92
NO_2^-	0.16	Na^+	87.58	IC	12.70
Br^-	0.00	NH_4^+	0.00	TOC	6.28
NO_3^-	23.11	K^+	20.85	TN	7.80
PO_4^{3-}	11.92	Mg^{2+}	4.28	NN	3.00
SO_4^{2-}	49.18	Ca^{2+}	15.91	TKN	4.80
pH 7.5					

TC: total carbon; IC: inorganic carbon; TOC: total organic carbon; TN: total nitrogen; NN: inorganic nitrogen; TKN: total Kjeldahl nitrogen

7.2.3.3. Microfiltration system

An Amicon stirred ultrafiltration cell 8200 (Millipore, Billerica, MA, USA) with 50 mL working volume was equipped with 0.22 µm cellulose acetate filter

(Millipore) was used for the continuous elimination of BPA. The reactor was operated at room temperature and fed with a solution containing 50 mM sodium malonate (pH 5.0), 1 mM $MnSO_4$, 555 µM glucose and 10 mg/L BPA at a flow rate of 0.55 mL/min, which corresponds to an addition rate of 110 µg/L·min. The run was started by adding VP-GPD-CLEA®s at a concentration of 25 U/L MnP activity, after 4 hours (**Figure 7.3**).
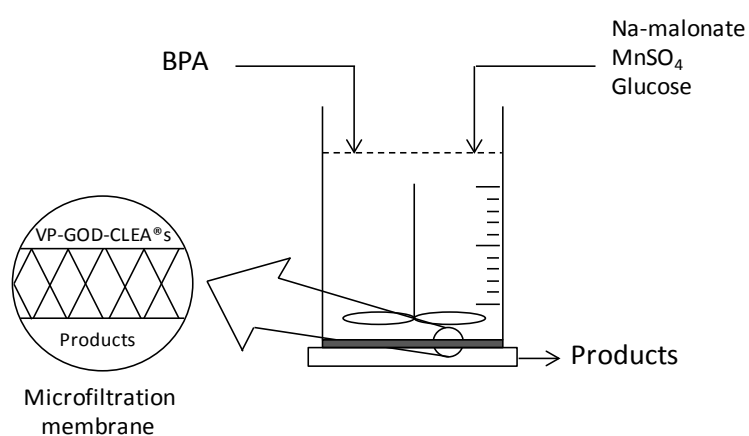

Figure 7.3. Schematic diagram of the microfiltration system for the continuous elimination of BPA.

7.3. Results and discussion

All the experiments carried out to evaluate the effect of x_1, x_2 and x_3 on the continuous generation of the complex Mn^{3+}-malonate and the deactivation of the enzyme were monitored for 8 h. **Figure 7.4** shows the typical Mn^{3+}-malonate production profile.
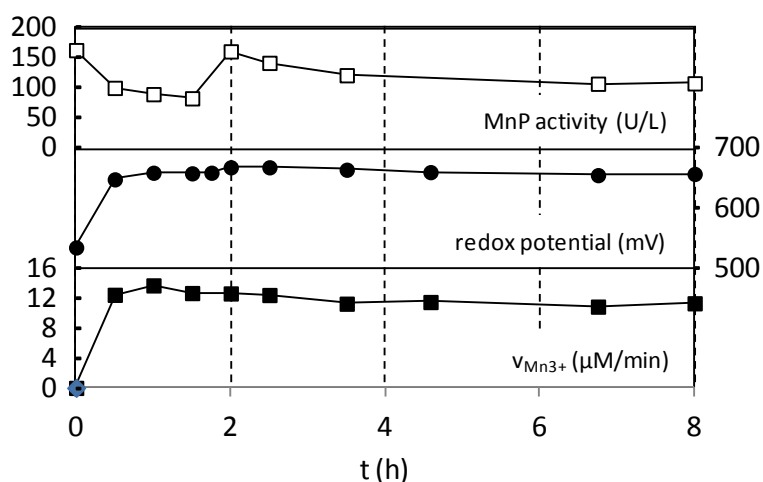
Figure 7.4. Typical Mn^{3+}-malonate continuous production profile in the "two-stage" system

It can be observed that during the beginning of the operation there is an increase in the Mn^{3+}-malonate production rate until a stable value is obtained after 30 min, approximately. Moreover, also during the first 30 min of operation there is a great enzymatic deactivation; presumably this may be due to the mechanic stress or due to adsorption in the ultrafiltration membrane. Concerning the enzymatic activity during the production of the oxidizing complex, the strategy was to perform the operation at 200 U/L, thereby when the MnP activity dropped below 100 U/L, a single pulse was added into the enzymatic reactor to recover the initial activity of 200 U/L. The measurement of

the online redox potential is very useful in order to easily predict when the steady state was reached.

7.3.1. Evaluation of the continuous production of Mn^{3+}-malonate in the "two-stage" system by response surface methodology

The data resulting from the 18 individual experiments to evaluate the effect of $v_{malonate}$ (x_1), v_{H2O2} (x_2) and HRT (x_3) are displayed in **Table 7.6**.

Table 7.6. Central composite Face Centered design matrix with response

Run	x_1	x_2	x_3	Y_1 (v_{Mn3+}, μM/min)	Y_2 ([Mn^{3+}], μM)	Y_3 (E.D., U/L·h)
1	-1	-1	-1	6.66	200	10.2
2	1	-1	-1	7.59	456	9.79
3	-1	1	-1	5.69	171	19.4
4	1	1	-1	6.87	206	22.3
5	-1	-1	1	5.88	412	14.0
6	1	-1	1	6.54	459	16.4
7	-1	1	1	7.68	537	21.8
8	1	1	1	7.46	523	20.8
9	-1	0	0	8.38	417	18.7
10	1	0	0	7.69	384	9.99
11	0	-1	0	9.24	467	16.8
12	0	1	0	15.1	753	16.5
13	0	0	-1	12.9	387	13.4
14	0	0	1	13.5	871	21.1
15	0	0	0	12.6	669	8.81
16	0	0	0	12.2	607	23.4
17	0	0	0	12.0	597	20.7
18	0	0	0	11.9	591	20.0

The experimental results were analyzed through three-dimensional response surface methodology in order to obtain as empirical model. Experimental data were fitted to a second order polynomial model with the

objective of explaining the mathematical relationship between the manipulated variables and the response variables, **equations [7.9-7.11]**.

$$Y_1 = 12.6 + 0.08 \cdot x_1 + 0.80 \cdot x_2 + 0.25 \cdot x_3 - 0.22 \cdot x_1 \cdot x_2 - 0.35 \cdot x_1 \cdot x_3 + 0.69 \cdot x_2 \cdot x_3 - 4.94 \cdot x_1^2 - 0.83 \cdot x_2^2 + 0.22 \cdot x_3^2 \qquad \textbf{[7.9]}$$

$$Y_2 = 621 + 21.4 \cdot x_1 + 27.4 \cdot x_2 + 146 \cdot x_3 - 44.8 \cdot x_1 \cdot x_2 - 42.1 \cdot x_1 \cdot x_3 + 68.3 \cdot x_2 \cdot x_3 - 226 \cdot x_1^2 - 16.4 \cdot x_2^2 + 2.52 \cdot x_3^2 \qquad \textbf{[7.10]}$$

$$Y_3 = 16.8 - 2.16 \cdot x_1 + 5.04 \cdot x_2 + 3.61 \cdot x_3 - 2.12 \cdot x_1 \cdot x_2 - 2.25 \cdot x_1 \cdot x_3 + 0.92 \cdot x_2 \cdot x_3 - 1.15 \cdot x_1^2 + 1.15 \cdot x_2^2 + 1.76 \cdot x_3^2 \qquad \textbf{[7.11]}$$

Statistical analysis shows (**Figure 7.5**) that the most statistically significant coefficients, at 10% level, were:

- Y_1, Mn^{3+}-malonate production rate: $x_1^2 > x_2$
- Y_2, Mn^{3+}-malonate concentration: $x_3 > x_1^2 > x_2 \cdot x_3$
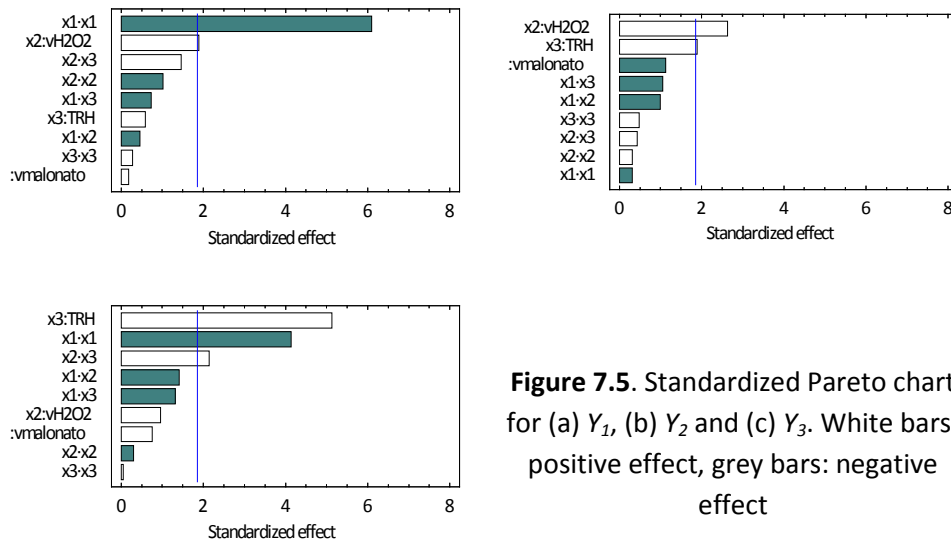- Y_3, enzymatic deactivation rate: $x_2 > x_3$

Figure 7.5. Standardized Pareto chart for (a) Y_1, (b) Y_2 and (c) Y_3. White bars: positive effect, grey bars: negative effect

The quadratic term of the Na-malonate feeding rate (x_1) had a negative effect on both Y_1 and Y_2. This effect may be explained because of the behavior of these response variables with the Na-malonate feeding rate (**Figure 7.6**) it can be observed that in both extreme values of x_1 (-1 and +1) the values of v_{Mn3+} and [Mn^{3+}] decrease; the same effect was observed when producing Mn^{3+}-malonate in batch mode.

In the case of the response variable Y_2, the most significant manipulated variable was the hydraulic retention time (x_3), which makes sense since the VP enzyme has more time to catalyzes the reaction between Mn^{2+} and H_2O_2, consequently produce more amount of Mn^{3+}.
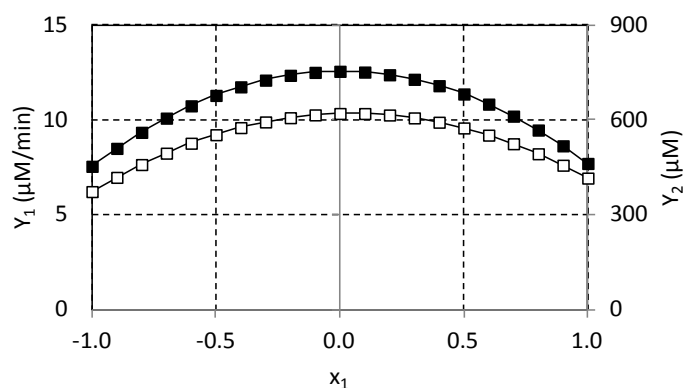
Figure 7.6. Effect of the manipulated variable x_1 on response variables (■) Y_1 and (□) Y_2.

Regarding the enzymatic deactivation rate (Y_3) the most significative effect was the individual effect of H_2O_2 feeding rate. The hydrogen peroxide concentration is, probably, the most important variable in the catalytic cycle of the VP. It is necessary to initiate the catalytic cycle of this enzyme but an excessively high concentration of H_2O_2 can inactivate the enzymatic ability through the formation of the inactive form Compound III [45].

The combined effects and the interactions between the three variables can be described quantificationally using RSM (**Figure 7.7-7.9**), which was successfully applied in this study to optimize the conditions to maximize both Y_1 and Y_2 and minimize Y_3 by using a non-linear optimization algorithm **Table 7.7**.

Table 7.7. Optimum conditions for the continuous production of Mn^{3+}-malonate in the "two-stage" system

Factor	Units	Response variables		
		v_{Mn3+} (μM/min)	$[Mn^{3+}]$ (μM)	E.D. (U/L·h)
$v_{malonate}$	μM/min	248	237	200
v_{H2O2}	μM/min	37.2	40	10
HRT	min	70	70	30

As a result of this analysis, it was concluded that the optimal conditions to reach a compromise rendering the highest production of Mn^{3+}-malonate (Y_1 and Y_2) is obtained with a reasonable enzymatic activity loss (Y_3), are 250 and 25 μM/min Na-malonate and H_2O_2 feeding rate, respectively, and 50 min HRT. The Mn^{3+}-malonate production profile with the optimal conditions is shown in **Figure 7.10**.
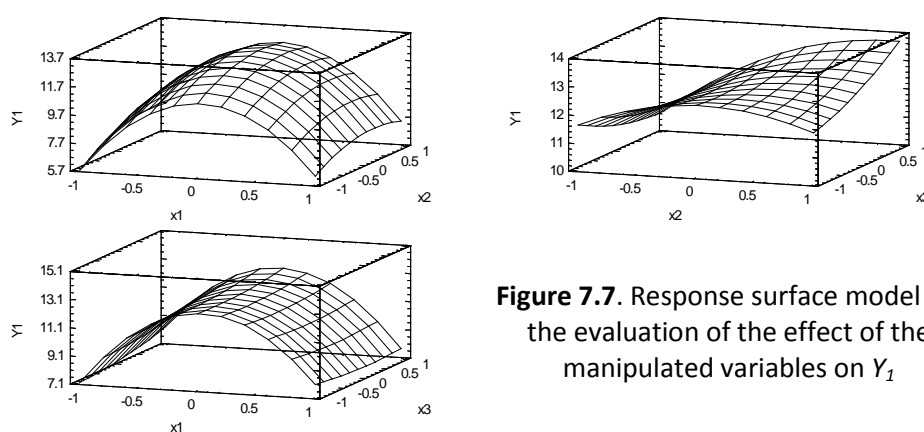
Figure 7.7. Response surface model for the evaluation of the effect of the manipulated variables on Y_1
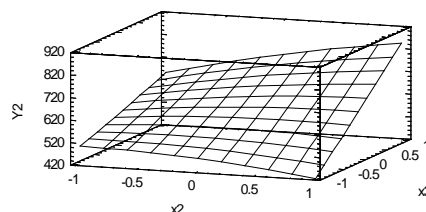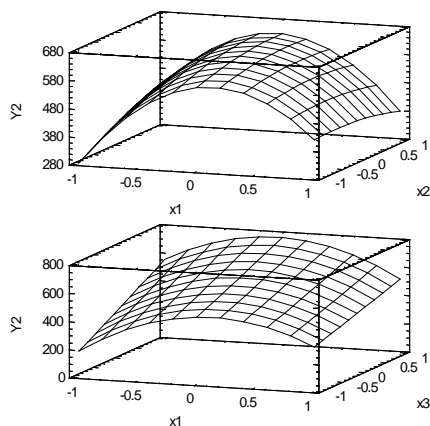
Figure 7.8. Response surface model for the evaluation of the effect of the manipulated variables on Y_2
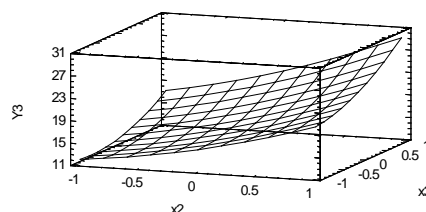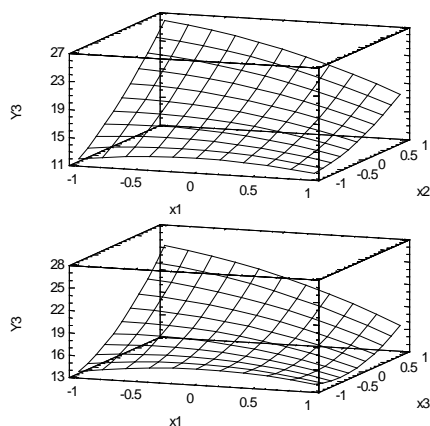
Figure 7.9. Response surface model for the evaluation of the effect of the manipulated variables on Y_3

Under these conditions the results were: 12.2±0.33 µM/min Mn^{3+}-malonate production rate, 616±35.6 µM Mn^{3+}-malonate concentration and 18.2±6.43 U/L·h enzymatic deactivation rate.

7.3.2. Design of the control system of the enzymatic reactor in the "two-stage system"

In most of equipments and process units, variables has to be controlled simultaneously, since in a multivariable process, a manipulated variable may affect more than one controlled variable and, vice versa, one controlled variable

can be affected by one or more manipulated variables. This type of processes is called *Multi-Input-Multi-Output* (MIMO).
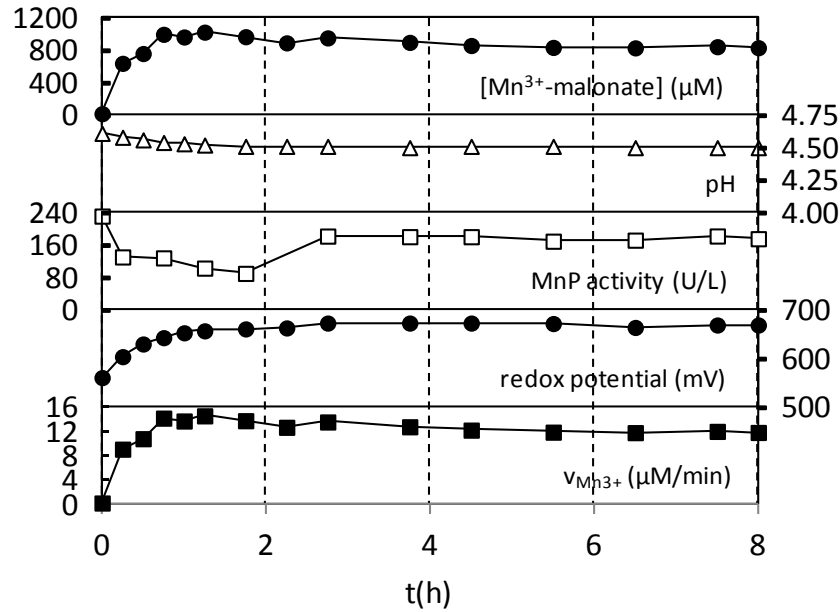
Figure 7.10. Profile of the production of Mn^{3+}-malonate under optimal conditions. (●) [Mn^{3+}-malonate], (△) pH, (□) MnP activity, (●) redox potential and (■) v_{Mn3+}

Therefore, the first question that arises when designing the structure of the control system is how to match the manipulated and controlled variables to form the loops. This issue is very important as it is closely related to the main problem of multivariable process control: the interactions between control loops. Interactions between loops may be minimized by properly pairing the manipulated and controlled variables. In this work, the methodology employed for the design and analysis of the continuous Mn^{3+}-malonate production process, was the Relative Gain Array (RGA).

After analyzing the profiles of each controlled variable in function of each manipulated variable, **Figure 7.11**, it can be observed that both Y_1 and Y_2

have a sign change and there is a maximum around $x_1 = 0$, the same behavior observed for Y_1 as a function of x_2.
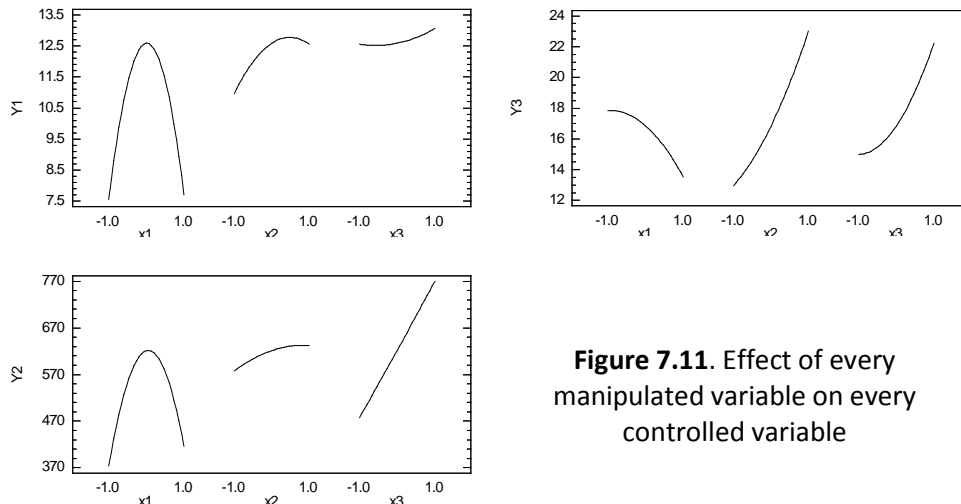
Figure 7.11. Effect of every manipulated variable on every controlled variable

Consequently, instead of calculating the RGA matrix for the entire range, from -1 to +1, it was calculated in two different segments, from -1 to 0 (segment A) and 0 to +1 (segment B). Thereby, it has been calculated how each controlled variable varies with an increment of the manipulated variables from -1 to 0 in the case of segment A, and from 0 to +1 in the case of segment B. The manipulated variables which are not evaluated, for each gain calculation, have remained in the central value, i.e. at zero. For example, when evaluating the effect of the variable x_1 on Y_1, the values of x_2 and x_3 were zero.

The considered restrictions were:

- Y_1 = 10 – 15 μmol/L·min
- Y_2 = 600 - 900 μM
- Y_3 = 0 - 15 min
- x_1 = 230 – 240 μmol/L·min
- x_2 = 20 – 30 μmol/L·min
- x_3 = 40 – 60 min

The results are shown below:

$$G_{(-1,0)} = \begin{bmatrix} 0.100 & 0.108 & 0.003 \\ 0.082 & 0.049 & 0.239 \\ -0.007 & 0.086 & 0.062 \end{bmatrix} \quad RGA_{(-1,0)} = \begin{bmatrix} 0.7123 & 0.2967 & -0.0090 \\ 0.2147 & -0.1240 & 0.9093 \\ 0.0731 & 0.8272 & 0.0997 \end{bmatrix}$$

$$G_{(0,1)} = \begin{bmatrix} -0.097 & -0.002 & 0.047 \\ -0.068 & 0.012 & 0.248 \\ -0.027 & 0.137 & 0.179 \end{bmatrix} \quad RGA_{(0,1)} = \begin{bmatrix} 1.1634 & -0.0041 & -0.1593 \\ -0.1742 & -0.0728 & 1.2469 \\ 0.0108 & 1.0769 & -0.0877 \end{bmatrix}$$

$$G_{(-1,1)} = \begin{bmatrix} 0.001 & 0.053 & 0.025 \\ 0.007 & 0.030 & 0.243 \\ -0.014 & 0.112 & 0.120 \end{bmatrix} \quad RGA_{(-1,1)} = \begin{bmatrix} 0.1082 & 1.0297 & -0.1379 \\ 0.1141 & -0.0646 & 0.9504 \\ 0.7777 & 0.0349 & 0.1874 \end{bmatrix}$$

The values of the condition number (γ) of each RGA matrix were $\gamma_{(-1,0)}$ = 4.2, $\gamma_{(0,1)}$ = 4.8 and $\gamma_{(-1,1)}$ = 35. This means that the pairing of variables calculated for the entire range (-1,1) is not suitable to be used since the gamma value is far from the unit.

According to the matrices $RGA_{(-1,0)}$ and $RGA_{(0,1)}$, the Mn^{3+}-malonate production rate (v_{Mn3+}, Y_1) must be controlled with the Na-malonate addition rate ($v_{malonate}$, x_1), the Mn^{3+}-concentration ($[Mn^{3+}]$, Y_2) must be controlled with the hydraulic retention time (*HRT*, x_3) and, finally, the enzymatic deactivation rate (*E.D.*, Y_3) must be controlled with the H_2O_2 addition rate (v_{H2O2}, x_2).

7.3.3. Continuous elimination of bisphenol A, triclosan, estrone, 17β-estradiol and 17α-ethinylestradiol in the "two-stage" system

The ability of the "two-stage" system to continuously eliminate BPA, TCS, E1, E2 and EE2 was evaluated. The oxidizing complex was produced in the enzymatic reactor (**[1]** in **Figure 6.2**) under the optimal conditions showed above, i.e. 250, 25 and 25 µM/min Na-malonate, $MnSO_4$ and H_2O_2 feeding rates, respectively, 200 U/L MnP activity, 50 min HRT, pH 4.5 and at 30ºC.

The elimination reaction was carried out in the oxidation reactor (**[2]** in **Figure 6.2**). In order to evaluate the effect of the EDCs concentration and the effect of the matrix where the EDCs are contained, four experiments were performed (**Table 7.4**).

Experiment 1 and experiment 2

Two different experiments were performed to evaluate the influence of the matrix in which the EDCs are contained.

In the first experiment, experiment 1, the matrix was real wastewater spiked with known concentrations of BPA, TCS, E1, E2 and EE2 (**Figure 7.12**). It can be observed that there is a positive relationship between production of the complex Mn^{3+}-malonate and the elimination of the EDCs, since during the first 30 min there is an increase in the production rate of the chelate up to 11.7 ± 0.9 µM/min and, in parallel, there is an increase in the degradation rate of all EDCs, until a 100% degradation extent is obtained. As expected, the change of the matrix from real wastewater to distilled water (assay 2) did not affect negatively neither the degradation rates nor degradation extents.

Experiment 3 and experiment 4

In order to evaluate the ability of the "two-stage" system to eliminate low concentration of EDCs (µg/L·min and ng/L·min), two different experiments were carried out in real wastewater spiked with known concentrations of EDCs. Results of feeding rate and degradation rate of each EDC are displayed in **Table 7.8**.
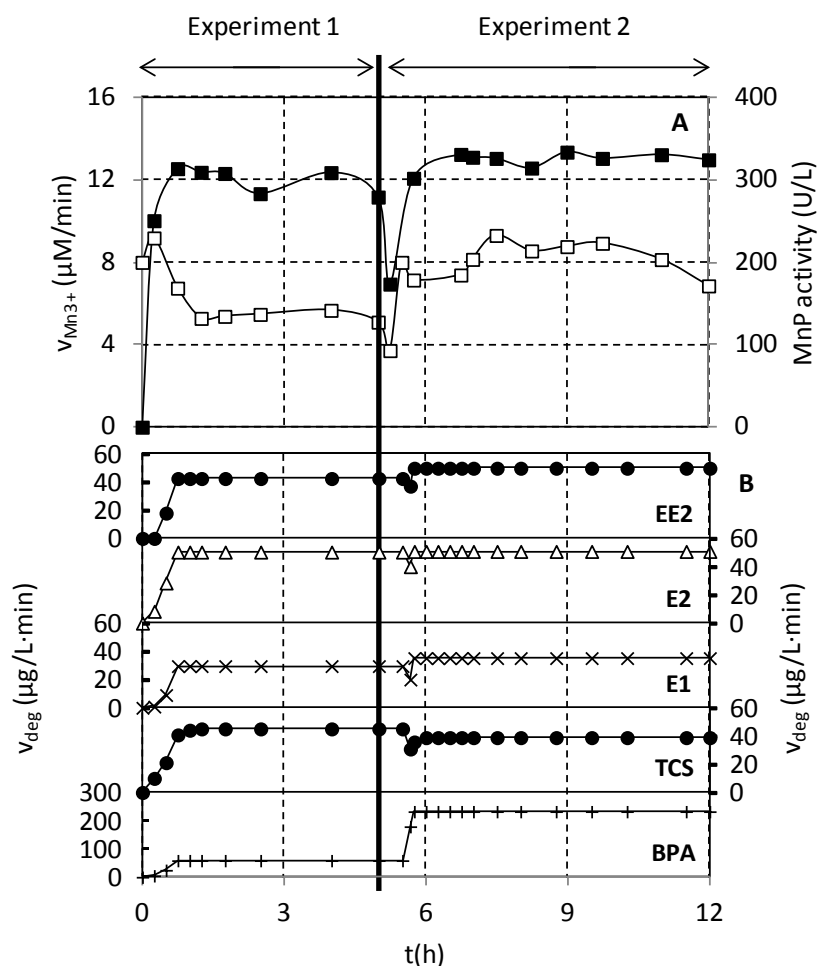
Figure 7.12. Continuous elimination of EDCs in the "two-stage" system: experiment 1 + experiment 2. (■) v_{Mn3+}, (□) MnP activity, (+) $v_{deg-BPA}$, (●) $v_{deg-TCS}$, (x) v_{deg-E1}, (△) v_{deg-E2} and (●)$v_{deg-EE2}$

These results demonstrate that the "two-stage" system is able to successfully eliminate all EDCs tested even when the feeding rate was very low. For all disruptors and in all conditions, the degradation rate was higher than 95%.

Table 7.8. Results from the experiments 3 and 4

	Experiment 3		Experiment 4	
	v_{feed} (µg/L·min)	v_{deg} (µg/L·min)	v_{feed} (ng/L·min)	v_{deg} (ng/L·min)
BPA	2.70	2.57	58.2	58.1
TCS	1.30	1.29	31.5	31.5
E1	-----	-----	99.8	99.8
E2	1.95	1.95	34.0	33.9
EE2	4.30	4.30	160	160
E.D. (U/L·h)	13.0		12.4	

7.3.4. Continuous elimination of bisphenol A, triclosan, estrone, 17β-estradiol and 17α-ethinylestradiol in an enzymatic ultrafiltration system

One of the main problems related to the use of enzymes in the degradation or removal of organic compounds is their deactivation. The loss of activity of the enzymes is typically due to the effect of the conditions in which the reaction has to be performed: pH, presence of organic solvents or denaturizing agents, mechanic stress, etc. Thereby, the ability of the enzyme VP to eliminate BPA, TCS, E1, E2 and EE2 in an enzymatic ultrafiltration system (**Figure 7.2**) was evaluated in two different matrixes: real wastewater (experiment 5, **Figure 7.13**) and distilled water (experiment 6, **Figure 7.14**).

The real wastewater had a negative effect in the ultrafiltration membrane as well as the enzymatic stability and the elimination rates of the EDCs (**Figure 7.13**). Even after the filtration of the wastewater before using (0.25 µm), the ultrafiltration membrane was clogged after three hours and a half (**Figure 7.15**), presumably due to the presence of colloidal solids [329] since colloidal particles have a diameter of between 0.001-1 µm, approximately [330].
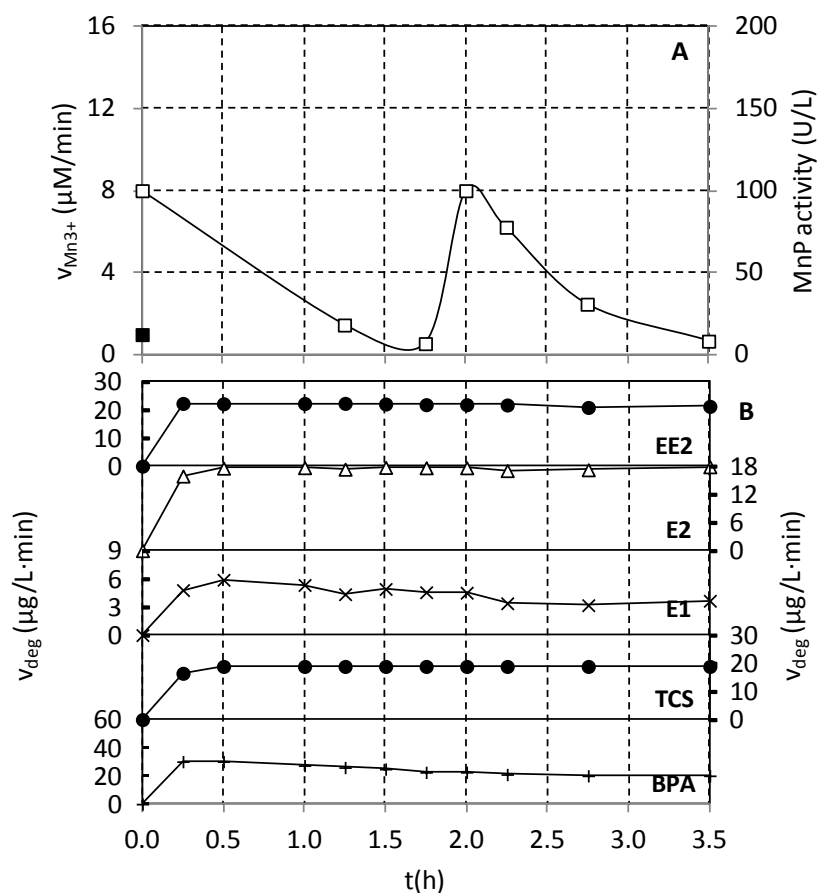
Figure 7.13. Continuous elimination of EDCs in the enzymatic ultrafiltration membrane system. Real wastewater, experiment 5. (■) v_{Mn3+}, (□) MnP activity, (+) $v_{deg-BPA}$, (●) $v_{deg-TCS}$, (x) v_{deg-E1}, (△) v_{deg-E2} and (●)$v_{deg-EE2}$

During ultrafiltration of colloidal suspensions, particles within the feed stream are convectively driven to the membrane surface where they accumulate and tend to form a cake or gel layer. This particle build-up near the membrane surface is known as concentration polarization, and results in increasing of hydraulic resistance to permeate flow; as a result the permeate flux declined with time, the pressure in the system increased more than 1.5 bars and the operation had to be stopped.
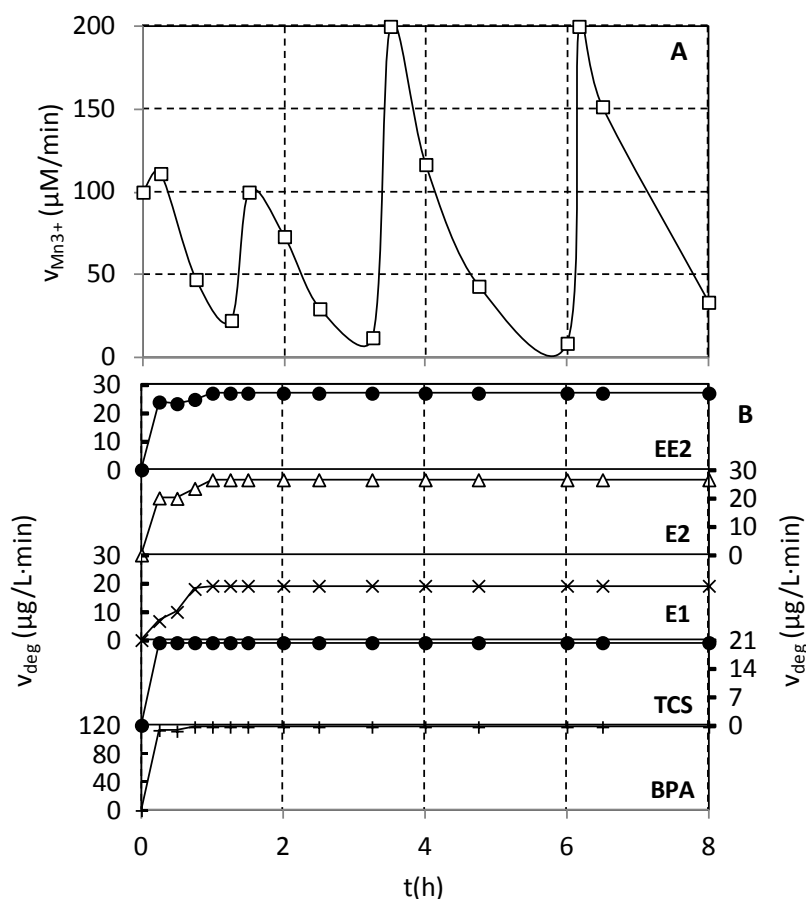
Figure 7.14. Continuous elimination of EDCs in the enzymatic ultrafiltration membrane system. Distilled wastewater, experiment 6. (■) v_{Mn3+}, (□) MnP activity, (+) $v_{deg-BPA}$, (●) $v_{deg-TCS}$, (x) v_{deg-E1}, (△) v_{deg-E2} and (●)$v_{deg-EE2}$

The wastewater also had a negative effect on the degradation rates and extents, and in the enzymatic deactivation rate (**Table 7.9**). The change of matrix to distilled water largely improved the degradation rate and extent (in all cases, the degradation extent was higher than 95%) but the enzymatic deactivation rate was still very high. Presumably, the deactivation in assay 6 was due to the mechanic stress.

Figure 7.15. Appearance of the ultrafiltration cartridges after their use to eliminate EDCs contained in real wastewater. (a) Enzymatic ultrafiltration membrane system and (b) "two stage" system.

Table 7.9. Results from the experiments 5 and 6

	Experiment 5		Experiment 6	
	v_{feed} (µg/L·min)	v_{deg} (µg/L·min)	v_{feed} (µg/L·min)	v_{deg} (µg/L·min)
BPA	30.2	24.5	117	117
TCS	18.9	18.6	20.4	20.4
E1	16.9	4.46	19.1	17.5
E2	24.9	17.4	26.5	25.3
EE2	24.9	21.8	27.0	26.3
E.D. (U/L·h)	83.1		91.4	

In order to compare the results from the "two stage" system experiments, working with real wastewater (experiment 1), with the results obtained in the enzymatic ultrafiltration system (experiment 5) a new variable, degradation yield (Y_d), was defined, **equation [7.12]**. Results are shown in **Table 7.10**.

$$Y_d = \frac{v_{deg}}{E.D.} \left(\frac{mg}{U}\right) \qquad \textbf{[7.12]}$$

The degradation yield allows quantifying, not only the ability of the enzyme to eliminate the EDCs but also the enzymatic stability and, consequently, the efficiency.

Table 7.10. Comparison of the results from enzymatic and "two-stage" system

	Enzymatic ultrafiltration system	"Two-stage" system
Compound	Y_d (mg/U)	
BPA	0.295	4.05
TCS	0.224	3.11
E1	0.054	2.03
E2	0.209	3.47
EE2	0.263	2.92

Comparing the results, from the enzymatic system with the results from the "two-stage" system, shown in **Table 7.10** it can be observed that the objective sought during the design of the "two-stage" system, improvement of the removal yield, is achieved, since there is an increase (10 fold) of the yield of the operation due to two factors: the reduction of enzyme inactivation and increased the degradation rate of EDCs.

7.3.5. Continuous elimination of bisphenol a by CLEA®s in a microfiltration system

The successful co-aggregation of VP and GOD provided an integrated system in which the oxidation of glucose in situ continuously produced H_2O_2 required by VP (**Figure 4.3b**). Moreover, due to the size of VP-GOD-CLEA®s (~5-10 μm diameter, determined by light microscopy, data not shown) the enzyme can be easily maintained in a continuously operated microfiltration membrane reactor.

In contrast to previously operated reactor systems with peroxidases, the setup (**Figure 7.3**) was simplified by the addition of glucose to the solution to be

treated, making a dosage of H_2O_2 unnecessary and allowing for a less controlled long-term operation. The continuous degradation of BPA from a 10 mg/L solution (110 µg/L·min) by VP-GOD-CLEA®s is shown in **Figure 7.16**. At a hydraulic retention time for 90 min more than 90% of BPA were constantly eliminated for 2 days, approximately. This finding is in agreement with the degradation results obtained from batch elimination assays of BPA using VP-GOD-CLEA®s (**Figure 5.8**). A similar reactor system was used by Cabana et al. (2009) [229]. Authors developed a perfusion basket reactor for the continuous elimination of EDCs (NP, BPA and TCS) using a laccase-CLEA®s, obtaining elimination of these disruptors up to 85%.

Problems in the application of membrane reactors for retention of free enzyme are fouling and clogging, even when they are well mixed. One major advantage of the CLEA®s and other forms of immobilized enzymes is the possibility to use large pore sizes for the membrane, thus minimizing the above mentioned problems. Moreover, the use of large pore sizes minimizes the deactivation due to the mechanic stress since high working pressure is not needed. In addition, the immobilization of enzymes enhances the stability against extremely pH values, presence of organic solvents, denaturant agents, etc. This is reflected in the enzymatic deactivation enzyme which in this system was lower compared to the enzymatic ultrafiltration membrane system and the "two-stage" system, 91.4, 12.4 and 1.20 U/L·h, respectively.
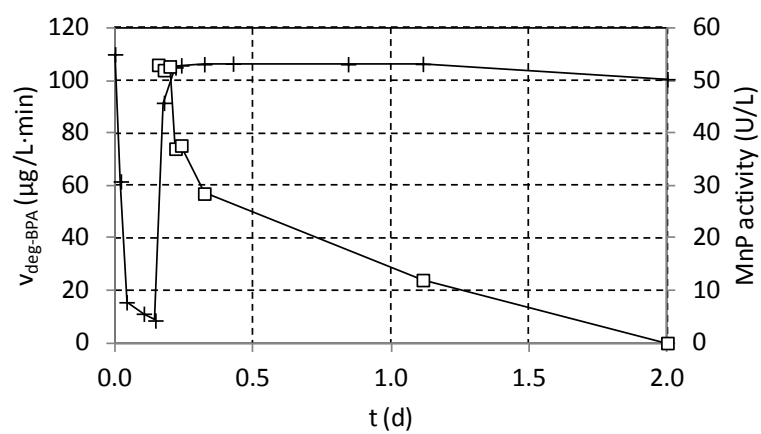
Figure 7.16. Continuous elimination of EDCs in the enzymatic microfiltration system. (□) MnP activity and (+) $v_{deg\text{-}BPA}$

7.4. Conclusions

In order to optimize the continuous production of the complex Mn^{3+}-malonate, a central composite face centered factorial design was chosen.   The independent variables were Na-malonate (x_1) and H_2O_2 (x_2) feeding rates and hydraulic retention time (x_3), whereas the response variables were Mn^{3+}-malonate production rate (Y_1), concentration of Mn^{3+}-malonate (Y_2) and enzymatic deactivation rate (Y_3).

Through an analysis of variance (ANOVA) the significance of an independent variable or the interaction between two of them was evaluated. The quadratic term of x_1 and the individual term of x_3 were the most statistically significant effects on Y_1, the individual effect of x_3 and the quadratic term of x_1 were the most significant effects on Y_2, and the individual term of x_2 and x_3 on Y_3.

Three-dimensional response surface model as a function of two factors, maintaining all other factors at fixed levels, hereby in at central point, was successfully applied. In this study, the objective was to maximize Y_1 and Y_2 and to minimize Y_3. As a compromise, the best conditions to maximize the production of the oxidizing complex having a reasonable deactivation rate where 250 and 25 µM/min feeding rate of Na-malonate and H_2O_2, respectively and a hydraulic retention time of 50 min.

The capability of the oxidizing chelate Mn^{3+}-malonate to eliminate five different disruptors, bisphenol A, triclosan, estrone, 17α-ethinylestradiol and 17β-estradiol, in a continuous mode was evaluated. It was demonstrated that the "two-stage" system was able to completely eliminate the five EDCs even when the feeding rate was in the order of ng/L·min.

With the purpose of confirming that this new set-up, "two-stage" system, reduces the deactivation rate of the enzyme, two experiments were carried out is an enzymatic ultrafiltration membrane system. In this system,

unlike the "two-stage" system, the enzyme is in direct contact with the contaminants, thus it was expected that the enzyme may have a faster deactivation due to the presence of the EDCs and the real wastewater. It was demonstrated that the deactivation of the VP was 7.5-fold lower in the "two-stage" system.

Finally, since an ultrafiltration cartridge leads to a high deactivation rate due to high pressure and mechanic stress, the elimination of the disruptor BPA was performed in a microfiltration reactor with the aim of further reducing the deactivation of the enzyme. In this system, the enzymatic deactivation decreased to 1.20 U/L·h, which means a 10.3-fold reduction.

Chapter 8

Polymerization of organic compounds, a different strategy for their removal

Chapter 8. Polymerization of organic compounds, a different strategy for their removal

8.1. Introduction

8.1.1. Dehydrogenation polymers

8.2. Materials and methods

8.2.1. Synthesis of coniferyl alcohol

8.2.2. Polymerization process in a fed-batch reactor

8.2.2.1. Polymerization of coniferyl alcohol

8.2.2.2. Polymerization of bisphenol A

8.2.3. Continuous polymerization of bisphenol A

8.2.4. Structural characterization of DHPs

8.3. Results and discussion

8.3.1. Polymerization of coniferyl alcohol for the production of dehydrogenation polymers (DHPs)

7.4.1.1. Enzymatic polymerization

7.4.1.2. Mn^{3+}-malonate mediated polymerization

8.3.2. Characterization of the DHPs

7.4.1.3. Size exclusion chromatography

7.4.1.4. Nuclear magnetic resonance

7.4.1.5. Pyrolysis-Gas Chromatography/Mass spectrometry

8.3.3. Polymerization of bisphenol A as a new approach of bioremediation

7.4.1.6. Effect of the $[H_2O_2]/[BPA]$ ratio (R_{BPA})

7.4.1.7. Effect of pH

7.4.1.8. Effect of reaction time (t_R)

8.3.4. Polymerization in a continuous process

8.4. Conclusions

Chapter 8. Polymerization of organic compounds, a different strategy for their removal

8.1. Introduction

Removal of bisphenol A (BPA) by advanced oxidation processes, such as photocatalytic degradation by TiO_2, photo-Fenton or enzymatic oxidation has attained satisfactory results [206, 331-333]. However, these processes occasionally result in the generation of secondary products that may be more harmful than the original compound [71, 182, 334].

According to Staples et al. (1998) [71] and Torres et al. (2008) [335], the intermediates from BPA with potential toxicity are phenol, 4-isopropylphenol, and semiquinone derivatives of BPA. To overcome the generation of more hazardous by-products derived from the oxidation of BPA, the physical separation of this compound by means of its polymerization is proposed in this chapter as an alternative. The polymerization of a compound involves the increase of size and molecular weight until a point where its solubility is exceeded, and consequently, the formed polymer precipitates. Thereby, the compound initially present in the aqueous phase would become a solid which can be separated by centrifugation or filtration.

The molecular structure of bisphenol A presents hydroxyl groups, which are prone to combine chemically to produce a very large chainlike or network molecule. The oxidizing agent, in this case the complex Mn^{3+}-malonate, oxidizes the molecule to form a free radical with the unpaired electron at the atom of the hydroxyl group (**Figure 8.1**).
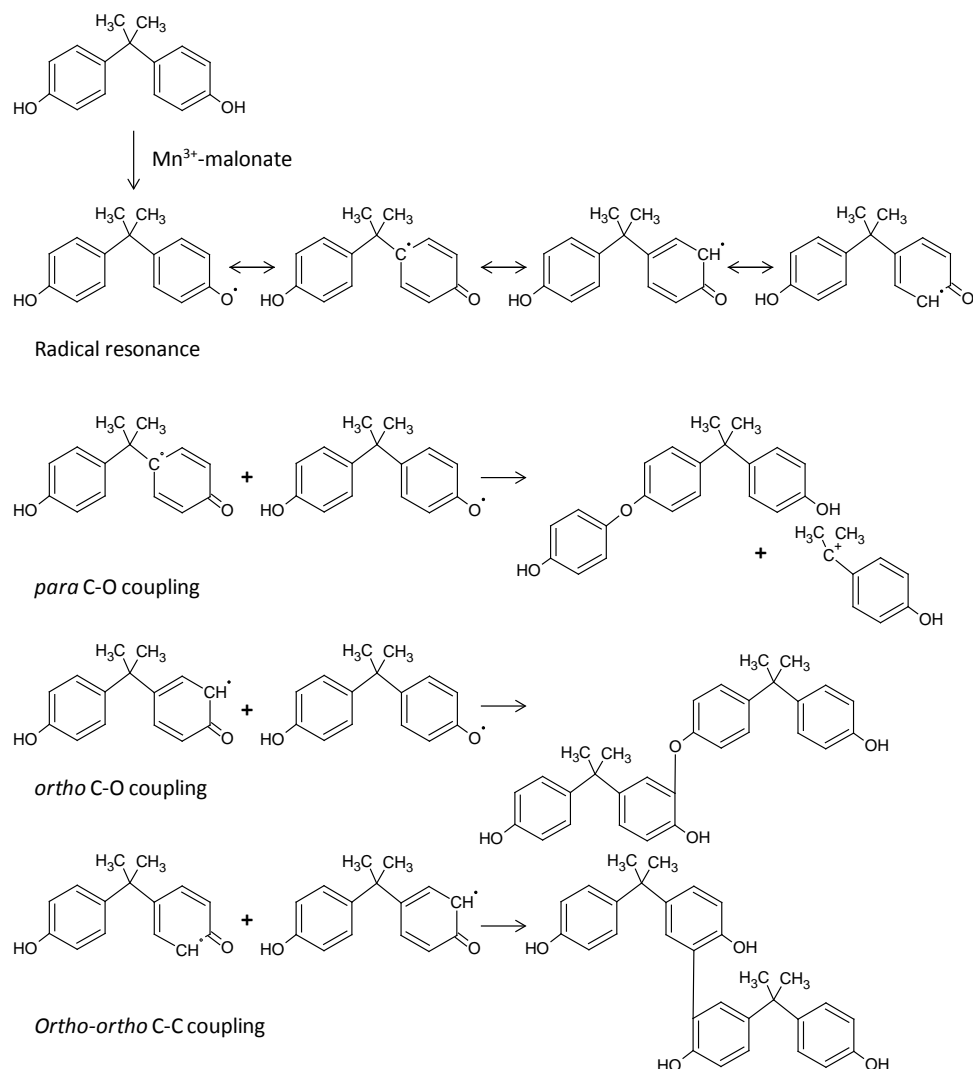
Figure 8.1. Polymerization of BPA, containing hydroxyl group, by the oxidative action of VP.

Polymerization can be divided in two steps, initiation and propagation. In the period of initiation, the reaction has a stoichiometry for Mn^{3+} and BPA of 1:1, whereas in the propagation step two ions are required for each molecule of BPA, i.e. in this step the stoichiometry for the Mn^{3+}:BPA ratio is 2:1 (**Figure 8.2**). For high molecular weight polymers, the reaction of propagation is likely to be

predominant. Since longs chains are required to accomplish precipitation, the molecular weight presumably will be high and, consequently, the stoichiometry leading the reaction will be 2:1. Considering that in the catalytic cycle of the enzyme versatile peroxidase, two ions of Mn^{3+} are produced for each molecule of H_2O_2, this would correspond to a $H_2O_2:Mn^{3+}$ ratio of 1:2, **equation [3.1]**. Consequently, from a theoretical point of view, the stoichiometry of the polymerization of BPA catalyzed by VP based on the $H_2O_2:BPA$ ratio should be 1:1.
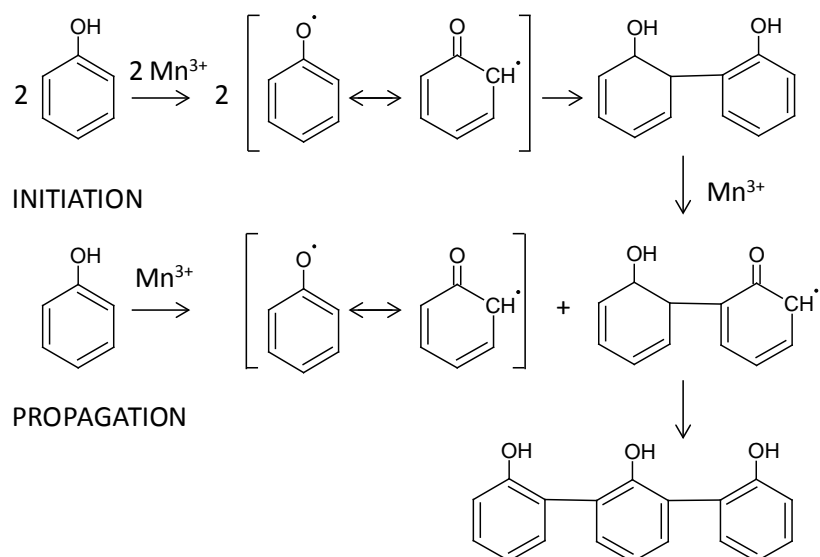
Figure 8.2. Polymerization of organic compounds, containing hydroxyl group, by the oxidative action of VP

8.1.1. Dehydrogenation polymers

Lignin is a heterogeneous polymer derived from phenylpropanoid monomers, mainly the hydroxycinnamyl alcohols coniferyl alcohol (CA) and sinapyl alcohol and minor amounts of *p*-coumaryl alcohol. These monolignols differ in their degree or aromatic methoxylation (-OCH_3 group, **Figure 8.3**).
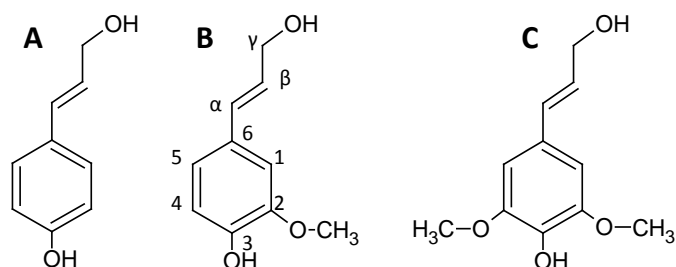
Figure 8.3. Chemical structures of three monolignols: (A) *p*-coumaryl alcohol, (B) coniferyl alcohol and (C) sinapyl alcohol

Although studies on lignin biosynthesis have started many years ago, there are still several aspects to elucidate such as lignin structure due to the difficulty of isolating lignin without damaging its structure and also related to lignin growth since polymerization reactions cannot be studied in vivo. To overcome these drawbacks, dehydrogenation polymers (DHPs) have been considered as lignin models for research purposes [336].

However, the structure and molecular weight of the DHPs differ from molecular weight and structures of milled wood lignin because the conditions of polymerization are different from those in the cell wall. Reaction systems containing organic solvents using Fe^{3+} as oxidant yielded DHPs with similar structure to that of natural lignin [337]. The main difference is related to the type of linkages between the monolignols, i.e. in natural lignin the most abundant linkage is β-O-4 and the most abundant one in DHPs is β-β or β-5. Polymerization of lignin precursors to lignin has been shown to be catalyzed by peroxidase/H_2O_2 in plant cell walls [338]. Therefore, a radical carrier which functions similarly to Fe^{3+} may function in the dehydrogenative polymerization catalyzed by peroxidase/H_2O_2. Versatile peroxidase, which produces two ions of Mn^{3+} during its Mn-oxidizing catalytic cycle, it is thought to produce β-O-4 rich DHP, which more closely approximates the structure of native lignin.

During the polymerization of CA, two moles of the oxidizing agent (Mn^{3+}) per mol of substrate (CA) are needed from a stoichiometric point of view (**Figure 8.4**), therefore one mol of H_2O_2 per mol of CA is necessary, **equation [3.1]**.
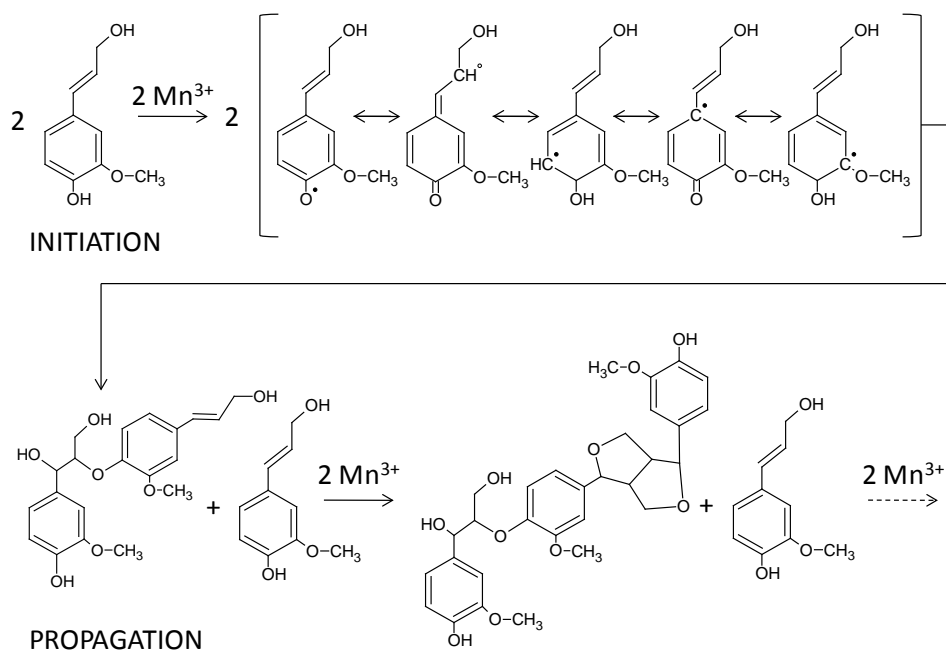
Figure 8.4. Mechanism of the polymerization of CA by the oxidative action of Mn^{3+}

The pH of the reaction medium affects both the stability of the enzyme and the structure of the DHPs. The highest oxidizing capability of this enzyme has been shown to be at pH 4.5 [339]. However, acidic pH is not very favourable for stability, corresponding the highest stability of this enzyme at pH 6 [300]. During polymerization, a quinone methide intermediate is formed (**Figure 8.5**). This intermediate is stabilized by the addition of hydroxyl groups from various nucleophiles depending on the pH value. In neutral and slightly acidic solutions (pH 6 and 7), the only dimeric product formed is the benzyl aryl ether (B). At pH 3, the addition of water becomes the predominant reaction to form

guaiacylglycerol-β-guaiacyl ether (A), which is the desired product. At near neutral or slightly basic pHs (7.5-8), the main dimeric reaction product is still the benzyl aryl ether (B), whereas the main dimeric product at pH higher than 9 is the retro aldol product (C) [340].
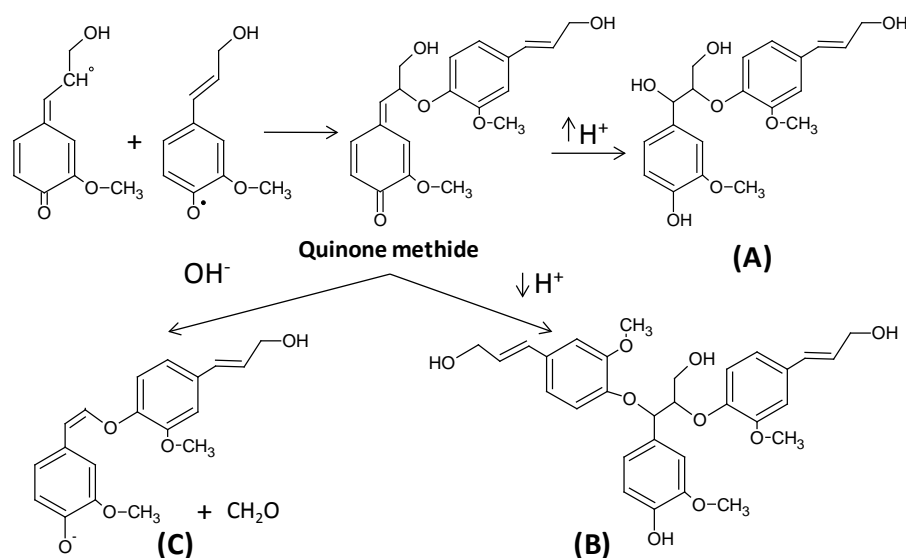
Figure 8.5. Effect of pH on DHP structure: (A) guaiacylglycerol-β-guaiacyl ether, (B) benzyl aryl ether and (C) retro aldol product

The use of organic solvents miscible in water as reaction media improves the solubility of the aromatic compounds and polymerization products which are poorly soluble in water. Therefore, organic solvents are expected to enhance the molecular weight of the DHPs.

The objective of this study is to analyze the ability of VP to polymerize organic compounds containing phenoxyl groups. Initially, the capability of VP and the complex Mn^{3+}-malonate to polymerize coniferyl alcohol, selected as model compound, to produce dehydrogenation polymers (DHPs) was evaluated. To do so, the effects of H_2O_2 concentration, pH and water-miscible organic solvents on the polymerization yield (Y_p) of coniferyl alcohol by VP were

assessed. Regarding the polymerization of BPA, the effect of three parameters: $[H_2O_2]$:[BPA] ratio, pH and reaction time (t_R) were investigated. Finally, once the optimal conditions for polymerization were established, the polymerization of BPA in a continuous process was proposed**.**

8.2. Materials and methods

8.2.1. Synthesis of coniferyl alcohol

Coniferyl alcohol was synthesized according to literature [341]. Ferulic acid was esterified with ethanol under acidic conditions into ethyl ferulate, which was purified and reduced to coniferyl alcohol by DIBAL-H.

8.2.2. Polymerization in a fed-batch reactor

8.2.2.1. Polymerization of coniferyl alcohol

Enzymatic polymerization

The enzymatic polymerization of coniferyl alcohol (CA) was performed as follows: 20 mg of CA was dissolved in a 20% mixture of 1,4-dioxane and sodium malonate buffer at pHs of 3, 4.5, 6 and 7.5 in a total volume of 5 mL and it was placed in a 5 mL-syringe. A second 5 mL-syringe contained a mixture of H_2O_2 (11.1–44.4 mM) and $MnSO_4$ (22.2 − 88.8 mM). Both solutions were added dropwise for 4 h to a 25 mL Erlenmeyer flask containing 10 mL of aqueous or water miscible organic solvent solution with VP (200 U/L as MnP activity, **Figure 8.6**). The reaction mixture was then stirred overnight at room temperature. After 24 h, the organic solvent was removed by evaporation under reduced pressure, pH adjusted to 2.5 and the precipitated polymer was finally recovered by centrifugation. The solid was washed with a large excess of acidic distilled water (pH 2.5) to remove unreacted coniferyl alcohol and low molecular weight oligomers. Thereafter, it was collected by centrifugation and vacuum-dried. The polymerization yield (Y_p) was determined as the ratio between the weight of the collected polymer and the initial amount of CA.
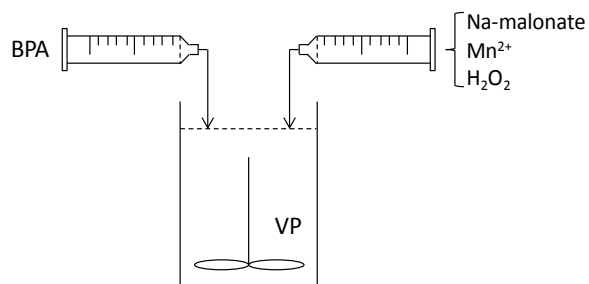
Figure 8.6. Schematic diagram of the fed-batch system for the polymerization of CA and BPA

Mn^{3+}-malonate mediated polymerization

The polymerization of CA by Mn^{3+}-malonate was performed as shown in **Figure 8.7**: 20 mg of CA was dissolved in a 20% mixture of 1,4-dioxane and sodium malonate buffer (pH 4.5) in a total volume of 5 mL. It was placed in a 5 mL-syringe and added dropwise for 4 h to the polymerization reactor with a CA feeding rate of 23.1 µM/min. Mn^{3+}-malonate was continuously added dropwise from a stock solution of 650 µM at feeding rate of 0.0625 mL/min, which means 2.03 µM/min. The complex had been previously produced in the "two-stage" system, which consisted of a stirred tank reactor [1] operated in continuous mode coupled to a 10 kDa cut-off ultrafiltration membrane [3] (Prep/Scale-TFF Millipore). Cofactors were added to the reactor from two stock solutions: H$_2$O$_2$ and a mixture of Mn^{2+} and Na- malonate at pH 4.5.

8.2.2.2. Polymerization of bisphenol A

In a typical procedure, the polymerization of BPA was performed as follows: 15 mg of BPA was dissolved in a 10% mixture of acetone and distilled water in a total volume of 10 mL, and it was placed in a 10 mL syringe. A mixture of Na-malonate (65.7 – 262.8 mM), H$_2$O$_2$ (3.28 – 13.14 mM) and Mn^{2+} (6.27- 26.28 mM) at different pH values (3 – 8) was placed in a second 5 mL-syringe. Both solutions were added dropwise for 1, 4, 10 or 12 h to an Erlenmeyer flask

containing 20 mL of distilled water with 200 U/L MnP (**Figure 8.6**). The reaction mixture was then stirred overnight at room temperature. After 24 h, one sample was withdrawn to measure enzymatic activity, pH was adjusted to 2.5 and the precipitated polymer was recovered by centrifugation. The solid was washed with a large excess of distilled water (pH 2.5) to remove low molecular weight oligomers. The unreacted BPA remaining in the liquid fraction was determined by HPLC analysis.
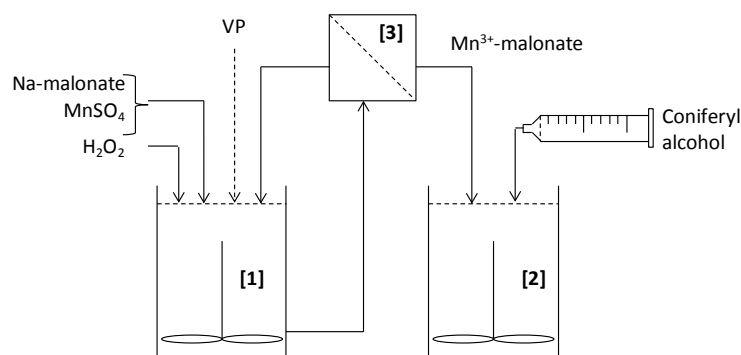
Figure 8.7. Schematic diagram of the "two-stage" system for the Mn^{3+}-malonate production. [1] Enzymatic reactor; [2] polymerization reactor; [3] ultrafiltration membrane

8.2.3. Continuous polymerization of bisphenol A

An Amicon stirred ultrafiltration cell 8200 (Millipore, Billerica, MA, USA) with 150 mL working volume equipped with a 0.1 μm cellulose acetate microfiltration membrane (Millipore) was used for the continuous polymerization of BPA. The reactor was operated at room temperature and fed with 182.5 nM/min of BPA (10 mg/L at 625 μL/min), 182.5 nM/min of H_2O_2 (10 mg/L at 625 μL/min), 365 nM/min of Mn^{2+} and 3.65 μM/min of Na-malonate at 625 μL/min (43.8 μmol/L, 87.6 μmol/L and 876 μmol/L, respectively). The experiment was started by adding VP enzyme at 200 U/L. Thereby, the membrane was able to retain the polymer formed into the Amicon cell but it was not able to retain the enzyme.

Subsequently, the reactor was coupled to a 10 kDa cut-off ultrafiltration membrane (Prep/Scale-TFF Millipore Corporation, Billerica, MA, USA), which allowed the recycling of the enzyme to the Amicon cell (**Figure 8.8**).

The experiment was performed for 43 h and samples were frequently taken from the Amicon cell and the system output to monitor the enzymatic activity. The samples taken from the reactor were centrifuged for 5 min at 5000 rpm before analysis. All samples from the system output were tested for residual BPA by HPLC.
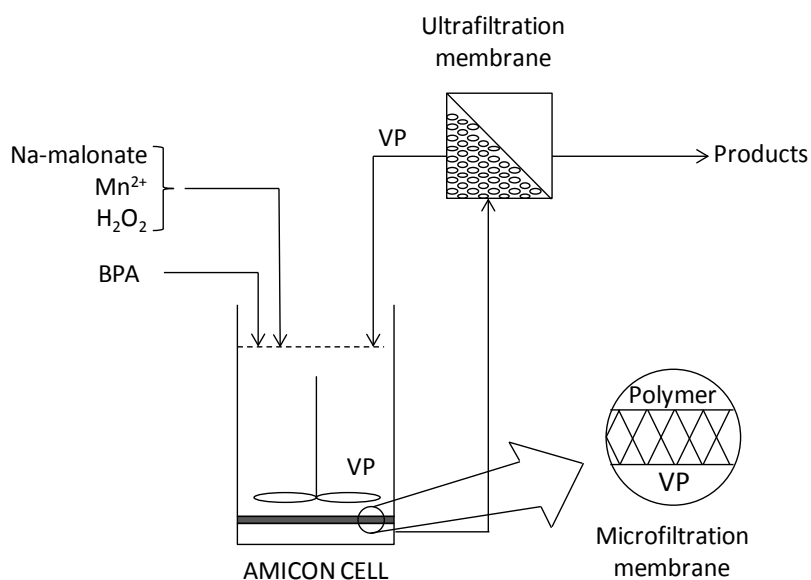
Figure 8.8. Schematic diagram of the continuous membrane system for the polymerization of BPA

8.2.4. Structural characterization of DHPs

Pyrolysis GC/MS was performed with a filament pulse pyrolyzer (Pyrola2000, Pyrol AB Sweden) which was connected to a GC/MS instrument (Varian 3800 GC/2000 MS). About 100 µg of the sample was pyrolyzed at 580°C for 2 s. Pyrolysis products were separated using a capillary column (J&W, DB-1701, 30 m

x 0.25 mm, film 1 μm) using carrier gas flow of 0.9 mL/min. Identification and quantification was done with an ion trap mass spectrometer (EI 70 eV). A more detailed description of the method is elsewhere [342]. Degradation products formed were identified using data from the literature [343-345].

For NMR analysis, the samples were acetylated with acetic anhydride/pyridine (1/1, v/v, reaction time 24 hours) and dissolved in $CDCl_3$. The spectra were acquired at 23°C on a Bruker Avance III 500MHz spectrometer equipped with a z-gradient double resonance probe. The semi-quantitative HSQC (1H-13C) experiments were carried out applying 5.0 s pulse delay, 0.11 s acquisition time, 128 transients and 1JC-H of 145Hz. Chromium(III)acetylacetonate was added to provide complete relaxation.

The molar mass measurements were performed by Waters HPLC in 0.1 M NaOH eluent using PSS's MCX 1000 and 100 000 Å columns with UV detection at 280 nm. The average molar masses (Mw, Mn) and the molar mass distributions were calculated relative to Na-polystyrene standards (Na-PSS, 3 420-148 500 g/mol) using Waters Empower 2 software. For the analysis, about 4 mg of sample was dissolved overnight in 4 ml analytical NaOH (0.1 M) and filtered with 0.45 μm PTFE membrane syringe filters (VWR).

8.3. Results and discussion

8.3.1. Polymerization of coniferyl alcohol for the production of dehydrogenation polymers (DHPs)

8.3.1.1. Enzymatic polymerization

Three parameters were assessed for their effect on the polymerization of coniferyl alcohol: H_2O_2/CA ratio (mol/mol), pH and use of water-miscible organic solvents. The H_2O_2/CA ratio (mol/mol, R_{CA}) was evaluated at five different levels: 0.5, 0.75, 1 (the stoichiometric ratio), 1.5 and 2 (**Figure 8.9a**). The highest polymerization yield value was obtained at $R_{CA} = 1$ (98.3±3.5%) but there is no statistical significant difference with the polymerization yield obtained at $R_{CA} = 0.75$ (91.8±9.6%). This could be explained because a ratio of 0.5 was enough during the initial polymerization step but during the propagation step a ratio of 1 was necessary (**Figure 8.4**). Therefore, a ratio between 0.75 and 1 is likely to be enough to fulfill complete polymerization. When R_{CA} was reduced to 0.5, the polymerization yield fell to 58.3±25.2%. This drop was probably due to the fact that the amount of oxidizing agent is half of the theoretically required value. A drop in the polymerization yield at values of R_{CA} greater than 1 was also observed, probably due to the deactivation of the enzyme. In fact, the residual activity of VP was 50.6±7.1% and 48.5±12.3% at ratios of 1.5 and 2.0, respectively.

The effect of pH was evaluated at four different levels: 3, 4.5 (highest oxidizing capacity of VP), 6 (highest stability of VP) and 7.5. The highest polymerization yield, 99.3±1.2%, was attained at pH 6; nevertheless no statistical differences were observed in comparison with the polymerization yield at pH 4.5: 91.7±10.4%. At those pH values, the observed enzymatic deactivation was negligible (pH 4.5) 29.0±3.4% (pH 6). The highest enzymatic deactivation was

observed at pH 3 and 7.5, which was reflected in the Y_p values, 84.2±9.3% and 77.5±19.3%, respectively (**Figure 8.9b**).
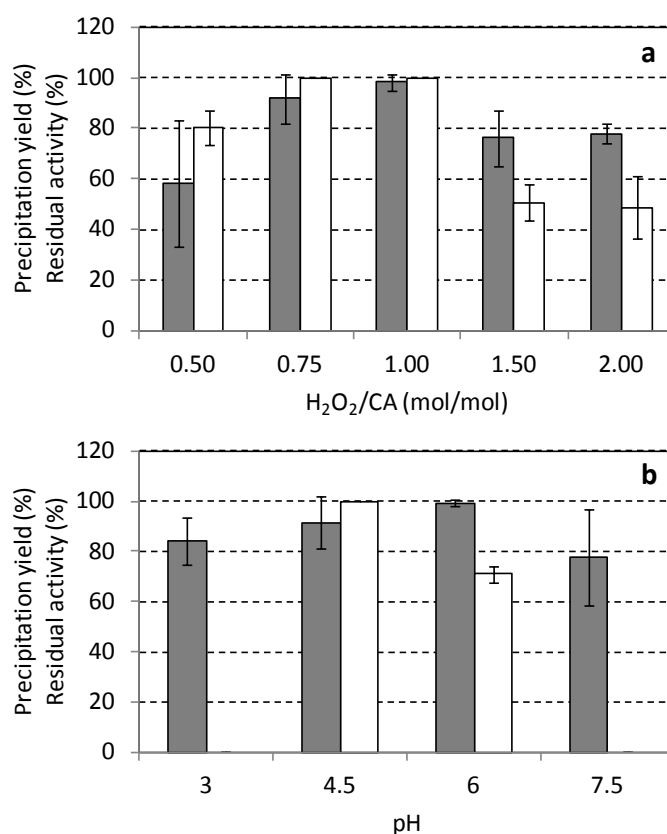
Figure 8.9. Effect of (a) H_2O_2/CA ratio and (b) treatment pH on precipitation yield and deactivation of the enzyme. Precipitation yield (grey columns) and residual activity (white columns).

The effect of three water miscible organic solvents was evaluated to perform the polymerization of coniferyl alcohol. The ability of the enzyme to produce DHPs drastically dropped due to the presence of the organic solvents (**Figure 8.10**), which is concomitantly reflected in the precipitation yield values, 57.5%, 25.5% and 21.5% for acetone, acetonitrile and 1,4-dioxane, respectively.

After 24 h of reaction, the residual enzymatic activity was negligible leading to very low polymerization yield.
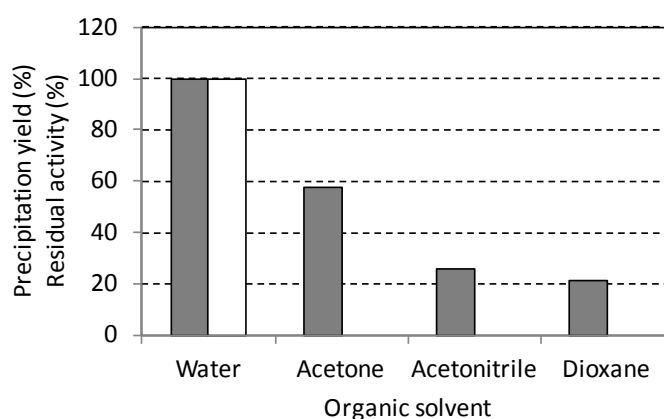
Figure 8.10. Effect of three water miscible organic solvents on precipitation yield and deactivation of the enzyme

8.3.1.2. Mn^{3+}-malonate mediated polymerization

The enzymatic reactor **([1], Figure 8.7**) was operated at the conditions found in **Chapter 7**, i.e. 240, 25 and 40 µM/min Na-malonate, MnSO$_4$ and H$_2$O$_2$ feeding rates, respectively, 200 U/L MnP activity and HRT of 70 min, to produce the highest level of Mn^{3+}-malonate. In these conditions, the concentration of the complex Mn^{3+}-malonate obtained after the ultrafiltration membrane was 875 µM. The complex was fed to the polymerization reactor (**[2], Figure 8.7**) at 62.5 µL/min, i.e. the feeding rate of the complex to the polymerization reactor was 2.73 µM/min, whereas the coniferyl alcohol was fed at 23.1 µM/min. Despite that the ratio Mn^{3+}:H$_2$O$_2$ was 0.12 while it should be 2, the results obtained from the Mn^{3+}-malonate mediated polymerization showed that the yield was almost complete (96.50%).

As a general conclusion of this part of the study, the VP-catalyzed polymerization of CA should be performed in aqueous solution with no organic solvent at pH between 4.5 and 6.0 and with a ratio between 0.75 and 1.

8.3.2. Characterization of the DHPs

Reaction conditions were expected to have a considerable effect on the structures of the formed DHPs. Thus, the second aim of this chapter was to identify the conditions that would be optimal regarding the similarity of the polymer to lignin structure rather than only optimizing the yield of the product. Detailed structural analyses of the formed DHPs were therefore performed.

8.3.2.1. Size exclusion chromatography

Size exclusion chromatography (SEC) analysis showed that the H_2O_2/CA ratio had clear effect on the degree of polymerization (**Table 8.1**). The highest values were obtained using ratios of 1-1.5. Polydispersities (Pd) were high, indicating very heterogeneous distributions. Significantly lower Mw values were measured for the samples prepared at pH values 3, 6 and 7.5. The samples from the Mn^{3+}-malonate experiments were not completely soluble in the eluent, and thus the high molar mass material may be excluded from the measurement.

Table 8.1. Effect of the H_2O_2/CA ratio and pH on molar mass and polydispersity.

pH	H_2O_2/CA ratio	Mw	Pd
4.5	0.50	4500	3.50
4.5	0.75	48800	24.50
4.5	1.00	80100	35.40
4.5	1.50	83600	29.90
4.5	2.00	41600	20.20
3.0	1.00	4600	3.60
6.0	1.00	1500	1.80
7.5	1.00	1300	1.70

8.3.2.2. Nuclear magnetic resonance

2D HSQC (1H-13C) NMR characterization of the sample was performed after acetylation. Unfortunately, the acetylation step was successful only to some of the samples due to limited solubility. Thus, only partial comparison of the effects of reaction conditions was possible. The poor solubility as such may be an indication of cross-linked structure.

The distributions of the main interunit linkages β-O-4 (A), phenyl coumaran (B) and resinol (C) in the samples obtained with the lowest H_2O_2/CA ratios 0.50 and 0.75 were determined (**Figure 8.11**). Analysis of the sample at ratio R_{CA} = 1 was successful only at pH 3. In addition to the interunit linkages, various α/γ-oxidised structures were detected (**Table 8.2**) [346].
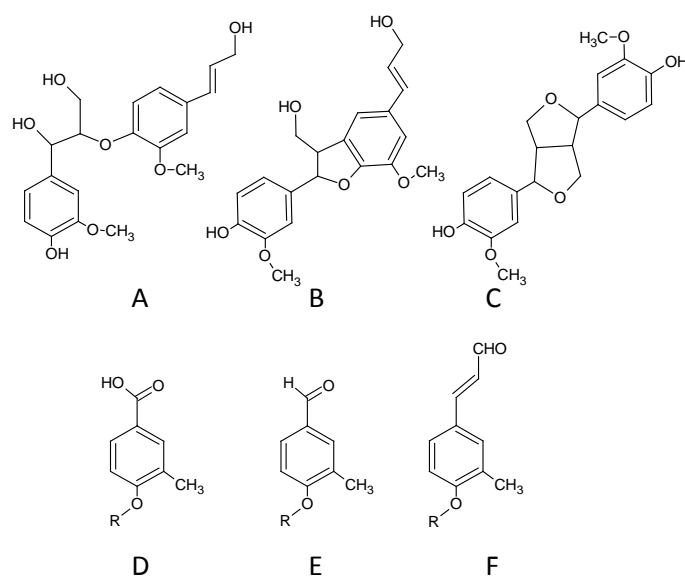
Figure 8.11. Main natural interunit linkages in lignin (A, B, C) and α/γ-oxidised structures (D, E, F) detected by NMR.

The proportion of the β-β resinol structures was found to be high at low (insufficient) H_2O_2 charge, as expected. The conditions had only minor effects on the distribution between the α/γ-oxidised structures.

Table 8.2. Effect of the H_2O_2/CA ratio on the relative abundance of natural interunit linkages and oxidized structures.

H_2O_2/CA ratio	A	B	C	E:D:F
0.5 (pH 4.5)	1	0.40	1.09	1.00:1.11:0.33
0.75 (pH 4.5)	1	0.55	0.60	1.00:1.36:0.32
1 (pH 3)	1	0.38	0.43	1.00:1.23:0.25

8.3.2.3. Pyrolysis-Gas Chromatography/Mass spectrometry

The analytical method of pyrolysis-GC/MS is widely used for the characterization of lignin structure. As the degradation is thermal, solubility of the samples is not required; therefore, the method complements 2D NMR, even if as detailed information cannot be obtained.

During the pyrolysis, lignin is degraded to rather simple phenols as a result of cleavage of ether and certain C-C linkages. Great advantage of this technique is that most of phenols retain their substitution patterns from the lignin polymer. Degradation products identified from the pyrograms of the DHP samples are listed in **Table 8.3**. It is possible to identify components from *p*-hydroxyphenyl, guaiacyl and syringyl units (**Figure 8.3**). Guaiacyl type components are mainly formed from softwood lignin, whereas hardwood lignin degrades to guaiacyl and syringyl type units. Also some *p*-hydroxyphenyl type components, which are typical structures for the non-wood materials, are formed from both wood types. In this study, pyrolysis was used to characterize DHPs polymerized from coniferyl alcohol. Thus, it is expected that pyrolysis of these DHPs will have similar type of degradation products than softwood lignin.

Table 8.3. Identified degradation products of DHPs

Compound	M_w	Compound	M_w
Catechol	110	trans-Isoeugenol	164
Phenol	94	Guaiacylpropyne	162
2-Methylphenol	108	Guaiacylallene	162
4-Methylphenol	108	Vanillin	152
Hydroxybenzaldehyde	122	Homovanillin	166
Guaiacol	124	Acetoguaiacone	166
m-Guaiacol	124	Guaiacylacetone	180
4-Methylguaiacol	138	4-(oxy-allyl)guaiacol	178
3-Ethylguaiacol	152	4-(1-Hydroxyprop-2-enyl)guaiacol	180
4-Ethylguaiacol	152	Dihydroconiferyl alcohol	182
4-Propylguaiacol	166	cis-Coniferyl alcohol	180
Vinylguaiacol	150	trans-Coniferyl alacohol	180
Eugenol	164	Coniferaldehyde	178

After integration, pyrolysis yield is calculated as the sum of peak areas of DHPs derived products normalized to the weight of the sample. The yield of pyrolysis products is related to the abundance of non-condensed structures, as only C-O bonds are expected to be extensively cleaved in pyrolysis [347]. In order to evaluate structural changes on various DHPs peak areas of *p*-hydroxypheny and guaiacyl derivatives were normalized to 100%. Two parallel py-GC/MS measurements were done for the each DHP samples and the averages of peak areas were calculated. The average variation between total peak areas of two parallel measurements was as high as 30%. Placement and staying of lignin sample on the filament, which is heated, is challenging that may explain the high variation between peak intensities. Profiles of lignin derived products between two parallel measurements were however alike.

Effect of H$_2$O$_2$/CA ratio

The DHPs produced by enzymatic polymerization of coniferyl alcohol with various H$_2$O$_2$/CA ratios were studied. Theoretical H$_2$O$_2$/CA ratio optimum is 1.0, therefore sample with R_{CA} = 1.0 was used as a reference. Yield of pyrolysis products with H$_2$O$_2$/CA ratios of 0.5, 0.75 and 1.0 was found to be same, and slightly higher than at ratios 1.5 and 2.0, suggesting that more condensed linkages are formed when excess of H$_2$O$_2$ is present (**Figure 8.12a**). Concerning the structure, only minor changes were observed in the different H$_2$O$_2$/CA ratios. At low H$_2$O$_2$ concentration more guaiacyl type structures with no oxygen in side chain were formed from DHP in comparison to reference DHP. Profiles were similar when H$_2$O$_2$/CA ratios were 0.75 and 1.0. The result indicates that H$_2$O$_2$/CA ratio of 0.75 is close to the theoretical optimum value, whereas when excess of H$_2$O$_2$ was used, the proportion of trans-coniferyl alcohol coniferaldehyde was changed in comparison to the reference DHP (**Figure 8.13a**).

Effect of pH

The effect of pH on the pyrolysis yield was more significant; clearly lower yields were obtained at high pH (**Figure 8.12b**). This result indicates that the higher pH is, the higher the amount of condensed structures originated in DHP. In addition to pyrolysis yield, the change of pH affected the proportions of degradation products formed from DHPs (**Figure 8.13b**).
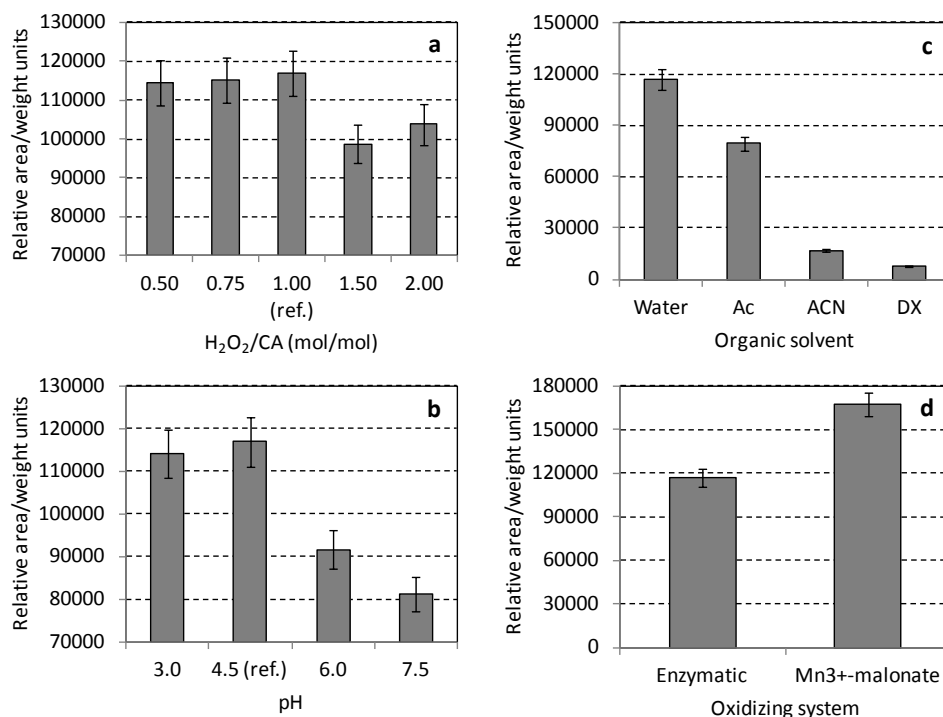
Figure 8.12. The effect of (a) H_2O_2/CA ratio and (b) treatment pH on pyrolysis yields.

The proportion of guaiacyl structures, mainly 4-methylguaiacol and trans-isoeugenol with no oxygen in the side chain, was increased at increasing pH value, whereas the proportion of coniferylaldehyde was decreased. Based on the model compound studies, 4-methylguaiacol is the main degradation product of β-5 structure [348]. Thus, the increase of 4-methylguaiacol may indicate higher proportions of β-5 structure in DHP at higher pH. The decrease of guaiacyl structures containing oxygen in the side chain, which are expected to be originated as a result of the cleavage of β-O-4 ether bonds in lignin, means lower proportion of β-O-4 bonds in DHP.
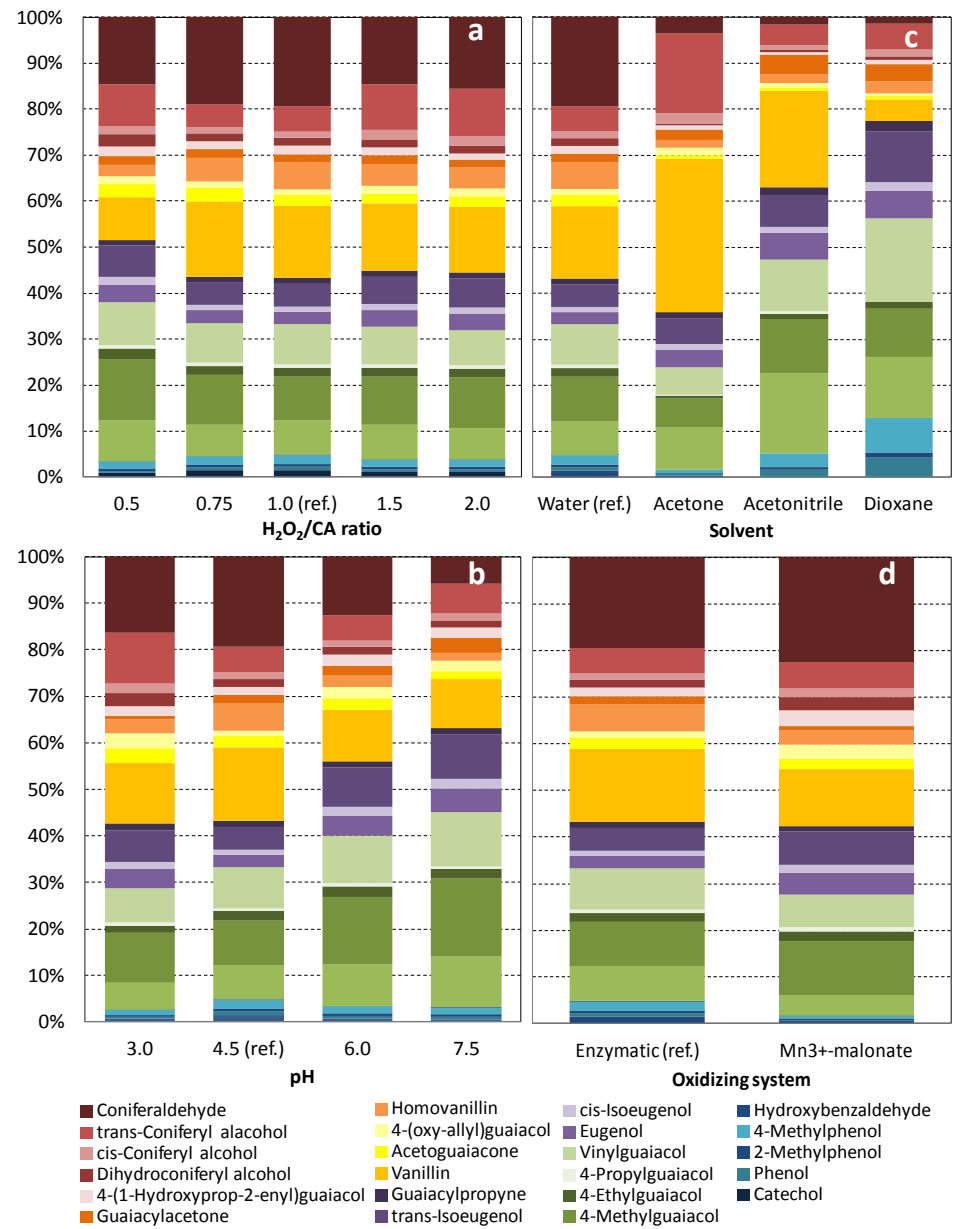
Figure 8.13. The effect of (a) H_2O_2/CA ratio, (b) treatment pH, (c) solvent and (d) oxidizing system, on the distribution of pyrolysis degradation products.

Effect of organic solvents

The DHPs obtained in the presence of organic solvents were unfortunately contaminated. Proportion of impurities in DHPs was much higher than that of original samples (**Figure 8.14**); thus the yields of pyrolysis derivatives of DHPs are not reliable (**Figure 8.12c**). Reference DHP polymerized in water media does not contain impurities like DHPs polymerized in organic solvents. It is assumed that the impurity was originated from the beakers that were used for freeze-drying. Based on the programs, the DHP polymerized in acetone is not so badly contaminated as DHPs polymerized in acetonitrile and dioxane. Profiles of pyrolysis degradation products of DHPs polymerized in different organic solvents were dissimilar between each other and, moreover, they have different profile in comparison to the reference DHP polymerized in water (**Figure 8.13c**).
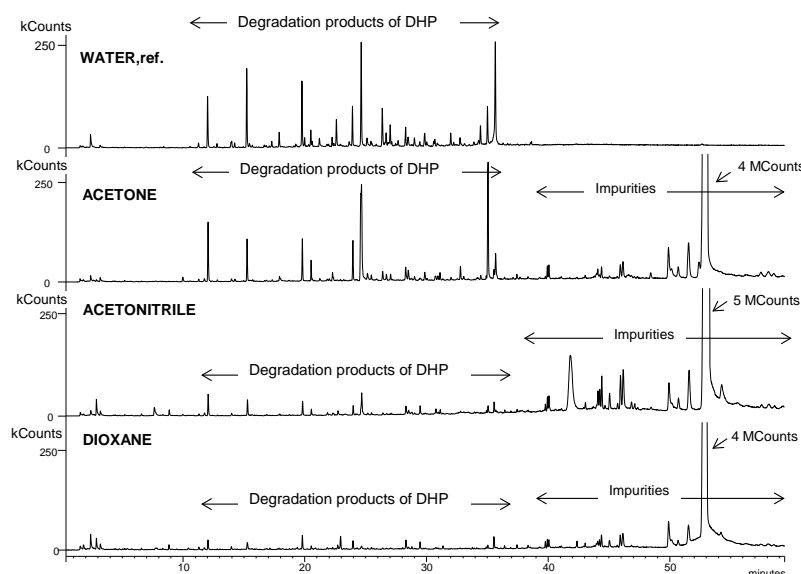
Figure 8.14. Pyrograms of DHPs polymerized in organic solvent media

Degradation products of DHP polymerized in acetone contains large amounts of vanillin and trans-coniferyl alcohol as well as lower proportion of 4-

methylguaiacol and vinylguaiacol in comparison to reference DHP. High proportion of guaiacyl structures with oxygen in the side chain may imply that acetone supports formation of β-O-4 linkages during DHP polymerization; however, lower proportion of *p*-hydroxyphenyl derivatives was present in DHP polymerized in acetone.

DHPs polymerized in the presence of acetonitrile and dioxane contained large proportions of guaiacyl derivatives with no oxygen in the side chain in comparison to reference DHP, suggesting that higher proportion of condensed structures in DHP structure prepared in organic solvent media in comparison to DHPs prepared in water. More vanillin was formed from the DHP polymerized in acetonitrile in comparison to the DHP polymerized in dioxane.

Mn^{3+}-malonate mediated polymerization

Yield of pyrolysis products was higher for the DHPs polymerized using Mn^{3+} – malonate in comparison to the polymerization attained with VP (**Figure 8.12d**). DHPs structures prepared by using Mn^{3+}-malonate were nearly identical to the ones obtained by enzymatic treatment at pH 4.5. The main difference is the proportion of guaiacol, vinylguaiacol and trans-coniferyl alcohol, which is higher in the DHPs produced by enzymatic treatment (**Figure 8.13d**).

As a summary, principle component analysis (PCA), which is designed for the visualization of similarities and differences between samples, was used to evaluate pyrolysis data obtained for the DHPs samples. Two principal components that describe the variance of the data were calculated. DHPs polymerized at various organic solvents were excluded for the PCA analysis due to the impurities in samples.

The score plot depicted in **Figure 8.15** shows how the samples are related to each other based on the pyrolysis data, whereas the loading plot

(**Figure 8.16**) shows which degradation products are important for the classification of the samples evaluated in the score plot.
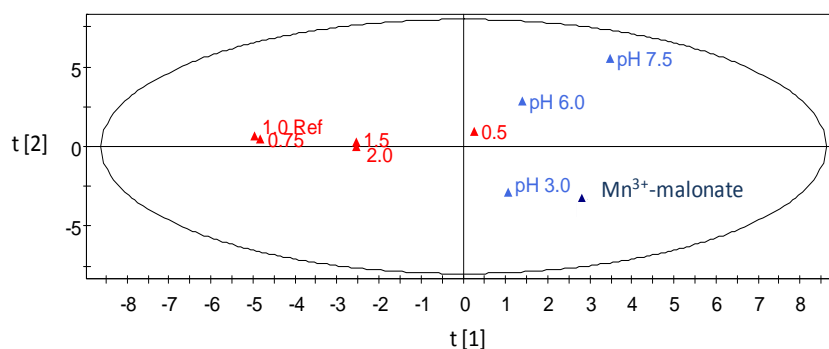
Figure 8.15. Score plot of the two principle components

Based on the pyrolysis results production of DHPs at various H_2O_2/CA ratios did not much change the polymer structure. Proportion of p-hydroxyphenyls and benzenediols as well as vanillin and homovanillin is higher in H_2O_2/CA series than that for the other DHPs. DHPs prepared at high pH produce, during the pyrolysis, high proportion of guaiacyl structures with no oxygen in the side chain whereas at low pH high proportion of guaiacyl structures with oxygen in the side chain is produced. DHPs polymerized by Mn^{3+}-malonate mediated polymerization processes have similar structure as DHP polymerized by enzymatic process at low pH.
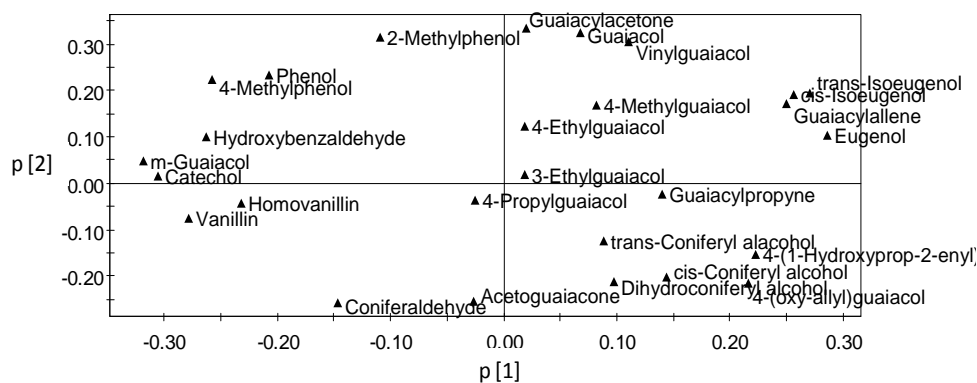
Figure 8.16. Loading plot

8.3.3. Polymerization of bisphenol A as a new approach of bioremediation

Bisphenol A was selected as a model compound to study the polymerization of EDCs. The polymerization was carried out in fed-batch mode in an Erlenmeyer flask with a final volume of 40 mL (**Figure 7.6**). The concentration of the starting material, BPA, was 1.5 g/L, higher than the solubility, 120 mg/L [136]; therefore, acetone was used to increase solubility (10% v/v).

Three parameters that may affect the polymerization yield on BPA were evaluated: [H_2O_2]/[BPA] ratio, pH and reaction time (t_R). The polymerization yield (Y_P, %) was calculated as the amount of obtained polymer referred to the initial amount of BPA. In addition, the residual concentration of soluble BPA was measured by HPLC. Results are shown in **Table 8.4**.

As shown, the polymerization yield of BPA in different conditions assayed is higher than 100%. This may be due to that the enzyme is produced in a complex medium containing phenolic compounds, such as polyethylene glycol (Tween 80) or phenolic compounds from the straw, which can react with the BPA molecules and, consequently, co-polymerize. Moreover, in some cases the amount of BPA contained in the polymer plus the residual amount of soluble BPA contained in the reaction medium at the end of the experiment, is less than

the initial amount of BPA. A possible explanation is that the molecules of bisphenol A can react to produce oligomers (dimers, trimers, tetramers, etc.) which are soluble in the reaction medium (they do not precipitate) but they cannot be detected by HPLC analysis.

Table 8.4. Results obtained during the polymerization of BPA.

$[H_2O_2]/[BPA]$ (mol/mol)	pH	t_R (h)	Y_p (%)	Residual soluble BPA (%)
4	4.5	4	147	1.41
2	4.5	4	191	0.15
1	4.5	4	113	0.00
0.5	4.5	4	63.6	26.7
0.25	4.5	4	33.8	40.0
1	3	4	68.8	43.9
1	6	4	141	0.04
1	8	4	40.1	1.01
1	4.5	1	159	0.71
1	4.5	10	109	0.29
1	4.5	12	140	0.27

8.3.3.1. Effect of the $[H_2O_2]/[BPA]$ ratio (R_{BPA})

From a theoretical point of view, the moles of hydrogen peroxide per mol of BPA required to perform the polymerization is 1. However, the effect of the $[H_2O_2]/[BPA]$ ratio was evaluated at five different levels: 0.25, 0.5, 1, 2 and 4 (**Table 8.4**). The lowest residual soluble BPA value was obtained at R_{BPA} = 1, but there is no difference with the values obtained at R_{BPA} = 2 (0.15%) and R_{BPA} = 4 (1.41%); in these three cases the polymerization yield was higher than 100%. When R_{BPA} was reduced to 0.5 or to 0.25, the Y_P values fell to 63.6% and 33.8%, respectively, whereas the residual soluble BPA dropped to 26.73% and 40.59%, respectively. These reductions were probably due to the fact that the amount of

oxidizing agent is half and quarter, respectively, of the theoretically required. As a conclusion of these experiments, the value of the $[H_2O_2]/[BPA]$ ratio selected to evaluate the effect of pH and reaction time was the unit.

8.3.3.2. Effect of pH

The pH of the reaction medium was evaluated at four different levels: 3, 4.5 (highest oxidizing capacity of VP), 6 (highest stability of VP) and 8 [339]. The lowest residual soluble BPA values were obtained at pH 4 and 7, Y_P = 0.00% and 0.04%, respectively (**Table 8.4**). When the reaction was performed in a very acidic medium (pH = 3), the polymerization yield dropped to 68.8%, whereas the residual soluble BPA dropped to 43.9%, which may be due to the fact that the enzyme is very unstable at pH lower than 4. When the pH of the reaction medium was 8, the polymerization yield also dropped drastically to 40.1% whereas the residual soluble BPA fell to 1.01%. This latter result suggests that in that pH conditions, oligomers are produced during the reaction. As a conclusion of these experiments, the pH value of the reaction medium selected to evaluate the effect of reaction time was 4.5.

8.3.3.3. Effect of reaction time (t_R)

The effect of the reaction time was evaluated at four different levels: 1, 4, 10 and 12 hours. As shown in **Table 8.4**, no improvement can be observed in the polymerization yield of in the residual soluble BPA at higher or lower values of t_R. Presumably the effect of this parameter may be observed on the structure of the obtained polymer, since that the frequencies of interunit linkages formed during the polymerization of BPA vary according to whether the substrate is all introduced at the beginning (Zulaufverfahren, ZL) into the enzyme containing solution or added gradually (Zutropfverfahren, ZT) to the same system [336]. ZT restricts radical coupling of monomers to occurring primarily with the growing

ends of polymer chains. In the ZL mode, a "bulk" polymer is obtained with low molecular weight, whereas by working in the ZT way, a "end-wise" polymer is obtained with higher molecular weight.

Concerning the enzymatic deactivation was almost complete after 24 hours of reaction except for the experiments with the lowest quantity of H_2O_2 (R_{BPA} = 0.25). In that case, an enzyme activity of 41 U/L was estimated at the end of the experiment. It may be explained by the action of the hydrogen peroxide since the concentration of H_2O_2 is crucial on the action and stability of the enzyme. An excessively concentrated reagent would cause the inactivation of the enzyme due to the formation of the catalytically inactive VPIII [45].

In summary, taking into account the effect of the three parameters, it can be concluded that the conditions which conduct to the best polymerization results are: R_{BPA} = 1, pH 4.5 and t_R = 4 hours.

8.3.4. Polymerization of BPA in continuous mode

The experiments carried out in the fed-batch system were performed with an initial concentration of BPA (1.5 g/L) much greater than the one detected in residual water [28], (**Table 1.7**). Moreover, the real wastewater does not contain aqueous organic solvents. For those reasons, a new challenge in this work was to try to polymerize the bisphenol A starting from a concentration lower than 1.5 g/L and closer to that observed in wastewater treatment plants (10 mg/L). A stirred microfiltration membrane operating in continuous mode was proposed since it can work with low concentration of BPA and it can retain the polymer produced inside, however it cannot retain the enzyme. To be able to perform the polymerization of BPA in continuous mode avoiding the use of a huge amount of VP, the coupling of an ultrafiltration membrane at the output of the stirred reactor to recover and to recycle the enzyme was proposed (**Figure 8.8**).

The system was fed with a BPA feed rate of 182.5 nM/min, 182.5 nM/min of H_2O_2, 365 nM/min of Mn^{2+} and 3.66 µM/min of Na-malonate. The results from the continuous BPA polymerization by using the micro-ultra-filtration system are shown in (**Figure 8.17**).
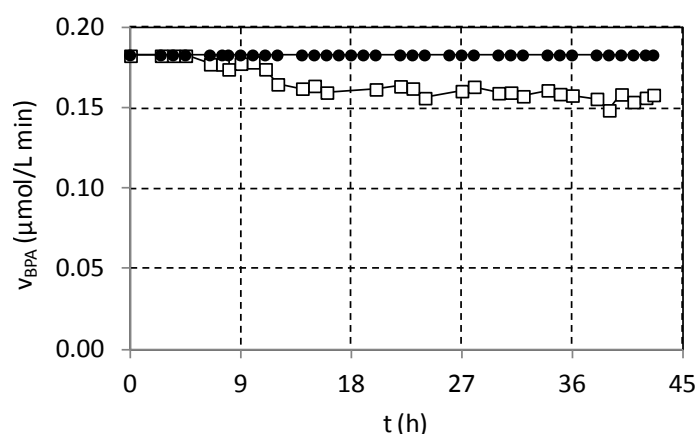
Figure 8.17. Profie of the continuous removal of BPA. ( ) Bisphenol A feeding rate and (□) removal rate

At the beginning of the operation the removal rate is exactly the same that the BPA feeding rate but this cannot be attributed to the polymerization of bisphenol A. This may be due to that, presumably, the EDC can be adsorbed in the ultrafiltration membrane cartridge. Thus during the first hours, BPA may be accumulated in the ultrafiltration membrane.

After 16 hours, approximately, it can be assumed that the steady state was reached. At this point and until the end of the operation (43 h), the removal rate of BPA was almost constant, 158.5±3.6 nM/min, i.e. the 86.8±1.98% of the BPA introduced in the system was eliminated.

During the 43 hours of the operation of the system, 16.125 mg of BPA was introduced into the reactor. After that time, 4.9 mg could be recovered which means that 30.39% of the total BPA introduced was polymerized. Possibly,

the rest of the BPA was retained in the ultrafiltration membrane module by adsorption, it was transformed into soluble oligomers which cannot be retained by the microfiltration membrane or it was transformed in a non-identified oxidized product.

8.4. Conclusions

VP-catalyzed polymerization of coniferyl alcohol (CA) into dehydrogenation polymer DHP was successful under various reaction conditions. For optimal polymerization yield, the reaction should be performed in aqueous solution with no organic solvent at pH between 4.5 and 6.0 and with a H_2O_2/CA ratio between 0.75 and 1.

Structural analyses of the DHPs revealed that high H_2O_2 addition and especially high pH during the reaction induced polymerization products that differ from native lignin. From the structural point of view, the optimal conditions for DHP formation using the presently studied system would be pH 3 or 4.5, using H_2O_2/CA ratio of 0.5. Even in this case, the formed DHP is enriched with resinol type linkages compared to native lignin.

For the first time, the polymerization of the endocrine disrupting compound, bisphenol A, by the oxidative action of the enzyme versatile peroxidase, was carried out. The ability of the enzyme to polymerize BPA was evaluated in a fed-batch configuration as well as in a continuous system.

Three parameters affecting the catalytic reaction were evaluated: the molar ration between H_2O_2 and BPA, pH of the medium and reaction time. The highest polymerization yield was obtained by using a $[H_2O_2]/[BPA]$ ratio of 1, pH of 4.5 and 4 hours of reaction time.

In order to polymerize the BPA in conditions closer to conditions of real wastewaters (i.e. with no organic solvent and lower concentration of BPA) a continuous systems using microfiltration and ultrafiltration membranes, was designed. After 16 h, it can be assumed that the steady state was reached. At this point and until the end of the operation (43 h), the removal rate of BPA was 158.5±3.6 nM/min, i.e. the 86.8±1.98% of the BPA in the input stream was removed.

This work demonstrates that the polymerization of organic compounds, carried out by the enzyme versatile peroxidase, it is a good alternative for the elimination of organic pollutants. Therefore, a new way for the elimination of EDCs is presented and further research is needed to optimize the operational conditions. Efforts may be focused on the use of other ligninolytic enzymes, such as laccase, effect of temperature, ability of this enzymatic system to treat real wastewater containing lower amount of contaminant, ability of the system to polymerize other EDCs.

General conclusions

The main conclusions obtained as a result of the work carried out in this PhD study are the ones detailed next:

1. A new fungus from Temuco, identified as an anamorphous form of *Bjerkandera* sp*,* was isolated and studied to produce ligninolytic enzymes. Among the lignin modifying enzymes evaluated during the fermentation of the fungus, only peroxidases were detected in the enzymatic crude. The highest enzyme production rate: 239 U/L·d, was obtained in a modified Kirk medium with 10 g/L glucose and 10 g/L peptone. Three purification steps were necessary to purify the enzymatic crude to obtain four hemeproteins. Among them, only the major one was identified as a versatile peroxidase (VP).

2. No cross-linking of versatile peroxidase has been reported so far in the literature. A number of factors affecting the production of CLEA®s have been evaluated: type of precipitants, glutaraldehyde (GLU) concentration, proteic feeder and glucose oxidase concentration. The best results in terms of aggregation yield were obtained when using polyethyleneglycol and 72 mM GLU concentration. Different VP/glucose oxidase (GOD) ratios (in terms of mg/mg) were evaluated with the purpose of finding the best results in terms of VP-GOD-CLEA®s yield. An optimum ratio was found to be 5/3.5. The co-aggregation of VP and GOD increased the stability of VP against H_2O_2. Finally, the use of GOD not only improved the CLEA®-yield but VP-GOD-CLEA®s affected MnP activity upon glucose addition; thereby demonstrating a functional catalytic cascade in which H_2O_2 produced *in situ* by GOD serves as a substrate for VPA functional catalytic cascade.

3. The capability of the fungus anamorph R1 of *Bjerkandera* to oxidize five endocrine disrupting chemicals, BPA, TCS, E1, E2 and EE2, and to reduce

their estrogenic activity, was demonstrated through *in vivo* static experiments. The effect of concentrations of Na-malonate and MnSO$_4$ and the initial enzymatic activity, in the *in vitro* oxidation of the above mentioned EDCs, was evaluated by response surface methodology. The individual effect of Na-malonate and MnSO$_4$ presented the most significant effect on both maximum degradation rate as well as degradation extent. Moreover, the quadratic term of the Na-malonate concentration had a very significant effect. The optimum conditions for the degradation were estimated to be 30-40 mM Na-malonate concentration, 0.8-1 mM MnSO$_4$ concentration and an initial enzymatic activity of 100 U/L. Three metabolites of BPA were found after 10 minutes of reaction, *BPA$_1$* (4-(2-hydroxypropan-2-yl)phenol), *BPA$_2$* (not identified) and *BPA$_3$* (2,2-bis(4-hydroxyphenyl)-1-propanol) and two degradation products of TCS, *TCS$_1$* (4-chlorocatechol or chlotohydroquinone) and *TCS$_2$* (hydroxylated triclosan). Concerning the estrogenic compounds, six, four and three degradation products were found for E1, E2 and EE2, respectively, after 10 minutes of reaction; however, their identification was not successful.

4. The ability of the enzyme VP to produce the oxidizing species Mn^{3+}-chelate was evaluated. Four parameters, such as type and concentration of the organic acid, Mn^{2+} and H$_2$O$_2$ concentrations, initial enzymatic activity and pH of the medium, were evaluated. The conditions which allowed the highest production were: 30 mM Na-malonate, 2 mM MnSO$_4$, 0.4 mM H$_2$O$_2$, 100 U/L initial activity and pH 4.5. The capability of the complex to oxidize the azo dye Orange II, the polycyclic aromatic hydrocarbon anthracene and three estrogens, was assessed. For all the pollutants, the oxidation extent was higher than 80%, thereby demonstrating that the complex is a strong and versatile oxidant. Moreover, a new set-up, the "two-stage" system in which

the Mn^{3+}-malonate complex can be produced in a continuous mode and can be applied in a second reactor to oxidize different organic compound, was designed and patented (ES 2373729 B2).

5. In order to optimize the continuous production of the complex Mn^{3+}-malonate, a central composite face centered factorial design was chosen. The independent variables were Na-malonate (x_1) and H_2O_2 (x_2) feeding rates and hydraulic retention time (x_3), whereas the response variables were Mn^{3+}-malonate production rate (Y_1), concentration of Mn^{3+}-malonate (Y_2) and enzymatic deactivation rate (Y_3). By means of the analysis of variance (ANOVA), the quadratic term of x_1 and the individual term of x_3 were found to be the most statistically significant effects on Y_1, the individual effect of x_3 and the quadratic term of x_1 were the most significant effects on Y_2, and the individual term of x_2 and x_3 on Y_3. The best conditions to maximize the production of the oxidizing complex having a reasonable deactivation rate where 250 and 25 µM/min feeding rate of Na-malonate and H_2O_2, respectively and a hydraulic retention time of 50 min. The capability of the oxidizing chelate Mn^{3+}-malonate to eliminate five different disruptors, bisphenol A, triclosan, estrone, 17α-ethinylestradiol and 17β-estradiol, in a continuous mode was evaluated. It was demonstrated that the "two-stage" system was able to completely eliminate the five EDCs even when the feeding rate was in the order of ng/L·min. It was demonstrated that the deactivation of the VP was 7.5-fold lower in the "two-stage" system, compared to the enzymatic ultrafiltration membrane.

6. VP-catalyzed polymerization of coniferyl alcohol (CA) into dehydrogenation polymer DHP was successful under various reaction conditions. For optimal polymerization yield, the reaction should be performed in aqueous solution with no organic solvent at pH between 4.5 and 6.0 and with a H_2O_2/CA ratio

between 0.75 and 1. Structural analyses of the DHPs revealed that high H_2O_2 addition and especially high pH during the reaction induced polymerization products that differ from native lignin. From the structural point of view, the optimal conditions for DHP formation using the presently studied system would be pH 3 or 4.5, using H_2O_2/CA ratio of 0.5. For the first time, the polymerization of the endocrine disrupting compound: bisphenol A (BPA), by the oxidative action of the enzyme versatile peroxidase, was carried out. The ability of the enzyme to polymerize BPA was evaluated in a fed-batch configuration as well as in a continuous system. Three parameters were evaluated: the molar ration between H_2O_2 and BPA, pH and reaction time. The highest polymerization yield was obtained by using a $[H_2O_2]$/[BPA] ratio of 1, pH of 4.5 and 4 h. A continuous systems using microfiltration and ultrafiltration membranes, was designed. The removal rate of BPA was 158.5±3.6 nM/min, i.e. the 86.8±1.98% of the BPA in the input stream was removed.

Conclusiones generales

Las principales conclusiones obtenidas como resultado de los trabajos realizados durante este estudio de doctorado son las siguientes:

1. Un nuevo hongo procedente de Temuco, identificado como un anamorfo (R1) de *Bjerkandera* sp, fue aislado y se estudió su capacidad para producir enzimas ligninolíticas. Entre las enzimas evaluadas durante la fermentación del hongo, sólo se detectaron peroxidasas. La velocidad máxima de producción de la enzima, 239 U/L·d, se obtuvo en un medio Kirk modificado suplementado con 10 g/L de glucosa y 10 g/L de peptona. Fueron necesarias tres etapas para purificar el crudo enzimático y, así, obtener cuatro hemoproteínas. Sólo R1B4, la más abundante, fue identificada como una peroxidasa versátil (VP).

2. Por primera vez se ha llevado a cabo la inmovilización de la enzima peroxidasa versátil a través de la formación de CLEA®s. Se han evaluado aquellos factores clave que afectan a la producción de CLEA®s: tipo de precipitante, concentración de glutaraldehido (GLU), tipo de aditivo proteico y concentración de la enzima glucosa oxidasa (GOD). Los mejores resultados, en términos de rendimiento de agregación, se obtuvieron con el precipitante polietilenglicol y 72 mM de GLU. Se evaluaron diferentes relaciones de VP/GOD (mg/mg) con el fin de encontrar el mejor rendimiento de producción de VP-GOD-CLEA®s. Se encontró una relación óptima igual a 5/3.5 (mg/mg). La coagregación de las enzimas VP y GOD aumentó la estabilidad de la peroxidase frente al H_2O_2. Finalmente, el uso de GOD no sólo mejoró el rendimiento de producción de CLEA®s sino que se demostró la posibilidad de un sistema catalítico en cascada en donde el H_2O_2 es producido *in situ* por GOD, empleando glucosa como sustrato, que es usado por la VP como sustrato.

3. A través de ensayos *in vivo*, en estático, se demostró la capacidad del anamorfo R1 de *Bjerkandera* sp. para eliminar y reducir la actividad estrogénica de cinco compuestos disruptores endocrinos (CDEs), BPA, TCS, E1, E2 y EE2. También se evaluó la capacidad de la enzima VP para eliminar, a través de ensayos *in vitro*, los CDEs mencionados; para ello se empleó una metodología de superficie de respuesta. El efecto de la concentración del malonato sódico y $MnSO_4$ fue el más importante en la velocidad máxima de degradación y rendimiento de eliminación. Por otra parte, se observó que el término cuadrático de la concentración de Na-malonato tuvo un efecto muy significativo, aunque negativo. Las condiciones óptimas para la degradación fueron una concentración de Na-malonato en torno a 30-40 mM, concentración de $MnSO_4$ de 0.8-1.0 mM y una actividad enzimática inicial de 100 U/L. Haciendo uso de GC-MS se encontraron tres metabolitos de BPA tras 10 minutos de reacción, *BPA$_1$* (4 -(2-hidroxipropan-2-il) fenol), *BPA$_2$* (no identificado) y *BPA$_3$* (2,2-bis (4-hidroxifenil-1-propanol) y dos productos de degradación de TCS, *TCS$_1$* (4-chlorocatechol o chlorohidroquinona) y *TCS$_2$* (triclosan hidroxilado). En cuanto a los compuestos estrogénicos, se han encontrado seis, cuatro y tres productos de degradación para E1, E2 y EE2, respectivamente, tras 10 minutos de reacción; sin embargo, su identificación no fue posible.

4. Se evaluó la capacidad de la enzima VP para producir especies de Mn^{3+}-quelato. Se evaluaron cuatro parámetros: tipo y concentración de ácido orgánico, concentración de Mn^{2+} y H_2O_2, actividad peroxidasa inicial y el pH del medio. Las condiciones en las cuales se obtuvo la más alta de complejo fueron: concentración 30 mM de Na-malonato, 2 mM de $MnSO_4$, 0,4 mM de H_2O_2, una actividad enzimática inicial de 100 U/L y pH 4,5. Se estudió la capacidad del complejo para oxidar el tinte azo Orange II, el hidrocarburo

aromático policíclico antraceno y tres estrógenos. Para todos los contaminantes, la eliminación fue mayor del 80%, lo que demuestra que el complejo es un oxidante fuerte y versátil. Además, se diseñó y patentó (ES 2373729 B2) un nuevo sistema, "sistema en dos etapas" en el que el complejo Mn^{3+}-malonato se produce y se aplica en un segundo reactor para oxidar compuestos orgánicos diferentes en continuo.

5. Con el fin de optimizar la producción en continuo del complejo Mn^{3+}-malonato, se diseñó un estudio factorial, en el que las variables independientes fueron la velocidad de alimentación de la sal Na-malonato (x_1) y H_2O_2 (x_2), y el tiempo de retención hidráulico (x_3), mientras que las variables respuesta fueron la velocidad de producción del complejo Mn^{3+}-malonato (Y_1), su concentración (Y_2) y la tasa de desactivación enzimática (Y_3). A través de un análisis de varianza (ANOVA) se observó que el término cuadrático de x_1 y el término individual de x_3 fueron los efectos estadísticamente más significativos en Y_1, el efecto individual de x_3 y el término cuadrático de x_1 fueron los efectos más significativos sobre Y_2, y el término individual de x_2 y x_3 en Y_3. Las condiciones óptimas para maximizar la producción del complejo y observar una velocidad de desactivación razonable fueron una velocidad de adición de Na-malonato y H_2O_2 de 250 y 25 μM/min, respectivamente, y un tiempo de retención hidráulica de 50 min. Se estudió la capacidad de Mn^{3+}-malonato de eliminar en continuo cinco CDEs, BPA, TCS, E1, E2 y EE2. Se demostró que el "sistema en dos etapas" es capaz de eliminar completamente los cinco CDEs aun cuando la velocidad de alimentación fue del orden de ng/L·min. Finalmente, se observó que la desactivación de la VP fue 7,5 veces menor en el "sistema de dos etapas", que en el sistema enzimático de membrana de ultrafiltración.

6. La polimerización del alcohol coniferílico (CA) con VP para obtener polímeros deshidrogenados (DHP) se evaluó bajo diversas condiciones de reacción. Se observó que el rendimiento óptimo de polimerización se obtiene cuando la reacción se lleva a cabo en solución acuosa, a un pH de entre 4,5 y 6,0, y con una relación de H_2O_2/CA entre 0,75 y 1. El análisis estructural de los DHPs reveló que una adición elevada de H_2O_2 y, especialmente, un pH alto durante la reacción, induce a la formación de productos de polimerización que difieren de la lignina nativa. Desde el punto de vista estructural, las condiciones óptimas para la formación de DHPs son pH entre 3 y 4,5 y una relación de H_2O_2/CA de 0,5. Por otra parte, se ha llevado a cabo, por primera vez, la polimerización de BPA por la acción de VP. Se evaluó la polimerización de BPA con VP tanto en una configuración "batch" como en un sistema en continuo. Se evaluaron tres parámetros: la relación molar entre H_2O_2 y BPA, pH del medio y tiempo de reacción. El mayor rendimiento de polimerización se obtuvo con una relación $[H_2O_2]/[BPA] = 1$, pH de 4,5 y un tiempo de reacción de 4 h. Se diseñó un nuevo sistema de membranas de micro- y ultrafiltración para poder llevar a cabo la polimerización en continuo de BPA. Con este sistema, se pudo eliminar el BPA con una velocidad de 158,5±3,6 nM/min. Consecuentemente, se eliminó el 86,8±1,98% del BPA introducido en el sistema.

Conclusións xerais

As principais conclusións, como resultado do traballo realizado durante esta tese de doutoramento son:

1. Un novo fungo procedente de Temuco, identificado como un anamorfo (R1) de *Bjerkandera* sp. foi illado e a súa capacidade para producir enzimas ligninolíticas foi avaliada. Entre as enzimas analizadas durante a fermentación do fungo, soamente foron detectadas peroxidasas no crudo enzimático. A produción máxima da enzima, 239 U/L·d obtiuse nun medio Kirk modificado e suplementado con 10 g/L de glucosa e 10 g/L de peptona. Empregáronse tres etapas para purificar o crudo enzimático e, así, obter catro hemoproteínas. Soamente R1B4, a máis abundante, foi identificada como unha peroxidasa versátil (VP).

2. É a primeira vez que se inmobiliza a enzima VP mediante a produción de CLEA®s. Avaliáronse os factores que afectan á produción dos CLEA®s: tipo de axente precipitante, concentración de glutaraldeído (GLU), tipo de aditivo proteico e a concentración da enzima glucosa oxidasa (GOD). Os mellores resultados en termos de rendemento de agregación obtivéronse co polietilén glicólico como axente precipitante e una concentración de 72 mM de glutaraldehído. Avaliáronse diferentes relación másicas VP:GOD (mg/mg) co fin de atopar os mellores rendementos de produción de VP-GOD-CLEA®s. Atopouse unha relación óptima igual a 5:3.5. A maiores, a coagregación de VP e GOD engadiu una maior estabilidade fronte ó H_2O_2. Finalmente, o uso de GOD non só mellorou o rendemento de produción de CLEA®s senón que demostrouse un sistema catalítico en fervenza, no que o H_2O_2 prodúcese *in situ* pola enzima GOD, empregando glucosa como sustrato, e actúa como sustrato da VP.

3. A capacidade do anamorfo R1 de *Bjerkandera* sp. para eliminar e reducir a actividade estroxénica de cinco compostos desreguladores endócrinos (CDEs), BPA, TCS, E1, E2 e EE2, foi avaliada satisfactoriamente en experimentos *in vivo* en estático. Tamén a capacidade da enzima VP para a eliminación dos CDEs nomeados anteriormente foi avaliada en ensaios *in vitro*. O efecto da concentración do Na-malonato e do $MnSO_4$, e a actividade enzimática inicial foi valorada por medio da metodoloxía de superficie de resposta. O efecto do Na-malonato e do $MnSO_4$ foi o máis salientable no que se refire tanto á velocidade de eliminación coma ó rendemento de eliminación; o termo cuadrático da concentración de Na-malonato tivo un efecto moi significativo, aínda que negativo. As condicións óptimas para a degradación estimáronse para ser: concentración de Na-malonato en torno a 30-40 mM, de 0,8-1,0 mM no caso do $MnSO_4$ e uhna actividade enzimática inicial de 100 U/L. Atopáronse tres metabolitos tras 10 minutos de reacción BPA_1 (4 - (2-hydroxypropan-2-il) fenol), BPA_2 (non identificado) e BPA_3 (2,2-bis (4-hidroxifenil)-1-propanol) e dous produtos de degradación, TCS_1 (4-clorocatecol ou chlorohidroquinona) e TCS_2 (triclosan hidroxilado) no caso do triclosán. En canto ós compostos estroxénicos, seis, catro e tres produtos de degradación atopáronse para E1, E2 e EE2, respectivamente, tras 10 minutos de reacción; sen embargo, no se acadou a súa identificación.

4. Avaliouse a capacidade da enzima peroxidasa versátil para producir especies de Mn^{3+}-quelato. Catro parámetros foron estudiados: tipo e concentración do ácido orgánico, a concentración de Mn^{2+} e H_2O_2, a actividade enzimática inicial e o pH do medio. As condicións que permitiron a produción máis alta foron: unha concentración de 30 mM de Na-malonato, 2 mM de $MnSO_4$, 0,4 mM de H_2O_2, unha actividade enzimática inicial de 100 U/L e pH 4,5. Estudouse a capacidade do complexo para oxidar o colorante azo Orange II,

o hidrocarburo aromático policíclico antraceno e tres estróxenos. Para todos os contaminantes, a eliminación foi superior ó 80%, o que demostra que o complexo é un oxidante forte e versátil. Ademais, foi deseñado e patentado (EEUU 2.373.729 B2) un novo "sistema de dúas etapas", en que o complexo Mn^{3+}-malonato pode ser producido e empregado nun segundo reactor para oxidación de compostos orgánicos diferentes de forma continua.

5. Co fin de optimizar a produción en continuo do complexo Mn^{3+}-malonato, realizouse un deseño factorial. As variables independentes foron a velocidade de alimentación de Na-malonato (x_1) e H_2O_2 (x_2) e o tempo de retención hidráulico (x_3), mentres que as variables resposta foron a velocidade de produción do complexo Mn^{3+}-malonato (Y_1), a súa concentración (Y_2) e a velocidade de desactivación da enzima (Y_3). A través dunha análise de varianza (ANOVA) mostrou que o termo cuadrático de x_1 e x_3 foron estatisticamente significativos en Y_1, o efecto individual x_3 e o término cuadrático de x_1 foron os efectos máis significativos sobre Y_2, e os termos x_2 e x_3 en Y_3. As condicións óptimas para maximizar a produción do complexo e observar unha velocidade razoable de desactivación foron: velocidade de alimentación do Na-malonato e do H_2O_2 250 e 25 µM/min, respectivamente, e un tempo de retención hidráulico de 50 min. Estudouse a capacidade de Mn^{3+}-malonato para eliminar en modo continuo BPA, TCS, E1, E2 e EE2. Demostrouse que o "sistema de dúas etapas" é capaz de eliminar completamente os cinco CDEs mesmo cando a velocidade de alimentación foi da orde de ng/L·min. Finalmente, demostrouse que a desactivación do VP foi 7,5 veces menor no "sistema de dúas fases", en comparación co sistema enzimático da membrana de ultrafiltración.

6. A polimerización enzimática do alcohol coniferílico (AC) coa VP para a produción de polímeros deshidroxenados (DHP) foi estudada baixo varias

condicións de reacción. Concluíuse que o rendemento óptimo é obtido cando a reacción de polimerización é conducida en solución acuosa, a un pH entre 4,5 e 6,0, e unha relación molar H_2O_2/AC de entre 0,75 e 1. A análise estrutural dos DHPs revelou que a adición elevada de H_2O_2 e, especialmente, un pH elevado, durante a reacción, leva á formación de produtos de polimerización que difiren da lignina nativa. Dende un punto de vista estrutural, as condicións óptimas para a formación de DHPs son: pH entre 3 e 4,5, cunha proporción de H_2O_2/CA de 0,5. Por outra banda, por primeira vez, levouse a cabo a polimerización do BPA, pola acción da VP. A capacidade da enzima para polimerizar BPA foi levada a cabo tanto nunha configuración "batch" coma nun sistema en continuo. Avaliáronse tres parámetros: a relación molar entre BPA e H_2O_2, pH do medio e o tempo de reacción. O rendemento de polimerización máis elevado foi obtido empregando una relación $[H_2O_2]/[BPA] = 1$, pH de 4,5 e un tempo de reacción de 4 h. ó cabo, foi deseñado un novo sistema de membranas de micro- e ultrafiltración para a polimerización en continuo do BPA. Con este sistema, eliminouse BPA cunha velocidade específica de 158,5±3,6 mM/min, ou sexa, eliminouse un 86,8±1,98% do BPA introducido no sistema.

References

[1] M. Kaneda, K.H. Rensing, J.C.T. Wong, B. Banno, S.D. Mansfield, A.L. Samuels, Tracking monolignols during wood development in lodgepole pine, Plant Physiology, 147 (2008) 1750-1760.

[2] F. Schwarze, S. Baum, S. Fink, Dual modes of degradation by Fistulina hepatica in xylem cell walls of Quercus robur, Mycological Research, 104 (2000) 846-852.

[3] T. Mester, M. Tien, Oxidation mechanism of ligninolytic enzymes involved in the degradation of environmental pollutants, International Biodeterioration & Biodegradation, 46 (2000) 51-59.

[4] E. Borras, G. Caminal, M. Sarra, C. Novotny, Effect of soil bacteria on the ability of polycyclic aromatic hydrocarbons (PAHs) removal by Trametes versicolor and Irpex lacteus from contaminated soil, Soil Biol. Biochem., 42 (2010) 2087-2093.

[5] S. Covino, M. Cvancarova, M. Muzikar, K. Svobodova, A. D'Annibale, M. Petruccioli, F. Federici, Z. Kresinova, T. Cajthaml, An efficient PAH-degrading Lentinus (Panus) tigrinus strain: Effect of inoculum formulation and pollutant bioavailability in solid matrices, Journal of Hazardous Materials, 183 (2010) 669-676.

[6] J. Ding, J. Cong, j. Zhou, S. Gao, Polycyclic aromatic hydrocarbon biodegradation and extracellular enzyme secretion in agitated and stationary cultures of Phanerochaete chrysosporium, Journal of Environmental Sciences-China, 20 (2008) 88-93.

[7] L. Valentín, T.A. Lú-Chau, C. López, G. Feijoo, M.T. Moreira, J.M. Lema, Biodegradation of dibenzothiophene, fluoranthene, pyrene and chrysene in a soil slurry reactor by the white-rot fungus *Bjerkandera* sp BOS55, Process Biochem, 42 (2007) 641-648.

[8] M. Cvancarova, Z. Kresinova, A. Filipova, S. Covino, T. Cajthaml, Biodegradation of PCBs by ligninolytic fungi and characterization of the degradation products, Chemosphere, 88 (2012) 1317-1323.

[9] J.C. Quintero, T.A. Lu-Chau, M.T. Moreira, G. Feijoo, J.M. Lema, Bioremediation of HCH present in soil by the white-rot fungus Bjerkandera adusta in a slurry batch bioreactor, International Biodeterioration & Biodegradation, 60 (2007) 319-326.

[10] P. Xiao, T. Mori, I. Kamei, H. Kiyota, K. Takagi, R. Kondo, Novel metabolic pathways of organochlorine pesticides dieldrin and aldrin by the white rot fungi of the genus Phlebia, Chemosphere, 85 (2011) 218-224.

[11] I. Eichlerova, L. Homolka, F. Nerud, Decolorization of high concentrations of synthetic dyes by the white rot fungus Bjerkandera adusta strain CCBAS 232, Dyes and Pigments, 75 (2007) 38-44.

[12] C. Novotny, B. Rawal, M. Bhatt, M. Patel, V. Sasek, H.P. Molitoris, Capacity of Irpex lacteus and Pleurotus ostreatus for decolorization of chemically different dyes, J. Biotechnol., 89 (2001) 113-122.

[13] N. Golan-Rozen, B. Chefetz, J. Ben-Ari, J. Geva, Y. Hadar, Transformation of the Recalcitrant Pharmaceutical Compound Carbamazepine by Pleurotus ostreatus: Role of Cytochrome P450 Monooxygenase and Manganese Peroxidase, Environmental Science & Technology, 45 (2011) 6800-6805.

[14] A. Prieto, M. Moeder, R. Rodil, L. Adrian, E. Marco-Urrea, Degradation of the antibiotics norfloxacin and ciprofloxacin by a white-rot fungus and identification of degradation products, Bioresource Technology, 102 (2011) 10987-10995.

[15] A.I. Rodarte-Morales, G. Feijoo, M.T. Moreira, J.M. Lema, Biotransformation of three pharmaceutical active compounds by the fungus Phanerochaete

chrysosporium in a fed batch stirred reactor under air and oxygen supply, Biodegradation, 23 (2012) 145-156.

[16] C.E. Rodriguez-Rodriguez, E. Marco-Urrea, G. Caminal, Degradation of naproxen and carbamazepine in spiked sludge by slurry and solid-phase *Trametes versicolor* systems, Bioresource Technology, 101 (2010) 2259-2266.

[17] D. Wesenberg, I. Kyriakides, S.N. Agathos, White-rot fungi and their enzymes for the treatment of industrial dye effluents, Biotechnology Advances, 22 (2003) 161-187.

[18] P. Kersten, D. Cullen, Extracellular oxidative systems of the lignin-degrading Basidiomycete Phanerochaete chrysosporium, Fungal Genetics and Biology, 44 (2007) 77-87.

[19] X. Hu, P. Wang, H.-m. Hwang, Oxidation of anthracene by immobilized laccase from Trametes versicolor, Bioresource Technol, 100 (2009) 4963-4968.

[20] G. Bayramoglu, M.Y. Arica, Immobilization of laccase onto poly(glycidylmethacrylate) brush grafted poly(hydroxyethylmethacrylate) films: Enzymatic oxidation of phenolic compounds, Materials Science & Engineering C-Materials for Biological Applications, 29 (2009) 1990-1997.

[21] A. Fillat, J.F. Colom, T. Vidal, A new approach to the biobleaching of flax pulp with laccase using natural mediators, Bioresource Technology, 101 (2010) 4104-4110.

[22] S. Georgieva, T. Godjevargova, D.G. Mita, N. Diano, C. Menale, C. Nicolucci, C.R. Carratelli, L. Mita, E. Golovinsky, Non-isothermal bioremediation of waters polluted by phenol and some of its derivatives by laccase covalently immobilized on polypropylene membranes, Journal of Molecular Catalysis B-Enzymatic, 66 (2010) 210-218.

[23] E. Franciscon, F. Piubeli, F. Fantinatti-Garboggini, C.R. de Menezes, I.S. Silva, A. Cavaco-Paulo, M.J. Grossman, L.R. Durrant, Polymerization study of the aromatic amines generated by the biodegradation of azo dyes using the laccase enzyme, Enzyme and Microbial Technology, 46 (2010) 360-365.

[24] I. Khouni, B. Marrot, R. Ben Amar, Decolourization of the reconstituted dye bath effluent by commercial laccase treatment: Optimization through response surface methodology, Chemical Engineering Journal, 156 (2010) 121-133.

[25] J.F. Osma, J.L. Toca-Herrera, S. Rodriguez-Couto, Biodegradation of a simulated textile effluent by immobilised-coated laccase in laboratory-scale reactors, Applied Catalysis a-General, 373 (2010) 147-153.

[26] M. Auriol, Y. Filali-Meknassi, C.D. Adams, R.D. Tyagi, T.N. Noguerol, B. Pina, Removal of estrogenic activity of natural and synthetic hormones from a municipal wastewater: Efficiency of horseradish peroxidase and laccase from *Trametes versicolor*, Chemosphere, 70 (2008) 445-452.

[27] M. Auriol, Y. Filali-Meknassi, R.D. Tyagi, C.D. Adams, Laccase-catalyzed conversion of natural and synthetic hormones from a municipal wastewater, Water Research, 41 (2007) 3281-3288.

[28] H. Cabana, J.P. Jones, S.N. Agathos, Elimination of endocrine disrupting chemicals using white rot fungi and their lignin modifying enzymes: A review, Eng. Life Sci., 7 (2007) 429-456.

[29] Z. Karim, Q. Husain, Redox-mediated oxidation and removal of aromatic amines from polluted water by partially purified bitter gourd (Momordica charantia) peroxidase, International Biodeterioration & Biodegradation, 63 (2009) 587-593.

[30] Z. Karim, Q. Husain, Removal of anthracene from model wastewater by immobilized peroxidase from Momordica charantia in batch process as

well as in a continuous spiral-bed reactor, Journal of Molecular Catalysis B-Enzymatic, 66 (2010) 302-310.

[31] H. Ashraf, Q. Husain, Studies on bitter gourd peroxidase catalyzed removal of p-bromophenol from wastewater, Desalination, 262 (2010) 267-272.

[32] H. Ashraf, Q. Husain, Use of DEAF cellulose adsorbed and crosslinked white radish (Raphanus sativus) peroxidase for the removal of alpha-naphthol in batch and continuous process, International Biodeterioration & Biodegradation, 64 (2010) 27-31.

[33] S. Cohen, P.A. Belinky, Y. Hadar, C.G. Dosoretz, Characterization of catechol derivative removal by lignin peroxidase in aqueous mixture, Bioresource Technology, 100 (2009) 2247-2253.

[34] C. López, M.T. Moreira, G. Feijoo, J.M. Lema, Dye decolorization by manganese peroxidase in an enzymatic membrane bioreactor, Biotechnol. Prog., 20 (2004) 74-81.

[35] I. Mielgo, C. López, M.T. Moreira, G. Feijoo, J.M. Lema, Oxidative degradation of azo dyes by manganese peroxidase under optimized conditions, Biotechnol. Prog., 19 (2003) 325-331.

[36] S. Pirillo, F.S. Garcia Einschlag, M. Lujan Ferreira, E.H. Rueda, Eriochrome Blue Black R and Fluorescein degradation by hydrogen peroxide oxidation with horseradish peroxidase and hematin as biocatalysts, Journal of Molecular Catalysis B-Enzymatic, 66 (2010) 63-71.

[37] D.W.S. Wong, Structure and Action Mechanism of Ligninolytic Enzymes, Applied Biochemistry and Biotechnology, 157 (2009) 174-209.

[38] S. Riva, Laccases: blue enzymes for green chemistry, Trends in Biotechnology, 24 (2006) 219-226.

[39] M. Tien, T.K. Kirk, Lignin peroxidase of *Phanerochaete chrysosporium*, Method Enzymol, 161 (1988) 238-249.

[40] M. Kuwahara, J.K. Glenn, M.A. Morgan, M.H. Gold, Separation and characterization of two extracellular H_2O_2 dependent oxidases from ligninolytic cultures of *Phanerochaete chrysosporium*, Febs Lett, 169 (1984) 247-250.

[41] M. Hofrichter, Review: lignin conversion by manganese peroxidase (MnP), Enzyme and Microbial Technology, 30 (2002) 454-466.

[42] L. Caramelo, M.J. Martinez, A.T. Martinez, A search for ligninolytic peroxidases in the fungus Pleurotus eryngii involving alpha-keto-gamma-thiomethylbutyric acid and lignin model dimers, Applied and Environmental Microbiology, 65 (1999) 916-922.

[43] A. Heinfling, F.J. Ruiz-Duenas, M.J. Martinez, M. Bergbauer, U. Szewzyk, A.T. Martinez, A study on reducing substrates of manganese-oxidizing peroxidases from Pleurotus eryngii and Bjerkandera adusta, Febs Letters, 428 (1998) 141-146.

[44] M. Perez-Boada, F.J. Ruiz-Duenas, R. Pogni, R. Basosi, T. Choinowski, M.J. Martinez, K. Piontek, A.T. Martinez, Versatile peroxidase oxidation of high redox potential aromatic compounds: Site-directed mutagenesis, spectroscopic and crystallographic investigation of three long-range electron transfer pathways, Journal of Molecular Biology, 354 (2005) 385-402.

[45] A.T. Martínez, Molecular biology and structure-function of lignin- degrading heme peroxidases, Enzyme Microb Tech, 30 (2002) 425-444.

[46] T. Mester, J.A. Field, Characterization of a novel manganese peroxidase-lignin peroxidase hybrid isozyme produced by Bjerkandera species strain BOS55 in the absence of manganese, Journal of Biological Chemistry, 273 (1998) 15412-15417.

[47] L.N. Vandenberg, M.V. Maffini, C. Sonnenschein, B.S. Rubin, A.M. Soto, Bisphenol-A and the Great Divide: A Review of Controversies in the Field of Endocrine Disruption, Endocrine Reviews, 30 (2009) 75-95.

[48] USEPA, Special report on endocrine disruption. An effects assessment and analysis., in, U.S. EPA, Washington, DC, 1997.

[49] Z.-h. Liu, Y. Kanjo, S. Mizutani, Removal mechanisms for endocrine disrupting compounds (EDCs) in wastewater treatment - physical means, biodegradation, and chemical advanced oxidation: A review, Science of the Total Environment, 407 (2009) 731-748.

[50] A.K. Hotchkiss, C.V. Rider, C.R. Blystone, V.S. Wilson, P.C. Hartig, G.T. Ankley, P.M. Foster, C.L. Gray, L.E. Gray, Fifteen years after "Wingspread" - Environmental endocrine disrupters and human and wildlife health: Where we are today and where we need to go, Toxicological Sciences, 105 (2008) 235-259.

[51] C.M. Markey, C.L. Michaelson, E.C. Veson, C. Sonnenschein, A.M. Soto, The mouse uterotrophic assay: A reevaluation of its validity in assessing the estrogenicity of bisphenol A, Environmental Health Perspectives, 109 (2001) 55-60.

[52] R.J. Witorsch, Endocrine disruptors: Can biological effects and environmental risks be predicted?, Regulatory Toxicology and Pharmacology, 36 (2002) 118-130.

[53] W.J. Biggers, H. Laufer, Identification of juvenile hormone-active alkylphenols in the lobster Homarus americanus and in marine sediments, Biological Bulletin, 206 (2004) 13-24.

[54] H.S. Marcial, A. Hagiwara, T.W. Snell, Estrogenic compounds affect development of harpacticoid copepod Tigriopus japonicus, Environmental Toxicology and Chemistry, 22 (2003) 3025-3030.

[55] M.M. Watts, D. Pascoe, K. Carroll, Exposure to 17 alpha-ethinylestradiol and bisphenol A-effects on larval moulting and mouthpart structure of Chironomus riparius, Ecotoxicology and Environmental Safety, 54 (2003) 207-215.

[56] M.F.L. Lemos, C.A.M. van Gestel, A.M.V.M. Soares, Endocrine disruption in a terrestrial isopod under exposure to bisphenol A and vinclozolin, Journal of Soils and Sediments, 9 (2009) 492-500.

[57] M.F.L. Lemos, C.A.M. van Gestel, A.M.V.M. Soares, Developmental Toxicity of Endocrine Disrupters Bisphenol A and Vinclozolin in a Terrestrial Isopod, Arch. Environ. Contam. Toxicol., 59 (2010) 274-281.

[58] M.F.L. Lemos, A.C. Esteves, B. Samyn, I. Timperman, J. van Beeumen, A. Correia, C.A.M. van Gestel, A.M.V.M. Soares, Protein differential expression induced by endocrine disrupting compounds in a terrestrial isopod, Chemosphere, 79 (2010) 570-576.

[59] M.F.L. Lemos, C.A.M. van Gestel, A.M.V.M. Soares, Reproductive toxicity of the endocrine disrupters vinclozolin and bisphenol A in the terrestrial isopod Porcellio scaber (Latreille, 1804), Chemosphere, 78 (2010) 907-913.

[60] M. Duft, U. Schulte-Oehlmann, L. Weltje, M. Tillmann, J. Oehlmann, Stimulated embryo production as a parameter of estrogenic exposure via sediments in the freshwater mudsnail Potamopyrgus antipodarum, Aquatic Toxicology, 64 (2003) 437-449.

[61] M. Hill, C. Stabile, L.K. Steffen, A. Hill, Toxic effects of endocrine disrupters on freshwater sponges: common developmental abnormalities, Environ. Pollut., 117 (2002) 295-300.

[62] F. Lahnsteiner, B. Berger, M. Kletzl, T. Weismann, Effect of bisphenol A on maturation and quality of semen and eggs in the brown trout, Salmo trutta f. fario, Aquatic Toxicology, 75 (2005) 213-224.

[63] A. Mandich, S. Bottero, E. Benfenati, A. Cevasco, C. Erratico, S. Maggioni, A. Massari, F. Pedemonte, L. Vigano, In vivo exposure of carp to graded concentrations of bisphenol A, General and Comparative Endocrinology, 153 (2007) 15-24.

[64] P. Sohoni, C.R. Tyler, K. Hurd, J. Caunter, M. Hetheridge, T. Williams, C. Woods, M. Evans, R. Toy, M. Gargas, J.P. Sumpter, Reproductive effects of long-term exposure to bisphenol a in the fathead minnow (Pimephales promelas), Environmental Science & Technology, 35 (2001) 2917-2925.

[65] D.A. Crain, M. Eriksen, T. Iguchi, S. Jobling, H. Laufer, G.A. LeBlanc, L.J. Guillette, Jr., An ecological assessment of bisphenol-A: Evidence from comparative biology, Reproductive Toxicology, 24 (2007) 225-239.

[66] G. Levy, I. Lutz, A. Kruger, W. Kloas, Bisphenol A induces feminization in Xenopus laevis tadpoles, Environmental Research, 94 (2004) 102-111.

[67] K. Sone, M. Hinago, A. Kitayama, J. Morokuma, N. Ueno, H. Watanabe, T. Iguchi, Effects of 17 beta-estradiol, nonylphenol, and bisphenol-A on developing Xenopus laevis embryos, General and Comparative Endocrinology, 138 (2004) 228-236.

[68] S. Iwamuro, M. Sakakibara, M. Terao, A. Ozawa, C. Kurobe, T. Shigeura, M. Kato, S. Kikuyama, Teratogenic and anti-metamorphic effects of bisphenol A on embryonic and larval Xenopus laevis, General and Comparative Endocrinology, 133 (2003) 189-198.

[69] C. Stoker, F. Rey, H. Rodriguez, J.G. Ramos, P. Sirosky, A. Larriera, E.H. Luque, M. Munoz-de-Toro, Sex reversal effects on Caiman latirostris exposed to environmentally relevant doses of the xenoestrogen bisphenol A, General and Comparative Endocrinology, 133 (2003) 287-296.

[70] C. Berg, K. Halldin, B. Brunstrom, Effects of bisphenol A and tetrabromobisphenol A on sex organ development in quail and chicken embryos, Environmental Toxicology and Chemistry, 20 (2001) 2836-2840.

[71] C.A. Staples, P.B. Dorn, G.M. Klecka, S.T. O'Block, L.R. Harris, A review of the environmental fate, effects, and exposures of bisphenol A, Chemosphere, 36 (1998) 2149-2173.

[72] W.-T. Tsai, Human health risk on environmental exposure to bisphenol-A: A review, Journal of Environmental Science and Health Part C-Environmental Carcinogenesis & Ecotoxicology Reviews, 24 (2006) 225-255.

[73] EFSA, Scientific Opinion of the Panel on Food additives, Flavourings, Processing aids and Materials in Contact with Food, The EFSA Journal, (2008).

[74] F.S. vom Saal, B.T. Akingbemi, S.M. Belcher, L.S. Birnbaum, D.A. Crain, M. Eriksen, F. Farabollini, L.J. Guillette, Jr., R. Hauser, J.J. Heindel, S.-M. Ho, P.A. Hunt, T. Iguchi, S. Jobling, J. Kanno, R.A. Keri, K.E. Knudsen, H. Laufer, G.A. LeBlanc, M. Marcus, J.A. McLachlan, J.P. Myers, A. Nadal, R.R. Newbold, N. Olea, G.S. Prins, C.A. Richter, B.S. Rubin, C. Sonnenschein, A.M. Soto, C.E. Talsness, J.G. Vandenbergh, L.N. Vandenberg, D.R. Walser-Kuntz, C.S. Watson, W.V. Welshons, Y. Wetherill, R.T. Zoeller, Chapel Hill bisphenol A expert panel consensus statement: Integration of mechanisms, effects in animals and potential to impact human health at current levels of exposure, Reproductive Toxicology, 24 (2007) 131-138.

[75] NTP-CERHR, Monograph on the potential human reproductive and developmental effects of bisphenol A, (2008).

[76] C.G., Canada Gazette Part II, 144 (2010).

[77] X. Wei, Y. Huang, M.H. Wong, J.P. Giesy, C.K.C. Wong, Assessment of risk to humans of bisphenol A in marine and freshwater fish from Pearl River Delta, China, Chemosphere, 85 (2011) 122-128.

[78] J. Sajiki, J. Yonekubo, Leaching of bisphenol A (BPA) from polycarbonate plastic to water containing amino acids and its degradation by radical oxygen species, Chemosphere, 55 (2004) 861-867.

[79] H. Asakura, T. Matsuto, N. Tanaka, Behavior of endocrine-disrupting chemicals in leachate from MSW landfill sites in Japan, Waste Management, 24 (2004) 613-622.

[80] H. Fromme, T. Kuchler, T. Otto, K. Pilz, J. Muller, A. Wenzel, Occurrence of phthalates and bisphenol A and F in the environment, Water Research, 36 (2002) 1429-1438.

[81] A. Ballesteros-Gomez, F.-J. Ruiz, S. Rubio, D. Perez-Bendito, Determination of bisphenols A and F and their diglycidyl ethers in wastewater and river water by coacervative extraction and liquid chromatography-fluorimetry, Analytica Chimica Acta, 603 (2007) 51-59.

[82] F.-J. Ruiz, S. Rubio, D. Perez-Bendito, Vesicular coacervative extraction of bisphenols and their diglycidyl ethers from sewage and river water, Journal of Chromatography A, 1163 (2007) 269-276.

[83] R.A. Rudel, J.G. Brody, J.C. Spengler, J. Vallarino, P.W. Geno, G. Sun, A. Yau, Identification of selected hormonally active agents and animal mammary carcinogens in commercial and residential air and dust samples, Journal of the Air & Waste Management Association, 51 (2001) 499-513.

[84] N.K. Wilson, J.C. Chuang, M.K. Morgan, R.A. Lordo, L.S. Sheldon, An observational study of the potential exposures of preschool children to pentachlorophenol, bisphenol-A, and nonylphenol at home and daycare, Environmental Research, 103 (2007) 9-20.

[85] A. Goodson, W. Summerfield, I. Cooper, Survey of bisphenol A and bisphenol F in canned foods, Food Additives and Contaminants, 19 (2002) 796-802.

[86] B.M. Thomson, P.R. Grounds, Bisphenol A in canned foods in New Zealand: An exposure assessment, Food Additives and Contaminants, 22 (2005) 65-72.

[87] H.C. Alexander, D.C. Dill, L.W. Smith, P.D. Guiney, P. Dorn, Bisphenol A: acute aquatic toxicity, Environmental Toxicology and Chemistry, 7 (1988) 19-26.

[88] S.J. Brennan, C.A. Brougham, J.J. Roche, A.M. Fogarty, Multi-generational effects of four selected environmental oestrogens on Daphnia magna, Chemosphere, 64 (2006) 49-55.

[89] M. Hirano, H. Ishibashi, N. Matsumura, Y. Nagao, N. Watanabe, A. Watanabe, N. Onikura, K. Kishi, K. Arizono, Acute toxicity responses of two crustaceans, Americamysis bahia and Daphnia magna, to endocrine disrupters, Journal of Health Science, 50 (2004) 97-100.

[90] S. Flint, T. Markle, S. Thompson, E. Wallace, Bisphenol A exposure, effects, and policy: A wildlife perspective, Journal of Environmental Management, 104 (2012) 19-34.

[91] R.D. Jones, H.B. Jampani, J.L. Newman, A.S. Lee, Triclosan: A review of effectiveness and safety in health care settings, American Journal of Infection Control, 28 (2000) 184-196.

[92] CEPA, Canadian Environmental Protection Act, (1999).

[93] C.G., Canada Gazette Part I, 146 (2012).

[94] K. Bester, Triclosan in a sewage treatment process - balances and monitoring data, Water Research, 37 (2003) 3891-3896.

[95] K. Bester, Fate of triclosan and triclosan-methyl in sewage treatment plants and surface waters, Arch. Environ. Contam. Toxicol., 49 (2005) 9-17.

[96] R. Kanda, P. Griffin, H.A. James, J. Fothergill, Pharmaceutical and personal care products in sewage treatment works, Journal of Environmental Monitoring, 5 (2003) 823-830.

[97] A. Lindstrom, I.J. Buerge, T. Poiger, P.A. Bergqvist, M.D. Muller, H.R. Buser, Occurrence and environmental behavior of the bactericide triclosan and its methyl derivative in surface waters and in wastewater, Environmental Science & Technology, 36 (2002) 2322-2329.

[98] L. Lishman, S.A. Smyth, K. Sarafin, S. Kleywegt, J. Toito, T. Peart, B. Lee, M. Servos, M. Beland, P. Seto, Occurrence and reductions of pharmaceuticals and personal care products and estrogens by municipal wastewater treatment plants in Ontario, Canada, Science of the Total Environment, 367 (2006) 544-558.

[99] V. Lopez-Avila, R.A. Hites, Organic compounds in an industrial wastewater. Their transport into sediments, Environmental Science & Technology, 14 (1980) 1382-1390.

[100] D.C. McAvoy, B. Schatowitz, M. Jacob, A. Hauk, W.S. Eckhoff, Measurement of triclosan in wastewater treatment systems, Environmental Toxicology and Chemistry, 21 (2002) 1323-1329.

[101] H. Singer, S. Muller, C. Tixier, L. Pillonel, Triclosan: Occurrence and fate of a widely used biocide in the aquatic environment: Field measurements in wastewater treatment plants, surface waters, and lake sediments, Environmental Science & Technology, 36 (2002) 4998-5004.

[102] T.A. Ternes, A. Joss, H. Siegrist, Scrutinizing pharmaceuticals and personal care products in wastewater treatment, Environmental Science & Technology, 38 (2004) 392A-399A.

[103] A. Thompson, P. Griffin, R. Stuetz, E. Cartmell, The fate and removal of triclosan during wastewater treatment, Water Environment Research, 77 (2005) 63-67.

[104] G. Bedoux, B. Roig, O. Thomas, V. Dupont, B. Le Bot, Occurrence and toxicity of antimicrobial triclosan and by-products in the environment, Environmental Science and Pollution Research, 19 (2012) 1044-1065.

[105] J. Heidler, R.U. Halden, Mass balance assessment of triclosan removal during conventional sewage treatment, Chemosphere, 66 (2007) 362-369.

[106] L. Racz, R.K. Goel, Fate and removal of estrogens in municipal wastewater, Journal of Environmental Monitoring, 12 (2010) 58-70.

[107] G.G. Ying, R.S. Kookana, Y.J. Ru, Occurrence and fate of hormone steroids in the environment, Environment International, 28 (2002) 545-551.

[108] D. Bendz, N.A. Paxeus, T.R. Ginn, F.J. Loge, Occurrence and fate of pharmaceutically active compounds in the environment, a case study: Hoje River in Sweden, Journal of Hazardous Materials, 122 (2005) 195-204.

[109] M.A. Coogan, R.E. Edziyie, T.W. La Point, B.J. Venables, Algal bioaccumulation of triclocarban, triclosan, and methyl-triclosan in a North Texas wastewater, treatment plant receiving stream, Chemosphere, 67 (2007) 1911-1918.

[110] M.A. Coogan, T.W. La Point, Snail bioaccumulation of triclocarban, triclosan, and methyltriclosan in a North Texas, USA, stream affected by wastewater treatment plant runoff, Environmental Toxicology and Chemistry, 27 (2008) 1788-1793.

[111] S.T. Glassmeyer, E.T. Furlong, D.W. Kolpin, J.D. Cahill, S.D. Zaugg, S.L. Werner, M.T. Meyer, D.D. Kryak, Transport of chemical and microbial compounds from known wastewater discharges: Potential for use as

indicators of human fecal contamination, Environmental Science & Technology, 39 (2005) 5157-5169.

[112] R.U. Halden, D.H. Paull, Co-occurrence of triclocarban and triclosan in US water resources, Environmental Science & Technology, 39 (2005) 1420-1426.

[113] D.W. Kolpin, E.T. Furlong, M.T. Meyer, E.M. Thurman, S.D. Zaugg, L.B. Barber, H.T. Buxton, Pharmaceuticals, hormones, and other organic wastewater contaminants in US streams, 1999-2000: A national reconnaissance, Environmental Science & Technology, 36 (2002) 1202-1211.

[114] D.W. Kolpin, M. Skopec, M.T. Meyer, E.T. Furlong, S.D. Zaugg, Urban contribution of pharmaceuticals and other organic wastewater contaminants to streams during differing flow conditions, Science of the Total Environment, 328 (2004) 119-130.

[115] K.S. Kumar, S.M. Priya, A.M. Peck, K.S. Sajwan, Mass Loadings of Triclosan and Triclocarbon from Four Wastewater Treatment Plants to Three Rivers and Landfill in Savannah, Georgia, USA, Arch. Environ. Contam. Toxicol., 58 (2010) 275-285.

[116] E.L. Waltman, B.J. Venables, W.Z. Waller, Triclosan in a North Texas wastewater treatment plant and the influent and effluent of an experimental constructed wetland, Environmental Toxicology and Chemistry, 25 (2006) 367-372.

[117] P.A. Fair, H.-B. Lee, J. Adams, C. Darling, G. Pacepavicius, M. Alaee, G.D. Bossart, N. Henry, D. Muir, Occurrence of triclosan in plasma of wild Atlantic bottlenose dolphins (Tursiops truncatus) and in their environment, Environ. Pollut., 157 (2009) 2248-2254.

[118] D. Sabaliunas, S.F. Webb, A. Hauk, M. Jacob, W.S. Eckhoff, Environmental fate of Triclosan in the River Aire Basin, UK, Water Research, 37 (2003) 3145-3154.

[119] G.-G. Ying, R.S. Kookana, Triclosan in wastewaters and biosolids from Australian wastewater treatment plants, Environment International, 33 (2007) 199-205.

[120] T. Okumura, Y. Nishikawa, Gas chromatography mass spectrometry determination of triclosans in water, sediment and fish samples via methylation with diazomethane, Analytica Chimica Acta, 325 (1996) 175-184.

[121] Z. Xie, R. Ebinghaus, G. Floeer, A. Caba, W. Ruck, Occurrence and distribution of triclosan in the German Bight (North Sea), Environ. Pollut., 156 (2008) 1190-1195.

[122] T.R. Miller, J. Heidler, S.N. Chillrud, A. Delaquil, J.C. Ritchie, J.N. Mihalic, R. Bopp, R.U. Halden, Fate of triclosan and evidence for reductive dechlorination of triclocarban in estuarine sediments, Environmental Science & Technology, 42 (2008) 4570-4576.

[123] S. Morales, P. Canosa, I. Rodriguez, E. Rubi, R. Cela, Microwave assisted extraction followed by gas chromatography with tandem mass spectrometry for the determination of triclosan and two related chlorophenols in sludge and sediments, Journal of Chromatography A, 1082 (2005) 128-135.

[124] J. Cha, A.M. Cupples, Detection of the antimicrobials triclocarban and triclosan in agricultural soils following land application of municipal biosolids, Water Research, 43 (2009) 2522-2530.

[125] S. Chu, C.D. Metcalfe, Simultaneous determination of triclocarban and triclosan in municipal biosolids by liquid chromatography tandem mass spectrometry, Journal of Chromatography A, 1164 (2007) 212-218.

[126] C.A. Kinney, E.T. Furlong, S.D. Zaugg, M.R. Burkhardt, S.L. Werner, J.D. Cahill, G.R. Jorgensen, Survey of organic wastewater contaminants in biosolids destined for land application, Environmental Science & Technology, 40 (2006) 7207-7215.

[127] A.C. Johnson, A. Belfroid, A. Di Corcia, Estimating steroid oestrogen inputs into activated sludge treatment works and observations on their removal from the effluent, Science of the Total Environment, 256 (2000) 163-173.

[128] H.H. Inhoffen, W. Hohlweg, New per os-effective female hipofisis gland hormone derivatives: 17-aethinyl-oesteridol and pregnen-in-on-3-ol-17, Naturwissenschaften, 26 (1938) 96-96.

[129] C. Baronti, R. Curini, G. D'Ascenzo, A. Di Corcia, A. Gentili, R. Samperi, Monitoring natural and synthetic estrogens at activated sludge sewage treatment plants and in a receiving river water, Environmental Science & Technology, 34 (2000) 5059-5066.

[130] A.C. Belfroid, A. Van der Horst, A.D. Vethaak, A.J. Schafer, G.B.J. Rijs, J. Wegener, W.P. Cofino, Analysis and occurrence of estrogenic hormones and their glucuronides in surface water and waste water in The Netherlands, Science of the Total Environment, 225 (1999) 101-108.

[131] H.M. Kuch, K. Ballschmiter, Determination of endocrine-disrupting phenolic compounds and estrogens in surface and drinking water by HRGC-(NCI)-MS in the picogram per liter range, Environmental Science & Technology, 35 (2001) 3201-3206.

[132] T.A. Ternes, P. Kreckel, J. Mueller, Behaviour and occurrence of estrogens in municipal sewage treatment plants - II. Aerobic batch experiments with activated sludge, Science of the Total Environment, 225 (1999) 91-99.

[133] T.A. Ternes, M. Stumpf, J. Mueller, K. Haberer, R.D. Wilken, M. Servos, Behavior and occurrence of estrogens in municipal sewage treatment plants - I. Investigations in Germany, Canada and Brazil, Science of the Total Environment, 225 (1999) 81-90.

[134] J.L. Zhou, R. Liu, A. Wilding, A. Hibberd, Sorption of selected endocrine disrupting chemicals to different aquatic colloids, Environmental Science & Technology, 41 (2007) 206-213.

[135] T.L. Jones-Lepp, R. Stevens, Pharmaceuticals and personal care products in biosolids/sewage sludge: the interface between analytical chemistry and regulation, Analytical and Bioanalytical Chemistry, 387 (2007) 1173-1183.

[136] A. Shareef, M.J. Angove, J.D. Wells, B.B. Johnson, Aqueous solubilities of estrone, 17β-estradiol, 17α- ethynylestradiol, and bisphenol A, Journal of Chemical and Engineering Data, 51 (2006) 879-881.

[137] K. Fujii, S. Kikuchi, M. Satomi, N. Ushio-Sata, N. Morita, Degradation of 17 beta-estradiol by a gram-negative bacterium isolated from activated sludge in a sewage treatment plant in Tokyo, Japan, Applied and Environmental Microbiology, 68 (2002) 2057-2060.

[138] H.B. Lee, D. Liu, Degradation of 17 beta-estradiol and its metabolites by sewage bacteria, Water Air and Soil Pollution, 134 (2002) 353-368.

[139] M. Nasu, M. Goto, H. Kato, Y. Oshima, H. Tanaka, Study on endocrine disrupting chemicals in wastewater treatment plants, Water Science and Technology, 43 (2001) 101-108.

[140] H. Tanaka, Y. Yakou, A. Takahashi, T. Higashitani, K. Komori, Comparison between estrogenicities estimated from DNA recombinant yeast assay and

from chemical analyses of endocrine disruptors during sewage treatment, Water Science and Technology, 43 (2001) 125-132.

[141] J. Xu, L. Wu, A.C. Chang, Degradation and adsorption of selected pharmaceuticals and personal care products (PPCPs) in agricultural soils, Chemosphere, 77 (2009) 1299-1305.

[142] F. Neira Ruiz, A. Arcos Arevalo, J.C. Duran Alvarez, B. Jimenez Cisneros, Operating conditions and membrane selection for the removal of conventional and emerging pollutants from spring water using nanofiltration technology: the Tula Valley case, Desalination and Water Treatment, 42 (2012) 117-124.

[143] T. Karpova, S. Preis, J. Kallas, A.L. Barros Torres, Selective photocatalytic oxidation of steroid estrogens in presence of saccharose and ethanol as co-pollutants, Environ. Chem. Lett., 5 (2007) 219-224.

[144] M. Deborde, S. Rabouan, H. Gallard, B. Legube, Aqueous chlorination kinetics of some endocrine disruptors, Environmental Science & Technology, 38 (2004) 5577-5583.

[145] A. Alum, Y. Yoon, P. Westerhoff, M. Abbaszadegan, Oxidation of bisphenol A, 17 beta-estradiol, and 17 alpha-ethynyl estradiol and byproduct estrogenicity, Environmental Toxicology, 19 (2004) 257-264.

[146] G. Li, L. Zu, P.-K. Wong, X. Hui, Y. Lu, J. Xiong, T. An, Biodegradation and detoxification of bisphenol A with one newly-isolated strain Bacillus sp GZB: Kinetics, mechanism and estrogenic transition, Bioresource Technology, 114 (2012) 224-230.

[147] T. Cajthaml, Z. Kresinova, K. Svobodova, M. Moder, Biodegradation of endocrine-disrupting compounds and suppression of estrogenic activity by ligninolytic fungi, Chemosphere, 75 (2009) 745-750.

[148] G. Eibes, G. Debernardi, G. Feijoo Costa, M.T. Moreira Vilar, J.M. Lema Rodicio, Oxidation of pharmaceutically active compounds by a ligninolytic fungal peroxidase, Biodegradation, (2010).

[149] A. Lagana, A. Bacaloni, I. De Leva, A. Faberi, G. Fago, A. Marino, Analytical methodologies for determining the occurrence of endocrine disrupting chemicals in sewage treatment plants and natural waters, Analytica Chimica Acta, 501 (2004) 79-88.

[150] A.D. Vethaak, J. Lahr, S.M. Schrap, A.C. Belfroid, G.B.J. Rijs, A. Gerritsen, J. de Boer, A.S. Bulder, G.C.M. Grinwis, R.V. Kuiper, J. Legler, T.A.J. Murk, W. Peijnenburg, H.J.M. Verhaar, P. de Voogt, An integrated assessment of estrogenic contamination and biological effects in the aquatic environment of The Netherlands, Chemosphere, 59 (2005) 511-524.

[151] M. Clara, N. Kreuzinger, B. Strenn, O. Gans, H. Kroiss, The solids retention time - a suitable design parameter to evaluate the capacity of wastewater treatment plants to remove micropollutants, Water Research, 39 (2005) 97-106.

[152] J.E. Drewes, J. Hemming, S.J. Ladenburger, J. Schauer, W. Sonzogni, An assessment of endocrine disrupting activity changes during wastewater treatment through the use of bioassays and chemical measurements, Water Environment Research, 77 (2005) 12-23.

[153] C.-P. Yu, K.-H. Chu, Occurrence of pharmaceuticals and personal care products along the West Prong Little Pigeon River in east Tennessee, USA, Chemosphere, 75 (2009) 1281-1286.

[154] J.-L. Wu, N.P. Lam, D. Martens, A. Kettrup, Z. Cai, Triclosan determination in water related to wastewater treatment, Talanta, 72 (2007) 1650-1654.

[155] N. Nakada, T. Tanishima, H. Shinohara, K. Kiri, H. Takada, Pharmaceutical chemicals and endocrine disrupters in municipal wastewater in Tokyo and

their removal during activated sludge treatment, Water Research, 40 (2006) 3297-3303.

[156] S. Weigel, U. Berger, E. Jensen, R. Kallenborn, H. Thoresen, H. Huhnerfuss, Determination of selected pharmaceuticals and caffeine in sewage and seawater from Tromso/Norway with emphasis on ibuprofen and its metabolites, Chemosphere, 56 (2004) 583-592.

[157] R. Montes, I. Rodriguez, E. Rubi, R. Cela, Dispersive liquid-liquid microextraction applied to the simultaneous derivatization and concentration of triclosan and methyltriclosan in water samples, Journal of Chromatography A, 1216 (2009) 205-210.

[158] J. Regueiro, E. Becerril, C. Garcia-Jares, M. Llompart, Trace analysis of parabens, triclosan and related chlorophenols in water by headspace solid-phase microextraction with in situ derivatization and gas chromatography-tandem mass spectrometry, Journal of Chromatography A, 1216 (2009) 4693-4702.

[159] E. Villaverde-de-Saa, I. Gonzalez-Marino, J. Benito Quintana, R. Rodil, I. Rodriguez, R. Cela, In-sample acetylation-non-porous membrane-assisted liquid-liquid extraction for the determination of parabens and triclosan in water samples, Analytical and Bioanalytical Chemistry, 397 (2010) 2559-2568.

[160] L. Kantiani, M. Farre, D. Asperger, F. Rubio, S. Gonzalez, M.J. Lopez de Alda, M. Petrovic, W.L. Shelver, D. Barcelo, Triclosan and methyl-triclosan monitoring study in the northeast of Spain using a magnetic particle enzyme immunoassay and confirmatory analysis by gas chromatography-mass spectrometry, Journal of Hydrology, 361 (2008) 1-9.

[161] P. Pothitou, D. Voutsa, Endocrine disrupting compounds in municipal and industrial wastewater treatment plants in Northern Greece, Chemosphere, 73 (2008) 1716-1723.

[162] G. D'Ascenzo, A. Di Corcia, A. Gentili, R. Mancini, R. Mastropasqua, M. Nazzari, R. Samperi, Fate of natural estrogen conjugates in municipal sewage transport and treatment facilities, Science of the Total Environment, 302 (2003) 199-209.

[163] M.R. Servos, D.T. Bennie, B.K. Burnison, A. Jurkovic, R. McInnis, T. Neheli, A. Schnell, P. Seto, S.A. Smyth, T.A. Ternes, Distribution of estrogens, 17 beta-estradiol and estrone, in Canadian municipal wastewater treatment plants, Science of the Total Environment, 336 (2005) 155-170.

[164] R.F. Chimchirian, R.P.S. Suri, H. Fu, Free synthetic and natural estrogen hormones in influent and effluent of three municipal wastewater treatment plants, Water Environment Research, 79 (2007) 969-974.

[165] M.P. Fernandez, M.G. Ikonomou, I. Buchanan, An assessment of estrogenic organic contaminants in Canadian wastewaters, Science of the Total Environment, 373 (2007) 250-269.

[166] O. Braga, G.A. Smythe, A.I. Schafer, A.J. Feitz, Fate of steroid estrogens in Australian inland and coastal wastewater treatment plants, Environmental Science & Technology, 39 (2005) 3351-3358.

[167] M. Cargouet, D. Perdiz, A. Mouatassim-Souali, S. Tamisier-Karolak, Y. Levi, Assessment of river contamination by estrogenic compounds in Paris area (France), Science of the Total Environment, 324 (2004) 55-66.

[168] W.H. Glaze, J.W. Kang, D.H. Chapin, The chemistry of water treatment processes involving ozone, hydrogen peroxide, and ultraviolet radiation, Ozone-Science & Engineering, 9 (1987) 335-352.

[169] I. Oller, S. Malato, J.A. Sanchez-Perez, Combination of Advanced Oxidation Processes and biological treatments for wastewater decontamination-A review, Science of the Total Environment, 409 (2011) 4141-4166.

[170] V. Augugliaro, M. Litter, L. Palmisano, J. Soria, The combination of heterogeneous photocatalysis with chemical and physical operations: A tool for improving the photoprocess performance, Journal of Photochemistry and Photobiology C-Photochemistry Reviews, 7 (2006) 127-144.

[171] Y.G. Adewuyi, Sonochemistry: Environmental science and engineering applications, Industrial & Engineering Chemistry Research, 40 (2001) 4681-4715.

[172] S. Esplugas, J. Gimenez, S. Contreras, E. Pascual, M. Rodriguez, Comparison of different advanced oxidation processes for phenol degradation, Water Research, 36 (2002) 1034-1042.

[173] D. Bila, A.F. Montalvão, D.d.A. Azevedo, M. Dezotti, Estrogenic activity removal of 17β-estradiol by ozonation and identification of by-products, Chemosphere, 69 (2007) 736-746.

[174] H.-s. Kim, H. Yamada, H. Tsuno, The removal of estrogenic activity and control of brominated by-products during ozonation of secondary effluents, Water Research, 41 (2007) 1441-1446.

[175] S.D. Kim, J. Cho, I.S. Kim, B.J. Vanderford, S.A. Snyder, Occurrence and removal of pharmaceuticals and endocrine disruptors in South Korean surface, drinking, and waste waters, Water Research, 41 (2007) 1013-1021.

[176] S.W. Krasner, H.S. Weinberg, S.D. Richardson, S.J. Pastor, R. Chinn, M.J. Sclimenti, G.D. Onstad, A.D. Thruston, Jr., Occurrence of a new generation

of disinfection byproducts, Environmental Science & Technology, 40 (2006) 7175-7185.

[177] H. Nakamura, T. Shiozawa, Y. Terao, F. Shiraishi, H. Fukazawa, By-products produced by the reaction of estrogens with hypochlorous acid and their estrogen activities, Journal of Health Science, 52 (2006) 124-131.

[178] M.J. Plewa, E.D. Wagner, S.D. Richardson, A.D. Thruston, Y.T. Woo, A.B. McKague, Chemical and biological characterization of newly discovered lodoacid drinking water disinfection byproducts, Environmental Science & Technology, 38 (2004) 4713-4722.

[179] N.W. Shappell, M.A. Vrabel, P.J. Madsen, G. Harrington, L.O. Billey, H. Hakk, G.L. Larsen, E.S. Beach, C.P. Horwitz, K. Ro, P.G. Hunt, T.J. Collins, Destruction of estrogens using Fe-TAML/peroxide catalysis, Environmental Science & Technology, 42 (2008) 1296-1300.

[180] N.A. Kulikova, O.I. Klein, E.V. Stepanova, O.V. Koroleva, Use of Basidiomycetes in Industrial Waste Processing and Utilization Technologies: Fundamental and Applied Aspects (Review), Applied Biochemistry and Microbiology, 47 (2011) 565-579.

[181] P. Demarche, C. Junghanns, R.R. Nair, S.N. Agathos, Harnessing the power of enzymes for environmental stewardship, Biotechnology Advances, 30 (2012) 933-953.

[182] K. Chiang, T.M. Lim, L. Tsen, C.C. Lee, Photocatalytic degradation and mineralization of bisphenol A by TiO2 and platinized TiO2, Applied Catalysis a-General, 261 (2004) 225-237.

[183] I. Ferrer, M. Mezcua, M.J. Gomez, E.M. Thurman, A. Aguera, M.D. Hernando, A.R. Fernandez-Alba, Liquid chromatography/time-of-flight mass spectrometric analyses for the elucidation of the photodegradation

products of triclosan in wastewater samples, Rapid Communications in Mass Spectrometry, 18 (2004) 443-450.

[184] B. Liu, X.L. Liu, Direct photolysis of estrogens in aqueous solutions, Science of the Total Environment, 320 (2004) 269-274.

[185] P. Mazellier, L. Méité, J.D. Laat, Photodegradation of the steroid hormones 17β-estradiol (E2) and 17α-ethinylestradiol (EE2) in dilute aqueous solution, Chemosphere, 73 (2008) 1216-1223.

[186] R. Thiruvenkatachari, T.O. Kwon, I.S. Moon, A total solution for simultaneous organic degradation and particle separation using photocatalytic oxidation and submerged microfiltration membrane hybrid process, Korean Journal of Chemical Engineering, 22 (2005) 938-944.

[187] G. Yu, X. Wen, R. Li, Y. Qian, In vitro degradation of a reactive azo dye by crude ligninolytic enzymes from nonimmersed liquid culture of Phanerochaete chrysosporium, Process Biochemistry, 41 (2006) 1987-1993.

[188] H.M. Coleman, E.J. Routledge, J.P. Sumpter, B.R. Eggins, J.A. Byrne, Rapid loss of estrogenicity of steroid estrogens by UVA photolysis and photocatalysis over an immobilised titanium dioxide catalyst, Water Research, 38 (2004) 3233-3240.

[189] J. Lee, H. Park, J. Yoon, Ozonation characteristics of bisphenol A in water, Environmental Technology, 24 (2003) 241-248.

[190] S. Suarez, M.C. Dodd, F. Omil, U. von Gunten, Kinetics of triclosan oxidation by aqueous ozone and consequent loss of antibacterial activity: Relevance to municipal wastewater ozonation, Water Research, 41 (2007) 2481-2490.

[191] T.A. Ternes, J. Stuber, N. Herrmann, D. McDowell, A. Ried, M. Kampmann, B. Teiser, Ozonation: a tool for removal of pharmaceuticals, contrast

media and musk fragrances from wastewater?, Water Research, 37 (2003) 1976-1982.

[192] S. Irmak, O. Erbatur, A. Akgerman, Degradation of 17 beta-estradiol and bisphenol A in aqueous medium by using ozone and ozone/UV techniques, Journal of Hazardous Materials, 126 (2005) 54-62.

[193] X. Zhang, P.Y. Chen, F. Wu, N.S. Deng, J.T. Liu, T. Fang, Degradation of 17 alpha-ethinylestradiol in aqueous solution by ozonation, Journal of Hazardous Materials, 133 (2006) 291-298.

[194] T. Yamamoto, A. Yasuhara, Chlorination of bisphenol A in aqueous media: formation of chlorinated bisphenol A congeners and degradation to chlorinated phenolic compounds, Chemosphere, 46 (2002) 1215-1223.

[195] P. Canosa, S. Morales, I. Rodriguez, E. Rubi, R. Cela, M. Gomez, Aquatic degradation of triclosan and formation of toxic chlorophenols in presence of low concentrations of free chlorine, Analytical and Bioanalytical Chemistry, 383 (2005) 1119-1126.

[196] J.Y. Hu, S.J. Cheng, T. Aizawa, Y. Terao, S. Kunikane, Products of aqueous chlorination of 17 beta-estradiol and their estrogenic activities, Environmental Science & Technology, 37 (2003) 5665-5670.

[197] C. Li, X.Z. Li, N. Graham, N.Y. Gao, The aqueous degradation of bisphenol A and steroid estrogens by ferrate, Water Research, 42 (2008) 109-120.

[198] B. Yang, G.-G. Ying, J.-L. Zhao, L.-J. Zhang, Y.-X. Fang, L.D. Nghiem, Oxidation of triclosan by ferrate: Reaction kinetics, products identification and toxicity evaluation, Journal of Hazardous Materials, 186 (2011) 227-235.

[199] K. Lin, W. Liu, J. Gan, Oxidative Removal of Bisphenol A by Manganese Dioxide: Efficacy, Products, and Pathways, Environmental Science & Technology, 43 (2009) 3860-3864.

[200] H.C. Zhang, C.H. Huang, Oxidative transformation of triclosan and chlorophene by manganese oxides, Environmental Science & Technology, 37 (2003) 2421-2430.

[201] L. Xu, C. Xu, M. Zhao, Y. Qiu, G.D. Sheng, Oxidative removal of aqueous steroid estrogens by manganese oxides, Water Research, 42 (2008) 5038-5044.

[202] L. Jiang, C. Huang, J. Chen, X. Chen, Oxidative Transformation of 17 beta-estradiol by MnO2 in Aqueous Solution, Arch. Environ. Contam. Toxicol., 57 (2009) 221-229.

[203] K. Nomiyama, T. Tanizaki, T. Koga, K. Arizono, R. Shinohara, Oxidative degradation of BPA using TiO2 in water, and transition of estrogenic activity in the degradation pathways, Arch. Environ. Contam. Toxicol., 52 (2007) 8-15.

[204] R.A. Torres-Palma, J.I. Nieto, E. Combet, C. Petrier, C. Pulgarin, An innovative ultrasound, Fe2+ and TiO2 photoassisted process for bisphenol a mineralization, Water Research, 44 (2010) 2245-2252.

[205] E.J. Rosenfeldt, P.J. Chen, S. Kullman, K.G. Linden, Destruction of estrogenic activity in water using UV advanced oxidation, Science of the Total Environment, 377 (2007) 105-113.

[206] H. Katsumata, S. Kawabe, S. Kaneco, T. Suzuki, K. Ohta, Degradation of bisphenol A in water by the photo-Fenton reaction, Journal of Photochemistry and Photobiology a-Chemistry, 162 (2004) 297-305.

[207] B. Gözmen, M.A. Oturan, N. Oturan, O. Erbatur, Indirect electrochemical treatment of bisphenol a in water via electrochemically generated Fenton's reagent, Environmental Science & Technology, 37 (2003) 3716-3723.

[208] M. Inoue, Y. Masuda, F. Okada, A. Sakurai, I. Takahashi, M. Sakakibara, Degradation of bisphenol A using sonochernical reactions, Water Research, 42 (2008) 1379-1386.

[209] R.P.S. Suri, M. Nayak, U. Devaiah, E. Helmig, Ultrasound assisted destruction of estrogen hormones in aqueous solution: Effect of power density, power intensity and reactor configuration, Journal of Hazardous Materials, 146 (2007) 472-478.

[210] H. Fu, R.P.S. Suri, R.F. Chimchirian, E. Helmig, R. Constable, Ultrasound-induced destruction of low levels of estrogen hormones in aqueous solutions, Environmental Science & Technology, 41 (2007) 5869-5874.

[211] C. Lopez, M. Teresa Moreira, G. Feijoo, J. Manuel Lema, Economic comparison of enzymatic reactors and advanced oxidation processes applied to the degradation of phenol as a model compound, Biocatalysis and Biotransformation, 29 (2011) 344-353.

[212] D. Ibarra, J. Romero, M.J. Martinez, A.T. Martinez, S. Camarero, Exploring the enzymatic parameters for optimal delignification of eucalypt pulp by laccase-mediator, Enzyme and Microbial Technology, 39 (2006) 1319-1327.

[213] L. Lloret, G. Eibes, T.A. Lu-Chau, M.T. Moreira, G. Feijoo, J.M. Lema, Laccase-catalyzed degradation of anti-inflammatories and estrogens, Biochemical Engineering Journal, 51 (2010) 124-131.

[214] G. Kabiersch, J. Rajasarkka, R. Ullrich, M. Tuomela, M. Hofrichter, M. Virta, A. Hatakka, K. Steffen, Fate of bisphenol A during treatment with the litter-decomposing fungi Stropharia rugosoannulata and Stropharia coronilla, Chemosphere, 83 (2011) 226-232.

[215] H. Kum, M.K. Kim, H.T. Choi, Degradation of endocrine disrupting chemicals by genetic transformants in Irpex lacteus with an inducible laccase gene of Phlebia tremellosa, Biodegradation, 20 (2009) 673-678.

[216] S.M. Lee, B.W. Koo, S.S. Lee, M.K. Kim, D.H. Choi, E.J. Hong, E.B. Jeung, I.G. Choi, Biodegradation of dibutylphthalate by white rot fungi and evaluation on its estrogenic activity, Enzyme and Microbial Technology, 35 (2004) 417-423.

[217] T. Hirano, Y. Honda, T. Watanabe, M. Kuwahara, Degradation of bisphenol a by the lignin-degrading enzyme, manganese peroxidase, produced by the white-rot basidiomycete, *Pleurotus ostreatus*, Biosci. Biotechnol. Biochem., 64 (2000) 1958-1962.

[218] K. Hundt, D. Martin, E. Hammer, U. Jonas, M.K. Kindermann, F. Schauer, Transformation of triclosan by *Trametes versicolor* and *Pycnoporus cinnabarinus*, Applied and Environmental Microbiology, 66 (2000) 4157-4160.

[219] Y. Tamagawa, H. Hirai, S. Kawai, T. Nishida, Removal of estrogenic activity of endocrine-disrupting genistein by ligninolytic enzymes from white rot fungi, Fems Microbiology Letters, 244 (2005) 93-98.

[220] P. Blanquez, B. Guieysse, Biodegradation of estrogenic compounds by white rot fungi, J. Biotechnol., 131 (2007) S244-S245.

[221] C.-S. Liao, S.-Y. Yuan, B.-H. Hung, B.-V. Chang, Removal of organic toxic chemicals using the spent mushroom compost of Ganoderma lucidum, Journal of Environmental Monitoring, 14 (2012) 1983-1988.

[222] C. Nicolucci, S. Rossi, C. Menale, T. Godjevargova, Y. Ivanov, M. Bianco, L. Mita, U. Bencivenga, D.G. Mita, N. Diano, Biodegradation of bisphenols with immobilized laccase or tyrosinase on polyacrylonitrile beads, Biodegradation, 22 (2011) 673-683.

[223] Y. Tsutsumi, T. Haneda, T. Nishida, Removal of estrogenic activities of bisphenol A and nonylphenol by oxidative enzymes from lignin-degrading basidiomycetes, Chemosphere, 42 (2001) 271-276.

[224] T. Fukuda, H. Uchida, M. Suzuki, H. Miyamoto, H. Morinaga, H. Nawata, T. Uwajima, Transformation products of bisphenol A by a recombinant *Trametes vilosa* laccase and their estrogenic activity, J. Chem. Technol. Biotechnol., 79 (2004) 1212-1218.

[225] T. Fukuda, H. Uchida, Y. Takashima, T. Uwajima, T. Kawabata, M. Suzuki, Degradation of bisphenol a by purified laccase from *Trametes villosa*, Biochemical and Biophysical Research Communications, 284 (2001) 704-706.

[226] H. Uchida, T. Fukuda, H. Miyamoto, T. Kawabata, M. Suzuki, T. Uwajima, Polymerization of Bisphenol A by Purified Laccase from Trametes villosa, Biochemical and Biophysical Research Communications, 287 (2001) 355-358.

[227] T. Saito, P. Hong, K. Kato, M. Okazaki, H. Inagaki, S. Maeda, Y. Yokogawa, Purification and characterization of an extracellular laccase of a fungus (family Chaetomiaceae) isolated from soil, Enzyme and Microbial Technology, 33 (2003) 520-526.

[228] T. Saito, K. Kato, Y. Yokogawa, M. Nishida, N. Yamashita, Detoxification of bisphenol A and nonylphenol by purified extracellular laccase from a fungus isolated from soil, Journal of Bioscience and Bioengineering, 98 (2004) 64-66.

[229] H. Cabana, C. Alexandre, S.N. Agathos, J.P. Jones, Immobilization of laccase from the white rot fungus Coriolopsis polyzona and use of the immobilized biocatalyst for the continuous elimination of endocrine disrupting chemicals, Bioresource Technology, 100 (2009) 3447-3458.

[230] H. Cabana, J.L.H. Jiwan, R. Rozenberg, V. Elisashvili, M. Penninckx, S.N. Agathos, J.P. Jones, Elimination of endocrine disrupting chemicals nonylphenol and bisphenol A and personal care product ingredient triclosan using enzyme preparation from the white rot fungus Coriolopsis polyzona, Chemosphere, 67 (2007) 770-778.

[231] S.-y. Okazaki, J. Michizoe, M. Goto, S. Furusaki, H. Wariishi, H. Tanaka, Oxidation of bisphenol A catalyzed by laccase hosted in reversed micelles in organic media, Enzyme and Microbial Technology, 31 (2002) 227-232.

[232] T. Tanaka, K. Yamada, T. Tonosaki, T. Konishi, H. Goto, M. Taniguchi, Enzymatic degradation of alkylphenols, bisphenol A, synthetic estrogen and phthalic ester, Water Sci. Technol., 42 (2000) 89-95.

[233] T. Tanaka, T. Tonosaki, M. Nose, N. Tomidokoro, N. Kadomura, T. Fujii, M. Taniguchi, Treatment of model soils contaminated with phenolic endocrine-disrupting chemicals with laccase from *Trametes* sp in a rotating reactor, J Biosci Bioeng, 92 (2001) 312-316.

[234] Y. Michizoe, H. Ichinose, N. Kamiya, T. Maruyama, M. Goto, Biodegradation of phenolic environmental pollutants by a surfactant-laccase complex in organic media, Journal of Bioscience and Bioengineering, 99 (2005) 642-647.

[235] G. Songulashvili, G.A. Jimenez-Tobon, C. Jaspers, M.J. Penninckx, Immobilized laccase of Cerrena unicolor for elimination of endocrine disruptor micropollutants, Fungal biology, 116 (2012) 883-889.

[236] H. Cabana, A. Ahamed, R. Leduc, Conjugation of laccase from the white rot fungus Trametes versicolor to chitosan and its utilization for the elimination of triclosan, Bioresource Technology, 102 (2011) 1656-1662.

[237] Y. Inoue, T. Hata, S. Kawai, H. Okamura, T. Nishida, Elimination and detoxification of triclosan by manganese peroxidase from white rot fungus, Journal of Hazardous Materials, 180 (2010) 764-767.

[238] K. Murugesan, Y.-Y. Chang, Y.-M. Kim, J.-R. Jeon, E.-J. Kim, Y.-S. Chang, Enhanced transformation of triclosan by laccase in the presence of redox mediators, Water Research, 44 (2010) 298-308.

[239] T. Tanaka, T. Tamura, Y. Ishizaki, A. Kawasaki, T. Kawase, M. Teraguchi, M. Taniguchi, Enzymatic treatment of estrogens and estrogen glucuronide, Journal of Environmental Sciences-China, 21 (2009) 731-735.

[240] J. Wang, N. Majima, H. Hirai, H. Kawagishi, Effective Removal of Endocrine-Disrupting Compounds by Lignin Peroxidase from the White-Rot Fungus Phanerochaete sordida YK-624, Current Microbiology, 64 (2012) 300-303.

[241] M. Kimura, J. Michizoe, S. Oakazaki, S. Furusaki, M. Goto, H. Tanaka, H. Wariishi, Activation of lignin peroxidase in organic media by reversed micelles, Biotechnology and Bioengineering, 88 (2004) 495-501.

[242] L. Mao, Q. Huang, J. Lu, S. Gao, Ligninase-Mediated Removal of Natural and Synthetic Estrogens from Water: I. Reaction Behaviors, Environmental Science & Technology, 43 (2009) 374-379.

[243] Y. Tamagawa, R. Yamaki, H. Hirai, S. Kawai, T. Nishida, Removal of estrogenic activity of natural steroidal hormone estrone by ligninolytic enzymes from white rot fungi, Chemosphere, 65 (2006) 97-101.

[244] K. Suzuki, H. Hirai, H. Murata, T. Nishida, Removal of estrogenic activities of 17 beta-estradiol and ethinylestradiol by ligninolytic enzymes from white rot fungi, Water Res, 37 (2003) 1972-1975.

[245] C. Muñoz, F. Guillén, A.T. Martínez, M.J. Martínez, Laccase isoenzymes of *Pleurotus eryngii*: Characterization, catalytic properties, and participation

in activation of molecular oxygen and Mn^{2+} oxidation, Appl Environ Microb, 63 (1997) 2166-2174.

[246] M.J. Martínez, F.J. Ruiz Dueñas, F. Guillén, A.T. Martínez, Purification and catalytic properties of two manganese peroxidase isoenzymes from *Pleurotus eryngii*, Eur J Biochem, 237 (1996) 424-432.

[247] J.A. Field, E. de Jong, G.F. Costa, J.A.M. Debont, Biodegradation of polycyclic aromatic-hydrocarbons by new isolates of white rot fungi, Appl Environ Microb, 58 (1992) 2219-2226.

[248] M. Bradford, A rapid and sensitive method for the quantitation of microgram quantities of proteins utilizing the principle of protein-dye binding, Anal Biochem, 72 (1976) 248-254.

[249] M. Somogyi, A new reagent for the determination of sugars, J Biol Chem, 160 (1945) 61-68.

[250] V.L. Singleton, J.A. Rossi, Colorimetry of Total Phenolics with Phosphomolybdic-Phosphotungstic Acid Reagents, American Journal of Enology and Viticulture, 16 (1965) 144-158.

[251] U. Urzua, P.J. Kersten, R. Vicuna, Kinetics of Mn^{3+}-oxalate formation and decay in reactions catalyzed by manganese peroxidase of *Ceriporiopsis subvermispora*, Arch. Biochem. Biophys., 360 (1998) 215-222.

[252] H. Wariishi, K. Valli, M.H. Gold, Manganese(II) oxidation by manganese peroxidase from the basidiomycete *Phanerochaete chrysosporium*: kinetic mechanism and role of chelators, J Biol Chem, 267 (1992) 23688-23695.

[253] T. Schultis, J.W. Metzger, Determination of estrogenic activity by LYES-assay (yeast estrogen screen-assay assisted by enzymatic digestion with lyticase), Chemosphere, 57 (2004) 1649-1655.

[254] A. Hatakka, Lignin modifying enzymes from selected white-rot fungi: production and role in lignin degradation, in, 1994, pp. 125-135.

[255] A. Hatakka, Lignin modifying enzymes from selected white-rot fungi: production and role from in lignin degradation, Fems Microbiology Reviews, 13 (1994) 125-135.

[256] F.J. Ruiz-Duenas, M. Morales, E. Garcia, Y. Miki, M.J. Martinez, A.T. Martinez, Substrate oxidation sites in versatile peroxidase and other basidiomycete peroxidases, Journal of Experimental Botany, 60 (2009) 441-452.

[257] A. Heinfling, M.J. Martinez, A.T. Martinez, M. Bergbauer, U. Szewzyk, Purification and characterization of peroxidases from the dye-decolorizing fungus *Bjerkandera adusta*, FEMS Microbiol. Lett., 165 (1998) 43-50.

[258] M. Chivukula, J.T. Spadaro, V. Renganathan, Lignin peroxidase-catalyzed oxidation of sulfonated azo dyes generates novel sulfophenyl hydroperoxides, Biochemistry, 34 (1995) 7765-7772.

[259] G. Davila-Vazquez, R. Tinoco, M.A. Pickard, R. Vazquez-Duhalt, Transformation of halogenated pesticides by versatile peroxidase from *Bjerkandera adusta*, Enzyme Microb Tech, 36 (2005) 223-231.

[260] T. Günther, U. Sack, M. Hofrichter, M. Latz, Oxidation of PAH and PAH-derivatives by fungal and plant oxidoreductases, J Basic Microb, 38 (1998) 113-122.

[261] O. Rubilar, G. Feijoo, C. Diez, T.A. Lú-Chau, M.T. Moreira, J.M. Lema, Biodegradation of pentachlorophenol in soil slurry cultures by *Bjerkandera adusta* and *Anthracophyllum discolor*, in, 2007, pp. 6744-6751.

[262] B.C. Okeke, A. Paterson, J.E. Smith, I.A. WatsonCraik, Comparative biotransformation of pentachlorophenol in soils by solid substrate cultures of *Lentinula edodes*, Appl Microbiol Biot, 48 (1997) 563-569.

[263] E. Romero, M. Speranza, J. García-Guinea, A.T. Martínez, M.J. Martínez, An anamorph of the white-rot fungus *Bjerkandera adusta* capable of

colonizing and degrading compact disc components, FEMS Microbiol. Lett., 275 (2007) 122-129.

[264] T. White, T. Bruns, S. Lee, J. Taylor, Amplification and direct sequencing of fungal ribosomal RNA genes for phylogenetics, in: M. Innis, D. Gelfand, J. Sninsky, T. White (Eds.) PCR Protocols: A Guide to Methods and Applications, Academic Press, Incorporated, San Diego, 1990, pp. 315-322.

[265] S.F. Altschul, T.L. Madden, A.A. Schaffer, J.H. Zhang, Z. Zhang, W. Miller, D.J. Lipman, Gapped BLAST and PSI-BLAST: a new generation of protein database search programs, Nucleic Acids Res, 25 (1997) 3389-3402.

[266] M. Gardes, T.D. Bruns, ITS primers with enhanced specificity for basidiomycetes: application to the identification of mycorrhizae and rusts, Mol Ecol, 2 (1993) 113-118.

[267] H. Barnett, B. Hunter, Descriptions and illustrations of genera, in: Illustrated Genera of Imperfect Fungi, American Phytopathological Society, St. Paul, Minnesota, 1998, pp. 68-69.

[268] T. Kornillowicz-Kowalska, M. Wrzosek, G. Ginalska, H. Iglik, R. Bancerz, Identification and application of a new fungal strain *Bjerkandera adusta* R59 in decolorization of daunomycin wastes, Enzyme Microb Tech, 38 (2006) 583-590.

[269] S.G.R. Wirsel, W. Leibinger, M. Ernst, K. Mendgen, Genetic diversity of fungi closely associated with common reed, New Phytol, 149 (2001) 589-598.

[270] F. Guillén, A.T. Martínez, M.J. Martínez, C.S. Evans, Hydrogen peroxide producing system of *Pleurotus eryngii* involving the extracellular enzyme aryl alcohol oxidase, Appl Biochem Biotech, 41 (1994) 465-470.

[271] B. Böckle, M.J. Martínez, F. Guillén, A.T. Martínez, Mechanism of peroxidase inactivation in liquid cultures of the ligninolytic fungus *Pleurotus pulmonarius*, Appl Environ Microb, 65 (1999) 923-928.

[272] C. Palma, A.T. Martínez, J.M. Lema, M.J. Martínez, Different fungal manganese-oxidizing peroxidases: a comparison between *Bjerkandera* sp and *Phanerochaete chrysosporium*, J Biotechnol, 77 (2000) 235-245.

[273] U.T. Bornscheuer, Immobilizing enzymes: How to create more suitable biocatalysts, Angewandte Chemie-International Edition, 42 (2003) 3336-3337.

[274] R.A. Sheldon, Enzyme immobilization: The quest for optimum performance, Adv. Synth. Catal., 349 (2007) 1289-1307.

[275] L.Q. Cao, L. van Langen, R.A. Sheldon, Immobilised enzymes: carrier-bound or carrier-free?, Current Opinion in Biotechnology, 14 (2003) 387-394.

[276] M.S. Doscher, F.M. Richards, Activity of an enzyme in crystalline state : Ribonuclease S., Journal of Biological Chemistry, 238 (1963) 2399-&.

[277] H. Cabana, J.P. Jones, S.N. Agathos, Preparation and characterization of cross-linked laccase aggregates and their application to the elimination of endocrine disrupting chemicals, J. Biotechnol., 132 (2007) 23-31.

[278] L.Q. Cao, F. van Rantwijk, R.A. Sheldon, Cross-linked enzyme aggregates: A simple and effective method for the immobilization of penicillin acylase, Organic Letters, 2 (2000) 1361-1364.

[279] R. Schoevaart, M.W. Wolbers, M. Golubovic, M. Ottens, A.P.G. Kieboom, F. van Rantwijk, L.A.M. van der Wielen, R.A. Sheldon, Preparation, optimization, and structures of cross-linked enzyme aggregates (CLEAs), Biotechnology and Bioengineering, 87 (2004) 754-762.

[280] R.A. Sheldon, R. Schoevaart, L.M. Van Langen, Cross-Linked Enzyme Aggregates, in: J.M. Guisan (Ed.) Methods in Biotechnology:

Immobilization of Enzymes and Cells, Humana Press Inc., Totowa, NJ, 2006, pp. 31-45.

[281] D.L. Brown, C.E. Glatz, Aggregate breakage in protein precipitation, Chemical Engineering Science, 42 (1987) 1831-1839.

[282] R.A. Sheldon, R. Schoevaart, L.M. Van Langen, Cross-linked enzyme aggregates (CLEAs): A novel and versatile method for enzyme immobilization (a review), Biocatalysis and Biotransformation, 23 (2005) 141-147.

[283] S. Shah, A. Sharma, M.N. Gupta, Preparation of cross-linked enzyme aggregates by using bovine serum albumin as a proteic feeder, Analytical Biochemistry, 351 (2006) 207-213.

[284] T. Dong, L. Zhao, Y. Huang, X. Tan, Preparation of cross-linked aggregates of aminoacylase from Aspergillus melleus by using bovine serum albumin as an inert additive, Bioresource Technology, 101 (2010) 6569-6571.

[285] B. Van Aken, P. Ledent, H. Naveau, S.N. Agathos, Co-immobilization of manganese peroxidase from Phlebia radiata and glucose oxidase from Aspergillus niger on porous silica beads, Biotechnology Letters, 22 (2000) 641-646.

[286] A. Bruggink, R. Schoevaart, T. Kieboom, Concepts of nature in organic synthesis: Cascade catalysis and multistep conversions in concert, Organic Process Research & Development, 7 (2003) 622-640.

[287] F. van de Velde, N.D. Lourenco, M. Bakker, F. van Rantwijk, R.A. Sheldon, Improved operational stability of peroxidases by coimmobilization with glucose oxidase, Biotechnology and Bioengineering, 69 (2000) 286-291.

[288] C. Mateo, A. Chmura, S. Rustler, F. van Rantwijk, A. Stolz, R.A. Sheldon, Synthesis of enantiomerically pure (S)-mandelic acid using an oxynitrilase-

nitrilase bienzymatic cascade: a nitrilase surprisingly shows nitrile hydratase activity, Tetrahedron-Asymmetry, 17 (2006) 320-323.

[289] H. Tsuge, O. Natsuaki, K. Ohashi, Purification, properties, and molecular features of glucose oxidase from *Aspergillus niger*, Journal of Biochemistry, 78 (1975) 835-843.

[290] G.P. Royer, Immobilized Enzymes, Antigens, Antibodies, and Peptides, Marcel Dekker, New York, 1975.

[291] C. Roberge, D. Amos, D. Pollard, P. Devine, Preparation and application of cross-linked aggregates of chloroperoxidase with enhanced hydrogen peroxide tolerance, Journal of Molecular Catalysis B-Enzymatic, 56 (2009) 41-45.

[292] I. Mielgo, C. Palma, J.M. Guisan, R. Fernandez-Lafuente, M.T. Moreira, G. Feijoo, J.M. Lema, Covalent immobilisation of manganese peroxidases (MnP) from *Phanerochaete chrysosporium* and *Bjerkandera* sp BOS55, Enzyme Microb Tech, 32 (2003) 769-775.

[293] L. Wilson, G. Fernandez-Lorente, R. Fernandez-Lafuente, A. Illanes, J.M. Guisan, J.M. Palomo, CLEAs of lipases and poly-ionic polymers: A simple way of preparing stable biocatalysts with improved properties, Enzyme and Microbial Technology, 39 (2006) 750-755.

[294] A.P.M. Tavares, R.O. Cristóvão, J.M. Loureiro, R.A.R. Boaventura, E.A. Macedo, Application of statistical experimental methodology to optimize reactive dye decolourization by commercial laccase, Journal of Hazardous Materials, 162 (2009) 1255-1260.

[295] G.E.P. Box, K.B. Wilson, On the experimental attainment of optimum conditions, Journal of the Royal Statistical Society Series B-Statistical Methodology, 13 (1951) 1-45.

[296] C.-Y. Chang, C.-L. Lee, T.-M. Pan, Statistical optimization of medium components for the production of Antrodia cinnamomea AC0623 in submerged cultures, Applied Microbiology and Biotechnology, 72 (2006) 654-661.

[297] I. Rodriguez, J.B. Quintana, J. Carpinteiro, A.M. Carro, R.A. Lorenzo, R. Cela, Determination of acidic drugs in sewage water by gas chromatography-mass spectrometry as tert.-butyldimethylsilyl derivatives, Journal of Chromatography A, 985 (2003) 265-274.

[298] C. Zhang, G.M. Zeng, L. Yuan, J. Yu, J.B. Li, G.H. Huang, B.D. Xi, H.L. Liu, Aerobic degradation of bisphenol A by Achromobacter xylosoxidans strain B-16 isolated from compost leachate of municipal solid waste, Chemosphere, 68 (2007) 181-190.

[299] G. Eibes, T. Lú-Chau, G. Feijoo, M.T. Moreira, J.M. Lema, Complete degradation of anthracene by Manganese Peroxidase in organic solvent mixtures, Enzyme Microb Tech, 37 (2005) 365-372.

[300] R. Taboada-Puig, T. Lú-Chau, G. Eibes, M.T. Moreira, G. Feijoo, J.M. Lema, Biocatalytic generation of Mn(III)-chelate as a chemical oxidant of different environmental contaminants, Biotechnol. Prog., 27 (2011) 10.1002/btpr.1585.

[301] S.A. Waters, J.S. Littler, Oxidation by Vanadium(V), Cobalt(III) and Manganese(III), in: K.B. Wiberg (Ed.) Oxidation in Organic Chemistry, Academic Press, New York and London, 1965.

[302] F.L.P. Gabriel, M. Cyris, W. Giger, H.-P.E. Kohler, ipso-substitution: A general biochemical and biodegradation mechanism to cleave alpha-quaternary alkylphenols and bisphenol A, Chemistry & Biodiversity, 4 (2007) 2123-2137.

[303] B. Kolvenbach, N. Schlaich, Z. Raoui, J. Prell, S. Zuhlke, A. Schaffer, F.P. Guengerich, P.F.X. Corvini, Degradation pathway of bisphenol A: Does ipso substitution apply to phenols containing a quaternary alpha-carbon structure in the para position?, Applied and Environmental Microbiology, 73 (2007) 4776-4784.

[304] J.H. Lobos, T.K. Leib, T.M. Su, Biodegradation of bisphenol A and other bisphenols by a gram-negative aerobic bacterium, Applied and Environmental Microbiology, 58 (1992) 1823-1831.

[305] J. Spivack, T.K. Leib, J.H. Lobos, Novel pathway for bacterial metabolim of bisphenol A. Rearrangements and stilbene cleavage in bisphenol a metabolism, Journal of Biological Chemistry, 269 (1994) 7323-7329.

[306] M. Sasaki, A. Akahira, K.I. Oshiman, T. Tsuchido, Y. Matsumura, Purification of cytochrome P450 and ferredoxin, involved in bisphenol A degradation, from Sphingomonas sp strain AO1, Applied and Environmental Microbiology, 71 (2005) 8024-8030.

[307] S. Kitamura, T. Suzuki, S. Sanoh, R. Kohta, N. Jinno, K. Sugihara, S. Yoshihara, N. Fujimoto, H. Watanabe, S. Ohta, Comparative study of the endocrine-disrupting activity of bisphenol A and 19 related compounds, Toxicological Sciences, 84 (2005) 249-259.

[308] I. Gültekin, N.H. Ince, Synthetic endocrine disruptors in the environment and water remediation by advanced oxidation processes, Journal of Environmental Management, 85 (2007) 816-832.

[309] Q.G. Huang, W.J. Weber, Transformation and removal of bisphenol A from aqueous phase via peroxidase-mediated oxidative coupling reactions: Efficacy, products, and pathways, Environmental Science & Technology, 39 (2005) 6029-6036.

[310] I. Sirés, N. Oturan, M.A. Oturan, R.M. Rodríguez, J.A. Garrido, E. Brillas, Electro-Fenton degradation of antimicrobials triclosan and triclocarban, Electrochimica Acta, 52 (2007) 5493-5503.

[311] S. Rafqah, P. Wong-Wah-Chung, S. Nelieu, J. Einhorn, M. Sarakha, Phototransformation of triclosan in the presence of TiO2 in aqueous suspension: Mechanistic approach, Applied Catalysis B-Environmental, 66 (2006) 119-125.

[312] K. Sankoda, H. Matsuo, M. Ito, K. Nomiyama, K. Arizono, R. Shinohara, Identification of Triclosan Intermediates Produced by Oxidative Degradation Using TiO(2) in Pure Water and Their Endocrine Disrupting Activities, Bulletin of Environmental Contamination and Toxicology, 86 (2011) 470-475.

[313] J.L. Wu, J. Liu, Z.W. Cai, Determination of triclosan metabolites by using in-source fragmentation from high-performance liquid chromatography/negative atmospheric pressure chemical ionization ion trap mass spectrometry, Rapid Communications in Mass Spectrometry, 24 (2010) 1828-1834.

[314] L. Lloret, G. Eibes, G. Feijoo, M.T. Moreira, J.M. Lema, Degradation of estrogens by laccase from Myceliophthora thermophila in fed-batch and enzymatic membrane reactors, Journal of Hazardous Materials, 213 (2012) 175-183.

[315] L. Mao, J. Lu, M. Habteselassie, Q. Luo, S. Gao, M. Cabrera, Q. Huang, Ligninase-Mediated Removal of Natural and Synthetic Estrogens from Water: II. Reactions of 17 beta-Estradiol, Environmental Science & Technology, 44 (2010) 2599-2604.

[316] S. Nicotra, A. Intra, G. Ottolina, S. Riva, B. Danieli, Laccase-mediated oxidation of the steroid hormone 17β-estradiol in organic solvents, Tetrahedron-Asymmetr, 15 (2004) 2927-2931.

[317] T.K. Kirk, R.L. Farrell, Enzymatic "combustion": the microbial degradation of lignin, Annu Rev Microbiol, 41 (1987) 465-505.

[318] K. Kishi, H. Wariishi, L. Marquez, H.B. Dunford, M.H. Gold, Mechanism of managanese peroxidase compound II reduction: effect of organic acid chelators and pH, Biochemistry, 33 (1994) 8694-8701.

[319] I.C. Kuan, M. Tien, Stimulation of Mn-peroxidase activity: a possible role for oxalate in lignin biodegradation, P Natl Acad Sci USA, 90 (1993) 1242-1246.

[320] G. Eibes, C. López, M.T. Moreira, G. Feijoo, J.M. Lema, Strategies for the design and operation of enzymatic reactors for the degradation of highly and poorly soluble recalcitrant compounds, Biocatal Biotransform, (2007) 260-268.

[321] F. Cui, D. Dolphin, The role of manganese in model systems related to lignin biodegradation, Holzforschung, 44 (1990) 279-283.

[322] J.K. Glenn, M.H. Gold, Purification and characterization of an extracellular Mn(II)-dependent peroxidase from the lignin-degrading basidiomycete, *Phanerochaete chrysosporium*, Arch. Biochem. Biophys., 242 (1985) 329-341.

[323] C. Lopez, J.C. Garcia-Monteagudo, M.T. Moreira, G. Feijoo, J.M. Lema, The presence of dicarboxylic acids required in the MnP cycle? Study of Mn^{3+} stability by cyclic voltammetry, Enzyme Microb Tech, 42 (2007) 70-75.

[324] Z. Lu, K. Lin, J. Gan, Oxidation of bisphenol F (BPF) by manganese dioxide, Environ. Pollut., 159 (2011) 2546-2551.

[325] A.G. Sharpe, Química Inorgánica, 2nd ed., Editorial Reverté, Barcelona, 1993.

[326] G. Eibes, T. Cajthaml, M.T. Moreira, G. Feijoo, J.M. Lema, Enzymatic degradation of anthracene, dibenzothiophene and pyrene by manganese peroxidase in media containing acetone, Chemosphere, 64 (2006) 408-414.

[327] A.C. Grabski, H.J. Grimek, R.R. Burgess, Immobilization of manganese peroxidase from *Lentinula edodes* and its biocalalytic generation of Mn-III-chelate as a chemical oxidant of chlorophenols, Biotechnol Bioeng, 60 (1998) 204-215.

[328] T. Sasaki, T. Kajino, B. Li, H. Sugiyama, H. Takahashi, New pulp biobleaching system involving manganese peroxidase immobilized in a silica support with controlled pore sizes, Appl Environ Microb, 67 (2001) 2208-2212.

[329] Y. Lee, M.M. Clark, Modeling of flux decline during crossflow ultrafiltration of colloidal suspensions, Journal of Membrane Science, 149 (1998) 181-202.

[330] I.N. Levine, Physical Chemistry, 5th ed., McGraw-Hill Science, 2001.

[331] M. Auriol, Y. Filali-Meknassi, R.D. Tyagi, C.D. Adams, Oxidation of natural and synthetic hormones by the horseradish peroxidase enzyme in wastewater, Chemosphere, 68 (2007) 1830-1837.

[332] S. Kaneco, M.A. Rahman, T. Suzuki, H. Katsumata, K. Ohta, Optimization of solar photocatalytic degradation conditions of bisphenol A in water using titanium dioxide, Journal of Photochemistry and Photobiology a-Chemistry, 163 (2004) 419-424.

[333] D. Zhou, W. Feng, N.S. Deng, X. Wu, Photooxidation of bisphenol A (BPA) in water in the presence of ferric and carboxylate salts, Water Research, 38 (2004) 4107-4116.

[334] E.M. Rodriguez, G. Fernandez, N. Klamerth, M.I. Maldonado, P.M. Alvarez, S. Malato, Efficiency of different solar advanced oxidation processes on the oxidation of bisphenol A in water, Applied Catalysis B-Environmental, 95 (2010) 228-237.

[335] R.A. Torres, G. Sarantakos, E. Combet, C. Petrier, C. Pulgarin, Sequential helio-photo-Fenton and sonication processes for the treatment of bisphenol A, Journal of Photochemistry and Photobiology a-Chemistry, 199 (2008) 197-203.

[336] K. Freudenberg, H.H. Hubner, Oxyzimtalkohole und ihre dehydrierungs-polymerisate, Chem. Ber.-Recl., 85 (1952) 1181-1191.

[337] S. Yoshida, M. Tanahashi, M. Shigematsu, Y. Shinoda, Effect of reaction medium on dehydrogenative polymerization of sinapyl alcohol, Mokuzai Gakkaishi, 40 (1994) 974-979.

[338] J.M. Harkin, J.R. Obst, Lignification in trees - Indication of exclusive peroxidase participation, Science, 180 (1973) 296-298.

[339] R. Taboada-Puig, T. Lú-Chau, M.T. Moreira, G. Feijoo, M.J. Martínez, J.M. Lema, A new strain of *Bjerkandera* sp. production, purification and characterization of versatile peroxidase, World J Microbiol Biotechnol, 27 (2011) 115-122.

[340] J. Sipila, G. Brunow, On the mechanism of formation of noncyclic benzyl ethers during lignin biosynthesis. 2. The effect of pH on the reaction between a beta-O-4-type quinone methide and vanillyl alcohol in water-dioxane solutions - The stability of noncyclic benzyl ethers during lignin biosynthesis, Holzforschung, 45 (1991) 275-278.

[341] S. Quideau, J. Ralph, Facile large-scale synthesis of coniferyl, sinapyl, and para-coumaryl alcohol, Journal of Agricultural and Food Chemistry, 40 (1992) 1108-1110.

[342] T. Ohra-aho, M. Tenkanen, T. Tamminen, Direct analysis of lignin and lignin-like components from softwood kraft pulp by Py-GC/MS techniques, Journal of Analytical and Applied Pyrolysis, 74 (2005) 123-128.

[343] O. Faix, I. Fortmann, J. Bremer, D. Meier, Thermal degradation products of wood - A colletion of electron-impact (EI) mass spectra of polysaccharide derived products, Holz Als Roh-Und Werkstoff, 49 (1991) 299-304.

[344] O. Faix, I. Fortmann, J. Bremer, D. Meier, Thermal degradation products of wood - Gas chromatographic separation and mass spectrometric characterization of polysaccharide derived productsT, Holz Als Roh-Und Werkstoff, 49 (1991) 213-219.

[345] J. Ralph, R.D. Hatfield, Pyrolysis-GC-MS characterization of forage materials, Journal of Agricultural and Food Chemistry, 39 (1991) 1426-1437.

[346] E.A. Capanema, M.Y. Balakshin, J.F. Kadla, A comprehensive approach for quantitative lignin characterization by NMR spectroscopy, Journal of Agricultural and Food Chemistry, 52 (2004) 1850-1860.

[347] K. Kuroda, A. Yamaguchi, K. Sakai, Analysis of sugi wood and its lignin preparations by pyrolysis-gas-chromatography, Mokuzai Gakkaishi, 40 (1994) 987-995.

[348] K. Kuroda, A. Nakagawa-izumi, Analytical pyrolysis of lignin: Products stemming from beta-5 substructures, Organic Geochemistry, 37 (2006) 665-673.